

FADING STAR

UNDERSTANDING ACCELERATED DECAY OF ORGANIC REMAINS AT STAR CARR

Kirsty High

PhD

University of York

Department of Chemistry

June 2014

ABSTRACT

The early Mesolithic site of Star Carr (approximately 11 ka BP) is widely acknowledged as one of the most important wetland sites in Northern Europe. It has provided some of the most informative archaeological evidence for hunter-gatherer lifestyles in Britain at that time. However, recent observations suggest that the site is no longer providing the conditions necessary for such remarkable archaeological preservation. In 2007 and 2008, excavations at the site uncovered artefacts displaying alarming levels of diagenesis, suggesting that current conditions may be leading to the destruction of any organic material yet to be uncovered. Geochemical and hydrological investigations suggest that this is closely linked to changes occurring due to drying out of the site. However, scientific data regarding the rates and mechanisms of decay in such acidic environments are severely lacking.

The aim of this thesis is to apply an experimental approach to investigate the observed deterioration, in order to answer some key questions: Is Star Carr undergoing accelerated deterioration, and if so, how are the changing site conditions contributing to this? Ultimately, by learning more about the key factors facilitating degradation in the specific burial environments at Star Carr, strategies to slow or stop the deterioration can be recommended, both for Star Carr and other wetland archaeological sites.

A suite of appropriate analytical methods have been tested and applied to assess deterioration in both bone and wood. It has been shown that as different techniques provide complementary and sometimes contradictory information, a multi-analytical approach is needed. Using these techniques it has been shown that bone mineral rapidly dissolves in acidic solutions, buffering the acidity. As a result, collagen is left exposed and also breaks down leading to the loss of bio-archaeological information. The effects of pH on wood degradation are more subtle, but burial experiments show that drying out of the burial environment can have a severely detrimental effect on the survival of structural polymers in wood.

Analysis of material excavated from Star Carr has shown that preservation differs across the site. For bone this is closely related to the geochemical conditions. It seems likely that bone in the current state of preservation would quickly deteriorate further at the low sediment pH recorded. Due to the localised differences in geochemistry and organic preservation across the site, any mitigation strategies aimed at slowing organic decay need to carefully consider all material that may yet be buried, and their varying states of diagenesis. Rapid changes in both materials (bone and wood) following excavation have also been observed. It is recommended that post-excavation strategies be designed to slow or stop these changes.

CONTENTS

Abstract	2
List of figures	13
List of Tables	24
Acknowledgements	26
Declaration	28
Chapter 1 - Introduction	30
1.1 Star Carr: The Stonehenge of the Mesolithic	31
1.1.1 Introduction	31
1.1.2 Archaeological excavation at Star Carr	32
1.1.2.1 <i>Wider context</i>	32
1.1.2.2 <i>Early excavations</i>	34
1.1.2.3 <i>Research by the Vale of Pickering Research Trust</i>	36
1.1.2.4 <i>Recent excavations</i>	36
1.1.3 Evidence for site deterioration	37
1.2 Bone deterioration	39
1.2.1 Introduction	39
1.2.2 The structure of bone	39
1.2.3 Bone deterioration.....	41
1.2.4 Analysis of bone deterioration.....	42
1.2.4.1 <i>Chemical analysis</i>	42
1.2.4.2 <i>Histological and bulk analysis</i>	44
1.3 Wood deterioration	45
1.3.1 Introduction	45
1.3.2 The structure of wood	45

1.3.3	Wood deterioration	46
1.3.4	Analysis of wood deterioration.....	48
1.3.4.1	<i>Chemical analysis</i>	48
1.3.4.2	<i>Histological and bulk analysis</i>	50
1.4	Summary of organic deterioration.....	51
1.5	Organic archaeological materials in wetlands	52
1.5.1	Introduction	52
1.5.2	The chemistry of wetland sites	52
1.5.3	The biology of wetland sites	55
1.5.3.1	<i>Aerobic decomposition</i>	56
1.5.3.2	<i>Anaerobic decomposition</i>	56
1.5.4	Summary of organic deterioration in wetland sites	57
1.5.5	Organic remains in wetland sites: <i>Case studies</i>	58
1.5.5.1	<i>Flag Fen, UK</i>	58
1.5.5.2	<i>Sweet Track, UK</i>	59
1.5.5.3	<i>Fiskerton, UK</i>	60
1.5.5.4	<i>Yoxall Bridge, UK</i>	60
1.5.5.5	<i>Nydam, Denmark</i>	61
1.5.6	Summary	61
1.6	Conclusions and aims	62
Chapter 2 – A review of geochemical observations at Star Carr.....		64
2.1	Introduction.....	65
2.2	Summary of previous studies	67
2.2.1	Background (wider context).....	67
2.2.2	The geochemistry of Star Carr	70
2.2.2.1	<i>Scope of previous study</i>	70
2.2.2.2	<i>pH and redox analysis</i>	70

2.2.2.3	<i>Elemental analysis</i>	72
2.2.3	The hydrology of Star Carr	73
2.2.3.1	<i>Scope of previous study</i>	73
2.2.3.2	<i>Summary of hydrology results</i>	73
2.3	Further geochemical analysis	75
2.3.1	Introduction	75
2.3.2	Methodology.....	75
2.3.2.1	<i>pH and redox analysis</i>	75
2.3.2.2	<i>Elemental analysis</i>	75
2.3.2.3	<i>Sampling strategy</i>	76
2.3.3	Results.....	78
2.3.3.1	<i>pH and redox</i>	78
2.3.3.2	<i>Sulfur content</i>	81
2.3.3.3	<i>Dipwell monitoring</i>	82
2.4	Discussion and review	84
2.4.1	Acid rock drainage (ARD)	84
2.4.2	Biological implications	86
2.4.3	Underlying geology	86
2.4.4	Hydrology.....	87
2.5	Conclusions.....	88
Chapter 3 – Development of methods of analysis		89
3.1	Introduction.....	90
3.2	Analysis of bone deterioration	91
3.2.1	Introduction	91
3.2.2	Experimental	91
3.2.3	Bulk assessment methods.....	92
3.2.3.1	<i>Methods</i>	92

3.2.3.2	<i>Assessment of bulk analysis techniques</i>	92
3.2.4	Amino acid analysis.....	93
3.2.4.1	<i>Method</i>	94
3.2.4.2	<i>Assessment of amino acid analysis technique</i>	97
3.2.5	Powder X-ray diffraction.....	99
3.2.5.1	<i>Method</i>	100
3.2.5.2	<i>Assessment of p-XRD for the analysis of bone mineral</i>	101
3.2.5.3	<i>Conclusions on the application of p-XRD</i>	103
3.2.6	Raman spectroscopy.....	104
3.2.6.1	<i>Method</i>	104
3.2.6.2	<i>Assessment of Raman spectroscopy for the analysis of bone</i>	104
3.2.7	FTIR spectroscopy	105
3.2.7.1	<i>Method</i>	105
3.2.7.2	<i>Assessment of FTIR for the analysis of bone</i>	106
3.2.7.3	<i>Conclusions</i>	108
3.2.8	Microscopy methods.....	108
3.2.8.1	<i>Method</i>	109
3.2.8.2	<i>Assessment of microscopy techniques</i>	110
3.2.9	Conclusions on bone analysis methods	112
3.3	Analysis of wood deterioration	113
3.3.1	Introduction	113
3.3.2	Experimental	113
3.3.3	Bulk assessment.....	113
3.3.3.1	<i>Methods</i>	113
3.3.3.2	<i>Assessment of bulk analysis techniques</i>	114
3.3.4	FTIR spectroscopy	115
3.3.4.1	<i>Method</i>	115

3.3.4.2	<i>Assessment of FTIR for the analysis of wood</i>	115
3.3.4.3	<i>Conclusions of FTIR for the analysis of wood</i>	119
3.3.5	Py-GC.....	119
3.3.5.1	<i>Method</i>	120
3.3.5.2	<i>Assessment of py- GC technique</i>	121
3.3.5.3	<i>Conclusions of py-GC analysis of wood</i>	124
3.3.6	Microscopic techniques	125
3.3.6.1	<i>Methodology</i>	125
3.3.6.2	<i>Assessment of techniques</i>	125
3.3.7	Conclusions on wood analysis methods	127
3.4	Summary of methods	129
4	Chapter 4 – Lab-based experiments	130
4.1	Introduction	131
4.2	Experimental	133
4.2.1	Materials	133
4.2.1.1	<i>Bone</i>	133
4.2.1.2	<i>Wood</i>	133
4.2.2	Method.....	134
4.2.3	Analysis of bone deterioration.....	135
4.2.3.1	<i>Bulk assessment</i>	135
4.2.3.2	<i>Chemical analysis</i>	135
1.1.1	Analysis of wood deterioration.....	136
1.1.1.1	<i>Bulk assessment</i>	136
1.1.1.2	<i>Chemical analysis</i>	136
4.3	Investigation into bone deterioration	137
4.3.1	Results: Bulk analysis	137
4.3.2	Results: Microscopy	139

4.3.2.1	SEM	139
4.3.2.2	TEM	140
4.3.3	Results: Chemical analysis.....	141
4.3.3.1	Powder X-ray diffraction (p-XRD).....	141
4.3.3.2	Amino acid racemisation analysis.....	144
4.3.4	Discussion.....	148
4.4	Investigation into wood deterioration	150
4.4.1	Results: Bulk assessment	150
4.4.2	Results: Microscopy (SEM).....	154
4.4.3	Results: Chemical analysis.....	156
4.4.3.1	FTIR spectroscopy.....	156
4.4.3.2	Py-GC.....	160
4.4.4	Discussion.....	162
4.5	Conclusions.....	164
Chapter 5	– Microcosm experiments.....	166
5.1	Introduction.....	167
5.2	Experimental	169
5.2.1	Method.....	169
5.2.1.1	Experimental set up.....	169
5.2.1.2	Sediment types.....	170
5.2.1.3	Analysis	173
5.2.2	Materials	173
5.2.2.1	Bone (3 modern, 2 archaeological).....	173
5.2.2.2	Wood (3 modern, 2 archaeological).....	173
5.3	Results and discussion.....	175
5.3.1	Sediment analysis.....	175
5.3.1.1	pH and redox analysis	175

5.3.2	Bone analysis.....	176
5.3.2.1	<i>Mass loss and visual analysis</i>	176
5.3.2.2	<i>Amino acid analysis</i>	179
5.3.2.3	<i>Powder X-ray diffraction</i>	181
5.3.2.4	<i>Microscopy</i>	184
5.3.2.5	<i>Summary of bone analysis</i>	185
5.3.3	Wood analysis.....	186
5.3.3.1	<i>Mass loss and visual analysis</i>	186
5.3.3.2	<i>FTIR spectroscopy</i>	188
5.3.3.3	<i>Py-GC</i>	191
5.3.3.4	<i>Microscopy</i>	193
5.3.3.5	<i>Summary of wood analysis</i>	194
5.4	Discussion and conclusions.....	195
Chapter 6 – In situ burial experiments		197
6.1	Introduction.....	198
6.2	Experimental	200
6.2.1	Materials.....	200
6.2.1.1	<i>Pilot study</i>	200
6.2.1.2	<i>Main study</i>	200
6.2.2	Burial locations.....	201
6.2.2.1	<i>SC29</i>	201
6.2.2.2	<i>Flixton Island</i>	201
6.2.3	Method.....	203
6.2.3.1	<i>Burial</i>	203
6.2.3.2	<i>Excavation</i>	204
6.2.3.3	<i>Analysis</i>	204
6.3	Results and discussion.....	205

6.3.1	Sediment analysis.....	205
6.3.1.1	<i>pH and redox analysis</i>	205
6.3.1.2	<i>Sulfur content analysis</i>	207
6.3.2	Bone analysis.....	208
6.3.2.1	<i>Pilot study in SC29</i>	208
6.3.2.2	<i>Main Study</i>	214
6.3.2.3	<i>Discussion</i>	220
6.3.3	Wood analysis	221
6.3.3.1	<i>Main study</i>	221
6.3.3.2	<i>Discussion</i>	227
6.4	Discussion and conclusions.....	228
Chapter 7 –Analysis of archaeological material.....		230
7.1	Introduction.....	231
7.2	Materials and burial locations	233
7.2.1	Bone from Star Carr	233
7.2.1.1	<i>Early excavations</i>	233
7.2.1.2	<i>2007/2008 excavations</i>	233
7.2.1.3	<i>2010 excavations</i>	233
7.2.1.4	<i>2013 excavations</i>	234
7.2.2	Comparative material (bone).....	234
7.2.3	Wood from Star Carr.....	237
7.2.3.1	<i>Early excavations</i>	237
7.2.3.2	<i>2007/2008 excavations</i>	237
7.2.3.3	<i>2013 excavations</i>	237
7.2.4	Comparative material (wood).....	238
7.2.4.1	<i>Flag Fen (National Grid Reference: TL 22841 991144)</i>	238
7.2.4.2	<i>Must Farm boats (National Grid Reference: TL 235 968)</i>	238

7.3	Results and discussion: Bone	242
7.3.1	A review of previous analysis.....	242
7.3.2	Further analysis.....	243
7.3.2.1	<i>Visual analysis</i>	243
7.3.2.2	<i>AAR analysis</i>	247
7.3.2.3	<i>Powder X-ray diffraction</i>	252
7.3.2.4	<i>Microscopy</i>	255
7.3.2.5	<i>Summary of bone analysis</i>	258
7.4	Results and discussion: Wood	259
7.4.1	A review of previous analysis.....	259
7.4.2	Further analysis.....	259
7.4.2.1	<i>Visual analysis</i>	259
7.4.2.2	<i>Surface pH analysis</i>	260
7.4.2.3	<i>Maximum water content (u_{max})</i>	261
7.4.2.4	<i>FTIR spectroscopy</i>	263
7.4.2.5	<i>Py-GC</i>	266
7.4.2.6	<i>Microscopy</i>	269
7.4.2.7	<i>Summary of wood analysis</i>	272
7.5	Discussion and conclusions	273
Chapter 8 – Conclusions and future work		275
8.1	Overall conclusions	276
8.2	Impact for Star Carr	278
8.2.1	Diagenesis of archaeological material.....	278
8.2.2	Site management.....	279
8.3	Future work	280
8.3.1	Method development.....	280
8.3.2	Biological assessment.....	280

8.3.3	Application to other wetland archaeological sites	281
8.3.4	Extended burial experiments	281
List of abbreviations		282
References.....		283

LIST OF FIGURES

Figure 1.1: Organic finds excavated from Star Carr. From left to right: an expanse of worked wood during excavations in 1952; a red deer antler barbed point uncovered during most recent excavations; an example of the iconic 'antler frontlets,' uncovered in 1952. Images reproduced with permission from Scarborough Archaeological and Historical society and 'Postglacial' project, University of York. (Originally in colour).	31
Figure 1.2: Location of Star Carr (yellow circle) in the Vale of Pickering, on the edge of prehistoric Lake Flixton. Red circles indicate the location of other Mesolithic sites around the lake (reproduced with permission from Milner, 2011b). (Originally in colour).....	33
Figure 1.3: Schematic of main trenches excavated during the three excavation phases at Star Carr. Trench SC34 was excavated in 2013 and discussed in further detail in Chapter 7. (Originally in colour).....	34
Figure 1.4: Plot of Clark's original excavation showing the location of barbed point finds. Those classified by Clark as 'firm' are shown in red and those classified as 'soft' shown in blue. Figure adapted from Clark (1954). (Originally in colour).	35
Figure 1.5: Image of the excavation of Cutting 2, taken from Clark (1954), compared to a reconstruction of the scene taken during re-excavation of the trench in 2010. The extent of the peat shrinkage is evident from the much smaller distance between the base of the trench and the ground surface in the later excavations. (Originally in colour).	38
Figure 1.6: Schematic illustrating the structure of bone on various hierarchical levels. Adapted from Rho et al. (1998) and Orgel et al. (2001). (Originally in colour).	40
Figure 1.7: Schematic showing the hierarchical structure of wood. Major sub units for lignin (red) and celluloses (blue) are indicated. (Adapted from Jane et al., 1970 and Hoffman & Jones, 1990). (Originally in colour).	46
Figure 1.8: Scheme showing how demethoxylation by fungal activity creates higher concentrations of phenol type sub-units in lignin.	47
Figure 2.1: Geological map of the Vale of Pickering, showing Star Carr located on alluvium bedrock. Inset shows detail of the site, bordered by the Hertford cut to the north and field drains to the east and west. Adapted from Brown et al. (2011).	67
Figure 2.2: Diagram showing the extent of the geochemical survey carried out in 2009 (top). Detailed stratigraphy through a transect of the site illustrates the local variability of the	

sediments underlying the archaeological deposits (bottom). Reproduced with permission from Boreham et al. (2011).(Originally in colour).	69
Figure 2.3: Plot of measured pH values of the transect illustrated in Figure 2.2, showing the variability in pH across the site; pH is lower directly above clay outcrops. Reproduced with permission from Boreham et al. (2011).(Originally in colour).	71
Figure 2.4: Schematic showing how column samples were taken into the virgin sediment from the trench face. In SC34 this trench face was newly exposed, whereas in VP85 the trench had been re-excavated, following previous excavation in 1985. The base of each trench represents the start of the archaeological zone (100 cm for SC34; 60 cm for VP85). (Originally in colour).	77
Figure 2.5: Plot of pH values measured across surface of SC34. Locations of column samples are indicated by a blue box, and black-outlined circles represent samples taken in association with organic artefacts. (Originally in colour).	80
Figure 2.6: Location of dipwells (indicated by circles) around the Star Carr site, along with the depth of the dipwells. Reproduced with permission from Bradley et al. (2012).	82
Figure 2.7: Proposed mechanisms of changes in acidity and redox potential upon exposure to oxygen. (Originally in colour).	85
Figure 2.8: Schematic illustrating a proposed mechanism of sulfuric acid formation due to alteration of the water-table. (Originally in colour).	87
Figure 3.1: Measured pH of solutions during the method development experiment, demonstrating that bone has a large capacity to buffer surrounding acidity. At each sampling point the solutions were readjusted to the starting pHs. The lines showing the increase in pH between the measured points are therefore indicative only as buffering is likely to have occurred more rapidly (Margolis & Moreno, 1992). (Originally in colour).....	93
Figure 3.2: Total amino acid concentrations (left) and Asx racemisation (right) in solution samples treated in 6 and 7 M HCl for a range of hydrolysis times. Alterations in concentration lie within the error (standard deviation calculated from two replicates of each sample) whilst Asx racemisation slightly increases with increased hydrolysis times. (Originally in colour).	96
Figure 3.3: Comparison of the three different sub-samples for the method development experiments: total amino acid content (left) and Asx racemisation (right). Error bars for the concentrations are one standard deviation derived from measurement of three replicates of a modern sheep long bone (0.32 mmol/ mg). Error bars for Asx racemisation are negligible. (Originally in colour).....	97

Figure 3.4: Total amino acid concentrations (left) and Asx racemisation (right) in solution over the course of the reaction period. Error bars are one standard deviation calculated from three replicate analyses of a sample. (Originally in colour).	98
Figure 3.5: Comparison of diffraction patterns for hand-milled vs freeze-milled sample excavated from Star Carr in 2008 (sample 92105). (Originally in colour).	101
Figure 3.6: Comparison of diffraction patterns for samples from the MDE. The position of the diffraction peaks in pure HA, determined by analysis of a commercially purchased standard, are marked with dashed lines. (Originally in colour).	102
Figure 3.7: Comparison of diffraction pattern for archaeological bones with modern fresh bone, showing no major alteration of diffraction patterns. Dashed lines indicate the position of diffraction peaks for pure HA, determined by analysis of a commercially purchased standard. (Originally in colour).....	103
Figure 3.8: Raman spectra obtained from MDE bone samples treated at pH 2 (top) and pH 3 (bottom), showing peaks characteristic of both HA and collagen, although no difference is observed between the two samples. (Originally in colour).....	105
Figure 3.9: Comparison of FTIR spectra for the four MDE samples. Key peaks relating to bone mineral and collagen are indicated, labelled according to Reiche et al. (2010). (Originally in colour).....	106
Figure 3.10: Comparison of FTIR spectra obtained from a sample excavated from Star Carr with an untreated modern bone and demineralised bone (collagen). (Originally in colour).....	107
Figure 3.11: Comparison of images obtained using light microscopy with a cross-polarised light source (top) and SEM (bottom), for bones treated in water and at pH 2.	110
Figure 3.12: TEM images of collagen from a modern cow bone (left) and a sample excavated in 2010 from Star Carr (right).....	111
Figure 3.13: FTIR spectra for the four MDE wood samples, showing calculation of peak heights from the four key absorption peaks (following the protocol of Gelbrich et al., 2008). (Originally in colour).	116
Figure 3.14: Comparison of ratios derived from FTIR peak heights for the four MDE wood samples. Error bars represent 1 standard deviation of three repeat readings for each sample. (Originally in colour).....	117
Figure 3.31: Comparison of FTIR spectra for untreated modern wood (bottom) and the wood sample excavated from Star Carr (top). (Originally in colour).	118

Figure 3.32: Ratios calculated for a series of archaeological samples compared to a modern birch sample. (Originally in colour).....	118
Figure 3.17: py-GC traces for MDE wood samples treated in pH 2 and pH 7 acid. Labelled peaks were identified by analysis of purchased standards, shown in Table 3.1. (Originally in colour).	122
Figure 3.18: Peak areas of phenol corrected for mass (left) and P: G peak area ratios (right) for the four MDE samples preliminary samples compared to an untreated birch sample. Error bars are one standard deviation calculated from replicate analysis of the each sample. (Originally in colour).....	123
Figure 3.19: Comparison of py-GC traces between the MDE sample at pH 7 and an archaeological sample from Star Carr. Degradation of both lignin and cellulose is indicated in the archaeological sample by an increased intensity of the phenol peak (P) and a decreased intensity of other lignin components, labelled according to Table 3.1. (Originally in colour).	124
Figure 3.20: SEM images of wood samples treated at pH 2 (left) and pH 3 (right). Wood structure is clearly observed under SEM, and no damage is seen in either sample.	126
Figure 4.1: Measured pH for dynamic conditions at room temperature for all bone samples. Data is shown for the pH 1 experiment (bottom) and pH 3 experiment (top) for 6 weeks. Buffering continues at similar levels for the duration of the 16 week experiments. (Originally in colour).	137
Figure 4.2 (Left to right): long bone A starting material; long bone A, pH1, 80°C, D after 3 days; long bone A, pH 1, RT, D after 6 weeks; long bone B, pH 1, RT, D after 6 weeks, illustrating differences between disintegrated, chalky and translucent samples. (Originally in colour). ..	138
Figure 4.3: SEM images of bone at 400 x magnification. Left: untreated bone; Centre: long bone B treated at pH3, RT, D; Right: long bone B treated at pH 1, RT, D (inset, zoomed in section – scale bar reads 2 µm).	140
Figure 4.4: Images obtained using TEM of long bone A sample treated in pH 2, RT under dynamic conditions (left) compared to a modern sample (right).	141
Figure 4.5: Example p-XRD patterns, illustrated by long bone A samples treated at 80°C at various pHs compared to an untreated modern bone (bottom), which displays the characteristic broad peaks of HA in fresh bone. Vertical lines indicate the positions of peaks characteristic of pure HA (dashed lines) and gypsum (dotted lines). (Originally in colour).	142

Figure 4.6: A and B show SEM images of gypsum rosette formation in different stages, reproduced with permission from Shih et al. (2005). Crystals pictured are in the 400-700 μm range. Image C is an SEM image of a crystal in the solution removed after 1 day from a bone sample displaying the X-ray diffraction pattern characteristic of gypsum (pH1, 80°C, D).	143
Figure 4.7: Total amino acid concentrations in all 4 bones under D conditions at RT and 80°C at 6 weeks. Water is given the description pH 7. Error bars are one standard deviation calculated from replicate analysis. (Originally in colour).	144
Figure 4.8: Aspartic acid (Asx; left) and serine (Ser; right) racemisation at 80°C, D for all 4 bone types after 6 weeks. Outlined data points represent samples which were removed early. Samples under dynamic conditions showed similar trends. Error bars were negligible and therefore not shown. (Originally in colour).	145
Figure 4.9: Aliquot solution amino acid concentrations over 6 week reaction period for all bone samples at 80°C for pH 3 and pH 1. (Originally in colour).	146
Figure 4.10: Racemisation values of Asx in solution at each sampling point during the experiment for modern rib and long bone A samples under dynamic conditions (the whole solution is replaced following each sampling point). Other bones show similar trends, with a slight increase in racemisation over time. (Originally in colour).	147
Figure 4.11: Schematic showing the proposed degradation mechanism of bone in different strength sulfuric acid solutions. (Originally in colour).	149
Figure 4.12: Measured pH for D conditions at 80°C for all 4 wood samples at pH 1(bottom) and pH 3 (top). A similar trend continues for the 16 week experiments. (Originally in colour).	150
Figure 4.13: Images showing the darkening occurring in samples of birch (left) and willow (right) after 3 and 42 days at pH 1, 80°C and D conditions. (Originally in colour).....	151
Figure 4.14: SEM images of modern willow and birch prior to the experiment (top) and after treatment for 16 weeks at pH 1 at 80°C, D conditions (bottom).....	155
Figure 4.15: FTIR spectra for birch samples treated at different pH at 80°C and under “D” conditions. Little difference is seen between spectra; this is illustrative of all samples treated for 6 weeks. (Originally in colour).....	156
Figure 4.16: Key ratios determined as markers of degradation for birch samples treated at 80°C for 6 weeks. An increase in L: C and 1507: C ratios is indicative of cellulose loss, and an increase in the 1507: 1240 ratio is indicative of lignin defunctionalisation. (Originally in colour).....	157

Figure 4.17: FTIR spectra of willow and birch following 16 weeks treatment in pH 1 sulfuric acid at 80°C, D conditions. (Originally in colour).....	158
Figure 4.18: Comparison of FTIR spectra for willow treated at 80°C in pH 1 sulfuric acid for 16 weeks with wood from Star Carr and Must Farm, illustrating the similarities observed between the archaeological materials. (Originally in colour).....	159
Figure 4.19: py-GC chromatograms for birch samples treated in various strength sulfuric acid solutions for 6 weeks at 80°C, D conditions. (Originally in colour).....	160
Figure 4.20: Comparison of py-GC traces for birch sample treated for 6 (top) and 16 (bottom) weeks in pH 1 sulfuric acid at, 80°C, D conditions. (Originally in colour).	161
Figure 4.21: Comparison of py-GC traces for archaeological starting material; Star Carr (top) and Must Farm (bottom). (Originally in colour).....	162
Figure 5.1: Schematic of the initial microcosm set up. Additional containers were also later set up.	169
Figure 5.2: Photos of materials laid out in the microcosms, showing the dipwells in the centre and the material spaced around the edge(left), and the outside of the microcosms (right). (Originally in colour).....	170
Figure 5.3: Image of buried bones before (top) and after burial in zone C2 (centre) and B2 (bottom). Note that C2 modern 'jellybone' is pictured after sub-sampling for analysis, and was in fact retrieved intact. (Originally in colour).....	177
Figure 5.4: Comparison of total amino acid concentrations in buried material compared to the starting material (left) and Asx racemisation in the same samples (right). (Originally in colour).	179
Figure 5.5: Comparison of total amino acid concentration (left) and Asx racemisation (right) in all bone samples excavated from microcosm C compared to the starting material. Error bars are calculated as the standard deviation of replicate measurements, except for the starting material where the error calculated in Chapter 3 is applied. (Originally in colour).	181
Figure 5.6: Comparison of diffraction patterns for the modern long bone and Star Carr rib samples from zone A2, where no alteration is seen (note that a small shoulder on the HA peak in the Star Carr rib pattern was present prior to burial), compared to the distinctive gypsum diffraction pattern in the modern long bone sample from zone C1. All analysed samples from zones C1, C2 and C3 displayed this pattern. (Originally in colour).	183

Figure 5.7: SEM image of modern long bone excavated from zone C3 (left), compared to untreated long bone (right).	184
Figure 5.8: Images of wood material before burial (top) compared to burial in zone A2 (centre) and C3 (bottom). (Originally in colour).	186
Figure 5.9: Comparison of FTIR spectra from untreated willow (bottom) and willow samples buried in zones A1 and C1. Note the complete loss of the methoxy signal at 1240 cm^{-1} in zone C1, although small cellulose peaks remain at 1325 and 1375 cm^{-1} . (Originally in colour).	189
Figure 5.10: Plot of peak height ratios indicating degradation parameters for willow samples excavated from zones A1, B1 and C1 compared to an untreated willow sample. Error bars are the standard deviation of three measurements of a modern willow sample. An increase in Lignin: Cellulose and 1507 : cellulose ratios is indicative of cellulose loss, and an increase in 1507 : 1240 ratio suggests lignin defunctionalisation. (Originally in colour).	190
Figure 5.11: Py-GC traces from all four zone C (Star Carr) willow samples, showing extensive degradation of all samples in damp or wet zones. (Originally in colour).	191
Figure 5.12: Comparison of py-GC traces for willow samples recovered from zones A1, B1 and C4. (Originally in colour).	192
Figure 5.13: SEM images of wood samples retrieved from microcosm C. Oak from zone 1 shows potential degradation of the inner cell walls (left) and Must Farm wood from zone 2 shows evidence for fungal activity (right).	193
Figure 6.1: Map showing approximate geographical location of both burial sites in relation to Star Carr. National Grid locations are shown. (Originally in colour).	202
Figure 6.2: Photographs of material buried during the pilot study at varying depths in SC29 (left) and at two levels at Flixton Island for the 12 month study (right). Note the water-table visible at the base of SC29. Depths are approximate. (Originally in colour).	203
Figure 6.3: Schematic showing location of samples buried for the 12 month study at SC29 (left) and Flixton Island (right). pH values recorded at time of burial are indicated. (Originally in colour).	204
Figure 6.4: Photographs of six samples retrieved from pilot study in 2007 after approximately 5 years burial. (Originally in colour).	209
Figure 6.5: Comparison of total amino acid content for all excavated bones, compared to a modern cooked chicken leg bone (left) and Asx racemisation values in all excavated bones	

(right). Error bars are one standard deviation calculated from replicate analysis. (Originally in colour).....	210
Figure 6.6: p-XRD patterns for all 3 samples retrieved from column A. The sharp peak at 28.5 °2θ is probably due to a quartz impurity (e.g. Person et al., 1995). (Originally in colour).....	211
Figure 6.7: SEM images of bone excavated from the pilot study in SC29, showing cortical bone (left) which is similar in appearance to bone treated in acid (Chapter 4). The more porous network of trabecular bone (right) makes it more difficult to observe damage.....	212
Figure 6.8: Features observed by SEM analysis of bone samples from SC29 which could be evidence for fungal activity (left). In other samples, fibres bear some resemblance to collagen fibrils (right) (Fantner et al., 2004).....	213
Figure 6.9: Images of the starting material (top) compared to after burial for 12 months at different locations. Orange deposits can be seen on the surface of bones from SC29, and the difference between material buried at 30 cm and 92 cm at SC29 is demonstrated by comparison of the cooked pig tibia (left). ‘Jellybones’ underwent discoloration and distortion at all burial locations (centre). (Originally in colour).	214
Figure 6.10: Total amino acid concentration (top) and Asx racemisation (bottom) in all excavated samples compared to the starting material. Error bars represent one standard deviation calculated from replicate analysis. (Originally in colour).....	216
Figure 6.11: p-XRD patterns for the pig rib excavated from Test pit SC29 at all depths compared to an untreated cooked pig rib, showing no alteration of the HA. (Originally in colour).	218
Figure 6.12: SEM images of pig ribs from SC29 (top) and Flixton Island (bottom) after 12 months. Different magnifications are used to highlight certain features, including crystals adhering to the bone surface (top left) and possible fungal activity (bottom right).....	219
Figure 6.13: Willow samples after 12 months at all burial locations, compared to the starting material, showing little alteration apart from some slight discoloration and some orange staining in the sample from SC29, 50 cm. (Originally in colour).....	221
Figure 6.14: Comparison of several indicators of degradation for willow samples from the 12 month burial experiment, compared to the Star Carr wood used in the experiments and an untreated willow sample. An increase in L: C and 1507: C ratios indicate an increase in cellulose loss, and an increase in the 1507: 1240 ratio is indicative of lignin defunctionalisation. (Originally in colour).....	223

Figure 6.15: Comparison of FTIR spectra of the birch samples excavated from Flixton Island, 60 cm where mould was present (bottom) and the bulk of the sample, showing loss of the phenol absorption.....	224
Figure 6.16: py-GC chromatograms for willow samples from Flixton Island, 60 cm and SC29, 30 cm.....	225
Figure 6.17: SEM images of wood samples excavated at both site, illustrating the extent of fungal activity.....	226
Figure 7.1: Location of all analysed bone samples from the 2013 excavations at Star Carr. (Originally in colour).....	236
Figure 7.2: Illustration of where samples from stake D00128 were taken (not drawn to scale).	238
Figure 7.3: Location of all analysed wood samples from most recent excavations (2013) at Star Carr. (Originally in colour).....	241
Figure 7.4: 2007 'jellybone' sample showing its flexibility, probably due to extensive demineralisation (reproduced with permission from Milner et al., 2011a). (Originally in colour).	242
Figure 7.5: Bone retrieved from the spoil heap in 1948 (top left) and bones held in the British Museum collection from original excavations at Star Carr. Site locations are unknown. Many were observed to be robust (bottom), but some bones show advanced degradation, with chalky deposits and severe cracking (top right). (Originally in colour).....	244
Figure 7.6: Chalky and brittle bone fragments, typical of all those found located in the dryland part of the site in 2007 and 2008. (Originally in colour).....	244
Figure 7.7: Bone excavated in 2010, showing splitting of rib bones (top), and a flaky surface on scapula (bottom left). Orange deposits formed post excavation. The 'jellybone' samples from SC33 (bottom right) are much darker in colour, and bendable. (Originally in colour).....	245
Figure 7.8: Examples of bones recovered in 2013, showing grey concretions adhering to the surface (top), white chalky deposits in the centre of the bones (bottom left) and translucent 'jelly' on the surface (bottom right). (Originally in colour).	246
Figure 7.9: Total amino acid concentrations (left) and Asx racemisation (right) measured in a number of samples excavated from Star Carr compared to a fresh untreated bone ('reference'). Those samples categorised as 'jellybone' following visual analysis are indicated. Full sample details are shown in Table 7.1. (Originally in colour).	247

Figure 7.10: Comparison of total amino acid content (left) and Asx racemisation (right) for inner and outer sub samples for a number of samples from 2010 excavations. Those bones identified as 'jellybone' are outlined in red (samples 92753 and 92811). (Originally in colour).	249
Figure 7.11: Total amino acid concentrations (left) and Asx racemisation (right) for bones excavated from Star Carr in 2013. Where known, the adjacent sediments pH is indicated, or estimated based on nearby sediments pH (in brackets). Where relevant, values for the jelly-like (J), chalky deposits (Ch) and firm (F) parts of the bone are shown. (Originally in colour).	251
Figure 7.12: Diffraction patterns for a number of Star Carr samples, compared to an untreated modern bone sample. Patterns have been classified according to as outlined in Chapter 4 (Section 4.3.3.1). (Originally in colour).	253
Figure 7.13: Diffraction pattern of the white powder present in several of the 2013 bones. Dotted lines indicate the typical position of peaks in pure gypsum (calcium sulfate).	254
Figure 7.14: SEM images of 'robust' rib bone excavated from the backfill of Cutting 2 in 2010; cracking is likely to be due to compression (top), compared to the chalky, brittle bones excavated from the dryland areas of the site (bottom).	255
Figure 7.15: SEM images of 'jellybone' samples excavated in 2010 (top left) and 2013 (top right and bottom left), showing extensive fungal network. Comparison is made to an image taken from Fantner et al. (2004).	256
Figure 7.16: Optical microscopy images of thin-sections of a 'robust' rib bone (left) compared to a 'jellybone' from the 2010 excavations (right). (Originally in colour).	257
Figure 7.17: Images of Must Farm log boat 1, and detail on log boat 3 (right), showing the excellent condition of the boat.	260
Figure 7.18: FTIR spectra for two samples from Star Carr compared to a fresh willow sample and a log boat from Must Farm. Important features are a reduction in the relative height of the cellulose peaks and splitting of the peak at 1240 cm^{-1} in archaeological samples (circled). These changes are slightly more significant in samples from Star Carr than the Must Farm boat. (Originally in colour).	263
Figure 7.19: Plot of ratios derived from FTIR analysis of samples from Star Carr (green), Flag Fen (blue) and Must Farm (red) compared to a willow standard. Error bars are one standard deviation of 3 readings from the willow standard. An increase in the L: C and 1507: Total	

Cellulose (TC) peaks indicates loss of cellulose, and an increase in the 1507: 1240 peak indicates lignin defunctionalisation. (Originally in colour).	264
Figure 7.20: Samples from Star Carr 2007 excavations that had been stored for several years prior to analysis, compared to an untreated willow sample. Cellulose is indicated to have completely depleted, and loss of the 1240 cm^{-1} peak indicates extensive defunctionalisation of the lignin. (Originally in colour).....	266
Figure 7.21: py-GC traces for 2 samples from Trench SC34 excavated in 2013 compared to a log boat excavated from the Bronze Age site of Must Farm (note that this sample was analysed using a longer GC column and as a result the peaks have slightly shifted). Whilst cellulose peaks are present, these are small, and an increase in the intensity of the phenol peak (indicated with an arrow for each sample) suggests lignin defunctionalisation. (Originally in colour). ...	267
Figure 7.22: Comparison of corrected peak areas for phenol in a number of samples excavated from Star Carr in 2013 compared to an untreated willow sample and two of the Must Farm log boats. (Originally in colour).....	268
Figure 7.23: py-GC chromatogram for sample excavated from Star Carr in 2007 and stored for four years prior to analysis, compared to a fresh modern willow sample. Very few peaks relating to lignin sub units remain in the Star Carr sample. (Originally in colour).	269
Figure 7.24: SEM images of archaeological wood compared to modern material (top left), showing the difference between the thick, cellulose-rich cell walls in undecayed wood compared to the lignin skeleton seen in wood from Star Carr. Cell collapse does however seem less extensive in the sample excavated in 2013 compared to 2007.	270

LIST OF TABLES

Table 2.1: pH recorded in the field and after 24 hours, and redox measurements for samples measured vertically down an exposed trench (Figure 2.4). Red values indicate where the pH decreased by more than 0.1 pH units after 24 hours.	78
Table 2.2: Geochemical data for soil samples taken from surface of excavated Trench SC34 in 2013. An asterisk indicates samples that were also analysed for sulfur content. When pH changed by more than 0.1 pH unit after 24 hours this is indicated by red for a negative change and blue for a positive change.	79
Table 2.3: Result of elemental analysis on selected sediment samples.	81
Table 2.4: pH values of selected groundwater samples analysed on four occasions from 2011-2012. Where no value is given, the dipwell was dry.	83
Table 3.1: Approximate retention times in applied GC method for important lignin related compounds.	121
Table 3.2: Summary of all analytical techniques targeted for the analysis of organic materials throughout the rest of the thesis. The rationale for each technique has been previously detailed.	128
Table 4.1: Summary of time points (in weeks) and planned experimental conditions for each bone type. Where samples had to be removed early due to rapid dissolution, the actual time point is shown in brackets.	134
Table 4.2: Summary of time points (in weeks) and experimental conditions for each wood type.	135
Table 4.3: Mass loss in bone after 6 weeks and 16 weeks (in brackets) where relevant. Mass loss is presented as a percentage of the starting mass.	139
Table 4.4: Summary of samples treated for analysis by TEM.	140
Table 4.5: Summary of changes to the p-XRD pattern for all analysed bones after 6 weeks, with characterisation after 16 weeks in brackets.	143
Table 4.6: Mass loss in wood after 6 weeks and 16 weeks (in brackets) where relevant. Mass loss is presented as a percentage of the starting mass.	152
Table 4.7: Maximum water content as a percentage of the end mass for all wood samples after 6 and 16 (in brackets) weeks.	153

Table 5.1: Summary of all conditions, or zones.	171
Table 5.2: Summary of geochemical data for each of the 10 experimental zones. Where data was not recorded, the box is left blank.	175
Table 5.3: Mass loss data for all bones from each of the 10 microcosm zones. No Tanner Row bone was buried in environment C4.....	178
Table 5.4: Summary of p-XRD patterns for all analysed bone sample, characterised according to classifications defined in Chapter 4 (section 4.3.3.1).	182
Table 5.5: Mass loss data for all wood samples from each of the 10 microcosm zones.	187
Table 6.1: Measured pH and redox values at both burial locations.	205
Table 6.2: Percentage values of sulfur and carbon in sediment samples from varying depths at Flixton Island and Test pit SC29.	207
Table 6.3: Visual analysis of samples retrieved from Test pit SC29 after five years burial.	208
Table 6.4: Mass loss in samples buried for 12 months in Test pit SC29 and Flixton Island site 2.	215
Table 6.5: Mass loss from wood samples buried for 12 months at both SC29 and Flixton Island site 2. Samples that were not recovered are indicated by a shaded box, and where there was no sample to begin with, this is indicated by a line through the box.	222
Table 7.1: Summary of all bone samples analysed from Star Carr. Where the species is known this is listed.	235
Table 7.2: Summary of all wood samples analysed from Star Carr. Where the wood species is known, this is listed.....	239
Table 7.3: Summary of all wood samples analysed for comparison.....	240
Table 7.4: Summary of p-XRD patterns for analysed bones from Star Carr, described according to classifications defined in Chapter 4 (Section 4.3.3.1).....	252
Table 7.5: pH measured from the water in which wood samples were stored or the surface of the sample where this was not possible.....	261
Table 7.6: u_{max} data for a number of samples from Star Car as well as comparative material from Flag Fen and the Must Farm log boats (provided by Ian Panter).....	262

ACKNOWLEDGEMENTS

I would like to thank all of my supervisors; Kirsty Penkman for her constant guidance, enthusiasm and support, and Ian Panter and Nicky Milner for introducing me to the worlds of conservation and archaeology and being exceptional sources of knowledge and advice. Thanks also to Bea Demarchi for being such an excellent substitute supervisor for a short time, and to my examiners Brendan Keely and Jim Spriggs for such helpful comments and an enjoyable viva! I'm grateful to NERC and York Archaeological Trust for funding this studentship, and to everyone who laid the groundwork for my research, in particular Steve Boreham, Chris Bradley and Tony Brown for all of the geochemical data and for being happy to chat to me about it.

Thanks to the rest of the Penkman group past and present (Bea, Molly, Jo, Keira, John, Pete and Sheila) for being such a pleasure to work with, and always being ready with cake (or beer for John – well, only if I'm buying) when things aren't going well. Also thanks to the BJK group for being great office mates and providing the laughs when they're needed. The same goes for the various students who have joined us; in particular to Emily for braving the rain to help me collect soil samples, Lucy for being so enthusiastic even when I asked for help digging bits of bone out of buckets, and Becky for getting as excited as me when we saw how slimy the 2013 jellybones were. For proofreading, thanks to Jo, Adam, Robyn and Em.

Thanks to everyone who has ever excavated at Star Carr – without you I would have had nothing to analyse. Thanks in particular to Mike Bamforth, Barry Taylor and Becky Knight who have provided me with various photos and maps, and dug out the best samples for me! Thanks to all of the current team for making me feel so welcome when I turned up to my first archaeological excavation entirely out of my depth - I am privileged to have been able to work with you all at Star Carr, and a special mention must go to Ed Blinkhorn and Emily Hellewell for inspiring in me an enthusiasm for all things Mesolithic early on.

I'm indebted to a huge number of people for technical help: Meg Stark for SEM, Adrian Whitwood for p-XRD, Paul Elliot for FTIR, Hannah Koon for TEM, Matt Pickering and Adam Pinder for py-GC, Scott Hicks for EA, Yvette Hancock for Raman, and Anthony Crawshaw for his help with analysis of archaeological woods. Over the years I have also received much help from Sheila Taylor, Richard Allen and Matt Von-Tersch; thanks for putting up with huge amounts of soil in the labs!

For providing me with modern materials, thanks to M&K butchers, various friend who have selflessly eaten ribs for me, and my Dad for sacrificing his firewood supply. Harry, Barry, Emily,

Andy, Adam and Lucy have to take some of the credit for digging up my burial experiments; thanks to Andy Needham in particular for having the foresight 7 years ago to carry out the pilot study, having an incredible ability to remember the exact spot the samples were buried 6 years later, and always being happy to spend time with me talking about the work at Star Carr he did previously.

Finally, I would like to thank the people who have provided me with moral support; all of the other PhD students in the archaeology department who have made me love archaeology, Robyn, who has inadvertently made me love academia, and Adam for sharing your passion for lignin, science and a good gin martini. I can't thank my parents enough: for helping me move house a million times, their constant support, and for always telling me to be the best that I can be.

DECLARATION

I hereby certify that the work described in this thesis is my own, except where otherwise acknowledged, and has not been submitted previously for a degree at this, or any other, university.

Kirsty High

*“It’s a capital mistake to theorise before one has data.
Insensibly one begins to twist facts to suit theories,
instead of theories to suit facts”*

Sherlock Holmes

(Sir Arthur Conan Doyle)

CHAPTER 1

UNDERSTANDING ORGANIC DETERIORATION AT STAR CARR (INTRODUCTION)

1.1 Star Carr: The Stonehenge of the Mesolithic

1.1.1 Introduction

Star Carr is an archaeological site located in North Yorkshire (UK), dating from the early Mesolithic period (approximately 9300 - 8700 BC; Mellars & Dark, 1998). Its importance for the understanding of life in Northern Europe during this time cannot be understated. The wealth of organic remains uncovered during initial excavations between 1948 and 1952 is unrivalled for sites of this age in Britain (Figure 1.1, Clark, 1954). Most spectacular of the artefacts were 21 red deer antler frontlets and 191 well preserved barbed points carved from deer antler – the most barbed points that have ever been found at a single Mesolithic site in Europe. The large quantities of animal bone recovered from Star Carr have provided extensive evidence for dietary practises, with a wide range of animal bones displaying cut marks and deposition patterns indicative of butchering (Caulfield, 1978). In addition, artefactual evidence of bone being utilised for other uses has been uncovered in the form of several tools manufactured out of bone (Clark, 1954). An abundance of well-preserved worked wood was also found, including what was interpreted as a ‘brushwood platform’ extending into the lake, potentially providing a living or working area (Clark, 1954). Later excavations also revealed evidence for woodworking, including an extensive platform made from split timbers: evidence for the earliest carpentry in Northern Europe (Mellars & Dark, 1998). Most recently, in 2008 evidence for a timber structure was uncovered, quite possibly the oldest structure, or ‘house’ ever to be found in Britain (Milner *et al.*, 2013a).



Figure 1.1: Organic finds excavated from Star Carr. From left to right: an expanse of worked wood during excavations in 1952; a red deer antler barbed point uncovered during most recent excavations; an example of the iconic 'antler frontlets,' uncovered in 1952. Images reproduced with permission from Scarborough Archaeological and Historical society and 'Postglacial' project, University of York. (Originally in colour).

Interpretation of the Star Carr site and the wealth of organic evidence uncovered has contributed greatly to how archaeologists have thought about the Mesolithic period in Europe, and stimulated much academic analysis (e.g. Caulfield, 1978; Wheeler, 1978; Conneller, 2004; Lane & Schadla-Hall, 2004). No Mesolithic sites discovered in Britain since have yielded the range and quantity of organic remains found at Star Carr, thus cementing its reputation as a site as important as Stonehenge is to our understanding of life in the past (Milner *et al.*, 2013a).

However, recent excavations at the site have uncovered artefacts in an alarming state of diagenesis, suggesting that conditions may no longer be conducive to such excellent preservation of organic remains (Milner *et al.*, 2011a; Section 1.1.2.4). In particular, observations of high acidity (pH < 2; Boreham *et al.*, 2011) in 2009 raised concerns for the future of the site; the effects of such high acidity on organic remains (specifically bone, wood and antler) are not well understood. This lack of scientific data regarding the decay of organic materials severely limited the confidence with which appropriate mitigation strategies could be implemented at the site.

This study investigates current site conditions and correlates these with the observed organic deterioration in bone and wood. An informed assessment of the rapidity of organic degradation at the site has been made through experimental studies and analysis of archaeological material, with the eventual aim of recommending potential mitigation strategies. This research is applicable not only to Star Carr, but to other archaeological sites that are undergoing similar changes.

1.1.2 Archaeological excavation at Star Carr

1.1.2.1 Wider context

Star Carr is one of several archaeological sites located on the banks of Lake Flixton, a shallow prehistoric lake in the Vale of Pickering, North Yorkshire (National Grid Reference TA 02864 80976). The location of Star Carr in relation to a number of other sites is indicated in Figure 1.2 (reproduced from Milner *et al.*, 2011b). At the beginning of the Holocene (approximately 9,000 years BC) the lake became gradually filled in with marl and organic mud over thousands of years. The edges of the lake have been established by extensive auger surveys carried out by the Vale of Pickering Research Trust (Milner *et al.*, 2011b). The surrounding flora (birch woodland, along with dense reed beds and wetland flora at the edges of the lake) has formed a thick blanket of organic-rich peat covering the muds and underlying gravels (Milner *et al.*, 2011a; 2011b; 2013a). Archaeological material has been uncovered from areas of the site that

were dry during the Mesolithic (dryland) as well as areas that extend into the edge of the lake (wetland) (Milner *et al.*, 2013a).

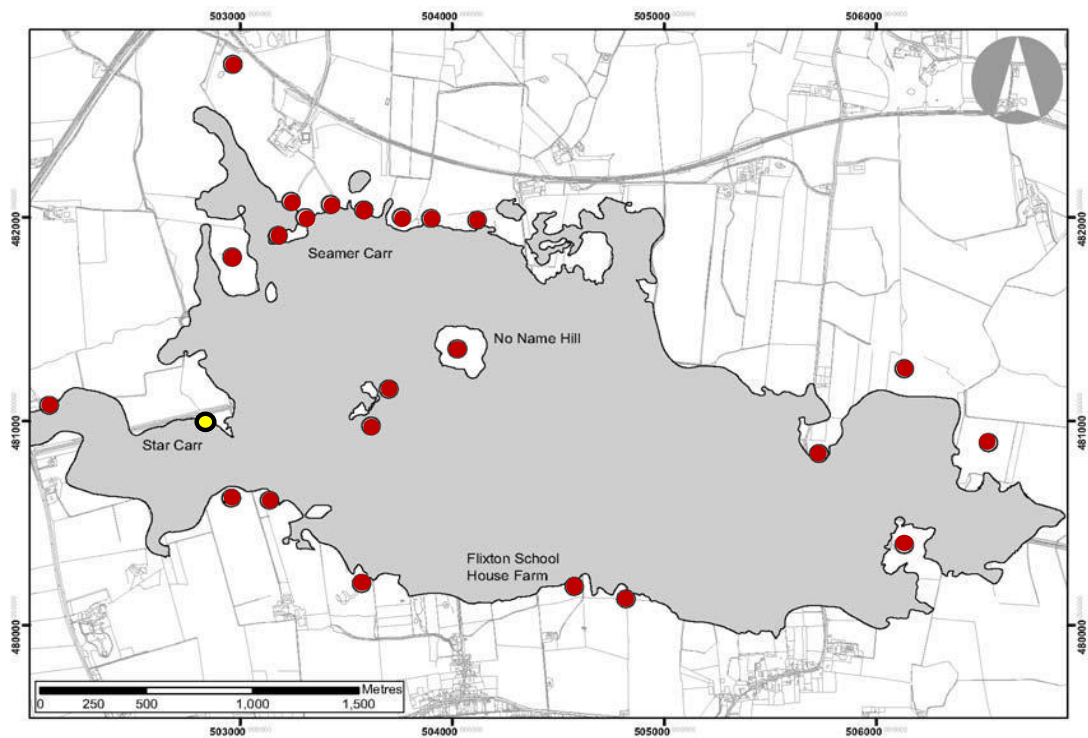


Figure 1.2: Location of Star Carr (yellow circle) in the Vale of Pickering, on the edge of prehistoric Lake Flixtan. Red circles indicate the location of other Mesolithic sites around the lake (reproduced with permission from Milner, 2011b). (Originally in colour).

Archaeological excavations have taken place at Star Carr in a number of phases since its discovery in 1948. Major trenches excavated over the 65-year period are illustrated in Figure 1.3 and described in further detail below.

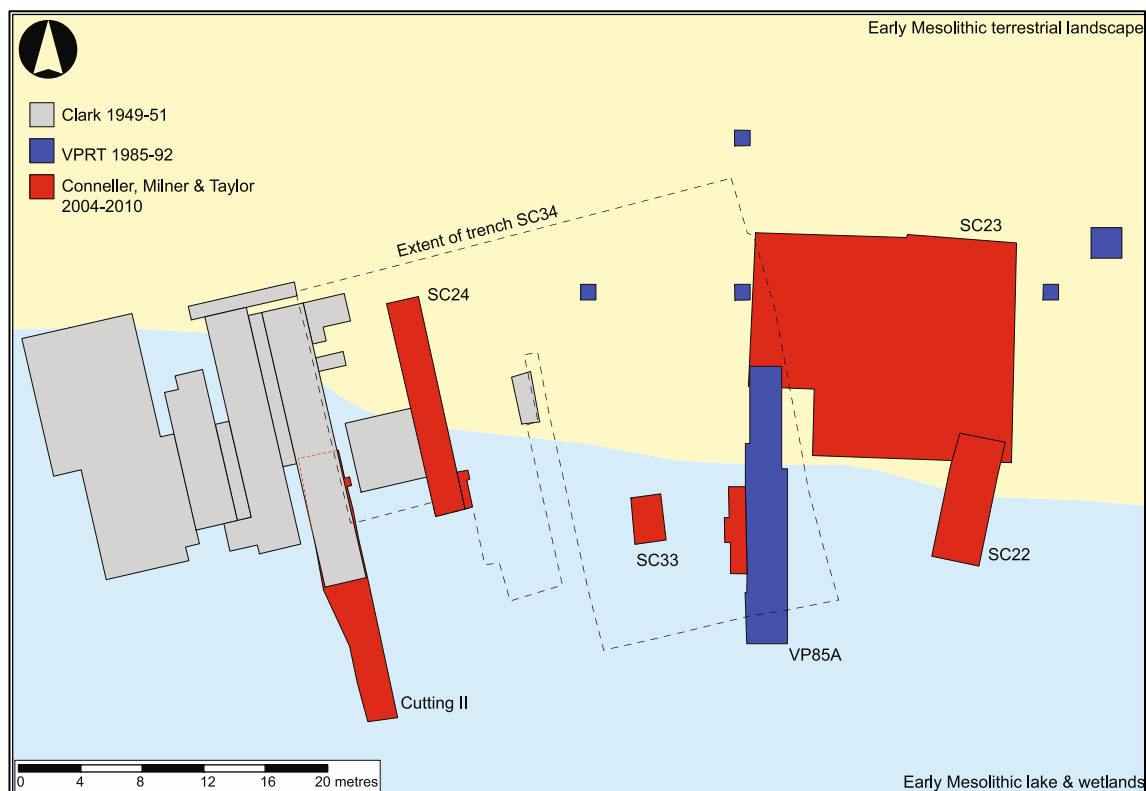


Figure 1.3: Schematic of main trenches excavated during the three excavation phases at Star Carr. Trench SC34 was excavated in 2013 and discussed in further detail in Chapter 7. (Originally in colour).

1.1.2.2 Early excavations

Star Carr was discovered by local archaeologist John Moore in the 1940s, although the first large scale excavations were carried out between 1949 and 1952 and led by Graham Clark (Clark, 1954). The excavations spanned a large area incorporating both wetland and dryland contexts (Figure 1.3, grey coloured trenches).

A large array of birch branches were excavated and interpreted as a platform that had been laid down at the edge of the lake. Within this brushwood was a vast quantity of well preserved animal bone, antler and wood, as well as more delicate remains such as wads of moss and bracket fungus. Perhaps the most important finds were a rare series of 21 worked antler frontlets. Carved and perforated for wearing, these are still the only examples of their kind in Britain, and only a handful of similar objects have ever been encountered from the Mesolithic across Europe (Milner *et al.*, 2013a). In addition to the organic remains, a large amount of flint tools and amber and shale beads were found across the excavations, another rarity in Mesolithic archaeology.

The sheer abundance of organic artefacts found in the 1950s excavations suggests that across the majority of the excavated area, conditions were largely conducive to organic preservation. Unfortunately, few records regarding the exact burial location of specific organic artefacts

exist, making a comparison of preservation in different parts of the site difficult. A plot of the location of a number of barbed points (constructed from red deer antler) discovered in the original excavations however, illustrates that organic material was found across the wetland areas of the excavations (Figure 1.4).

Visual analysis of most of the antler barbed points discovered in the wetland parts of the trench, as well as many of the bone tools, declared them to be “firm” (Clark, 1954, pg 7). In contrast, in the northeast corner towards the dryland deposits they were softer, and in the dryland itself, no barbed points were recorded despite the lithic evidence for occupation being abundant. This perhaps indicates that the dryland parts of the site were less conducive to the preservation of organic material even in the early excavations. Clark himself notes some less well-preserved fragments of bone found further away from the lake edge and reports that degrees of organic preservation varied across the site. He describes some pieces of bone and antler as “dark in colour and soft as leather” (Clark, 1954, pg 1). He also noted that the brushwood platform did not extend into the dryland area and was better preserved where the site was waterlogged (Clark, 1954).

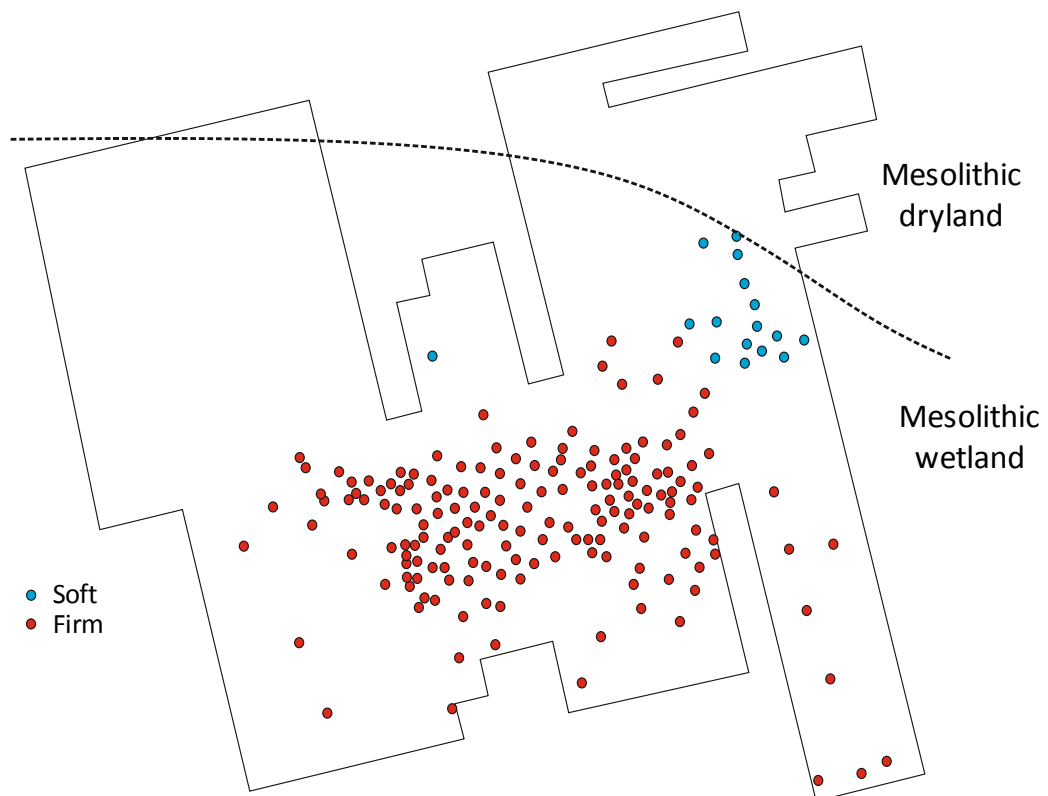


Figure 1.4: Plot of Clark's original excavation showing the location of barbed point finds. Those classified by Clark as 'firm' are shown in red and those classified as 'soft' shown in blue. Figure adapted from Clark (1954). (Originally in colour).

1.1.2.3 Research by the Vale of Pickering Research Trust

Further excavations in 1985 and 1989 were on a smaller scale and aimed primarily at understanding the environmental context of Star Carr (Mellars & Dark, 1998). It was discovered during excavation of a trench some distance to the east of Clark's excavations (VP85A; coloured blue in Figure 1.3) that the site was much larger than previously thought. Further organic remains were uncovered, including a large worked timber platform and an additional barbed antler point, as well as an abundance of flint material. The platform, made from timbers split by stone tools, is considered the earliest evidence for carpentry in Europe. Evidence for controlled burning, and more detailed radiocarbon dating, also indicated that the site had been occupied for much longer than previously thought (Dark, 1998).

During the 1980s excavations, some fragments of bone and antler were reportedly in a poor state of preservation. Similarly to Clark, Rowley-Conwy reported that organic preservation was better in the peat nearest the wooden platform, i.e. near the lake edge (Rowley-Conwy, 1998). Despite this, excavations yielded a wealth of organic environmental evidence, suggesting that even delicate plant remains were still reasonably well preserved in parts of the site.

1.1.2.4 Recent excavations

Further excavations were carried out between 2006 and 2010, again spanning both wetland and dryland parts of the site. Large trenches were newly dug as well as re-excavation and extension of previous trenches, notably Cutting 2 from Clark's excavations (Figure 1.3, extension is shown in red). In addition, test pitting was carried out further away from the main site with the aim of establishing the extent of the archaeology. Excavations established that the site extended even further than estimated by Mellars & Dark (1998); in particular the worked timber 'trackway' uncovered in 1985 was found to extend into the lake edge (Milner *et al.*, 2013a).

Whilst large numbers of lithic materials were uncovered, organic artefacts were noticeably sparse, even in the waterlogged parts of the site, which had previously yielded a huge array of material. Two clusters of severely compressed worked antler were found and had to be excavated on a layer of peat. Others were in such advanced states of degradation that they have been described as "only tentatively identifiable as antler" (Milner *et al.*, 2011a, pg. 2823). In 2007, only two certain pieces of bone were found and these were observed to be spongy in texture. The only bone discovered in 2008 has been termed the 'jellybone' due to the fact that it seems to have completely lost any mineral content, leaving only the collagen matrix (Milner *et al.*, 2011a). In the dryland areas (Trench SC23), fragments of unidentified bone were found, but were largely chalky and brittle.

The wood material was better preserved than the bone and antler; analysis by I. Panter showed wooden artefacts to be degraded, but comparable to other waterlogged archaeological wood (Panter, 2009). Much of it was severely flattened however; M. Taylor (in Milner *et al.*, 2011a) reported difficulties in establishing the peat/wood interface in the wetland part of Trench SC24.

1.1.3 Evidence for site deterioration

Following the discovery of the 'jellybones' and flattened antler in 2007/2008, a review of the organic material from each stage of excavation was carried out, and resulted in the hypothesis that the burial conditions had severely deteriorated since the initial excavations (Milner *et al.*, 2011a). It became clear that the organic artefacts found in the 1985 excavations were both less abundant and considerably less well preserved than those found by Clark in the 1950s, whilst organic remains recovered in the most recent excavations were often barely identifiable.

There was however a clear difference in organic preservation between the wetland and dryland areas of the site; a fact acknowledged even in the first excavations (Clark, 1954). In the northern end of the trenches where the deposits constituted gravelly sand instead of peat, "leathery" pieces of bone and antler were reported, with better organic preservation observed towards the lake. Barbed points were also observed to be more flattened in some parts of the trench than others, highlighting the spatial variability across the site (Clark, 1954). This spatial variation must therefore be considered when assessing preservation across the site.

Despite this, there is clear evidence that the site has altered in recent years. Evidence for the peat having shrunk due to drying out was first observed during excavations in 1985 and 1989 (Mellars & Dark, 1998). Between 2002 and 2005, further concerns were raised following field walking and test pitting, during which it was noticed that the previously invisible contours of the lake edge could now be observed (Milner *et al.*, 2011a). Furthermore, photographic comparison of the re-excavation of Clarks' Cutting 2 Trench in 2010 with photographs from the original excavations appears to show further evidence of the extent of peat shrinkage; the trench wall extends much further above the height of the excavator in the photograph from 1952 compared to in 2010, suggesting that the depth of the trench has significantly decreased (Figure 1.5).

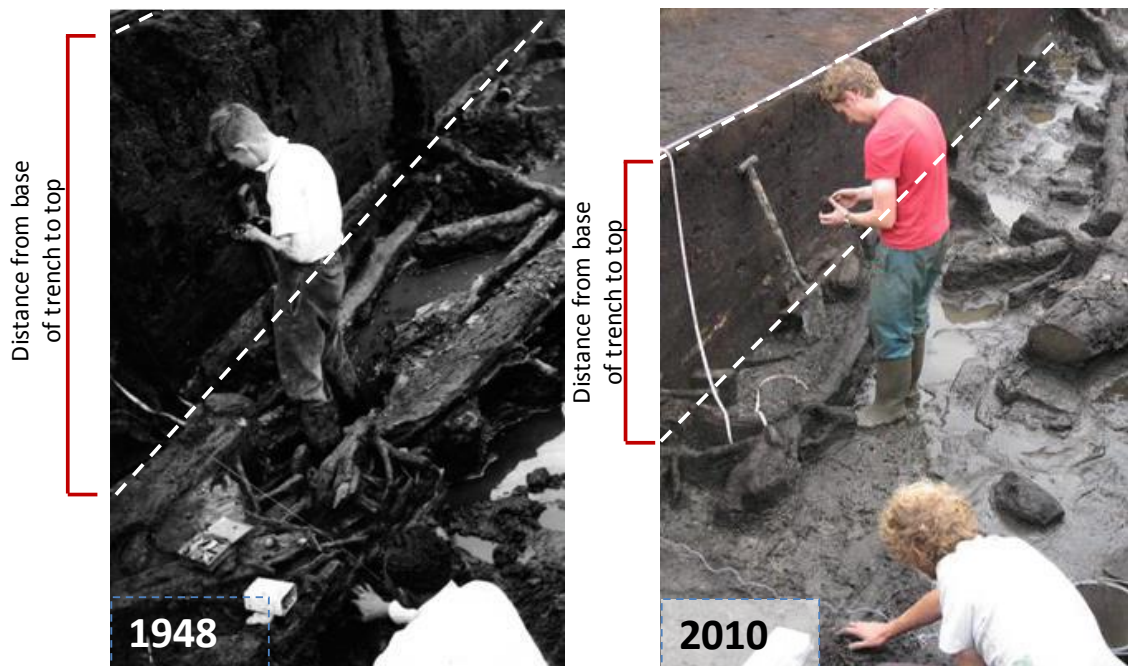


Figure 1.5: Image of the excavation of Cutting 2, taken from Clark (1954), compared to a reconstruction of the scene taken during re-excavation of the trench in 2010. The extent of the peat shrinkage is evident from the much smaller distance between the base of the trench and the ground surface in the later excavations. (Originally in colour).

In 2009, metrical analysis was carried out on antler recovered from all three phases of excavation (Milner *et al.*, 2011a). Results showed that whilst antler excavated by Clark had largely preserved its original shape and texture, those excavated in the 80s were visibly more flattened in comparison, and those from most recent excavations even more so. This was taken as further evidence that peat shrinkage had occurred, possibly resulting in compression, or flattening, of the organic remains.

The most compelling evidence for extreme site conditions has been provided by an extensive geochemical survey carried out in 2009, where high sediment acidity was observed (< pH 2 in parts of the site) in association with high levels of sulfur, indicating that sulfuric acid formation may be occurring (Boreham *et al.*, 2011; Chapter 2). As no geochemical survey had previously been carried out at the site, it is difficult to determine whether this has occurred recently, or if site conditions have always been acidic. A key aim of this study is to assess organic (bone and wood) deterioration at Star Carr in light of the observed geochemical conditions, and to determine the time frame in which these changes may have occurred. In order to do so, the current state of preservation and potential degradation mechanisms of the organic remains must first be considered.

1.2 Bone deterioration

1.2.1 Introduction

Some of the most important artefacts excavated at Star Carr have been bone or antler, including the iconic antler frontlets. For the purposes of this study, the discussion has been limited to bone, as it is the most abundant material, allowing a more thorough assessment of material from across the site. However, as antler is similarly composed of type 1 collagen and hydroxyapatite (although in different relative proportions) it can be expected to deteriorate via similar mechanisms (e.g. O'Connor, 1987). The rate and mechanisms by which bone decays in archaeological sites has been an important area of research, particularly as bone artefacts are often utilised for methods such as radio carbon dating (e.g. Child, 1995; Hedges *et al.*, 1995; Collins *et al.*, 2002).

1.2.2 The structure of bone

Bone has a highly complex hierarchical structure that is still not entirely understood (e.g. Weiner & Traub, 1992; Rho *et al.*, 1998). However, for the purposes of discussing bone diagenesis it may be somewhat simplified into two major components: an organic fraction (primarily type 1 collagen) and an inorganic fraction (hydroxyapatite). In addition to these, bone contains a range of non-structural proteins and lipids (e.g. Glimcher & Katz, 1965; Currey, 2002). Although these components could still be present in archaeological bone, they are found in low abundance in comparison to the collagen (e.g. Evershed *et al.*, 1995).

Collagen provides bones with their mechanical strength and composes approximately 22 % by mass, depending on the age, species and type of bone (e.g. Aerssons *et al.*, 1998; Hedges, 2002). Type 1 collagen is composed of triple helices of protein chains, held together by hydrogen bonding (e.g. Rich & Crick, 1961). In two of these protein chains, glycine represents every third residue, resulting in an amino acid concentration profile that is dominated by glycine (e.g. Shoulders & Rains, 2009). These helices are arranged into fibrils where they are axially staggered (Figure 1.6; Orgel *et al.*, 2001). This staggered pattern manifests as a characteristic banding at a width of ~ 67 nm that can be seen under electron microscopy (e.g. Rho *et al.*, 1998). These fibrils are then arranged in a series of concentric lamellae, making up osteons, which are packed longitudinally to form the bone macrostructure (Figure 1.6). The highly organised and stable structure of collagen means that it can survive extremely well in the archaeological record (e.g. San Antonio *et al.*, 2011). This, along with its high natural abundance, means that collagen is one of the most commonly utilised proteins in

archaeological research, for example in radio-carbon dating (e.g. Hedges & Law, 1989) and isotope analysis for dietary reconstructions (e.g. Ambrose & DeNiro, 1986).

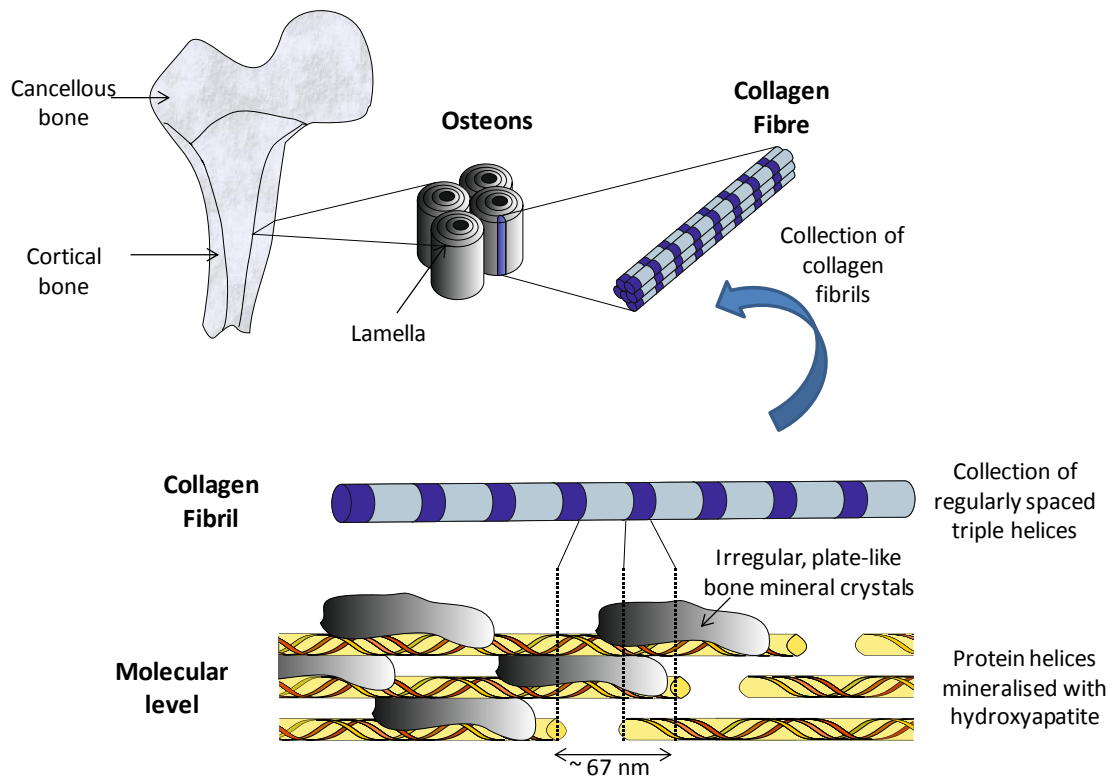


Figure 1.6: Schematic illustrating the structure of bone on various hierarchical levels. Adapted from Rho *et al.* (1998) and Orgel *et al.* (2001). (Originally in colour).

Bone collagen is mineralised by an impure, non-crystalline form of hydroxyapatite (HA; $\text{Ca}_{10}(\text{PO}_4)_6(\text{OH})_2$) containing a number of imperfections such as carbonate, magnesium and fluoride (Brown & Chow, 1979). The HA is deposited in the collagen matrix in plate-like crystals as an animal grows; the way in which this occurs is poorly understood (Weiner & Traub, 1992). The level of mineralisation differs with animal age as well as bone type; for example, load bearing bones (such as long bones) are composed of more heavily mineralised cortical bone, compared to flat bones (such as ribs) which consist mainly of less dense cancellous bone (e.g. Rho *et al.*, 1998). However, as a general rule HA typically accounts for approximately two thirds of the total mass of bone (Green & Kleeman, 1991; Aerssons *et al.*, 1998).

Whilst the exact relationship between the two fractions of bone is not well understood, it is clear that they are intimately associated. This means that the deterioration of one is effected by deterioration of the other (e.g. Collins *et al.*, 2002; Hedges, 2002).

1.2.3 Bone deterioration

Collins *et al.* (2002) summarise the modes of bone deterioration as: “chemical deterioration of the organic phase; chemical deterioration of the mineral phase; and biological attack of the composite.” Which process dominates is dictated by the burial environment, as well as the condition of the bone when it enters the burial environment (for example, whether the bone is cooked or uncooked, fleshed or defleshed) (e.g. Nicholson 1996; 1998; Dixon *et al.*, 2008).

HA is relatively vulnerable to chemical deterioration; at low pH it can rapidly dissolve to buffer the acidity of the environment, leading to its destruction in a relatively short space of time (Gordon & Buikstra, 1981; Margolis & Moreno, 1992). Due to its highly cross-linked and constrained structure however, collagen is generally not soluble except at extremes of pH (Glimcher & Katz, 1965) or high temperature (Koon, 2006). Under these conditions, collagen can undergo ‘denaturing’, or loss of the strong cross-links between the protein strands, allowing the fibrils to swell and melt, eventually turning to gelatine (Glimcher & Katz, 1965; Neilsen-Marsh *et al.*, 2000; Koon, 2006). It is understood that in an archaeological context these processes can be prevented by the presence of the HA, both by buffering of the acidity and stabilising the fibrils by physically constraining them (Covington *et al.*, 2008). Chemical deterioration of the collagen is therefore unlikely to occur without prior loss of the mineral fraction (Collins *et al.*, 2002), although the exact conditions at which sufficient HA is lost to allow collagen degradation by chemical means are unclear (Child, 1995).

Biological deterioration of both phases can occur in the burial environment, and is most likely to occur immediately following deposition (Child, 1995). Hedges *et al.* (1995) predict that biological attack can lead to the complete destruction of bone within 500 years. Experimental studies such as those by Dixon *et al.* (2008) and Nicholson (1996; 1998) support this, showing that processes such as tunnelling by erosion bacteria and surface damage to the bone mineral do proceed quickly under certain conditions. Collagen degradation by biological means is also largely prevented by the HA however, as the small size of the crystals restricts the extent to which collagen-digesting enzymes (collagenases) can access the collagen (Nielsen-Marsh *et al.*, 2000).

1.2.4 Analysis of bone deterioration

An understanding of bone deterioration is important not only in archaeology but in biomedicine, and as such a range of analytical methods are routinely employed. Different analytical approaches are often required to determine levels of deterioration in the organic and inorganic fractions. In addition, multi-analytical approaches are often utilised (e.g. Nielsen-Marsh & Hedges, 2000; Turner-Walker & Peacock, 2008).

1.2.4.1 Chemical analysis

Analysis of the collagen fraction of bone often focuses on the quantification of the amino acid content (Ezra & Cook, 1957; Bada, 1972; Collins *et al.*, 2009). For estimating the relative concentration of collagen, simple measurements such as nitrogen: carbon values or total amino acid content can be utilised (e.g. Dobberstein *et al.*, 2009). Relative increases or decreases in bulk collagen content can inform on the levels of HA and/or protein loss (e.g. Roberts *et al.*, 2002). Furthermore, enrichment of aspartic and glutamic acids (due to their high abundance in non-collagenous proteins) can also signify degradation of the collagen or an inclusion of microbes into the structure, suggesting that biological deterioration may be occurring (Dennison, 1980; Child *et al.*, 1993).

When the chiral forms of each amino acid can be separated, for example by reverse phase high performance liquid chromatography (HPLC), the extent of racemisation for each amino acid can be quantified (e.g. Kaufman & Manley, 1998). Due to the highly stable nature of collagen, racemisation is not expected to occur unless collagen is significantly broken down, increasing the number of terminal amino acids (e.g. Child *et al.*, 1993). The degree of racemisation in each amino acid can therefore be used as a proxy indicator for the degree of damage within the collagen helix, and has been applied as an indicator of biomolecular preservation (e.g. Dobberstein *et al.*, 2008). Most amino acids racemise very slowly, even when terminally bound (for example alanine racemisation has a half-life of 12,000 years at 25°C), and as such, significant racemisation is not likely to be observed in samples from a Mesolithic site, where low temperatures may further slow racemisation (e.g. Bada & Schroeder, 1975). However, aspartic acid (Asp) is a fast racemiser, and is therefore most commonly applied as a diagenetic indicator in archaeological bone (Child *et al.*, 1993; Collins *et al.*, 1999; Dobberstein *et al.*, 2008). It is also able to racemise in-chain, so can indicate an increase in conformational freedom, for example by loss of cross-link between protein chains (Collins *et al.*, 2009). Recent studies show that serine (Ser) may also be able to racemise in-chain and relatively quickly (Demarchi *et al.*, 2013), and may also be able to serve as a diagenetic indicator.

Other methods of analysis of the protein fraction of bone include spectroscopic methods. Examples include Fourier transform infrared spectroscopy (FTIR) (e.g. Pleshko *et al.*, 1991) and Raman spectroscopy (e.g. Timlin *et al.*, 2000; Ragahavan, 2011). Spectroscopic methods are useful for the analysis of archaeological or fossil samples as they are potentially non-destructive, and probe alteration on a molecular level, revealing changes such as a loss of cross-linking. An advantage of spectroscopic methods is that they often allow the simultaneous analysis of the HA.

Loss of collagen also results in an increase in porosity of the bone. Quantification of this using a method such as mercury intrusion porosity, where mercury is introduced to a sample under vacuum and the volume taken up is recorded, can therefore also be an indicator of diagenesis (e.g. Nielsen-Marsh & Hedges, 1999). This method has a major disadvantage in that it requires a large sized sample to gain a reliable result.

Analysis of the HA content is achieved in part by quantification of the protein content, as it indicates the relative composition of the bone; however, several methods of analysing the deterioration in HA in more detail and independently of the collagen fraction are possible. Many of these focus on the phenomenon of increased HA crystallinity with diagenesis (Pleshko *et al.*, 1991; Hiller & Wess, 2006). The reasons for this increase in crystallinity occurring are not well understood, but are possibly due to preferential dissolution of the smallest crystals (Surovel & Stiner, 2000) or recrystallisation of dissolved HA in a stagnant environment (Hedges & Millard, 1995). This manifests as a sharpening of peaks in X-ray techniques, as shown by Hiller & Wess (2006) for small angle X-ray scattering, and by Bonar *et al.* (1983) for powder X-ray diffraction (p-XRD). Diffraction methods are used to probe long-range crystallinity of the HA structure, obtaining an 'average' assessment of the properties of a crystal. This is in contrast to spectroscopic methods which detail molecular changes only on the surface of the sample, and as such can be more influenced by sample preparation techniques (e.g. polishing or grinding samples) (e.g. Surovell & Stiner, 2001).

As diagenetic alteration often involves exchange with the burial environment (Lee-Thorp & van der Merwe, 1991), analytical techniques such as emission spectroscopy (Reiche *et al.*, 1999; Zapata *et al.*, 2006) may be employed to investigate trace element inclusions. Uptake of, for example carbonate, can also be identified using spectroscopy, most often FTIR (Lee-Thorp & van der Merwe, 1991). Often however, these techniques require advanced equipment, such as a synchrotron radiation source, to achieve resolution appropriate for the analysis of archaeological bones. Other advanced methods include 2 D spectroscopies, where Raman or

FTIR spectra are taken across the surface of a sample, providing analysis of spatial variations in preservation (e.g. Penel *et al.*, 1998; Paschalis *et al.*, 2001).

1.2.4.2 Histological and bulk analysis

Macroscopic preservation of archaeological bone is often evaluated using a scoring system from 1 to 5, where 1 represents well preserved bone and 5 indicates a highly degraded bone (Gordon & Buikstra, 1981; Hedges *et al.*, 1995). However, this can be subjective and cannot assess small diagenetic changes (Jans *et al.*, 2002).

The most common methods of detecting small levels of histological alteration are microscopic techniques. Thin-sectioning in combination with optical microscopy is often employed to observe characteristic changes to bone histology due to microbial activity (e.g. Jans, 2005; Dixon *et al.*, 2008). In thin-section, characteristic bone features such as osteons should be observable if HA is still present, as well as features such as cracking, tunnelling characteristic of biological deterioration, or the incorporation of extraneous material into the bone structure (Jans *et al.*, 2002). If used with cross-polarised light, the presence of protein can be indicated by the presence of birefringence (alternating patterns of light and dark); this occurs due to the orientation of the collagen fibres (Giraud-Guille, 1988).

Scanning electron microscopy (SEM) (which achieves a much higher magnification than optical microscopy with minimal sample preparation) can also be used to look at histological alteration of bone during burial and is often used to complement studies that also apply quantitative chemical methods (e.g. Bell, 1990; Turner-Walker & Peacock, 2008). Nicholson (1993) shows how SEM can reveal changes to the surface texture of bone when it has undergone alteration due to burning. When used in back-scattered electron mode, where changes in bone mineral density can be observed, variations in diagenesis across a sample can be better assessed (Turner-Walker, 2008).

Under transmission electron microscopy (TEM) using uranyl acetate stain, the characteristic banding of collagen fibrils can be observed (Giraud-Guille, 1988). Koon (2006) developed a method to isolate the fibrils from the HA so that they can be observed in isolation; using this method, swelling or distortion of collagen fibrils can be identified. TEM can also be utilised for the observation of HA crystals, allowing the identification of changes to crystallinity (Nudelman *et al.*, 2010). As with all microscopic methods however, this assessment can be subjective and user dependent.

1.3 Wood deterioration

1.3.1 Introduction

Wood is often found in high abundance in wetland archaeological sites (Caple, 2004). At Star Carr, some important examples of wooden artefacts have been uncovered, including the timber 'trackway' and several smaller artefacts such as a birch-wood paddle (Milner *et al.*, 2013a).

1.3.2 The structure of wood

Wood can be broadly considered a complex composition of two types of biological polymer: lignin and polysaccharides (cellulose and hemi-cellulose) (e.g. Jane *et al.*, 1970; Figure 1.7). The exact relative composition is dependent on a range of factors such as species, age and type of wood (i.e. trunk or branch) (Pandey & Pitman, 2003), but fresh wood is considered roughly 70-80 % celluloses and 15-35 % lignin (Fengel & Wegener, 1984). A small amount of non-structural components, such as pectic acid, proteins and metal ions, can compose up to 10 % by mass of fresh wood (Hedges, 1990; Martinez *et al.*, 2005). These can easily be extracted however, and are unlikely to survive in any great abundance in archaeological wood (Hedges, 1990). In addition, these non-structural components can be replaced by material from the burial environment such as metals and minerals, particularly those containing iron (Hedges, 1990). This uptake can result in a higher 'ash content,' that is, the material left behind when the wood is burnt at 650°C (e.g. Panter & Spriggs, 1996).

The inner cell walls (or secondary cell walls) are composed mainly of very long sugars (cellulose; up to 15,000 glucose units) and shorter branched chains (hemi-celluloses) (e.g. Hoffman & Jones, 1990). These are organised into fibrils, which also contain some lignin (Jane *et al.*, 1970). Celluloses are readily broken down by both biological and chemical processes and are often lost in an archaeological context, with the order of stability being lignin > cellulose > hemi-cellulose (Florian, 1990).

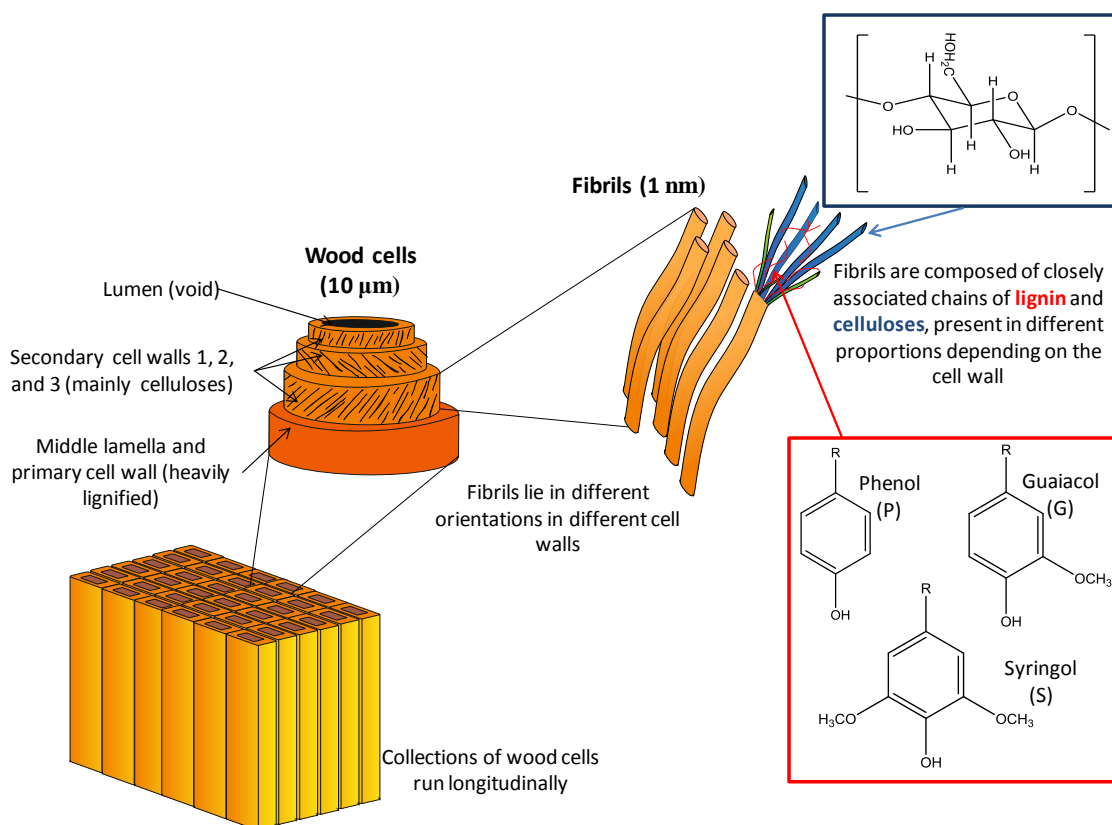


Figure 1.7: Schematic showing the hierarchical structure of wood. Major sub units for lignin (red) and celluloses (blue) are indicated. (Adapted from Jane *et al.*, 1970 and Hoffman & Jones, 1990). (Originally in colour).

Lignin is mainly located within the outer primary cell walls and middle lamellae; the interfaces between the cells (Jones & Eaton, 2006). Lignin is composed of three main phenol sub units: non-methoxylated (phenol, P), monomethoxylated (guaiacol, G), and dimethoxylated (syringol, S) (Martinez *et al.*, 2005; Figure 1.7). These are present in different proportions depending on the wood species (softwood for example, has no syringyl units). These sub units form a large three-dimensional network containing a large variety of types of chemical bonds and cross-links, resulting in a highly stable structure (Martinez *et al.*, 2005).

1.3.3 Wood deterioration

Both cellulose and hemi-cellulose break down relatively easily via biological activity, primarily due to hydrolase and oxidase enzymatic activity from both microbes and fungi (Blanchette *et al.*, 1991; Jones & Eaton, 2006). In addition to biological activity, celluloses can undergo chemical hydrolysis; for example they can be dissolved in strong acids or 10 % sodium hydroxide (Fengel & Wegener, 1984; Kamide *et al.*, 1984). This is often preceded by swelling of the cellulose fibres (Kamide *et al.*, 1984). This swelling process may be accelerated by the presence of certain chemical species, or prevented in the cell walls that are more lignified (Fengel & Wegener, 1984). In most circumstances in archaeological wood, chemical

deterioration is insignificant in comparison to the levels of biological deterioration (Jones & Eaton, 2006).

Lignin degradation is much slower due to the complexity of the types of chemical bond that hold it together (Jones & Eaton, 2006) and occurs primarily by fungal attack (Blanchette *et al.*, 1990; Kim & Singh, 2000). Chemical deterioration of lignin is much less likely; indeed its resilience to acid hydrolysis is illustrated by the commonly applied method of isolating lignin from wood by dissolving cellulose in 72 % sulfuric acid without loss of the lignin (TAPPI standard T 222 om-88). Lignin therefore tends to survive more readily than cellulose; however certain fungi (soft rot fungi) do preferentially decay lignin before cellulose (Pandey & Pitman, 2003; Martinez *et al.*, 2005). This mode of biological degradation occurs by enzymatic oxidation of the phenol-type units, causing a number of breakdown reactions including aromatic ring cleavage and demethoxylation of the G and S units. Degraded lignin therefore has altered ratios of P: G: S (Hatcher, 1984; Martinez *et al.*, 2005; Figure 1.8).

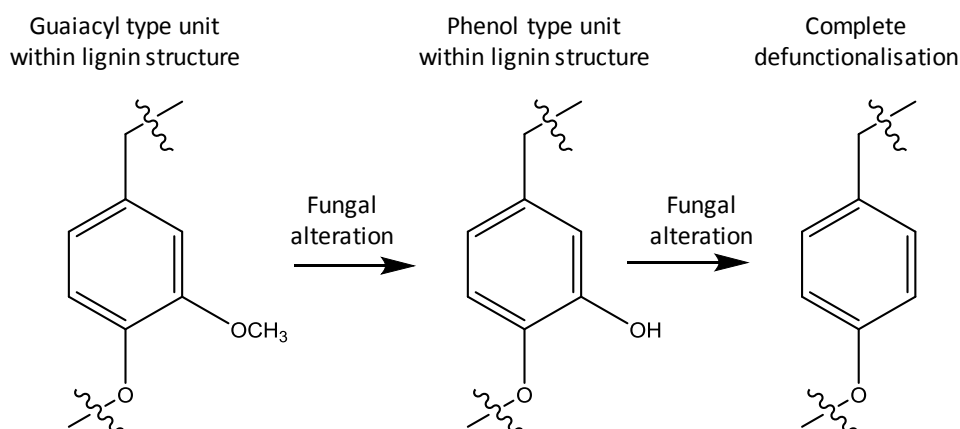


Figure 1.8: Scheme showing how demethoxylation by fungal activity creates higher concentrations of phenol type sub-units in lignin.

As many classes of both microbes and fungi are aerobic, and therefore not active in a waterlogged context, wood can survive for long periods in wetland environments (e.g. Hedges, 1990; Section 1.4.3.1). Despite this, low levels of deterioration do occur via the activity of small numbers of anaerobic organisms (Section 1.4.3.2), although the exact level of oxygen tolerance of such species is relatively unknown (Caple, 1994). Due to the faster loss of cellulose, archaeological wood deterioration is often characterised by an increased lignin: cellulose ratio (e.g. Bjordal *et al.*, 1999; Gelbrich *et al.*, 2008) and waterlogged wood can sometimes be found as a lignin rich skeleton consisting of only the primary cell walls (Hedges, 1990).

Aside from polymer degradation, the chemical composition of archaeological wood can also alter due to the incorporation of various minerals into the highly porous structure; in particular, iron (III) is actively chelated by cellulose (Jones & Eaton, 2006). As some anaerobic

bacteria utilise inorganic iron as an electron donor in their metabolic processes (Postgate, 1965), this may in turn lead to an increase in biological activity within the cell walls. Another major problem with archaeological wood is a build-up of sulfates, particularly in material from marine environments (e.g. Almkvist, 2008). These sulfates can then undergo oxidation upon exposure to air to form sulfuric acid, which may cause chemical hydrolysis of the celluloses (Jones & Eaton, 2006). Upon exposure to air, an increase in biological activity can also lead to accelerated degradation of both cellulose and lignin. This presents problems for the storage of wood post-excavation, or when a site becomes no longer waterlogged (see Flag Fen, Section 1.4.5.1).

1.3.4 Analysis of wood deterioration

The assessment of the condition of archaeological wood is a large area of research due to its importance in informing conservation processes. Celluloses and lignin deteriorate very differently, but are much more closely associated than bone protein and mineral, making them difficult to physically separate (Fengel & Wegener, 1984). Therefore, many analytical techniques involve the simultaneous analysis of both polymers.

1.3.4.1 Chemical analysis

Deterioration of wood, although mainly driven by biological factors, is characterised by alterations in the chemical composition of the wood, primarily alteration of the lignin: cellulose ratios, as well as P: G: S ratios in lignin (Gelbrich *et al.*, 2008; Martinez *et al.*, 2005).

Lignin: cellulose ratios in wood are routinely analysed in the paper and pulp industry using bulk wet chemical methods that have been adopted for the analysis of archaeological wood (e.g. Hoffman, 1981; TAPPI standards). These involve a series of dissolution steps using solvents including 72 % sulfuric acid and strong sodium hydroxide, from which the relative composition of different wood components can be calculated. However, it has often been found that this presents yields of over 100 %, suggesting error in the methods (Fengel & Wegener, 1984). In addition, it requires large amounts of sample, making it not ideally suited to the analysis of archaeological materials.

Spectroscopic methods present a solution to the problem of the large quantities of sample required for wet chemical methods; these can also often be non-destructive. FTIR in particular is commonly used to investigate changes in the lignin: cellulose ratios of degraded wood (Pandey, 1998; Gelbrich *et al.*, 2008; Pandey & Pitman, 2008). The development of FTIR spectrometers fitted with an attenuated total reflectance unit (ATR) removes the necessity to prepare wood samples in a potassium bromide matrix, making it ideal for the rapid screening

of wood deterioration (e.g. Gelbrich *et al.*, 2008). Whilst most FTIR absorption bands contain contributions from each polymer, some can be attributed to only lignin (e.g. 1507 cm^{-1} relating to the aromatic ring; 1240 cm^{-1} relating to the ether bond) and only cellulose (1325 cm^{-1} relating to a CH_2 wagging; 1375 cm^{-1} relating to OH deformations) (Pandey, 1998). Changes in the relative heights and integrations of these four peaks are interpreted as degradation of the polymers (e.g. Gelbrich *et al.*, 2008). In addition, Pandey & Pitman (2008) show how FTIR can reveal alterations to the lignin structure: changes such as peak splitting, peak shifting or a reduction in the intensity of the peaks relating to methoxy groups in lignin can indicate a change in the chemical environments in which they are present, or a reduction in their abundance. Loss of aromatic rings can also be identified by a reduction of characteristic absorption, and this is another key indicator of fungal decay of lignin (Faix *et al.*, 1991).

Although widely used to qualitatively assess the condition of archaeological wood, FTIR is not ideally suited to quantitative analysis. Gas chromatography using pyrolysis (py-GC) in the absence of oxygen provides a more detailed analysis of wood degradation products (e.g. Vinciguerra *et al.*, 2007), and has the potential to provide an absolute measure of composition if an internal standard is used (Bocchini *et al.*, 1997). Pyrolysis breaks down polymers into small fragments, which can then be separated using GC. When used in conjunction with mass spectrometry, peaks can be confidently assigned to different sub-units of both cellulose and lignin, giving an overview of the ratio of the different monomeric units present in the starting material (e.g. Vinciguerra *et al.*, 2007; Alves *et al.*, 2006). In addition, it requires minimal sample preparation and a very small amount of sample (Martinez *et al.*, 2005). Alves *et al.* (2006) show how even without an internal standard, py-GC can reliably reveal P: S: G ratios, signifying chemical changes to the lignin itself. This may be particularly indicative of biological decay, where demethoxylation due to enzymatic activity will result in a higher P content. The presence of smaller, carbohydrate-derived molecules can also confirm the presence of cellulose (e.g. van Bergen *et al.*, 2000).

Solid-state ^{13}C NMR has been shown as an alternative method for the analysis of archaeological wood (Wilson *et al.*, 1993; Gilardi *et al.*, 1994; Almqvist, 2008). Similarly to FTIR, alteration of the peak areas and chemical shift indicate alteration of the chemical environments, although NMR has the advantage of distinguishing between G or S lignin subunits (Wilson *et al.*, 1993). NMR can also be quantitative with the use of an internal standard (Almqvist, 2008); however the limitation of this technique is mainly in the lack of availability of appropriate NMR instruments (samples will be in the solid state) as well as the expertise required to run them (Hedges, 1990).

In many cases, a multi-analytical approach is taken (e.g. Faix *et al.*, 1991; Wilson *et al.*, 1993; Almkvist, 2008). Due to the complexity of the composition of wood, it is acknowledged that this application of complementary techniques, rather than relying on an individual measure, provides a more reliable assessment of the levels of deterioration.

1.3.4.2 Histological and bulk analysis

Many studies on biological degradation of wood focus on microscopic analysis, both optical (e.g. Bjordal *et al.*, 2000) and SEM (Blanchette, 2000). In thin-section (and in more detail in SEM), it is often possible to identify the separate cell walls (Fengel & Wegener, 1984).

Characteristic microbial decay patterns and fungal hyphae are identifiable, as well as features such as shrinking and collapse of the cell walls (Bjordal *et al.*, 2000; Powell, 2011). The use of biological stains such as astra-blue and chrysoidine red in thin-section can further reveal biological activity (e.g. Hoffman, 1986; Humar *et al.*, 2008).

A range of standard decay-assessment tests are often applied to archaeological wood prior to conservation, providing a measure of the bulk condition of the wood. These include measurements such as wood density and maximum water content (u_{\max}) (Panter & Spriggs, 1996). An increase in u_{\max} suggests greater levels of damage to the wood structure, primarily loss of cellulose, creating larger voids within the structure, which allows a greater uptake of water (Hoffman, 1986). In experimental degradation experiments, mass loss has also been shown to correlate with levels of degradation measured using chemical methods (Faix *et al.*, 1991). Due to the high porosity of wood however, it can be difficult to obtain the mass of absolutely dry samples, leading to high levels of error in such measurements (Fengel & Wegener, 1984). In addition, the values can be altered by the presence of non-structural components, such as iron and minerals (Panter & Spriggs, 1996).

The inorganic components of archaeological wood can be determined by burning a sample at 650 °C to remove all organic components, leaving behind an ash composing minerals such as iron and sulfur (Hedges, 1990). Increased ash content is often taken to be indicative of increased diagenesis as a result of interaction with the burial environment. The presence of inorganic components can also cause error in measurements such as wood density, maximum water content and chemical composition as measured by wet chemical methods, as they contribute to the total mass (Hedges, 1990).

1.4 Summary of organic deterioration

There are a range of analytical techniques that provide both qualitative and quantitative information regarding the deterioration of bone and wood. Each of these have merits and downfalls, and therefore considering the most appropriate technique will be driven in part by the degradation mechanisms that need to be studied.

Degradation mechanisms for organic archaeological materials are driven primarily by the nature of the burial environment. Degradation of bone and wood in peatland environments can occur via a number of different pathways driven by the specific conditions of such environments.

1.5 Organic archaeological materials in wetlands

1.5.1 Introduction

Bone and wood can deteriorate by both chemical and biological means (Sections 1.2.3 and 1.3.3). The rate by which organic degradation proceeds depends almost entirely on the chemical and biological nature of the burial environment (e.g. Hedges, 1995; Caple, 2004). The reasons that wetlands preserve such vast amounts of organic material are complex; anaerobic, waterlogged and slightly acidic conditions are often cited as the major requirements as they suppress biological activity and provide a chemically stagnant environment (Gearey *et al.*, 2010).

Wetland peat deposits are formed when plant material decomposes *in situ* in an area where waterlogging means that microbial decomposition is slow to occur, leaving an organic rich peat (Bain *et al.*, 2011). Star Carr is located on the bank of a prehistoric lake, where the original reed beds and wetland fauna have resulted in the formation of a reedy peat blanket bog covering the area (Milner *et al.*, 2011b). In places, this peat layer is relatively thin, for example areas of the site away from the banks of the lake, which were previously dryland in the Mesolithic. In other parts of the Star Carr site the peat can be metres thick (Boreham *et al.*, 2011). The Mesolithic archaeology is almost all contained within these peat layers.

Gearey *et al.* (2010) suggest that an estimated 22,500 archaeological sites are preserved in peat in Britain alone. As such, these environments have been extensively studied. Although their complex and vulnerable nature is often acknowledged (e.g. Kenward & Hall, 2000; Caple, 2004), the major factors contributing to organic preservation in peatland sites can be broadly categorised into chemical and biological components, although there is much overlap between the two.

1.5.2 The chemistry of wetland sites

The most important factors affecting soil chemistry can be briefly summarised: water content, oxygen content, cation/anion identity, pH, soil density and redox behaviour; all of which are closely interlinked (e.g. Caple, 2004; Lillie & Smith, 2007). Characterisation of the chemical nature of the burial environment can to some extent allow the prediction of the potential for organic archaeological remains to survive (Caple, 2004).

The water content of peat environments is often high (up to 95 %), due to the high density of the peat restricting water movement (e.g. Chapman & Van de Noort, 2001). Drainage of the

peat therefore leads to severe shrinkage, which is often irreversible (Schwarzel *et al.*, 2002). Waterlogging also leads to an anaerobic environment; often cited as the main factor promoting organic preservation. This is because fungal and bacterial growth will be suppressed in the absence of oxygen, leading to a reduction in biological degradation (Holden *et al.*, 2006; Section 1.4.3).

The restricted movement of water also means that any reactive chemical species do not move through the sediment as quickly as, for example, in environments where rainwater rapidly percolates (Bartlett *et al.*, 2010). This results in a stagnant chemical environment. Experimental studies such as those by Crowther (2002) and Nicholson (1996; 1998) show that the rate at which dissolved components of deteriorated bone are washed away is a key factor determining the rate at which it decays. Hedges & Millard (1995) suggest that interaction with groundwater is the one major underlying feature that dictates the rate at which organic decay proceeds. The hydrology of a wetland site is also influenced by the underlying geology which may further restrict its movement, as well as the source of groundwater, which determines its chemical composition (Welch & Thomas, 1996; Holden *et al.*, 2006).

A variety of organic and inorganic species may be mobilised in a waterlogged environment, originating from minerals, agricultural activities and decayed organic matter (Faulkner & Richardson, 1989). Although the environment is stagnant, the presence of water allows a closer interaction of these species with any buried archaeological material (e.g. Pollard, 1996). A fluctuating water-table has been shown by Nicholson (1996) and Williams *et al.* (2006; Section 1.4.5.3) to be even more destructive, as it causes the constant movement of reactive species. If this fluctuation occurs through an archaeological layer, this can exacerbate the rates of degradation as it constantly bring new species into contact with the archaeological material. The identity and movement of reactive chemical species within a burial environment define properties such as pH and redox potential (Pollard, 1996; Caple, 2004). As such, measurements of these parameters can indicate the propensity of an environment to preserve organic matter (e.g. Mattheisen, 2004). Peat bogs are often slightly acidic (pH < 6) due to the high concentrations of organic acids such as humic acids, which are formed from the decay of plant material. These humic acids and tannins often cause severe discolouration by staining, which normally characterises archaeological finds from peatland areas (Clark, 1954; Mellars & Dark, 1998; Hedges, 2002).

Whilst low pH can have a beneficial effect on delicate organic remains, as it restricts biological deterioration (Section 1.4.3), it often has a negative effect on the preservation of bone, as HA can rapidly dissolve to buffer the acidity of the surrounding environment (e.g. Gordon &

Buikstra, 1981). The extent to which it does this is not well understood (Child, 1995). In addition, low pH may be detrimental to the preservation of wood as cellulose can undergo acid catalysed hydrolysis, causing break down of the long polysaccharides (Fengel & Wegener, 1984).

Redox potential is a measure of the tendency of sediments to cause oxidation or reduction, and is strongly influenced by pH and the availability of oxygen, which is in turn influenced by the degree of waterlogging (Caple, 1994). With regards to a burial environment, a more positive redox potential indicates a higher tendency for the sediments to gain electrons, thus causing oxidation of mobilised reactive species or buried remains (Atkins *et al.*, 2006). Acids are often highly oxidising as they readily gain electrons (Luder, 1942).

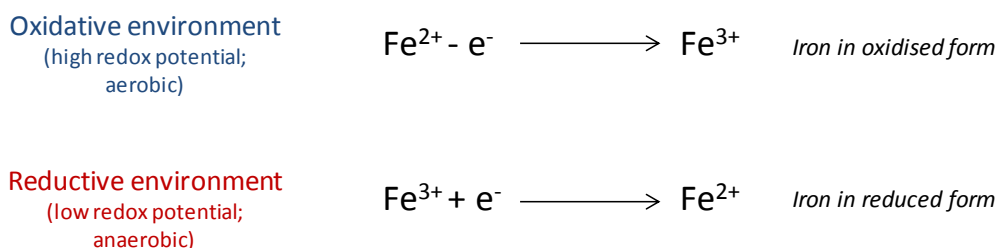
Sediments with low redox potential (low oxygen content; reducing) are often considered the most likely to preserve archaeological materials; peatland sites often display low redox (e.g. -200 to -400 mV) (Caple, 1996). Redox measurements are often interpreted as proxy indicators of biological activity of a burial environment, as this is likely to be higher in more aerobic sediments (e.g. Lillie & Smith, 2007). An increase in redox potential can occur when oxygen becomes available and sediments oxidise; often this has been seen to correlate to an increase in organic degradation (Caple, 1996). In addition, environments with a fluctuating water-table may undergo cyclic changes in redox potential (Pollard, 1996).

The concentrations of reactive species that can participate in electron transfer reactions have important impacts on both the chemical and biological (Section 1.4.3) nature of a burial environment (Caple, 2004). High sulfur content in peat is often seen due to the high levels of decomposed organic material, resulting in the formation of sulfates (Price & Casagrande, 1991; Sposito, 2008). However, in a number of wetland sites (e.g. Yoxall Bridge, described further in Section 1.4.5.4), the sulfur concentrations are too high to be explained by this and have instead been attributed to underlying sulfur containing mineral deposits (Brown *et al.*, 2010). This inorganic sulfur can exist in minerals (e.g. pyrite, FeS_2 ; gypsum, CaSO_4), or dissolve to form H_2S . When this comes into contact with oxygen (i.e. when redox potential is high) it can form sulfates (SO_4^{2-} ; Brown, 1985). High levels of sulfur have been hypothesised by previous studies as a serious factor in the altered site conditions at Star Carr (e.g. Boreham *et al.*, 2011; Brown *et al.*, 2011). A full review of these studies is given in Chapter 2.

Other important reactive species include metals such as iron and copper (Faulker & Richardson, 1989), which can serve as indicators of redox potential as well as influence the biological nature of the burial environment. In reducing (anaerobic) environments, ions are

often present in a reduced form, whilst in oxidising sediments more of the oxidised form will be present (Hong & Kester, 1986). This is illustrated for iron in Equation 1.1.

Equation 1.1: redox states of iron in different environments.



Other chemical species can add to the complexity of the chemistry of a burial environment. Examples include clay particles, which may act as cation exchange sites to buffer acidity, or aluminium which may buffer by forming chelated complexes (Caple 1996; Holden *et al.*, 2006). Elements such as calcium are able to form complexes with a multitude of other species, thus altering the chemical environment (Pollard, 1996).

The presence of a number of chemical species such as methane, phosphate and nitrogen containing compounds are dictated by the biological activity occurring within the burial environment (e.g. Caple, 1994).

1.5.3 The biology of wetland sites

Biological activity (enzymatic decomposition by microbes and fungi) is generally accepted as the primary cause of degradation of organic materials in archaeological sites, particularly with regards to wood (e.g. Hopkins, 1996). Many studies have attempted to look closer at the effect of microbial degradation specifically on bone (e.g. Child *et al.*, 1993; Section 1.2.3) and wood (e.g. Blanchette, 2000; Section 1.3.3).

Traditionally, biological deterioration of organic remains in wetland archaeological sites has been assumed to be negligible, and this is often cited as the main reason that so many wetland sites yield vast numbers of organic remains (e.g. Hedges, 1990, Bjordal *et al.*, 1999). However, recent research shows that this is rather a simplistic view of the complicated nature of wetland environments (e.g. Kim & Singh, 2000; Caple, 2004). The biological activity of wetland sites is controlled by a multitude of factors; the number and variety of microbes present in soil have been shown to be vast, and the decomposition methods of each of these varied and not well understood (Hamilton, 1985; Sanchez, 2009).

Biological activity can both be influenced by and influence the chemical nature of the burial environment; for example, some inorganic compounds such as copper may contribute

favourably to organic preservation as they can inhibit some microbial decay processes (e.g. Zevenhuizen *et al.*, 1979). Biological activity can itself cause fluctuations in pH and redox as well as alter concentrations of organic compounds such as sulfates and nitrates (Pollard, 1996; Section 1.4.3.2)

In addition, seasonal fluctuations in biological activity may occur due to changes in moisture content and temperature, making it difficult to predict (e.g. Bandick & Dick, 1999).

Broadly, two types of biological deterioration can occur: aerobic and anaerobic; however, research also shows that when an environment alternates between the two (i.e. a fluctuating water-table) biological activity is stimulated (Reddy & Patrick Jr, 1975).

1.5.3.1 Aerobic decomposition

Aerobic decomposition is the primary mode of natural decay of organic materials. It eventually results in the total oxidative breakdown of organic material into carbon dioxide, nitrates and methane via the metabolic processes of microbes and fungi (Cagle & Dungworth, 1998).

Wood is particularly susceptible to aerobic decay by fungi, resulting in the demethoxylation of phenolic sub units and aromatic cleavage (Section 1.3.3; Blanchette, 2000). However, bone protein is somewhat protected from deterioration by collagenase enzymes, as these are too big to access the small gaps between HA crystals (Section 1.2.3; Dixon *et al.*, 2008).

In waterlogged environments aerobic decomposition is assumed to be severely suppressed as the high water content prevents the sediments from becoming aerated. Fungi, particularly those which cause the rapid breakdown of lignin in wood (brown rot and wet rot) are observed to exist only in very limited numbers in anaerobic environments (Holt & Jones, 1983). Although some species of aerobic bacteria (specifically erosion bacteria which cause cavities in the cellulose rich secondary cell walls) can be active at very low concentrations of oxygen, these facilitate degradation at very slow rates (Blanchette *et al.*, 1990; Bjordal *et al.*, 1999).

Another factor causing the suppression of aerobic decomposition in peatland sites is the high concentration of toxic compounds, such as the polyphenols from plant remains, which causes the de-activation of the digestive mechanisms of many aerobic micro-organisms (Rosswall, 1975). In addition, many peatland environments are slightly acidic (generally < pH 6); many species of fungi in particular are less able to thrive at extremes of pH (Kim & Singh, 2000).

1.5.3.2 Anaerobic decomposition

Although aerobic decomposition is often restricted in peatland sites, certain classes of microbes can survive in these anaerobic environments. In peat in particular, sulfate-reducing bacteria have often been identified (Postgate, 1965). These utilise sulfate as an alternative to

oxygen in their metabolic processes, causing its oxidation to sulfides (Equation 1.2). Sulfate reducing bacteria tend to be most active in environments with low redox potential (< -20 mV) and can survive at relatively low pH, being observed to thrive between pH 4.1 and 9.9 (Cappenberg, 1974).

Equation 1.2: Mechanism of sulfate reduction by bacterial metabolism (Singleton & Sainsbury, 1991).



Other anaerobic bacteria can utilise a variety of other electron donors, for example NO_3^- or inorganic iron. Often, the metabolic processes of these bacteria contribute to altering the chemical environment (Holden *et al.*, 2006). Whilst this may further suppress the activity of some microbes, others can adapt to increasingly extreme environments.

Aside from bacteria, certain types of fungi have been shown to be more tolerant to anaerobic environments than other types and are generally more destructive to wood than other degrading species (Highley & Kirk, 1979).

1.5.4 Summary of organic deterioration in wetland sites

A number of factors (biological and chemical) contribute to determine whether organic material is preserved in an archaeological site. In wetland sites, waterlogging is considered the major factor contributing to the excellent preservation often seen; exclusion of oxygen leads to the suppression of aerobic microbial decay, one of the main degradation pathways for organic material (e.g. Pollard, 1996; Caple, 2004; Mattheisen, 2004).

Wetland sites are also incredibly vulnerable to alteration and destruction via changes such as alteration of the water-table and changes to the groundwater chemistry (e.g. Buckland, 1993; Kenward & Hall, 2000). This vulnerability can be illustrated using a few important case studies.

1.5.5 Organic remains in wetland sites: *Case studies*

Examples of peatland sites preserving a vast array of organic material can be found all over the world. Examples of Mesolithic sites are most common in countries with large wetland areas such as Denmark and the Netherlands (e.g. Coles, 1998; Van de Noort & O'Sullivan, 2006). In Britain, areas such as the Somerset Levels (Cole & Coles, 1986), the East Anglian Fenlands (Pryor, 1991) and the Humber Wetlands (Van de Noort, 1998) have provided archaeologists with a wealth of environmental and material information.

A review by Bain *et al.* (2011) underlines the risks that peat deposits are facing, as processes such as land drainage, peat cutting and agricultural activities put them increasingly at risk. The detrimental effect that this has on the archaeology contained within them is well documented; indeed the fact that so many archaeological sites are now known is testament to the risk that they face, as they often become visible only when they become desiccated, or are revealed by farming activities (e.g. Buckland, 1993). The effects of changing burial conditions on organic archaeology are illustrated by several examples that have relevance to the situation at Star Carr, outlined below.

1.5.5.1 Flag Fen, UK

Flag Fen, near Peterborough (National Grid Reference TL 22841 991144) is an Iron Age site discovered in 1982, in which both organic and inorganic material has been well preserved within a waterlogged peat land environment. In recent years, extensive drainage and peat cutting has led to an extreme level of peat shrinkage across the Fens, with documented shrinkage of several metres occurring over the last century (Pryor, 1991).

The impact of this changing environment on the archaeology is clear; originally, the wood excavated from Flag Fen in 1982 was so well preserved that tool marks, wood species and wear marks were all easily identifiable (Taylor, 1992). Recently however, in parts of the site wood has been excavated in much poorer condition (Powell *et al.*, 2001). This has been attributed to the recorded land drainage, and resulting peat shrinkage. This has had the combined effect of increasing the compression factor of the peat (causing compression of the delicate archaeological wood) and creating an oxygenated environment in which aerobic bacteria may thrive, causing increased degradation of both the lignin and cellulose components of wood. A programme of *in situ* preservation is now in place at the site, and a large-scale investigation of microbial decay is being carried out in conjunction with this (Powell *et al.*, 2001). A number of modern wood samples have been buried across the site and have

been removed periodically for analysis by SEM, in order to identify any increase in biological activity (Powell *et al.*, 2001).

1.5.5.2 Sweet Track, UK

Perhaps one of the most well-known archaeological wetland areas in Britain is the Somerset Levels (Coles & Coles, 1986; National Grid Reference ST 42133 40079). Some unique examples of woodworking have been discovered there, such as Neolithic arrow shafts and bows (Coles & Coles, 1986). In contrast to the well-preserved archaeological wood, faunal remains have only ever been found where pH is slightly elevated due to alkaline mineral deposits, illustrating the tendency for bone to dissolve in low pH environments (Gordon & Buikstra, 1981).

One of the most remarkable finds on the levels is a long track of carved wood dating to the 4th millennium B.C. – the ‘Sweet Track’, a raised walkway of oak, ash and lime timbers, reaching for approximately 2 km. SEM analysis of the wood in the 1980s by Coles & Coles (1986) found that the condition of the wood was variable from section to section, depending on the depth of the overlying peat.

Studies of the Levels in the 1980s aimed to establish the factors affecting preservation and led to a long term project of monitoring and *in situ* preservation, which continues today under an English Heritage initiative (Brunning *et al.*, 2000). The main objective is to monitor water-levels along the track and maintain these via a water pumping system if necessary. With the system currently in place, the water-table has been successfully kept above the Sweet Track since 1993. Research in 2000 by the Royal Holloway Institute for Environmental Research showed that the height of this was more or less stable (Brunning *et al.*, 2000). In recent years, peat extraction has also been tightly controlled and tree felling undertaken to prevent root damage to the archaeology.

In the wider region however, recent intensification of drainage of the wetlands for agricultural purposes could be putting undiscovered wooden artefacts at more risk (e.g. Brunning *et al.*, 2000; Geary *et al.*, 2010). Cox *et al.* (2001) compared the Sweet Track site to the nearby site of Abbot’s Way (National Grid Reference ST 4180 4278) where the water-table had not been maintained. It was found that wood still present was in extremely poor condition, with some of it being impossible to identify, illustrating the negative impact that land drainage can have on the preservation of wood.

1.5.5.3 Fiskerton, UK

A large timber causeway, along with other organic and inorganic artefacts, was uncovered at the Iron Age site of Fiskerton, Lincolnshire in 1981 (Field & Parker-Pearson, 2003). During later years, the site underwent an extended period of drainage and intensive farming before the threat to the archaeology was recognised and re-watering of the site instigated (Fell, 2005).

The effects of re-watering were closely studied by implementing a series of *in situ* burial experiments and programme of hydrological monitoring (Williams *et al.*, 2006). Prior to the rewetting of the site, pieces of archaeological and modern animal bone (cooked and uncooked) were suspended using plastic tubes, at different depths in the peat for a period of three years, and the water chemistry and level of the water-table monitored during this time. Some pieces were suspended at a depth that was permanently water saturated (anaerobic conditions) and some were permanently dry (aerobic conditions), but others were situated in an area of alternating wet/dry conditions as the water-table moved vertically seasonally. Deterioration of bone was measured by mass loss and assessment of damage to the collagen structure carried out using TEM. Within three years significant degradation of the bone was observed. The worst affected pieces were those in the region of the fluctuating water-table, illustrating the important role that the water-table plays in preserving organic materials (Williams *et al.*, 2006).

1.5.5.4 Yoxall Bridge, UK

An accumulation of Bronze Age timbers was found in 1994 at Yoxall Bridge, Staffordshire (National Grid Reference SK 13120 17748). Archaeological investigations at the site have consisted mainly of sediment, pollen and macrofossil analysis with the aim of understanding the wider regional context (Smith *et al.*, 2001).

Routine soil analysis revealed pH values of < 2 at Yoxall Bridge as well as another site in the region (Brown *et al.*, 2010); this is of a similar pH to areas of Star Carr (Boreham *et al.*, 2011). A sulfur content of over 3.5 % was recorded (soils typically have a sulfur content of 0.005 – 0.05 %; Steinburgs *et al.*, 1961), leading to the hypothesis that the acidity had been caused by underlying gypsum deposits causing sulfuric acid formation upon oxidation (Brown *et al.*, 2010). Despite the high acidity at Yoxall Bridge, wooden artefacts were well preserved and it was concluded that such acidity may even be conducive to this level of preservation (Brown *et al.*, 2010). However, little further research was undertaken into the effects this high acidity may have had on any other archaeological remains, particularly bone.

1.5.5.5 Nydam, Denmark

The site of Nydam in Jutland, Denmark is an Iron Age site located on the banks of a prehistoric lake, where it is believed that sacrificial offerings were deposited. As a result, an abundance of organic and inorganic remains have been found (e.g. Rieck, 1997). Due to the quantity of artefacts present, it was decided in 1997 to preserve the site *in situ*.

Over a 7-year period following the decision to stop excavations, thorough *in situ* monitoring of geochemical parameters (water-levels, pH, redox, and chemical composition) was carried out in order to establish the stability of the site (Mattheisen 2004; Mattheisen *et al.*, 2006). The study illustrated the importance of long term monitoring in determining future management of the site (e.g. whether to continue to preserve the site *in situ*). Throughout the monitoring period, it was deemed essential to maintain a neutral pH and a high water-table, a strategy which enabled the continued survival of both organic and inorganic remains.

1.5.6 Summary

These case studies serve to illustrate the importance of gaining an understanding of a burial environment and the impact that changes within it might have on the survival of organic archaeological materials. Through successful monitoring (e.g. Nydam), chemical and biological changes can be quickly identified and mitigation strategies put in place to ensure the continued preservation at the site (e.g. Sweet Track).

The research undertaken in this study, whilst focused on Star Carr, is applicable to other archaeological sites that are at risk of undergoing similar processes. Gaining an understanding of the threshold conditions at which organic materials can survive is critical to informing the management of wetland sites.

1.6 Conclusions and aims

The site of Star Carr has recently revealed potential evidence for accelerated organic deterioration (Milner *et al.*, 2011a; Section 1.1.3). Geochemical analysis strongly indicates that this is due to changing site conditions, primarily site drainage and a resulting increased acidity (a full review of this is given in Chapter 2). A review of several other wetland archaeological sites illustrates how changing burial conditions can have adverse effects on the survival of organic remains (e.g. Powell, 2001; Williams *et al.*, 2006). The example of Flag Fen illustrates the detrimental effect of a lowering water-table on the survival of wooden artefacts in particular (Section 1.4.5.1), whilst the studies at Fiskerton showed that a water-table which fluctuates through the archaeological layer may lead to the loss of bone in a relatively short period of time (Section 1.4.5.3).

Although a great deal of research has previously been carried out regarding bone and wood deterioration, both in archaeological and other contexts, the current conditions at Star Carr present some unknowns. In particular, archaeological sites with acidity as high as observed at Star Carr (< pH 2; Boreham *et al.*, 2011) that still contain bone, antler and wood are not known. In addition, experimental diagenetic studies do not consider the effects of as low pH as has been observed at Star Carr, and as such our understanding of organic preservation under these conditions is very limited.

The aim of this study was to generate relevant data to further understand the preservation of organic materials at Star Carr. This has been achieved by following several key objectives:

- To assess the current geochemical conditions at Star Carr
- To determine whether these conditions could be solely responsible for the observed organic decay
- To assess the state of preservation of archaeological material excavated from the Star Carr site, and compare this to experimental data

By achieving this greater understanding, questions raised following observations reported by Milner *et al.* (2011a; Section 1.1.2.4) and Boreham *et al.* (2011; Chapter 2) could be assessed; primarily, whether deterioration at Star Carr had indeed occurred recently, and whether increased acidity was the major cause of this. By answering these questions, the aim was to provide the scientific evidence to enable the appropriate authorities to assess whether anything can be done to mitigate against the deterioration. This study has important archaeological implications of these results on both the unexcavated archaeology at Star Carr and for preservation at other wetland sites, particularly acidic sites.

An experimental approach has been taken, with the aim of answering these questions. A review of the current burial conditions at Star Carr was first carried out (Chapter 2) and appropriate methods of analysis of deterioration established (Chapter 3). Following that, the effects of high acidity alone on the degradation of bone and wood has been considered (Chapter 4). However, as burial conditions are more complex than can be estimated by one parameter, burial experiments have been carried out alongside this controlled study. To begin with, these were performed under semi-controlled conditions in a lab (Chapter 5). *In situ* burial experiments were then carried out, in order to represent true site conditions as close as possible (Chapter 6).

Comparison of results from these experiments has been made with archaeological material, both from Star Carr and other sites, through the application of a suite of appropriate analytical techniques (Chapter 7). This has expanded the understanding of the deterioration of organic remains not only at Star Carr but other archaeological sites that have similar burial conditions, or are at risk of undergoing similar alterations in site conditions.

CHAPTER 2

A REVIEW OF GEOCHEMICAL OBSERVATIONS AT STAR CARR

2.1 Introduction

The mechanisms and rate by which any archaeological material deteriorates is heavily dependent on factors such as local hydrology, pH and microbial activity of the burial environment (Caple, 1994; Nicholson, 1996; Turner-Walker, 2008; Chapter 1, Section 4). Several studies show how important it is to characterise and understand these factors when making decisions regarding the management of an archaeological site; for example whether to preserve the site *in situ* (e.g. Williams *et al.*, 2006) or whether to implement long-term management strategies such as artificially increasing the water-table (e.g. Brunning *et al.*, 2000). In recent years, as more and more archaeological sites are preserved *in situ* (e.g. Mattheisen *et al.*, 2006; Pollard, 2006) it has also become more important to closely monitor any alterations in the burial conditions and anticipate the effects these might have on any remaining archaeology (e.g. Kars, 1998; Mattheisen, 2004).

Examples of monitored sites are now found across the UK and Northern Europe, where policies of *in situ* preservation are regularly advised (Mosely, 1996; Oxley, 1996). Water-table depths and variations in site hydrology are often surveyed adjacent to an archaeological site, either continuously, using automatic data loggers, or by regular manual measurements (e.g. Davis, 1996; Brunning, 2006). Alongside this, recording of pH and redox can serve as a proxy for preservation potential; redox in particular can indicate potential levels of biological activity. In addition, changes to pH and redox serve as a marker for changing chemical conditions of the burial environment (e.g. Pollard, 1996; Mattheisen, 2006). Characterisation often goes further than this, constituting analyses such as total organic carbon, calcium, phosphate and sulfur content to provide a detailed understanding of the chemical nature of the burial environment (Nicholson, 1996; Crowther, 2002).

Until recently, no prolonged period of hydrological or geochemical analysis had taken place at the Star Carr site. However, there were indications that deterioration of organic remains at the site was linked to changes within the burial environment, although much of this evidence could be considered largely anecdotal. During field walking in 2002 and 2003, the presence of large numbers of lithics on the ground surface, and the observation of a previously hidden contour led to the hypothesis that peat shrinkage had occurred (Boreham *et al.*, 2011). In addition, comparison of water levels in the trenches during excavations in 2007 and 2008 with photographic records of original excavations (Clark, 1954), suggested that the water-table had lowered (Chapter 1, Section 1.1.2).

Following these observations, a small-scale survey of pH across the site was carried out and results showed that parts of the site were highly acidic, reaching < pH 3 in places (Needham, 2007). Between 2009 and 2012, a number of larger scale projects were implemented, in order to more fully understand the site conditions. More specifically, it was hoped to ascertain whether changes were recent, and how the changes were linked to the observed organic decay (Boreham *et al.*, 2011; Brown *et al.*, 2011; Milner *et al.*, 2011a; Bradley *et al.*, 2012).

As part of this study, the results of these previous assessments have been compiled and used as a starting point from which to investigate organic deterioration at the site. While these studies have provided a great deal of geochemical and hydrological data, they still span a relatively short period. Therefore, in order to slightly extend the time-scale of the geochemical assessment and determine whether data from those studies represent current site conditions, further small-scale measurements have been recorded as part of the current study. In most cases, these measurements have been taken alongside the excavation of organic remains, and therefore cover only a small area of the site.

2.2 Summary of previous studies

The following discussion is compiled from results published by Needham (2007), Boreham *et al.* (2011), Brown *et al.* (2011) and Bradley *et al.* (2012).

2.2.1 Background (wider context)

Star Carr is located within the Vale of Pickering, which is bordered by Cretaceous chalk to the south and Jurassic limestone to the north (Figure 2.1). The base of the vale, in which Star Carr is situated, is primarily sand and gravel post-glacial alluvium, surrounded by Cretaceous and Jurassic clay and chalk outcrops. Above this bedrock lie more gravel, glacial sands and Speeton and Kimmeridge clays; both types of clay are very low in permeability and high in pyrite concentrations (Dypvik, 1984). Above these formations are the Mesolithic reedy and wood peats.

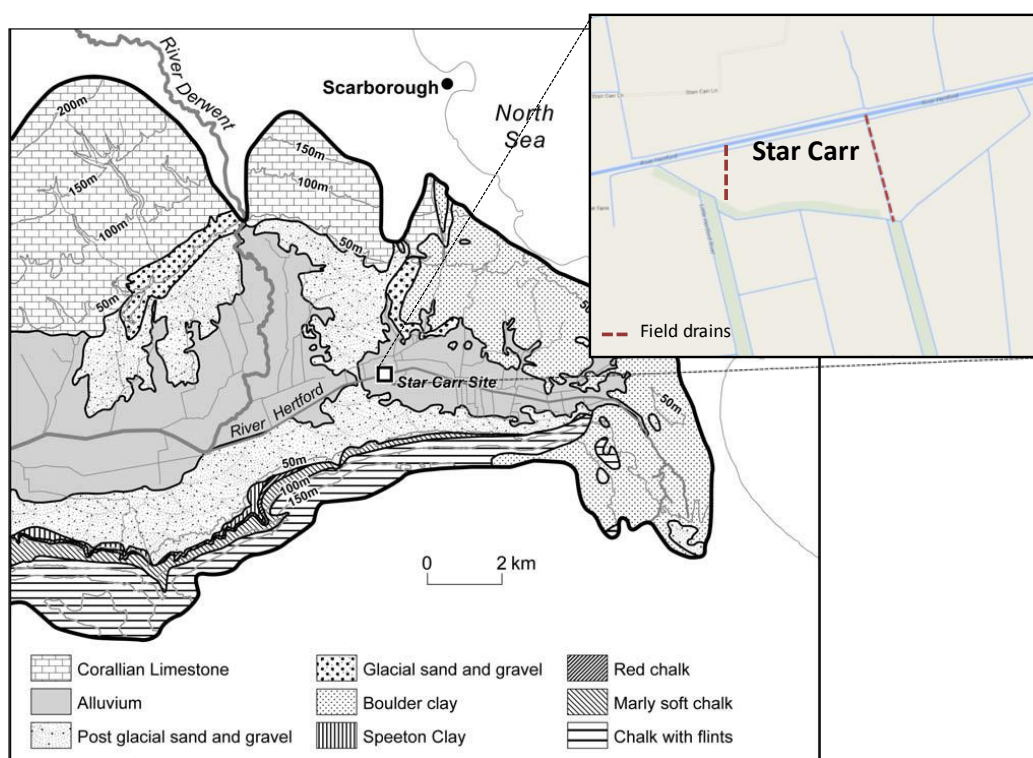


Figure 2.1: Geological map of the Vale of Pickering, showing Star Carr located on alluvium bedrock. Inset shows detail of the site, bordered by the Hertford cut to the north and field drains to the east and west. Adapted from Brown *et al.* (2011).

The majority of the Mesolithic archaeology is located within these peats at a depth of between ~ 0.8 and 1.2 m below ground level, which has probably contributed to the preservation of organic materials (Chapter 1, Section 1.4). A high-resolution auger survey conducted by Boreham *et al.* (2011), consisting of three transects across the site established that the sediments directly underlying the peats vary locally (Figure 2.2, bottom). Speeton or

Kimmeridge clay outcrops of varying thickness lie between the peat and the alluvium gravels in places. These may cause local variations in soil chemistry and hydrology (Welch & Thomas, 1996).

Upwelling groundwater at the site is believed to originate primarily from a calcium-rich local aquifer, and the nearby river Derwent may also have an effect on local hydrology. Both water sources are neutral or slightly alkaline, due to the influence of the local chalk and limestone. A man-made channel, the river Hertford, closely borders the site to the north, and field ditches extend down the east and west side of the field in which Star Carr is contained. The Hertford cut is fed mainly from a nearby chalk spring. In addition, in 2000 AD underground field drains were installed across the field for agricultural purposes, running parallel to the Hertford cut and discharging into the east and west ditches.

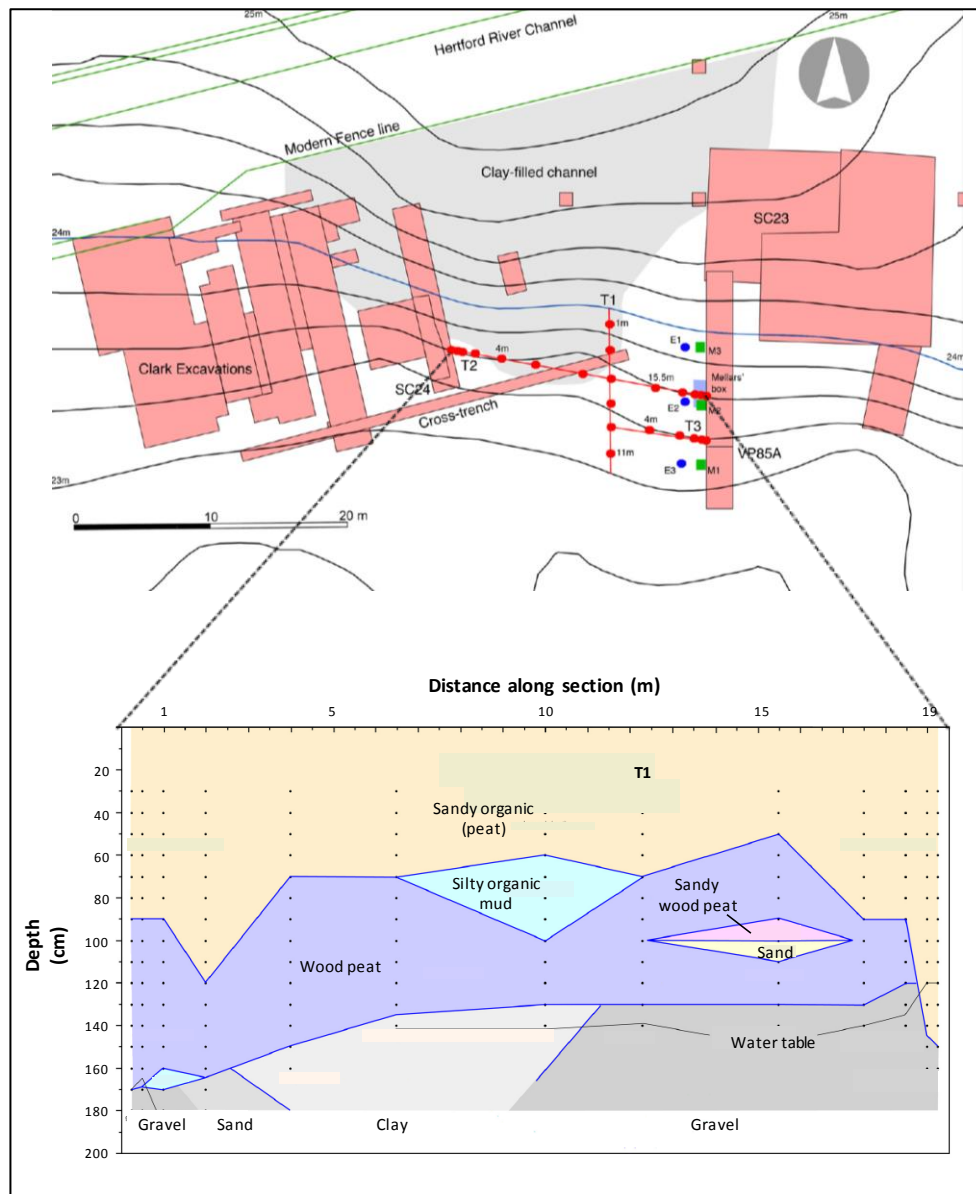


Figure 2.2: Diagram showing the extent of the geochemical survey carried out in 2009 (top). Detailed stratigraphy through a transect of the site illustrates the local variability of the sediments underlying the archaeological deposits (bottom). Reproduced with permission from Boreham et al. (2011). (Originally in colour).

2.2.2 The geochemistry of Star Carr

2.2.2.1 Scope of previous study

In 2007, pH values recorded during excavations at Star Carr were found to be lower than pH 3 in the southern end of Trench SC24 (located in the wetland area of the site; see Chapter 1, Figure 1.3) (Needham, 2007). Although peat is often slightly acidic (pH <6), values this low are unusual, and the effects of such high acidity on organic archaeological remains not well understood (Chapter 1, Sections 1.2 and 1.3). This led to the hypothesis that the organic deterioration observed in the material from the 2007 and 2008 excavations was likely to be linked to geochemical changes, primarily increased acidity. In addition to this, a number of observations made during excavations were judged to be indicative of unusual geochemical activity; for example, orange residues forming in the flotation tank (used to sieve the excavated sediments for small finds) were characterised by their colour as iron oxide (Schwertmann & Cornell, 2000; Needham, 2007). An extensive survey carried out in 2009 aimed to build upon this initial evidence, and ascertain the extent of the potential acidification (Boreham *et al.*, 2011).

The 2009 survey involved analysis of a series of cores, encompassing the three transects across the site indicated in Figure 2.2. Two of these transects cut through previous trenches, with the aim of establishing any influence of excavation on the chemistry of the sediments. The sequences were measured for pH and redox at 10 cm depth intervals, and cores taken at approximately 2 m intervals, providing high resolution analysis of spatial variations in pH. In addition, identical analysis was carried out on archive auger cores, removed during excavations in 1985 and stored at the University of Cambridge in the intervening years. The aim of this was to determine whether any post-excavation alteration of the sediments had occurred. Further time-dependent pH tests were carried out on a number of fresh sediment samples, with pH and redox recorded at intervals on samples left exposed to the air (Boreham in Milner *et al.*, 2010).

In addition to pH and redox analysis, measurements such as total organic content, iron II: iron III ratios and sulfate: sulfide ratios and aluminium and manganese concentrations were carried out at each sampling point to provide a more detailed survey of the site chemistry.

2.2.2.2 pH and redox analysis

The pH of sediments analysed in the field differed hugely, spanning between pH < 2 and 8.43; similar variability was observed upon analysis of the archive cores. Sediments tended to become more acidic with depth, with the region of the archaeology displaying the lowest pH

(Figure 2.3). Below the archaeology, pH tended to rise again. This could be due to the presence of groundwater, resulting in less oxidation of sulfides to acidic sulfates (Boreham *et al.*, 2011).

Correlation with the stratigraphy of the sediments indicated that these local variations could be the direct result of the variations in the underlying sediments (Figure 2.3). In particular, the presence of thin clay lenses underlying the peats in areas of the site seems to correlate with increased acidification. In areas where the peat is underlain by thick gravel, pH tended to be higher; this is likely to be explained by the absence of pyrite-rich clays resulting in a lower sulfate concentration. Closer to the lake edge, an increase in pH was also observed, attributed to carbonate-rich lake marls causing buffering (Boreham *et al.*, 2011)

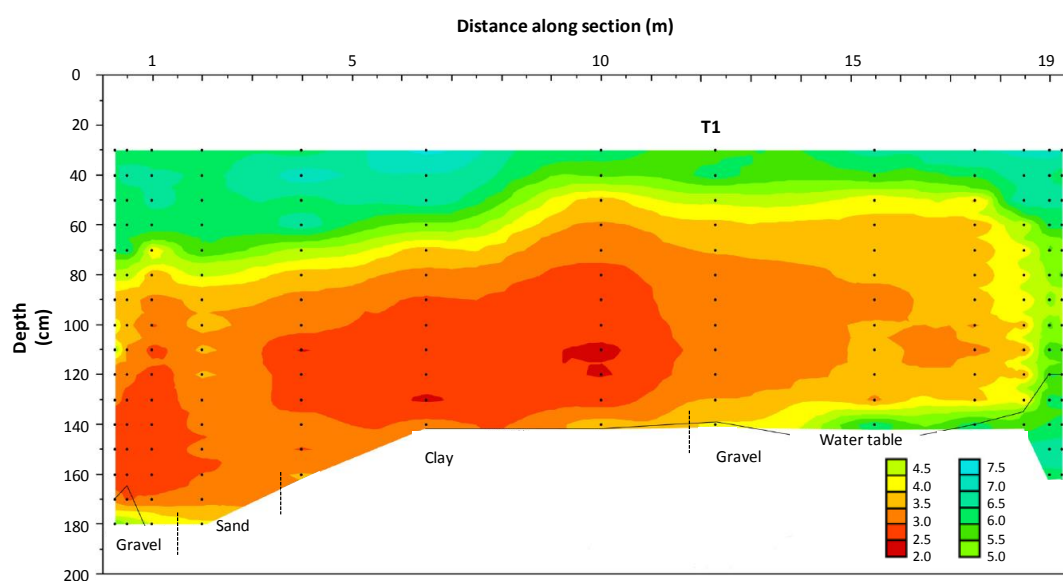


Figure 2.3: Plot of measured pH values of the transect illustrated in Figure 2.2, showing the variability in pH across the site; pH is lower directly above clay outcrops. Reproduced with permission from Boreham *et al.* (2011). (Originally in colour).

Where the survey transected through previously excavated trenches, some evidence for a 'halo' effect was observed; pH was increased in the backfill and extending horizontally into fresh sediments, compared to the surrounding sediment. A possible explanation for this is the mixing up of less acidic plough soil with the peats during backfilling of the trench.

Time-dependent analysis, where measurements of pH were taken at intervals of several minutes following exposure to air, revealed evidence for rapid alteration upon exposure to oxygen. The response differed in different samples however; in samples already displaying acidity, pH decreased logarithmically indicating a tendency to undergo oxidation rapidly upon exposure to air (e.g. Patrick & Mahapatra, 1968). In more neutral samples (closer to the surface) however, pH increased slightly. These changes in pH indicate that the sediments are 'vulnerable' and can easily oxidise on contact with air (Boreham *et al.*, 2011).

A wide range of redox potentials (- 44mV to + 600 mV) were also measured across the site, further indicating that different chemical processes may be occurring in different parts of the site. A high redox potential indicates a tendency of sediments to become reduced, catalysing oxidation reactions (e.g. Patrick & Mahapatra, 1968). Redox measurements recorded by Boreham *et al.* (2011) at Star Carr were most elevated in regions where pH was low (+400 mV to +600 mV); sediments with redox values > 400 mV are generally described as highly oxidative (Patrick & Mahapatra, 1968). As well as indicating the presence of oxygen, high redox potential can be attributed to high concentrations of acid, as acids readily accept electrons, facilitating oxidation (Atkins *et al.*, 2006). In the more neutral topsoil, redox potential was lower (< 200 mV). Changes in redox potential between the field and lab further confirmed the vulnerability to oxidation displayed by the sediments at Star Carr.

2.2.2.3 Elemental analysis

Elevated levels of total iron were determined in the base and top of most boreholes. The oxidation state of iron serves as an indicator of the state of oxidation of the sediments (Boreham *et al.*, 2011); low levels of iron III present indicated that much of the sediment was not completely oxidised at the time of analysis.

The concentrations of sulfur were found to be elevated throughout each transect. High concentrations were often associated with elevated iron concentrations, leading to the hypothesis that both originated from pyrite (FeS₂) in the underlying Speeton and Kimmeridge clay deposits. In addition, sulfur concentrations tended to be higher towards the base of the sequences, indicating the source of the sulfur as from below the sequence. The high concentrations of sulfur indicate that high acidity across the site is likely to be caused by the formation of high levels of sulfuric acid due to oxidation of the sediments.

Comparison of the sulfide: sulfate ratios revealed increased levels of sulfate in archive boreholes compared to those taken as part of the study. This suggests that oxidation of the sulfide had occurred in the archive boreholes over time, and is likely to explain the increase in acidity through sulfuric acid formation. The overall reaction is shown in Equation 2.1.

Equation 2.1: Oxidation of sulfide to sulfuric acid.



This rapid oxidation of sulfides to sulfates further indicates that sediments from parts of the site have the potential to undergo redox reactions once exposed, further illustrating their vulnerability.

2.2.3 The hydrology of Star Carr

2.2.3.1 Scope of previous study

During excavations in 2006 and 2007, it was noticed that the level of water in excavated wetland trenches appeared a lot lower than indicated by photographic evidence of the original excavations, reported by Clark (1954). Concerns were raised that this may have been the direct result of the land drainage undertaken for agricultural purposes. Hydrological assessment of the area surrounding Star Carr was therefore carried out in order to determine the source of groundwater at the site and infer the effects that drainage may be having on the land (Brown *et al.*, 2011). This was done using computer modelling as well as by collating existing hydrological data from the British Atmospheric Data Centre, the Environment Agency and the British Geological Survey.

Between September 2010 and September 2011, a series of dipwells across the Star Carr site and surrounding area was monitored monthly, in order to provide realistic data on the height of the water-table and complement the previous modelling-based study conducted by Brown *et al.* (2011). In one of these dipwells, an automatic data logger was placed to record a higher time resolution of water level data.

Isotopic analysis of hydrogen and oxygen present in groundwater can be used to identify the source of the groundwater, as processes occurring during the water cycle cause the relative proportions of heavy and light isotopes to alter (Bradley *et al.*, 2007). Isotopic analysis was therefore carried out during both studies, on water samples taken from the dipwells, the Hertford cut, the bordering field ditches and a nearby chalk spring that is believed to come directly from the local limestone aquifer.

2.2.3.2 Summary of hydrology results

It was hypothesised from the computer modelling survey and field data that the insertion of the underground drainage system in 2000 AD may have lowered the water-table by as much as 0.5 m, and as such resulted in the Star Carr site effectively being isolated from any regional hydrological influences. Data obtained for water levels in the Hertford cut revealed no reduction in water levels since 1989, further confirming that changes in hydrology of the Star Carr site are localised. Over the period from 2000, since the insertion of the field drains, data from the British Atmospheric Data Centre shows that the area was predominantly wetter than average, suggesting that any drainage of the land was not climate driven. Hydrogen and oxygen isotopic analysis of groundwater from in and around the Star Carr site indicated that residence times of the groundwater were short, confirming the hydrological isolation of the

site. This suggests that groundwater is likely to originate from precipitation, rather than any local aquifers.

Measurements of water levels in the series of dipwells between September 2010 and September 2011 confirmed these findings, further suggesting that recent drainage at the Star Carr site has occurred, and is the result of field drainage rather than wider hydrological influences.

Boreham *et al.*, (2011) had also hypothesised that Star Carr is hydrologically isolated, based on the stark differences in groundwater chemistry between acidic water at the site and the neutral to alkaline local chalk spring and Hertford cut. The formation of sulfuric acid due to oxidation of sulfides was also hypothesised to be linked to the reduction of the water-table (see Section 2.4 for discussion).

2.3 Further geochemical analysis

2.3.1 Introduction

Previous geochemical analysis afforded a wealth of information regarding the geochemistry and hydrology of the Star Carr site. Rapidly altering pH values and high redox potential in sediment samples from parts of the site following exposure to air demonstrated that sediments in parts of the Star Carr site are highly vulnerable, and that further exposure to air may cause oxidation of these sediments, increasing their acidity even more (Boreham *et al.*, 2011). For these reasons, it was decided that a further extensive geochemical investigation (for example by conducting an auger survey) would not add sufficiently to previous surveys to justify the possible damage to the archaeology, and would therefore not be carried out as part of this study.

Despite this, opportunities for limited geochemical analysis were undertaken during archaeological excavations. This minimised the impact of further analysis, as well as allowing the direct correlation of the geochemical data with the preservation of archaeological material; the majority of samples were taken in association with bone artefacts and from the surface of exposed trenches. The aim was to supplement existing data, and test whether conditions at the site had significantly altered since analysis in 2009, rather than carry out an independent survey.

2.3.2 Methodology

2.3.2.1 pH and redox analysis

Sediment pH and redox potential were measured, using a method developed by Needham (2007) and based on that described by Nicholson (1996). Approximately 50 cm³ of soil was mixed with 20 cm³ of deionised water and agitated. pH and redox values of the resulting suspension were recorded using a hand held pH probe (Hanna Instrument). An adjustment of the values due to the addition of water is not necessary (e.g. Boreham *et al.*, 2011).

For groundwater samples, measurements were taken directly, using a hand held field probe (HI-98121 pH and ORP pocket probe, Hanna Instrument) calibrated using pH 4 and pH 7 reference solutions.

2.3.2.2 Elemental analysis

Total sulfur, hydrogen, carbon and nitrogen content analysis of soils was carried out on freeze-dried sediment samples. A Thermo Flash 2000 Elemental Analyser fitted with a MAS200R

autosampler, chromatographic column and thermal conductivity detector was used with helium as a carrier gas (Green, *in prep*). Soil samples (10-15 mg) were weighed into tin foil capsules and the capsules folded to exclude air. Samples were introduced for combustion, with a pulse of oxygen (250 ml min⁻¹, 5 s) into a quartz reactor tube, packed with copper oxide granules and electrolytic copper wires, held at 900°C. Sulfanilamide and cystine were used as standards.

2.3.2.3 Sampling strategy

2.3.2.3.1 Sediment analysis

The majority of geochemical analysis undertaken as part of this study was carried out in a large trench excavated in 2013 (SC34; Chapter 1, Figure 1.3) that extended into both the wetland and dryland areas of the site. Further analysis was carried out at nearby Flixton Island and a small test pit located to the North of Star Carr as part of *in situ* burial experiments; however, the discussion here has been limited specifically to the Star Carr site, and therefore only analysis from SC34 is presented. Results from the *in situ* experiments are discussed in Chapter 6.

In order to assess the vertical variation in pH, two series of samples were taken down the exposed wall of Trench SC34 during excavation (Figure 2.4). The first series was located at the interface between the backfill of VP85 (first excavated in 1985) and the unexcavated sediment). It was expected, based on the hypothesis of a 'halo' effect caused by excavation, developed by Boreham *et al.* (2011) that the previous exposure of the sediments may have had a localised impact on the surrounding sediments. The second series was located entirely within newly excavated sediment. The locations of both 'column' samples are indicated by a blue box in Figure 2.5.

Samples for these series down the trench were taken by clearing approximately 3 cm of sediment from the exposed surface and removing ~50 cm³ of new sediment for analysis at regular intervals down the profile. pH and redox were recorded for each sample.

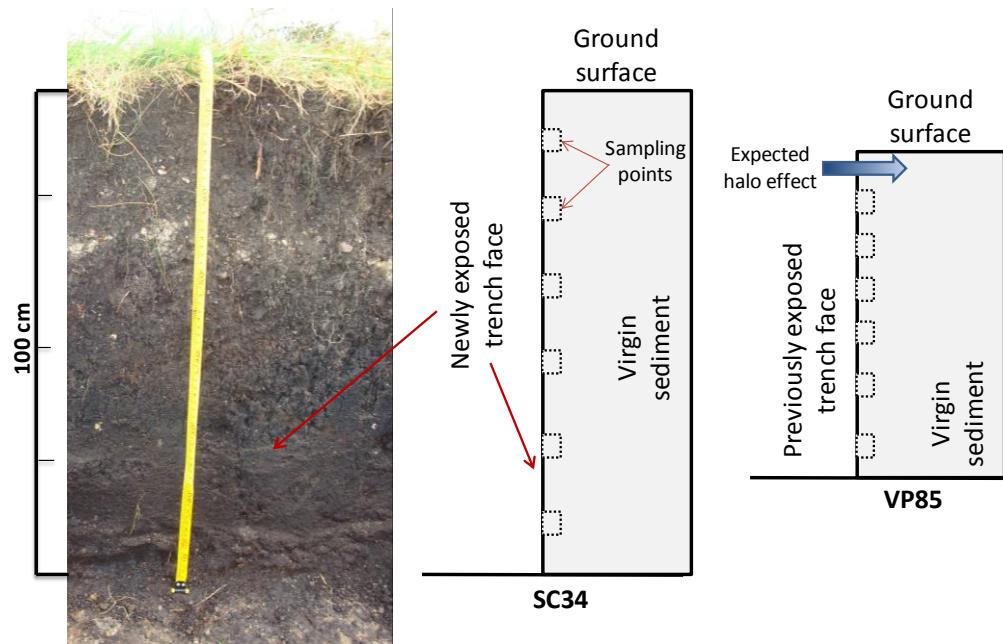


Figure 2.4: Schematic showing how column samples were taken into the virgin sediment from the trench face. In SC34 this trench face was newly exposed, whereas in VP85 the trench had been re-excavated, following previous excavation in 1985. The base of each trench represents the start of the archaeological zone (100 cm for SC34; 60 cm for VP85). (Originally in colour).

Additional samples were taken across the exposed surface of Trench SC34 during excavations, mainly in association with recovered organic artefacts. To minimise the effects of oxidation, immediately prior to sampling the exposed surface was cleared and fresh sediment removed for analysis. These samples were analysed for pH and redox, and summarised in Table 2.2.

2.3.2.3.2 Groundwater monitoring

A series of dipwells were installed around the perimeter of the Star Carr field by Brown *et al.* (2011) and monitored between September 2010 and September 2011 as part of the study by Bradley *et al.* (2012). In order to slightly expand the monitoring period and confirm that the current situation at the site is represented by the previous study, additional measurements and groundwater samples were taken from these on four occasions (October 2011; May, June and July 2012). The opportunity was also taken to record pH and redox values for groundwater in each dipwell, and make a comparison with the Hertford cut, field ditches and nearby spring. This was done by removing a ~20 mL sample of groundwater using a syringe after the water level had been recorded. The pH and redox of the water were measured immediately using hand held field probes (HI-98121 pH and ORP and HI-98130 EC pocket probes, Hanna Instrument).

2.3.3 Results

2.3.3.1 pH and redox

Sediment samples measured down the profile of the trench (column samples) reveal the vertical variation in the geochemistry of the Star Carr site (Table 2.1). Samples taken close to the backfill of a previously excavated trench (VP85) were much less acidic than those in a newly excavated trench. An explanation for this could be that neutralised topsoil was mixed into the peat during backfilling in 1985, further supporting the proposal by Boreham *et al.* (2011) that excavation of the site may alter the burial environment.

Table 2.1: pH recorded in the field and after 24 hours, and redox measurements for samples measured vertically down an exposed trench (Figure 2.4). Red values indicate where the pH decreased by more than 0.1 pH units after 24 hours. (Originally in colour).

Depth (cm)	Column samples					
	SC34 (fresh sediment)			VP85 (Backfill)		
	pH	pH + 24 hours	Redox (mV)	pH	pH + 24 hours	Redox (mV)
Surface				3.92	3.82	364
10	6.41	5.98	214	3.97	3.72	314
20				4.00	3.78	220
30	4.85	4.33	310	5.34	4.86	123
40				6.06	5.57	-20
50	3.41	3.36	384	6.11	5.96	-4
60				6.30	5.88	-84
70	2.60	2.58	440			
90	2.93	2.66	276			
100	3.23	2.99	198			

In the sediments adjacent to the backfilled trench (VP85), the soil becomes more neutral with depth, whereas adjacent to the new excavations it becomes more acidic. This is potentially due to differences in the underlying sediments, although it could also be due to oxidation occurring in the sediments close to VP85 following the original excavation in 1985. The diverse pH values in SC34 are comparable to those observed during the auger survey carried out in 2009, where pH also decreased in the region of the archaeology (Boreham *et al.*, 2011).

Low redox values (< 200 mV) in the region of the archaeology near VP85 shows that sediments are reduced, despite displaying low pH. This suggests that they are no longer as 'vulnerable' as

those from SC34, which are highly oxidising. However, differences in pH after 24 hours were observed in the backfill samples as well as those adjacent to fresh sediment (Table 2.1). This suggests that some oxidation post-excavation has occurred, signifying that the sediments were not completely oxidised prior to excavation.

Values of pH and redox recorded in the field across Trench SC34 (as well as pH after 24 hours for some samples) are shown in Table 2.2. Where sediment samples were taken alongside organic artefacts, the artefact sample number is given (left hand column), and additional sediment samples, that were not associated with artefacts, are numbered sequentially (right hand column).

Table 2.2: Geochemical data for soil samples taken from surface of excavated Trench SC34 in 2013. An asterisk indicates samples that were also analysed for sulfur content. When pH changed by more than 0.1 pH unit after 24 hours this is indicated by red for a negative change and blue for a positive change. (Originally in colour).

Soil samples adjacent to organic artefacts			Soil samples from across surface of trench			
Sample number	pH	Redox (mV)	Sample code	pH	pH + 24 hours	Redox (mV)
99342*	2.92	425	KH-S-01*	1.98	2.12	383
99755	2.24	365	KH-S-02*	2.13	2.24	385
99760	3.22	328	KH-S-03	2.36	2.20	430
99762*	2.22	369	KH-S-04	2.06	2.14	420
99790	2.29	306	KH-S-05	2.13	2.17	375
99876*	2.09	333	KH-S-06	3.21	3.14	287
99871*	2.30	322	KH-S-07	3.27	2.79	345
103369	3.98	240	KH-S-08	2.12	1.83	420
103423*	5.60	102	KH-S-09	2.86	2.83	238
103425	4.87	154	KH-S-10	4.58	4.76	191
103426*	4.44	190	KH-S-11	3.57	3.30	380
103639	6.58	84	KH-S-12	3.94	3.75	375
103644	6.58	20	KH-S-13	3.18	3.03	426
103645*	6.57	26	KH-S-14*	3.08	2.96	315
103646	6.48	135				
103648	4.49	282				

Measurements of pH and redox across the surface of Trench SC34 further confirmed that spatial variability in the geochemistry is significant. Even within the wetland areas of the trench, pH ranged from approximately neutral to less than 2.

In Figure 2.5, pH values have been plotted spatially. For these purposes it has been assumed that the pH measured at a point is broadly representative of the pH for approximately 0.5 m around the sample. This illustrates clearly the variability in sediment pH across the surface of Trench SC34: pH varies between 2.2 and 6.57 within metres in the southwest corner of the trench. This is therefore likely to have a localised impact on organic preservation.

Where high acidity (low pH) was recorded, sediments also displayed high redox (> 400 mV), which is to be expected due to the oxidising nature of acid (Atkins *et al.*, 2006). High redox also indicates a tendency for further redox reactions to occur, again supporting observations by Boreham *et al.* (2011) that sediments across the site are 'vulnerable.' Indeed, in all samples where pH was measured after 24 hours, pH had altered suggesting that oxidation had occurred.

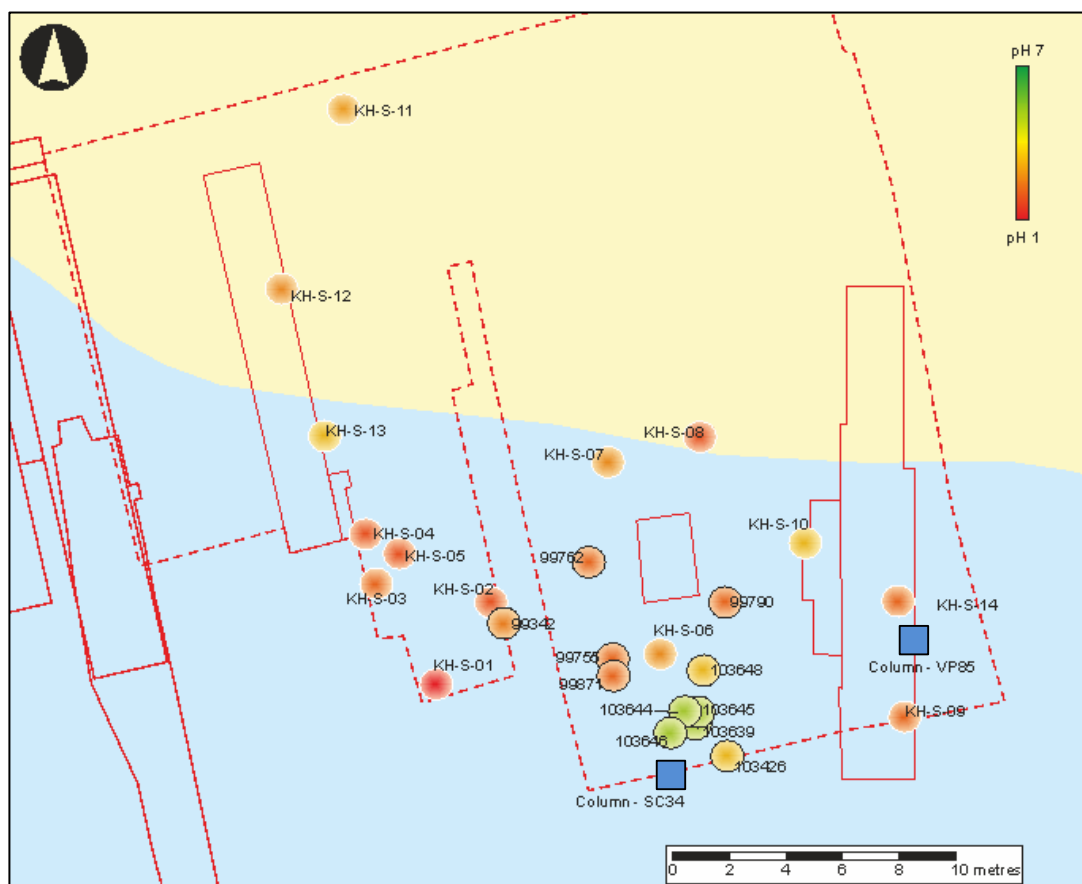


Figure 2.5: Plot of pH values measured across surface of SC34. Locations of column samples are indicated by a blue box, and black-outlined circles represent samples taken in association with organic artefacts. (Originally in colour).

2.3.3.2 Sulfur content

Percentage sulfur and carbon content was analysed for a small number of the samples in Table 2.1, with the aim of determining whether the high levels of sulfur across the site reported by Boreham *et al.* (2011) persist.

Soils typically range from 0.005 – 0.05 % sulfur content (Steinburgs *et al.*, 1961), meaning that sulfur content is elevated in all samples analysed from SC34, ranging from 1.4 – 20 % (Table 2.3). It is also highly variable however. This corroborates what was found in the larger scale investigation in 2009 (Boreham *et al.*, 2011). No correlation is seen between pH and sulfur content, although there does seem to be a lower level of carbon present in samples with a higher pH. This could be the result of higher clay content of the soil, as clay is less carbon rich than peat (e.g. Dypvik, 1984).

Table 2.3: Result of elemental analysis on selected sediment samples.

% Sulfur and carbon in analysed samples			
Sample	pH	% Sulfur	% Carbon
KH-S-01	1.98	7.3	34.3
KH-S-01	2.13	6.4	35.3
99342	2.92	1.4	46.5
99762	2.22	9.5	24.2
99876	2.09	10.0	33.2
99871	2.30	20.0	14.6
103423	5.60	6.1	2.9
103426	4.44	8.6	4.2
103645	6.57	7.6	2.2

2.3.3.3 Dipwell monitoring

Groundwater samples were collected from 11 dipwells around the Star Carr site in October 2011, May, June and July 2012, as well as from the field ditches, Hertford cut and the local spring, expected to originate from the limestone aquifer (Bradley *et al.*, 2012) (Figure 2.6). Data from the pH analysis is shown in Table 2.4.

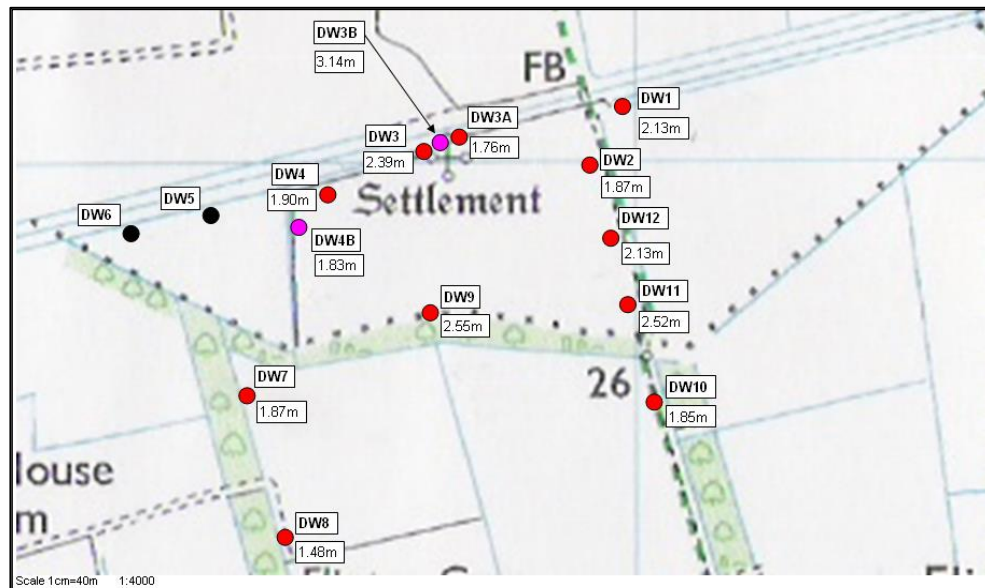


Figure 2.6: Location of dipwells (indicated by circles) around the Star Carr site, along with the depth of the dipwells. Reproduced with permission from Bradley *et al.* (2012).

All dipwell samples were slightly acidic or neutral, ranging from pH 5.4 to 7.5 (Table 2.4). Analysis of water from both the Hertford cut and local spring showed that both potential water sources were slightly more alkaline, reading pH 7.3 to 8.3. This is in agreement with the hypothesis proposed by Brown *et al.* (2011) that Star Carr is hydrologically isolated from regional water sources, and that the observed acidity originates from chemical conditions within the site itself. Slightly lower values in the field ditches support this, as these contain groundwater that has originated from the site itself, which may have increased their observed acidity.

Water levels remained at similar levels to those in 2010/11 reported by Bradley *et al.* (2012) indicating that data obtained during the earlier study is representative of site conditions a year later. No clear correlation was observed between water-table depth and pH. However, the time-scale of the period of monitoring was not long enough to establish long term trends.

Table 2.4: pH values of selected groundwater samples analysed on four occasions from 2011-2012. Where no value is given, the dipwell was dry.

pH of groundwater samples				
Dipwell	October 2011	May 2012	June 2012	July 2012
DW-1	5.43	6.37	6.49	
DW-2	6.31	6.63	6.62	7.00
DW-3		7.35	7.47	7.71
DW-7	7.27	7.02	6.96	
DW-9	7.42	6.98	7.27	7.48
DW-11	7.35	7.37	7.55	7.81
West field ditch	6.57	7.99	7.94	8.03
East field ditch	7.17	7.94	7.52	7.57
Local spring	7.54	7.54	7.62	7.88
Hertford Cut	7.35	8.32	7.54	7.95

Evidence for high levels of iron oxide was noted during water sampling, in the form of orange-brown deposits in and around the field ditches (Schwertmann & Cornell, 2000).

2.4 Discussion and review

From geochemical analysis carried out by Boreham *et al.* (2011), it is clear that parts of Star Carr are highly acidic. High levels of sulfur present across the site suggest that this is likely to be due to the formation of sulfuric acid. Further analysis as part of this study confirmed those observations, indicating that the conditions observed in 2009 are representative of current conditions at Star Carr.

Both Boreham *et al.* (2011) and Brown *et al.* (2011) suggested that this high acidity is likely to be a major factor stimulating organic decay at the site. Evidence closely links this high acidity to alterations in the hydrology of the site; oxidation of sulfides to sulfate occurs following introduction of oxygen into the sediments. Archive hydrological data suggests that this alteration has occurred recently (compiled in Brown *et al.*, 2011). This is in agreement with the hypothesis that organic decay has occurred recently and is caused primarily by alterations of burial conditions at the Star Carr site, as proposed by Milner *et al.* (2011a).

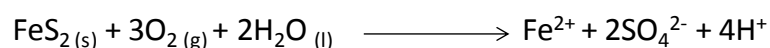
The complex underlying stratigraphy of the site, reported by Boreham *et al.* (2011), combined with changes in the water-table appears to have contributed to altering the specific chemical environment of the Star Carr site. Importantly, it appears to have resulted in highly localised spatial variations in the acidity of the site, and although parts of the site are highly acidic, areas remain that are almost neutral.

The complex geochemistry observed across the site is likely to be caused by a number of contributing and conflicting factors. Several are summarised below.

2.4.1 Acid rock drainage (ARD)

Evidence for high levels of iron and sulfur indicate that a process similar to acid rock drainage (ARD) may be occurring at the Star Carr site (e.g. Robb & Robinson, 1995; Warren, 2011). This is a process often seen in association with some mining activities, where the exposure of sulfide-containing minerals to both air and oxygen results in the formation of sulfuric acid. The most common geological source of sulfide is pyrite (FeS₂). The exact mechanism of its oxidation is not fully understood; the process is likely to involve a series of oxidation and reduction steps, driven by both chemical and biological influences (Egiebor & Oni, 2007). However, the overall conversion can be simplified according to Equation 2.1.

Equation 2.2: Formation of sulfuric acid from pyrite.



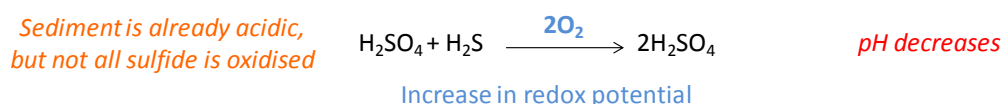
Pyrite had been hypothesised to be the main source of high levels of sulfur at the Star Carr site (Boreham *et al.*, 2011; Brown *et al.*, 2011). It is likely to originate from the underlying Speeton and Kimmeridge clay deposits, sediments characterised by high pyrite content (Dypvik, 1984). Indeed, the proposed hydrological isolation of the site strongly indicates that the sulfur must originate from within the site. Although agricultural activities such as fertilisation may also have some contribution (Needham, 2007), hydrogen and oxygen isotope analysis and the pattern of sulfate concentrations in the sediments suggest that the source of the sulfur lies primarily below the archaeology (Brown *et al.*, 2011; Boreham *et al.*, 2011).

The alterations in pH and redox potential in the sediments following exposure to air reported by Boreham *et al.* (2011) strongly supports the hypothesis that the presence of sulfides and sulfates are responsible for the high levels of acidity at the site. Three different scenarios were noted:

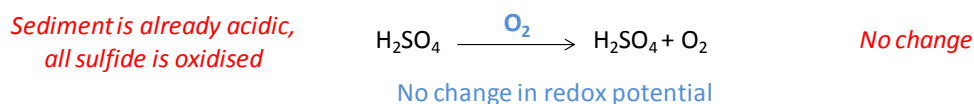
- Where sediments that were already acidic became more acidic and underwent an increase in redox potential
- Where acidic sediments underwent little or no change in pH or redox potential
- Where near neutral sediments underwent an increase in pH and decrease in redox potential.

This third scenario has been attributed to the presence of calcium in the topsoils, causing the reaction of sulfate to gypsum following exposure to air. All three processes and explanations are summarised in Figure 2.7.

Scenario 1:



Scenario 2:



Scenario 3:

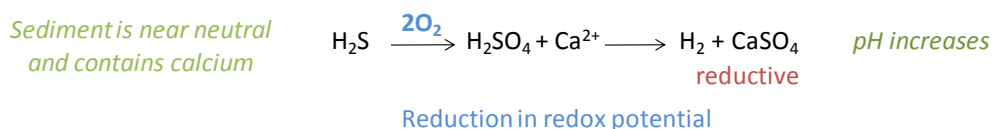


Figure 2.7: Proposed mechanisms of changes in acidity and redox potential upon exposure to oxygen. (Originally in colour).

2.4.2 Biological implications

It is normally assumed that under anaerobic (i.e. waterlogged) conditions, microbial activity is suppressed and thus biological activity can be considered a minor factor in the deterioration of wood and bone (e.g. Kim & Singh, 2000; Chapter 1 Section 1.4.3.1). It is possible however, that anaerobic bacteria are present (Chapter 1, Section 1.4.3.2). The formation of sulfuric acid from pyrite is likely to be catalysed by certain strains of anaerobic bacteria which oxidise iron as part of the metabolic process, assisting in the initial breakdown of pyrite (Egebor & Oni, 2007). Such bacteria are often acidophilic, surviving or indeed flourishing at low pH, meaning that high levels of acidity do not necessarily lead to the absence of biological activity.

Conversely, the presence of sulfate-reducing bacteria may mitigate the sulfuric acid formation by reducing the sulfates to sulfides via Equation 2.3 (Robb & Robinson, 1995). These bacteria are also strictly anaerobic (Postgate, 1965). Hydrogen sulfide (H₂S) can be identified by its characteristic smell and has frequently been noted during recent excavations at Star Carr (various excavators, pers. comm.), suggesting that this process is occurring.

Equation 2.3: Bacterial reduction of sulfates.



In areas of the site where pH is higher, it is possible that increases in acidity caused by the metabolism of pyrite by some anaerobic bacteria is therefore mitigated by the co-existence of sulfate reducing bacteria. In other areas however, it appears that the lowered water-table allows ARD to proceed at a rate that is not mitigated by the reduction of sulfates to hydrogen sulfide by microbial activity.

2.4.3 Underlying geology

The spatial variations in pH and redox potential across the Star Carr site are more difficult to justify; regions of high acidity lie in close proximity to almost neutral sediments. In trench SC34, this variability was most obvious in the southwest corner of the trench, where pH values ranged between 2.2 (sample 99762) and 6.57 (sample 103645) within metres (Figure 2.5). Boreham *et al.* (2011) discuss the role played by differences in the sediments directly underlying the peat deposits in causing these inconsistencies. Where thin layers of clay lie between the peat and the gravelly bedrock, movement of the water-table is likely to be more restricted, meaning that when the water levels drop below the level of the archaeology, they take longer to rise again, resulting in more oxidation of sulfides. Boreham *et al.* (2011) suggest that if the water-table was constantly above this clay lens, the effects would be benign or even

beneficial, as the proposed 'sulfur pump' system, which causes an accumulation of acid above the clay, could not occur; however, when this clay is thicker the presence of carbonates may be causing a buffering effect, mitigating the acidification.

2.4.4 Hydrology

A lowered water-table appears to be the most significant event instigating the formation of sulfuric acid in the archaeological zone at Star Carr, and has been attributed to the insertion of field drains in 2000 AD (Brown *et al.*, 2011). Monitoring of water levels showed that at dry periods, the water-table was at more than 1 m below ground level. As the recognised archaeological zone exists between approximately 0.8 and 1.2 m below ground level, this indicates that there are periods of time where parts of the archaeology in previously waterlogged parts of the site lies dry. It also suggests that the archaeology could lie within a zone of seasonal fluctuation of the water-table. High redox potential (> 400 mV) was measured by Boreham *et al.* (2011) in parts of the site, further indicating that sediments have become oxygenated due to the site no longer being waterlogged. The potential effects of this are illustrated in Figure 2.8, showing a proposed mechanism by which sulfuric acid forms in the archaeological zone.

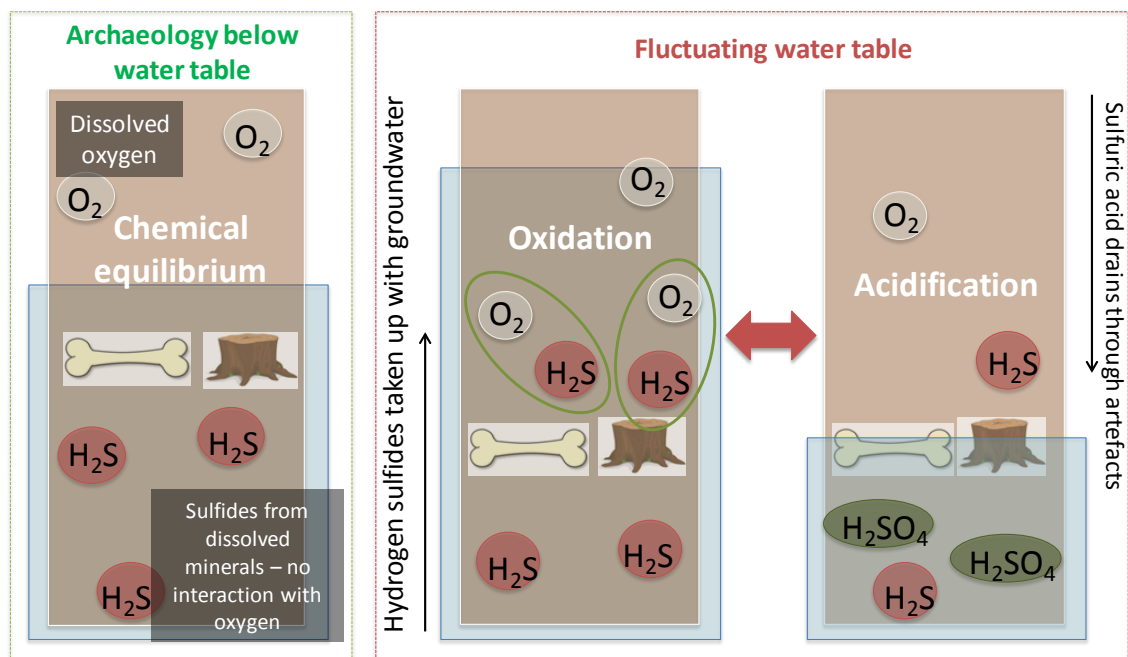


Figure 2.8: Schematic illustrating a proposed mechanism of sulfuric acid formation due to alteration of the water-table. (Originally in colour).

2.5 Conclusions

Geochemical observations at Star Carr in recent years have indicated that areas of the site are highly acidic. Furthermore, the observation of a potential 'halo' effect, causing oxidation of sediments extending horizontally from previously excavated trenches, along with the rapid oxidation of sediment within 24 hours, illustrates that sediments are vulnerable to redox reactions which may further increase the levels of acidity (Boreham *et al.*, 2011). Further drainage of the land is therefore likely to lead to further oxidation and the formation of more sulfuric acid. Indeed, the proposed mechanism of sulfuric acid formation is likely to continue even under current conditions, and it is not impossible that acidity will increase even without any further modification. This highlights the care that must be taken during management of the site, and suggests that research into the effects of this acidity must account for the possibility of sediments becoming even more acidic.

In addition, the changing hydrology of the site may have wider implications than simply increasing the acidity. Assessment by Brown *et al.* (2011) indicated that artefacts could be located in the region of dynamic hydrology, potentially putting them at further risk of deterioration (Hedges *et al.*, 1995; Williams *et al.*, 2006). Furthermore, biological activity is widely acknowledged to be suppressed in waterlogged, or anaerobic, environments (e.g. Blanchette, 2000). With a lowering water-table, oxygen will be introduced into the sediments and microbial activity may flourish. In addition, the high concentration of iron and sulfur present in the peat indicate that even in the absence of oxygen, anaerobic bacteria which instead utilise iron and sulfur in their metabolic processes, could survive. Biological degradation may therefore be another major factor facilitating the decay of organic remains. However, no direct evidence for biological degradation (for example fungal hyphae or surface damage characteristic of tunnelling bacteria; Nicholson, 1996) has been reported on artefacts excavated from the site.

Based on the geochemical assessment of Star Carr, it was proposed that the investigation of organic decay at the site should focus initially on the effects of acidification, specifically high concentrations of sulfuric acid. In order to do this, methods for the analysis of deterioration of bone and wood have first been investigated, to ensure that appropriate methods are utilised in order to elucidate the information relevant to the research questions posed (Chapter 3).

CHAPTER 3

DEVELOPMENT OF METHODS FOR THE ANALYSIS OF ORGANIC DETERIORATION

3.1 Introduction

A number of methods for the qualitative and quantitative analysis of organic deterioration are available, and each has its merits and disadvantages. The information provided by these different analytical methods ranges from structural to chemical, and microscopic to bulk changes. A number of applicable analytical techniques have been briefly reviewed in Chapter 1.

Previous studies have often highlighted the importance of applying a suite of complementary techniques for the analysis of organic archaeological materials. For example, analysis of wood degradation in the Vasa shipwreck utilised methods ranging from SEM to detect microscopic changes, to NMR to detect chemical alteration of the polymers (Almkvist, 2008). Analysis of bone deterioration commonly utilises microscopic methods (e.g. Jans *et al.*, 2002; Turner-Walker & Peacock, 2008), although measurements such as calcium and phosphate ratios, and amino acid content provide more detailed information on the overall chemical composition of a bone sample (e.g. Bada, 1972; Dobberstein *et al.*, 2008; Turner-Walker & Peacock, 2008).

Given the range of potential methods, in order to assess organic preservation at Star Carr, appropriate methods of determining the extent of deterioration were first investigated. Several important requirements were identified; firstly, that the methods chosen were appropriate for the analysis of both archaeological and modern materials (used for degradation experiments), and provided a broad overview of deterioration. It was also important that they were minimally destructive, and readily available at minimal cost, as this makes it possible to apply these protocols to other archaeological material and research questions in future.

In this study, a range of different techniques applicable to the research questions posed in Chapter 1 were first explored, and assessed with respect to the utility of the information they were able to provide. For the preliminary assessment of techniques, a series of modern material (bone & wood) at different levels of degradation was created in a short method development experiment (MDE), using sulfuric acid solutions comparable to the pH observed at Star Carr. The aim was to provide 4 samples of each material in progressing states of degradation. Where necessary, additional archaeological samples were also analysed as part of this assessment in order to determine whether the methods are applicable to materials that may have already undergone diagenesis. Where alternative samples were used, this is indicated.

3.2 Analysis of bone deterioration

3.2.1 Introduction

Many of the most important artefacts uncovered at Star Carr are bone and antler. Examples include bone tools, barbed hunting points crafted from red deer antler, and a series of frontlets, interpreted as headdresses, comprising both bone and antler (e.g. Clarke, 1954; Mellars & Dark, 1998). Both materials are forms of mineralised collagen, although antler contains a much higher proportion of collagen (approximately 34 % compared to 22 % in bone; Landete-Castillejos *et al.*, 2007). This study has been limited to the investigation of bone degradation, although it is expected that antler would degrade in a similar way (e.g. O'Connor, 1987).

The rates and different modes by which bone deteriorates are complex, and have been discussed in Chapter 1 (Section 1.2.3). Due to the differences between the mineral (HA) and collagen fractions, some analytical techniques provide information on only one component, whilst others can detect changes in both.

3.2.2 Experimental

For bone, a modern sheep long bone was obtained from a butcher (M&K Butchers, York). This was de-fleshed by gentle warming in biological washing powder, and the epiphyses removed with a hacksaw and discarded, allowing removal of marrow from the mid-section of cortical bone (according to Turner-Walker & Peacock, 2008). This was sliced into approximately 3 mm thick slices using a water-cooled diamond edged band saw.

Solutions of pH 2, 3, and 5 sulfuric acid were made by diluting 12 M sulfuric acid (Fisher Scientific) with MilliQ water. Slices of bone were sealed into separate glass vials containing a solution of the appropriate pH, or MilliQ water (approximately pH 7) as a control. These were incubated at 80°C for 10 days, thereby providing a set of four samples heated at different pHs. At 1, 3 and 8 days the pH of the surrounding solution was recorded and readjusted to the starting pH using 1 M sulfuric acid. At each of these points, an aliquot of the surrounding solution was also removed.

After 10 days, the samples were removed from solution and left to dry at room temperature for approximately 2 weeks.

3.2.3 Bulk assessment methods

Alongside chemical methods to characterise molecular change, it can be useful to apply methods to assess changes to bulk (macroscopic) properties of the samples. Although often less quantitative than chemical methods, they can provide an immediate comparison between different samples. Three methods of bulk assessment were carried out during the Method Development Experiment (MDE): visual, mass loss and pH analysis.

3.2.3.1 Methods

3.2.3.1.1 Visual analysis

Photographic recording of samples was carried out before and after experimentation using a 10 MP digital camera, as well as during the experiment where possible.

3.2.3.1.2 Mass loss analysis

Mass loss occurs by dissolution of material into the surrounding environment, and provides a semi-quantitative method of directly comparing experimental samples. Mass loss is reported as a percentage of the starting mass and was calculated by recording dry masses of the samples before and after experimentation.

3.2.3.1.3 pH analysis

Any change to the pH of the surrounding solution could be the direct result of dissolution. In experimental samples, monitoring of the surrounding pH may therefore provide a time dependent analysis of dissolution. pH was recorded throughout using a temperature sensitive calibrated glass pH probe (Denver instrument) unless otherwise stated.

3.2.3.2 Assessment of bulk analysis techniques

Mass analysis of the four bone samples from the method development experiments showed that in pH 3, pH 5 and water (pH 7), only 5 % mass was lost after 10 days, compared to 28 % at pH 2. Similarly, no apparent visual alteration occurred in the samples apart from that at pH 2, where a chalky texture was observed after the 10 days.

Analysis of the pH of the surrounding solution showed that the acidity was rapidly buffered, presumably by dissolution of HA, releasing carbonate and phosphate ions and increasing the pH of the surrounding solution (e.g. Green & Kleeman, 1991; Collins *et al.*, 1995) (Figure 3.1). At pH 2 a much larger amount of bone mineral would have to dissolve to buffer the acidity due to the logarithmic nature of the pH scale. In the region of 10 times more HA would be required to facilitate a change from pH 2 to 5, than pH 3 to 8. Although an accurate calculation of the

mass of HA required to dissolve was not possible due to readjustment of the pH throughout the experiment, this may explain why a greater mass loss was seen at pH 2 despite an apparent lower capacity to neutralise the surrounding solution.

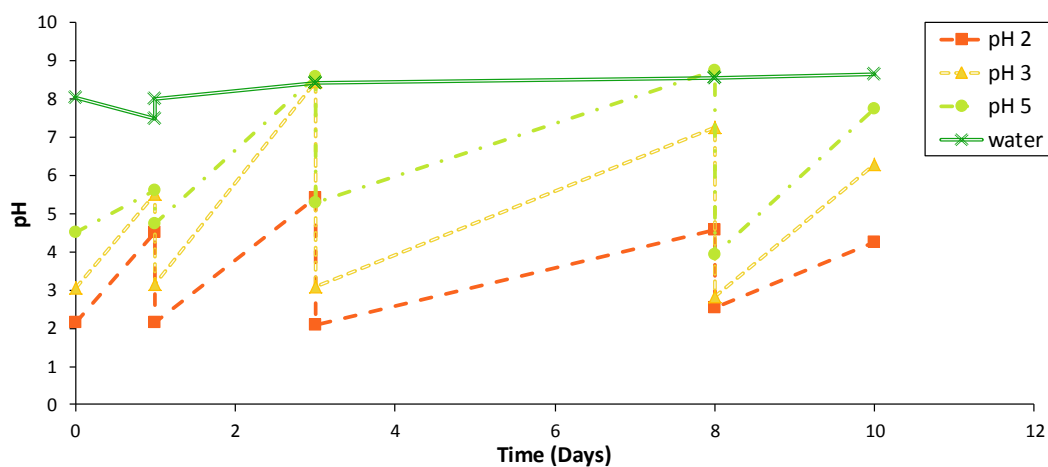


Figure 3.1: Measured pH of solutions during the method development experiment, demonstrating that bone has a large capacity to buffer surrounding acidity. At each sampling point the solutions were readjusted to the starting pHs. The lines showing the increase in pH between the measured points are therefore indicative only as buffering is likely to have occurred more rapidly (Margolis & Moreno, 1992). (Originally in colour).

3.2.3.2.1 Conclusions

Bulk assessment methods applied to samples from the MDE suggest that they are useful tools for the broad assessment of experimental diagenesis. Although mass loss analysis cannot be applied to archaeological material, comparison of mass loss can provide an easy comparison of deterioration in modern samples. Buffering of the pH of the solution, along with the mass loss, suggests that bone mineral is dissolving under acidic conditions. In this case, pH analysis provides a suitable method of quantifying the bone mineral deterioration as a function of time under experimental conditions.

3.2.4 Amino acid analysis

Amino acid analysis is a well-established technique for the assessment of the preservation of archaeological and fossil bone (e.g. Bada, 1972).

The total amino acid concentration can indicate loss of the HA and/or protein, by alteration of the relative composition of a bone sample. As type 1 collagen accounts for 85-90 % of protein in bone, the amino acid content can be considered to be primarily collagen (Currey, 2002).

In addition to this, racemisation of amino acids may be indicative of collagen damage, as racemisation in bone is very slow, unless the triple helix is disrupted (e.g. Collins *et al.*, 1999; Orgel *et al.*, 2001). Aspartic acid (Asp) and serine (Ser) are both relatively fast racemising

amino acids (e.g. Smith & Evans, 1980; Collins *et al.*, 1999) and can also racemise in-chain (e.g. Clarke, 1987; Demarchi *et al.*, 2013). Therefore, an increase in racemisation of these two amino acids within collagen is likely to reflect an increase in both the levels of conformational freedom (for example by loss of cross-linking within the helix; Vitagliano *et al.*, 1993) and degree of protein breakdown. Racemisation in other amino acids would only occur upon significant breakdown of the collagen helix, although many are very slow to racemise even when in a terminal position in the peptide (e.g. free alanine racemisation has a half-life of 12,000 years at 25°C; Bada & Schroeder, 1975).

3.2.4.1 Method

3.2.4.1.1 Analysis of solid samples

Analysis of the 4 MDE samples was first carried out on unpowdered material, with sub samples taken both from the inner cortical bone and thin outer layer (periosteum). In an archaeological context bone samples are often small fragments, and it is often not possible to distinguish between these layers. Therefore, in order to create samples that are representative of both layers, samples were also powdered using an agate pestle and mortar, or a freezer mill (SPEX) if manual powdering was not possible, and homogenised before analysis.

The method of analysis of amino acid racemisation has been developed over the course of several decades and has been adapted for application to a range of biomaterials, (e.g. Penkman *et al.*, 2008; Crisp *et al.*, 2013). The analysis of bone used here is based on a method reported by Buckley *et al.*, (2008). Dissolution of the HA and hydrolysis of the collagen was achieved by heating the sample in excess acid (7 M HCl) for 18 hours. The acid was then evaporated under vacuum, and the sample rehydrated with 500 µL per mg of sample with a weak acid solution containing an internal standard of L-homo-arginine (L-hArg). Each sample was analysed using reverse phase high-performance liquid chromatography (RP-HPLC) using a C₁₈ HyperSil BDS column (5 mm x 250 mm) at 25°C, using o-phthalaldehyde (OPA) as a derivatising agent (2 µl of sample mixed online with 2.2 µl of a derivatising agent containing 260 mM n-Iso-L-butyryl L-cysteine (IBLC) and 170mM o-phthalaldehyde in 1M potassium borate buffer). Separation was achieved using three solvents: sodium acetate buffer (23 mM sodium acetate tri-hydrate, 1.5 mM sodium azide and 1.3 µM EDTA, adjusted to pH 6.00), methanol and acetonitrile on an Agilent 1100 HPLC using fluorescence detection (xenon-arc flash lamp at a frequency of 55 Hz, with an excitation wavelength of 230 nm and emission wavelength of 445 nm) over a 2 hour elution period (adapted from Kaufman & Manley, 1998). Standards and blanks were analysed routinely.

Asparagine and glutamine undergo rapid deamidation to aspartic acid and glutamic acid respectively during the hydrolysis preparation step. As asparagine and glutamine cannot be distinguished from aspartic acid and glutamic acid using RP-HPLC, they are therefore reported as Asx and Glx, where Asx includes contributions from asparagine, and Glx includes contributions from glutamine. In order of elution, the amino acids detected were: L-Asx, D-Asx, L-Glx, D-Glx, L-Ser, D-Ser, L-Thr, His, Gly, L-Arg, D-Arg, L-Ala, L-hArg, D-Ala, L-Tyr, L-Val, L-Met, D-Met, D-Val, L-Phe, L-Ile, D-Phe, L-Leu, D-Ile and D-Leu. The concentrations of each isomer of each amino acid were used to derive a D/L value.

3.2.4.1.2 Estimation of error in solid samples

Racemisation (expressed by a D/L value) induced by the preparation steps was determined by analysis of a powdered untreated modern sheep bone sample and was found to be approximately 0.06 in Asx and 0.03 in Ser, with a standard deviation of less than 1 % and 7 % respectively, measured by analysis of three replicates. Total amino acid concentrations were approximately 1.33 mmol/mg, with a standard deviation of 0.32 (18 %), thus illustrating that assessment of total amino acid concentrations should account for a higher level of error than measurements of D/L values. The error in concentration measurements is likely to arise due to the high degree of sample dilution prior to analysis, as well as the small mass of sample used. This is unlikely to affect the D/L measurements, as preparation error is cancelled out when the concentrations of both D and L isomers are considered.

3.2.4.1.3 Analysis of liquid samples

As it may be useful to quantify any proteins leaching into solution during experimental diagenesis, analysis of the solution aliquot samples was also carried out. A short study to test the ideal conditions for hydrolysis was carried out here, using the supernatant removed from the pH 2 sample at the end of the method development experiment. Solutions of 2, 6 and 7 M HCl with 12, 18 and 24 hour hydrolysis times were compared. It was found that hydrolysis in 2 M acid yielded much lower concentrations of amino acids, and as such probably did not achieve full hydrolysis. Solutions of 6 M and 7 M HCl yielded similar concentrations (Figure 3.2, left) and therefore 6 M HCl has been used in order to avoid catalysing racemisation (Kaufman & Manley, 1998). Although differences in amino acid concentration were seen between replicate samples, these differences did not appear to be dependent on the hydrolysis time and were within the margins of error (calculated as the standard deviation of three replicate analyses). High levels of error are likely to occur in analysis of liquid samples due to high levels of dilution employed along with the small sample sizes. Although a slight increase in

racemisation was observed with increased hydrolysis time, the increase was minimal. Therefore, for convenience a 24 hour heating has been applied.

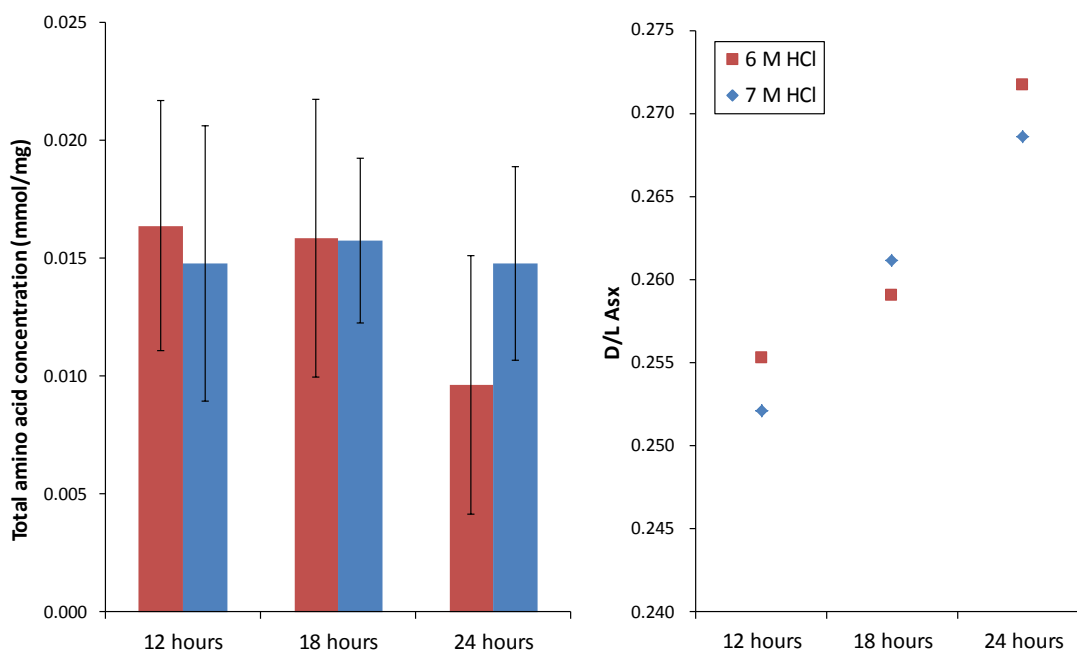


Figure 3.2: Total amino acid concentrations (left) and Asx racemisation (right) in solution samples treated in 6 and 7 M HCl for a range of hydrolysis times. Alterations in concentration lie within the error (standard deviation calculated from two replicates of each sample) whilst Asx racemisation slightly increases with increased hydrolysis times. (Originally in colour).

For the analysis of all aliquot samples a 100 μ L sample of the solution was hydrolysed at 110°C for 24 hours with 100 μ L 6M HCl and then dried under vacuum. Samples were rehydrated with 100 μ L of rehydration fluid and further diluted in L-hArg if required, before analysis by HPLC as described for solid samples (Section 2.3.1.1).

3.2.4.1.4 Estimations of error in liquid samples

Error in concentration measurements was determined by three replicate analyses of the liquid sample. Using the 24 hour, 6M HCl hydrolysis, total amino acid concentration values varied by up to 58 %. Therefore concentrations of amino acids in solution have been interpreted with caution, as error is likely to be high due to the high order of dilutions and small mass of original sample. In addition, evaporation may have occurred from the samples during the experiment, resulting in an altered concentration. Errors in racemisation were less; 8 and 12 % for Asx and Ser respectively. Replicate analysis of all aliquot samples was not possible, as the minimal amount of liquid was removed from the 'stagnant' samples during the experiment. The error calculated here has therefore been applied throughout.

3.2.4.2 Assessment of amino acid analysis technique

3.2.4.2.1 Application to solid samples

Both powdered and un-powdered sub samples from the MDE were analysed. Results showed differences in amino acid concentrations between the inner layer, outer layer and powdered samples. In most cases, the differences between the three samples are greater than the standard deviation calculated in Section 2.3.1.1 (0.32) (Figure 3.3) suggesting that sample preparation needs to be consistent. Due to the variability between subsections of the bone (inner and outer un-powdered samples), it is likely that milling and homogenising the samples provides a better analysis of the whole bone and should therefore be done throughout. In addition, for archaeological samples it may be difficult to identify the periosteum. Although total concentrations differed, Asx racemisation was consistent between the powdered and inner samples (Figure 3.4, right) suggesting that avoiding analysis of the outer surface alone provides a better measure of racemisation across the bone.

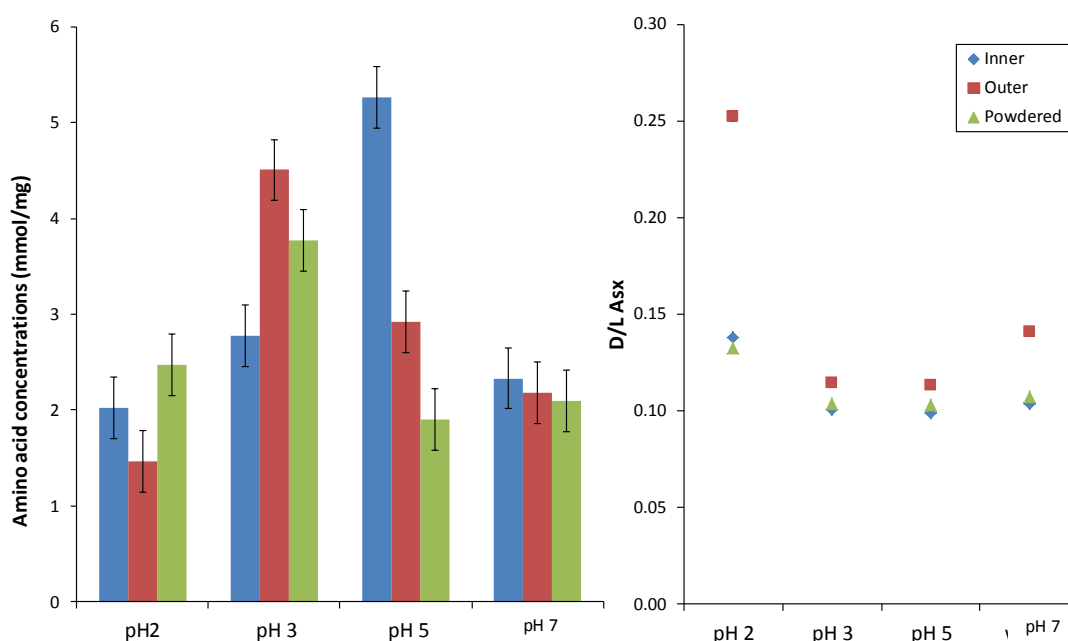


Figure 3.3: Comparison of the three different sub-samples for the method development experiments: total amino acid content (left) and Asx racemisation (right). Error bars for the concentrations are one standard deviation derived from measurement of three replicates of a modern sheep long bone (0.32 mmol/mg). Error bars for Asx racemisation are negligible. (Originally in colour).

In both powdered and non-powdered samples, an increase in Asx racemisation was seen at pH 2, indicating significant collagen breakdown within the 10 days (Figure 3.3, right). Racemisation was considerably higher in the 'outer' sample at all pHs. As the samples were longitudinal slices, this is not likely to be due to greater contact with the solution, and it is possible that analysis of the periosteum is not representative of the behaviour of the whole bone, possibly

because of higher mineral density in the outer layers (e.g. Gong *et al.*, 1964). This again suggests that milling and homogenising samples is the best method of sample preparation.

3.2.4.2.2 Application to liquid samples

Analysis of the amino acids present in the aliquot samples required adapting the dilution factors prior to analysis by HPLC dependent on the conditions of the experiment. Therefore, no standard dilution factor can be proposed.

Detectable concentrations of amino acids were present in all solutions (Figure 3.4), and an increase in both concentration and racemisation is seen over time. This is somewhat expected; increased levels of amino acids leach out of the sample as degradation proceeds. At pH 2, there is increased leaching of amino acids into solution, and interestingly these are less racemised than those leaching out into the higher pH solutions, which might be because the leached collagen is more intact at lower pH. The difference between the pH 2 sample and samples at higher pH corroborates results from the bulk analysis.

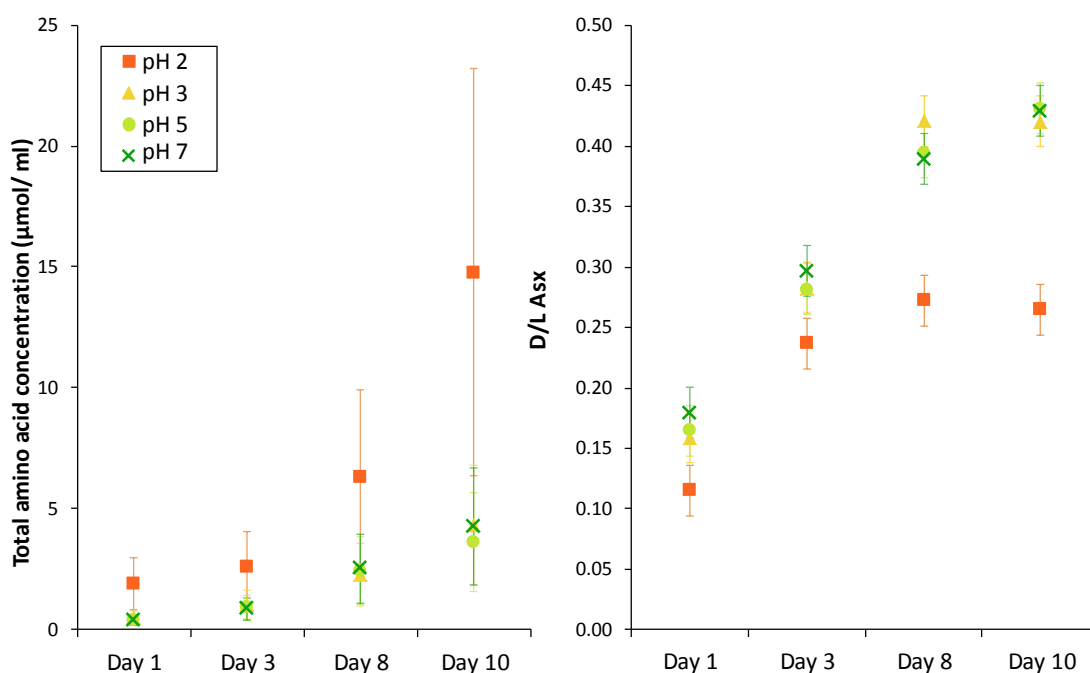


Figure 3.4: Total amino acid concentrations (left) and Asx racemisation (right) in solution over the course of the reaction period. Error bars are one standard deviation calculated from three replicate analyses of a sample. (Originally in colour).

3.2.4.2.3 Conclusions

Amino acid analysis of the four samples from the MDE suggests that it is an appropriate method for analysing the levels of degradation in solid samples, and levels of leaching by analysis of the liquid samples. Whilst care needs to be taken to distinguish between inner and

outer layers of bone when comparing material, powdering and homogenising the bones may offer the best method of sample preparation. Error in the concentration data must be taken into account when interpreting analysis of the bone samples. Despite this, an obvious difference has been seen here in the sample treated at pH 2, suggesting that degradation is accelerated at lower pHs.

3.2.5 Powder X-ray diffraction

Several studies show that increased HA crystallinity can be a marker of bone diagenesis (Pleshko, 1991; Hiller & Wess, 2006), although the reasons for the increase are not well understood. Potential explanations have been proposed as preferential loss of the smallest crystals, or dissolution of the HA followed by rapid recrystallisation; as the HA would not be biologically constrained during recrystallisation, it is likely to do so in a more crystalline form than when originally laid down in the bone (Hedges & Millard, 1995). It has been shown that an increase in HA crystallinity cannot be directly related to the age of archaeological bone, but rather indicates the extent of diagenetic transformations (Person *et al.*, 1995).

Powder X-ray diffraction (p-XRD) analysis of bone material provides a general measure of crystallinity of the HA, with characteristic diffraction peaks sharpening with increased crystallinity (e.g. Bonar *et al.*, 1983; Boskey, 2003). The peak characteristic of HA that appears at approximately $32^\circ 2\theta$ is normally broad as it is actually two coalescing peaks. When a sample is extremely degraded, the band resolves into two peaks, appearing at around 32 and $33^\circ 2\theta$ (Person *et al.*, 1995). p-XRD can also allow the identification of mineral inclusions within the HA, for example quartz or fluoride which indicate exchange with the burial environment (Person *et al.*, 1995). Unlike spectroscopic methods, p-XRD provides an average characterisation of the HA crystallinity rather than focussing on a small area, allowing assessment of structural changes throughout the bone (e.g. Wess *et al.*, 2001). p-XRD also has the potential to be applied in a minimally destructive manner, for example by using synchrotron X-ray sources (Wess *et al.*, 2001), although this was not carried out here.

As mass loss and amino acid content already provide a quantitative measure of HA loss, p-XRD was assessed as a possible complementary qualitative method of analysing structural changes to the HA fraction.

3.2.5.1 Method

All p-XRD analysis was carried out using a Bruker-AXS D8 diffractometer fitted with a copper anode (1.54 \AA) and a rotating position sensitive detector. Powdered bone samples were packed into an aluminium plate with a shallow circular well, and loaded onto a rotating sample holder. For analysis, the X-ray generator was set to 40 KV and 30 mA and samples scanned between $24\text{-}36^\circ 2\theta$ using a scan rate of 0.3 seconds/step and an increment of 0.025 degrees (adapted from Person *et al.*, 1995).

In order to ascertain the diffraction pattern of pure HA, a commercially produced standard was purchased (Aldrich) and analysed using the same parameters.

3.2.5.1.1 Investigation into sample preparation methods

Most modern samples (e.g. the MDE samples) could not be powdered by hand-milling as they were too robust, and a method such as freeze-milling using a ball mill had to be used; however, this has the potential to introduce contamination into a sample, and therefore for degraded archaeological samples, hand-milling may present a better option.

Previous studies applying p-XRD have used different milling methods, for example drilling (Bartsiokas & Middleton, 1992), freeze-milling, (Bonar *et al.*, 1983) and hand-milling using a pestle and mortar (Person *et al.*, 1995). However, whilst it is recognised that sample preparation techniques have implications for FTIR analysis of bone (Surovell & Stiner, 2001), the effects of different milling methods in p-XRD studies have not been compared previously.

Here, a small study was conducted to compare the effects of hand-milling using an agate pestle and mortar, and freeze-milling using a pulverising mill in liquid nitrogen (SPEX). As the MDE samples were small in size and too robust for hand-milling, an archaeological sample excavated from Star Carr in 2008 was used for this comparison (sample 92105; see Chapter 7 for further detail). Diffraction patterns for the unsieved hand and freeze-milled fractions are shown in Figure 3.5.

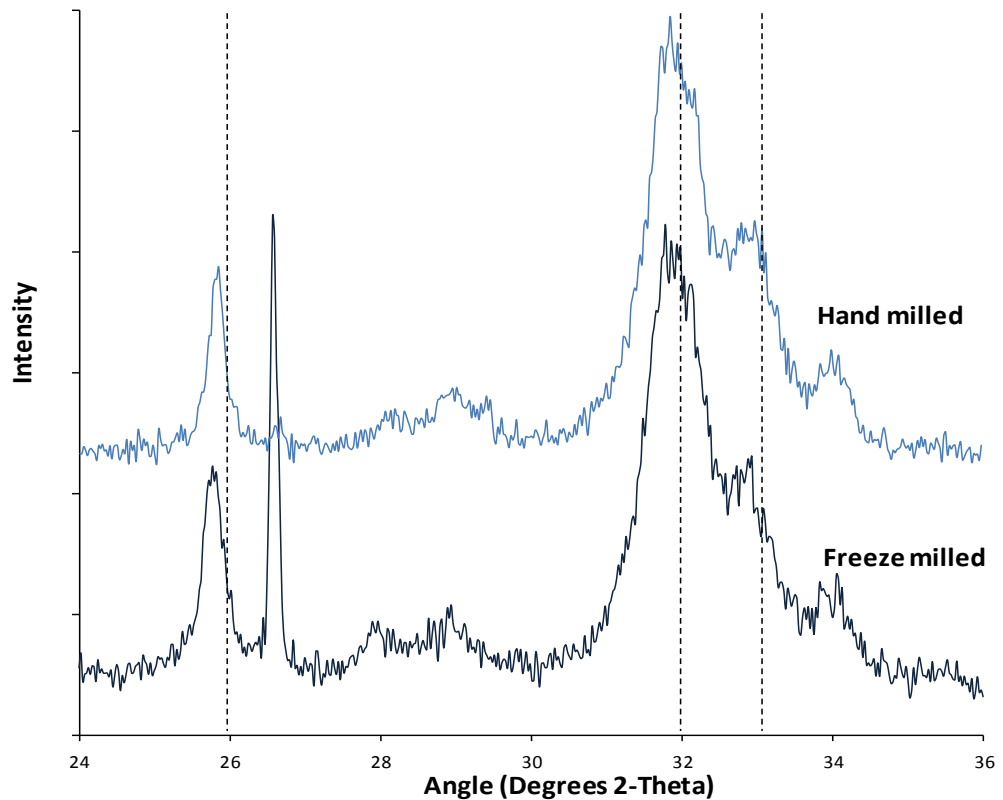


Figure 3.5: Comparison of diffraction patterns for hand-milled vs freeze-milled sample excavated from Star Carr in 2008 (sample 92105). (Originally in colour).

The sharp peak at $26.5^{\circ}2\theta$ in the freeze-milled sample is likely to be a quartz inclusion, which is commonly found in fossil samples (Person *et al.*, 1995). Visual analysis of the spectra shows that different milling methods do not impact on the intensity or position of the HA peaks, and no difference in the degree of peak splitting can be discerned. This suggests that the milling method has no impact on the crystallinity of the sample.

In several literature sources, particle size fractionation of bone is carried out by sieving prior to analysis by p-XRD (e.g. Bonar, 1983; Very & Baud, 1984). However, more recently studies have been carried out where bone samples were not sieved prior to analysis, resulting in no increased error (e.g. Piga *et al.*, 2009). The use of sieves may introduce a source of contamination as well as create the potential to lose significant amounts of small samples, and therefore size fractionation was not carried out in this study.

3.2.5.2 Assessment of p-XRD for the analysis of bone mineral

The four MDE bone samples were powdered using a freezer mill (SPEX). Analysis by p-XRD shows no difference in crystallinity between the bones at pH 3, pH 5 and in water. Slight resolution of the peak characteristic of HA into its two component peaks can however be determined at pH 2. This indicates increased crystallinity of the sample at this higher acidity (Figure 3.6).

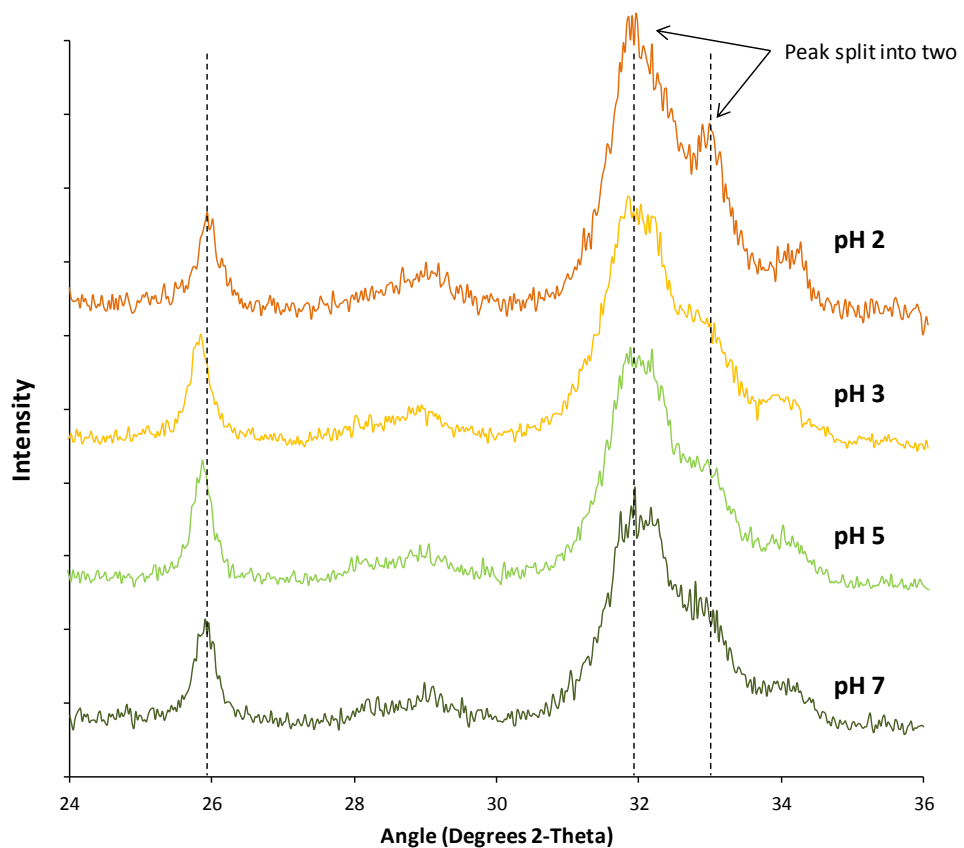


Figure 3.6: Comparison of diffraction patterns for samples from the MDE. The position of the diffraction peaks in pure HA, determined by analysis of a commercially purchased standard, are marked with dashed lines. (Originally in colour).

Clear separation of the broad peak at $32^{\circ}2\theta$ does not occur even at pH 2, making it difficult to apply statistical assessment, as has been done in previous studies on archaeological material (e.g. Bartsiokas & Middleton, 1992). Person *et al.* (1995) also show that unambiguous splitting of the peaks occurs only in severely degraded bone. To investigate this, analysis was also carried out on a rib bone excavated from Star Carr in 2010 and a cow metatarsal from the late Roman site of Tanner Row (York), which may be expected to display a greater degree of HA alteration. Further sample information is provided in Chapter 7 (Section 7.2.2). Neither bone displayed unambiguous splitting of the peak characteristic of HA (Figure 3.7).

In light of these results, it is proposed that p-XRD is utilised as a non-quantitative method to detect major changes in the bone mineral, rather than use statistical assessment of the data to provide quantitative results. It was expected that p-XRD would allow the identification of samples where HA alteration is significantly progressed.

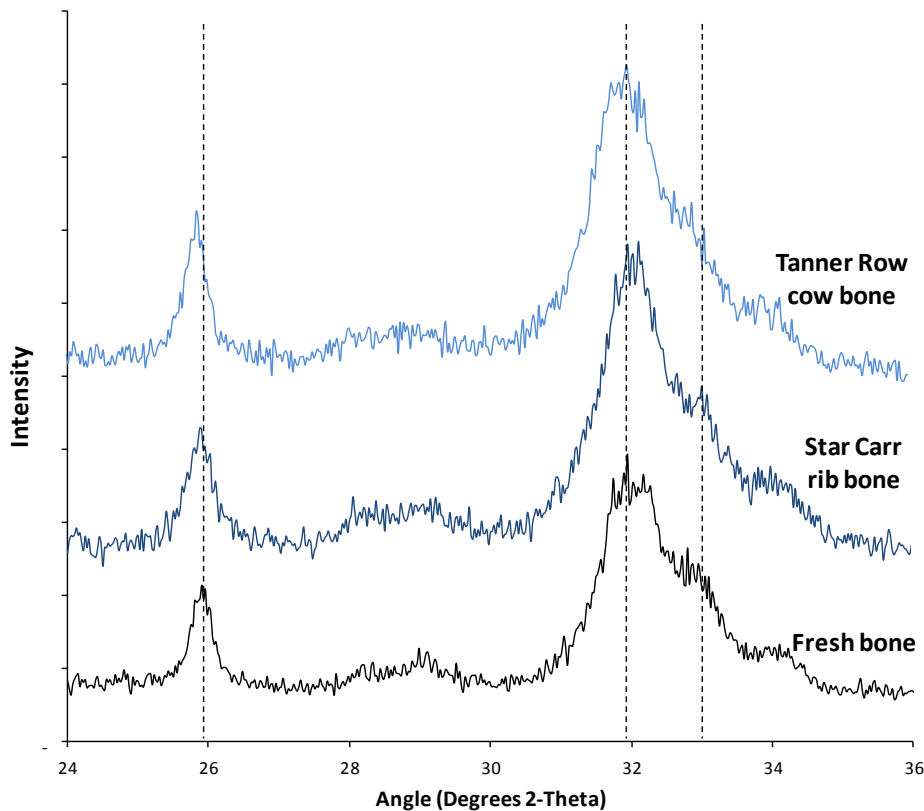


Figure 3.7: Comparison of diffraction pattern for archaeological bones with modern fresh bone, showing no major alteration of diffraction patterns. Dashed lines indicate the position of diffraction peaks for pure HA, determined by analysis of a commercially purchased standard. (Originally in colour).

3.2.5.3 Conclusions on the application of p-XRD

As it is possible that milling methods can alter the crystallinity of the bone sample, it is recommended that preparation methods for p-XRD are standardised. The best option is therefore freeze-milling, as this is done for a standard period of time and conditions such as time, temperature and milling rate can be controlled. As sieving introduces the possibility of contamination as well as the potential loss of sample, this has been discounted as a necessary sample preparation step.

It has been shown that minor differences between samples may be attributed to the sample preparation steps. This further suggests that p-XRD analysis is better considered a qualitative rather than quantitative technique. However, information provided regarding alteration of the HA in the four MDE samples is in agreement with results from other analysis techniques; the bone at pH 2 is the only sample to display significant alteration of the HA structure, consistent with the significant mass loss observed in Section 2.2.2.

3.2.6 Raman spectroscopy

Studies such as those by Timlin *et al.* (2000) and Raghavan (2011) have shown that Raman microscopic analysis is effective in the analysis of bone, as changes in the bonding and structure of the bone mineral translate into changes in the Raman spectrum. Sharpening of the peak identified as characteristic of bone phosphate at approximately 950cm^{-1} is primarily caused by an increase in crystallinity of the bone mineral, reducing the vibrational modes of the mineral lattice (Timlin *et al.*, 2000). Changes in the association between the collagen and bone mineral are signified by changes in the position of this phosphate peak, as well as a number of peaks identified as relating to collagen (Raghavan, 2011). The ability to analyse both bone mineral and collagen simultaneously gives Raman spectroscopy a potential advantage over analytical techniques that focus only on one component.

3.2.6.1 Method

Although no sample preparation is typically needed in Raman spectroscopy, focus of the microscope proved impossible without a flat sample surface. For bone samples this was achieved by setting a small sub-sample in epoxy resin and polishing the surface until the bone was revealed. Raman spectra were collected using an HORIBA XploRa Raman microscope with a 532 nm laser applying a 50 % filter and 2400 g/mm grating, between 400 and 1800 cm^{-1} (adapted from Raghavan, 2011). 16 spectra were collected over a small area of the bone surface using a 1s laser exposure and averaged, according to Timlin *et al.* (2000).

3.2.6.2 Assessment of Raman spectroscopy for the analysis of bone

Once a flat surface was achieved, spectra were obtained that displayed the peaks characteristic of HA phosphate groups (950 cm^{-1}) and carbonate imperfections (1100 cm^{-1}). In addition, very low intensity peaks at higher wavenumbers are possibly attributable to collagen (Figure 3.8).

No differences between the pH 2 and pH 3 samples from the MDE were discerned, despite the obvious increase in degradation detected by other methods (Sections 2.2, 2.3, & 2.4). The theoretical benefits of Raman spectroscopy (non-destructive analysis, ability to detect both the HA and collagen) were difficult to achieve in practise. This is potentially because of the wavelength of the laser available (532 nm); both Timlin *et al.* (2000) and Raghavan (2011) showed that a 785 nm laser resulted in good peak resolution. For these reasons, it was decided that the Raman spectroscopic techniques available were not suitable for the analysis of bone in this study.

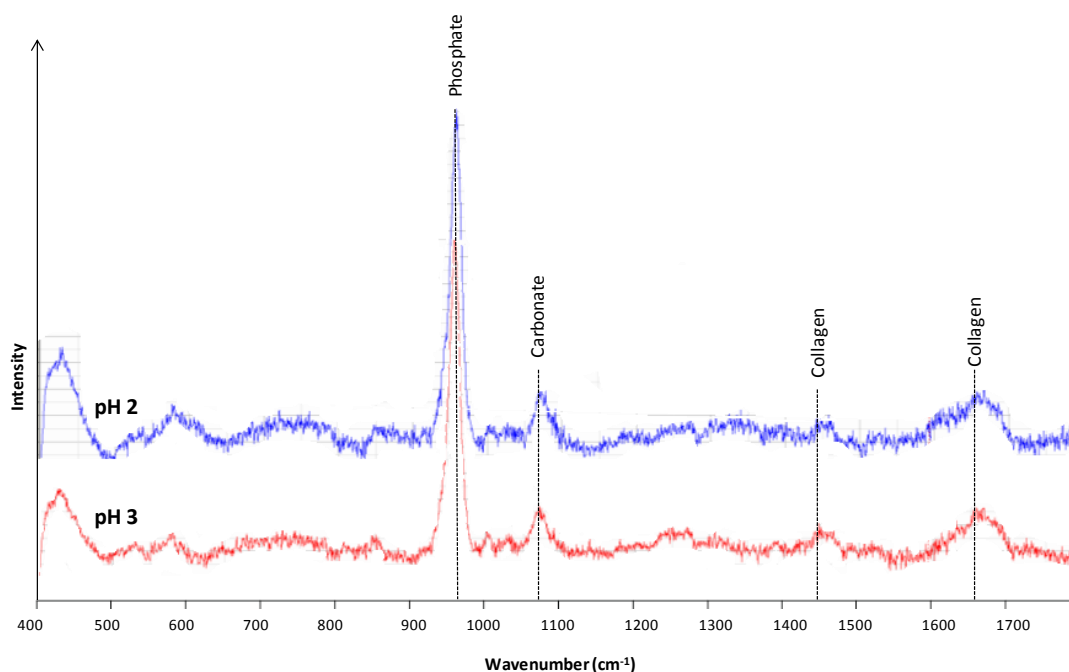


Figure 3.8: Raman spectra obtained from MDE bone samples treated at pH 2 (top) and pH 3 (bottom), showing peaks characteristic of both HA and collagen, although no difference is observed between the two samples. (Originally in colour).

3.2.7 FTIR spectroscopy

FT-Infrared spectroscopy (FTIR) is an established method of detecting molecular changes within archaeological bone, with advanced technologies such as FTIR imaging and synchrotron FTIR exposing more detailed information (e.g. Pleshko *et al.*, 1991; Reiche *et al.*, 2003). The potential benefits of FTIR are that it can be applied non-destructively, and can be combined with microscopy, allowing spatial variations to be detected (Reiche *et al.*, 2010). Alterations of the HA can be indicated by increased splitting of the characteristic phosphate absorption peak at 950 cm^{-1} , signifying alteration of crystal size; or increased intensity of the carbonate peak at $1350\text{--}1550\text{ cm}^{-1}$ (an increased carbonate: phosphate ratio), suggesting exchange with the burial environment (Lee-Thorp & van der Merwe, 1991; Piga *et al.*, 2011). Further information regarding the protein fraction may be discerned; Paschalis *et al.* (2001) show how molecular information obtained from absorption characteristic of collagen can even reveal the extent of cross-linking.

3.2.7.1 Method

Analysis was carried out on a Vertex 70 FTIR spectrometer fitted with an ATR (attenuated total reflectance) unit. A resolution of 4 cm^{-1} was used to scan between $600\text{ and }3600\text{ cm}^{-1}$ using an averaged 16 scans (adapted from Surovell & Stiner, 2001). Minimum sample preparation is necessary for FTIR-ATR measurements; however it was found that a better resolution of peaks

was achieved when samples were powdered. This was achieved by milling in a freezer mill (SPEX).

3.2.7.2 Assessment of FTIR for the analysis of bone

Four bone samples from the MDE were analysed and the key peaks in the fingerprint region of the spectra identified according to Reiche *et al.* (2010) (Figure 3.9). Analysis indicated that samples treated at pH 3, pH 5 and in water are identical. This is in agreement with analysis by p-XRD and mass loss analysis. Slight alteration of the spectra for the sample at pH 2 can be discerned; broadening of the amide peak at approximately 1650 cm^{-1} and disappearance of the peak at 1250 cm^{-1} suggests alteration of the collagen (Reiche *et al.*, 2003). Increased resolution (manifesting in an altered peak shape) of the phosphate peak at approximately 900 cm^{-1} (indicated in Figure 3.9) indicates an increase in crystallinity of the HA (Reiche *et al.*, 2010), in agreement with p-XRD analysis. In general, alterations of the ratio between collagen and HA peaks indicates that there is a change in relative composition in the bone treated at pH 2, again corroborating analysis using other methods.

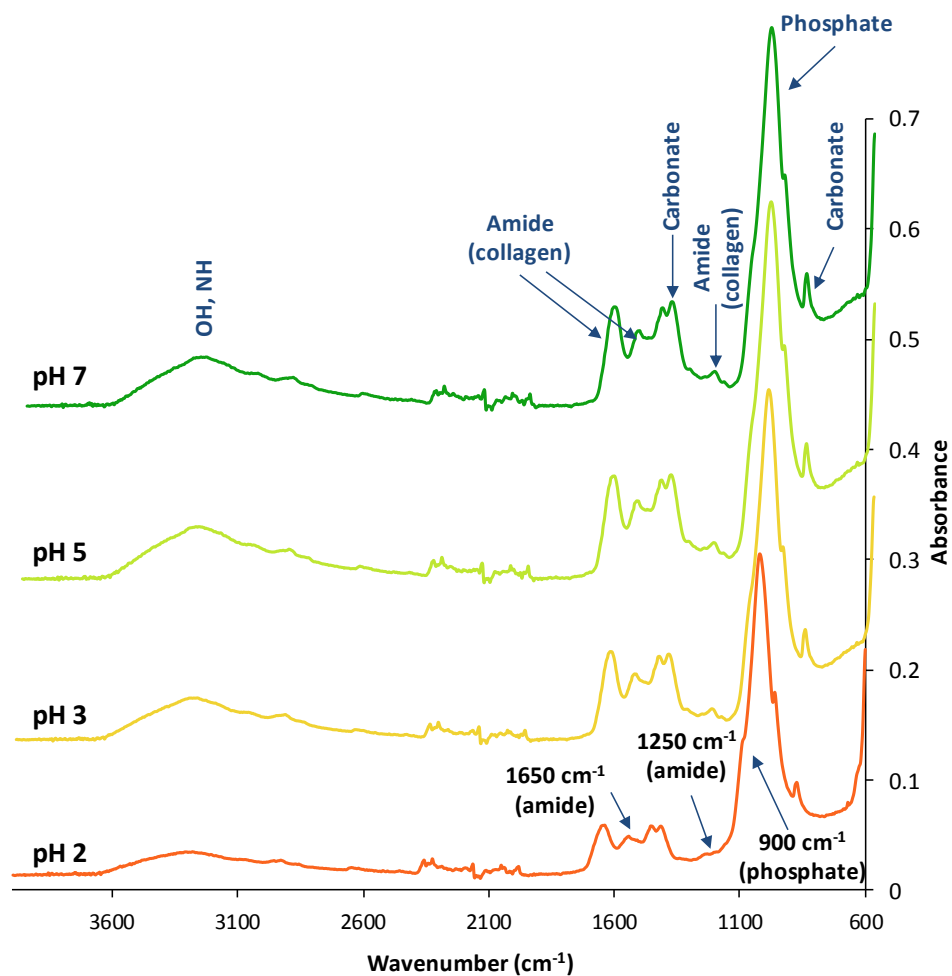


Figure 3.9: Comparison of FTIR spectra for the four MDE samples. Key peaks relating to bone mineral and collagen are indicated, labelled according to Reiche *et al.* (2010). (Originally in colour).

In archaeological samples, an increase in the levels of carbonate may signify diagenetic alteration, through exchange with the burial environment (e.g. Lee-Thorp & van der Merwe, 1991). In order to assess whether this is discernible using FTIR, a sample excavated from Star Carr in 2010 was also analysed. The carbonate peak appeared small in the archaeological sample, although the amide peaks appeared at much higher absorption (Figure 3.10, top), suggesting that the sample had undergone extensive demineralisation (e.g. Very *et al.*, 1997). Comparison with both an untreated bone and bone demineralised in 0.6 M HCl (assumed to be only collagen) suggests that the relative composition of the bone from Star Carr lies somewhere between fresh bone and ‘collagen.’

Preliminary FTIR analysis suggests that it provides a semi-quantitative measure of the extent of demineralisation, although alteration of the HA fraction alone is more difficult to discern.

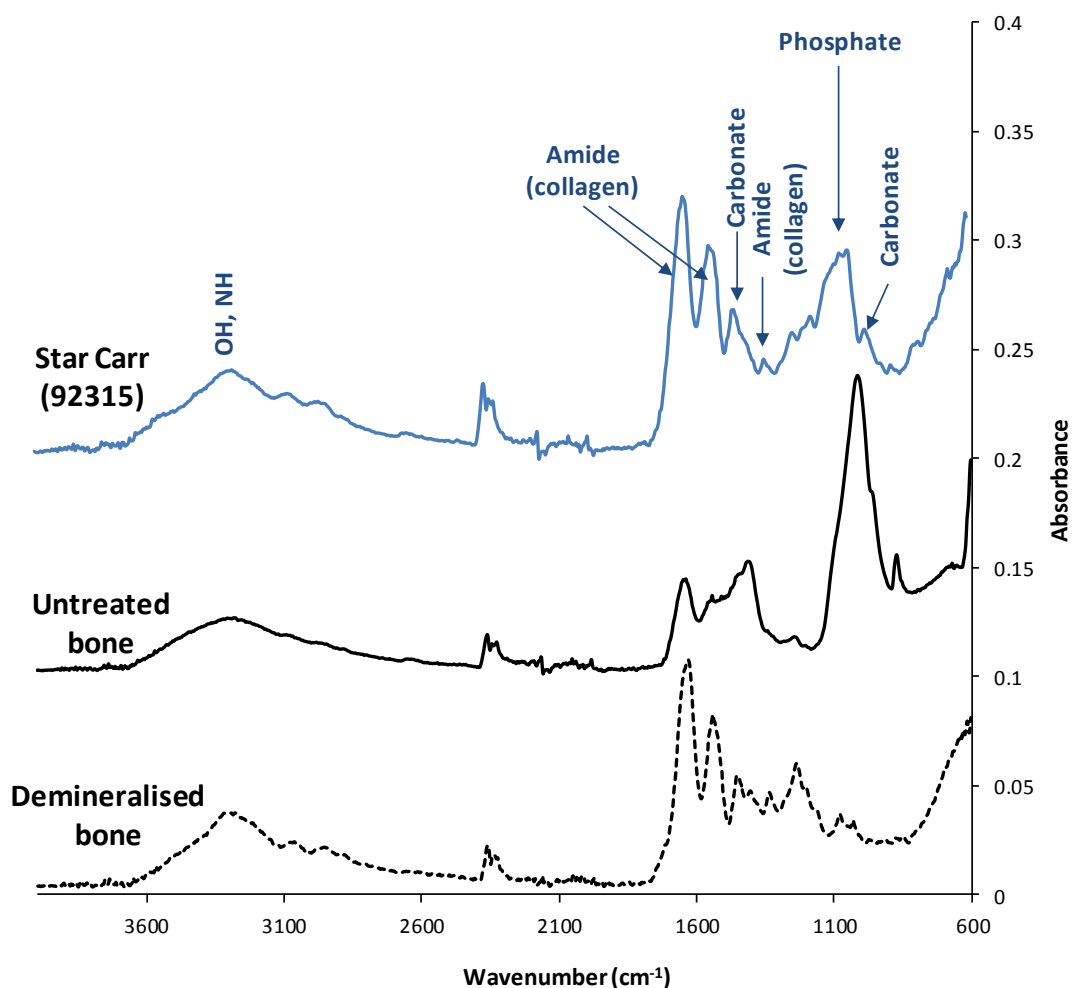


Figure 3.10: Comparison of FTIR spectra obtained from a sample excavated from Star Carr with an untreated modern bone and demineralised bone (collagen). (Originally in colour).

3.2.7.3 Conclusions

FTIR analysis of the MDE samples indicates that degradation is only seen at pH 2, in agreement with amino acid and p-XRD analysis. In addition, comparison of a sample from Star Carr with fresh and demineralised bone suggests that it could be a complementary technique to amino acid analysis for determining the extent of bone demineralisation.

The aim of applying FTIR was primarily to determine HA crystallinity. The alteration of the phosphate peak in FTIR is only very slight, in comparison to p-XRD where splitting of the HA peak was more obvious, suggesting that FTIR is a less sensitive technique for this purpose. In addition, Surovel & Stiner (2001) show that FTIR can be affected by sample preparation techniques. A method such as FTIR imaging may be more appropriate as it does not involve the analysis of such a small area of sample as conventional FTIR and is therefore less likely to be affected by sample preparation methods (Paschalis *et al.*, 2001). However, this is not a technique that is readily available.

For these reasons, FTIR has been applied only on selected samples throughout this study, where the extent of demineralisation has been examined, rather than has a routine technique for the analysis of HA crystallinity.

3.2.8 Microscopy methods

Microscopic methods of analysing bone deterioration provide information on histological deterioration, and have often been reported as complementary to chemical analysis techniques (e.g. Nielsen-Marsh & Hedges, 2000; Turner-Walker & Peacock, 2008).

Thin-section optical microscopy has a long history of application to the analysis of archaeological bones (e.g. Stout & Teitelbaum, 1976; Jans *et al.*, 2002). If the bone is mineralised, osteons should be observable in thin-section (Jans, 2005). In addition, collagen can be identified when plane-polarised light is used to view a thin-sectioned bone, as collagen demonstrates birefringence due to the alignment of fibrils (Girouad-Guille, 1988). Different classes of microbe may also be detected by characteristic tunnelling (Jans *et al.*, 2002; 2004), and fungal activity signified by characteristic porosity of the bone (Stout & Teitelbaum, 1976). Such features can also be seen using scanning electron microscopy (SEM) alongside other diagenetic features such as cracking, mineral inclusions and changes in mineral density (e.g. Bell, 1990; Turner-Walker & Syversen, 2002).

Koon (2006) developed a method of demineralisation and reverse staining using phosphotungstic acid and uranyl acetate that allows the visualisation of individual collagen

fibrils under transmission electron microscopy (TEM). Using this method, it is possible to visualise alteration of collagen as a result of degradation.

3.2.8.1 Method

3.2.8.1.1 Light microscopy

Samples were prepared for optical microscopy in thin-section by setting a small (3 mm x 3 mm) sub sample in epoxy resin using a cylindrical plastic mould. The resin was cured under vacuum and sliced using a water-cooled saw to expose the sample. This was affixed to a microscopy slide using more resin. Once dry, this was sanded to approximately 30-50 μm (e.g. Jans *et al.*, 2002) and polished.

Samples were viewed using a Zeiss AxioScope binocular microscope with a motorised stage, using both plane-polarised and cross-polarised light.

3.2.8.1.2 SEM imaging

Minimal sample preparation was carried out for SEM. A sub-section of each sample (approximately 3 mm x 3 mm) was fixed to aluminium pin stubs and earthed using silver glue. Samples were sputter-coated with a 7 nm layer of gold/palladium and images obtained under vacuum using a JEOL JSM-6490LV SEM.

3.2.8.1.3 TEM imaging

Samples were prepared for TEM using the reverse staining method developed by Koon (2006).

Bone samples were fragmented using a hammer, and fragments of approx 3 mm picked out. These were demineralised over a 2 week period in 0.5 M EDTA, replaced every 2-3 days.

Samples were washed thoroughly with MilliQ water and homogenised for a total of 3 minutes in 3 mL of a 1% w/v solution of phosphotungstic acid (PTA). Samples were then centrifuged at 3000 g and 4°C for 15 minutes. The supernatant was removed and the sample re-suspended in 1 mL PTA. A drop of this solution was then pipetted onto a formvar film TEM grid with a carbon coating (Agar Scientific) and allowed to settle for 5 minutes. The grids were then dried with filter paper and stained with uranyl acetate (Agar Scientific). Grids were thoroughly washed with a 50:50 solution of ethanol: water and allowed to air dry.

TEM imaging was carried out using a Tecrai 12 TEM with a beam setting of 100 kV.

3.2.8.2 Assessment of microscopy techniques

All four samples from the MDE were prepared for thin sectioning and SEM imaging. Bone histology was clearly visible using both techniques, confirming the presence of HA (Figure 3.11). Collagen was also identified by birefringence in both bones, shown by regions of light and dark in Figure 3.11.

In the sample heated in water, the appearance under both optical and SEM is what would be expected for fresh bone (e.g. Hedges, 1995; Jans *et al.*, 2004), with no damage observable. In comparison to this, deep cracks are seen in the sample treated at pH 2. This damage is much clearer under SEM imaging, where it can be seen that the cracking follows the histological structure of the bone.

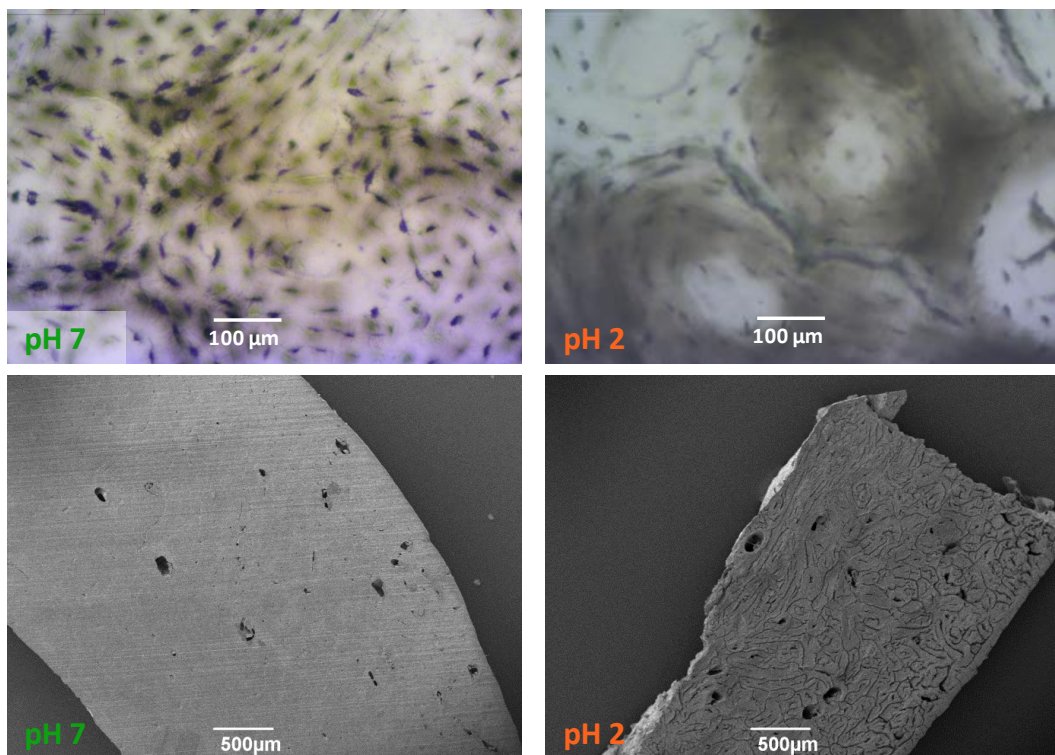


Figure 3.11: Comparison of images obtained using light microscopy with a cross-polarised light source (top) and SEM (bottom), for bones treated in water and at pH 2.

TEM analysis was not carried out on the MDE samples, but was tested on modern untreated bone and a bone excavated from Star Carr in 2010. In both cases, collagen fibrils were observed, although they were far less abundant in the Star Carr sample (Figure 3.12).

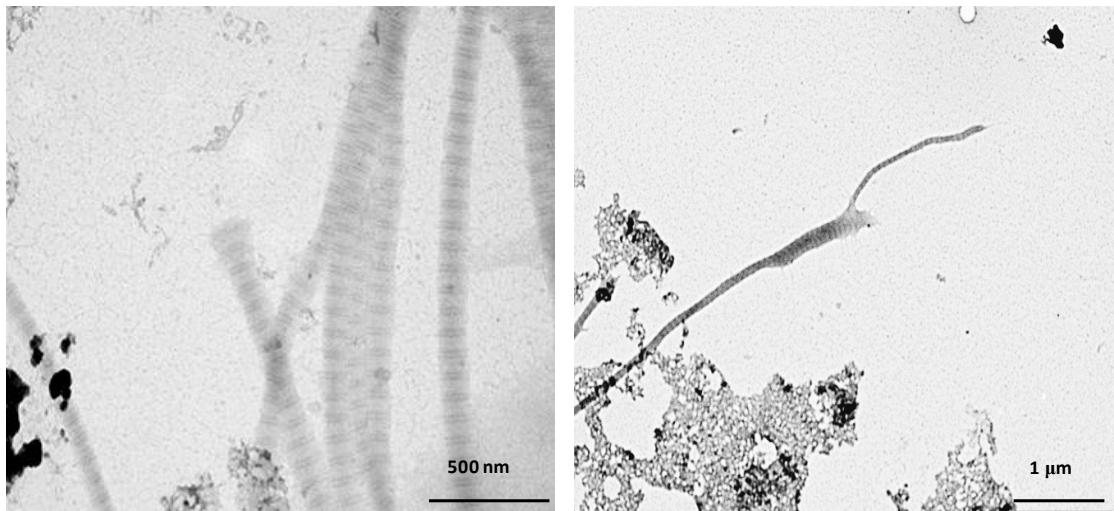


Figure 3.12: TEM images of collagen from a modern cow bone (left) and a sample excavated in 2010 from Star Carr (right).

Collagen is easily identified by its characteristic banding - a result of the regular organisation of collagen fibrils (e.g. Rho *et al.*, 1998). This banding is less obvious in the archaeological sample (Figure 3.12, right). Along with apparent ‘fraying’ of the fibrils at the end, this may signify collagen damage (Koon, 2006; Koon *et al.*, 2010).

3.2.8.2.1 Conclusions on microscopy methods

It was noted that during the preparation of thin-sections for optical microscopy, pieces of the bone treated at pH 2 tended to flake away from the slide very easily. It is possible therefore that the preparation could be causing additional damage to the bone. For SEM analysis, preparation techniques are minimal, and alteration of the histological structure at pH 2 was clearer. SEM was therefore recommended for future analysis.

TEM analysis successfully revealed collagen microstructure, whereas SEM and optical microscopy cannot. However, the preparation method requires a large amount of sample to be destroyed, and TEM is not a technique that is readily available. This makes it more suitable for providing further information on selected samples after other chemical techniques have been applied.

3.2.9 Conclusions on bone analysis methods

Several methods of analysis have been tested and shown to provide complementary information. Whilst mass loss and visual analysis provide a quick and easy comparison between samples, determination of the amino acid content and the racemisation of Asx provides more detailed information regarding loss of HA and degradation of the collagen. Differences between bones in different states of deterioration are easily elucidated by application of all methods combined. With archaeological samples, the mass loss and pH buffering methods are not possible, but they are useful for assessing degradation in laboratory experiments.

Several methods of analysing changes in the HA fraction of the bones have been discussed and each have advantages and disadvantages. The use of Raman spectroscopy proved in this study to be largely unsuccessful, possibly due to the lack of availability of a laser with an appropriate wavelength. Both p-XRD and FTIR provide suitable alternatives, although without further method development both have been concluded to be only qualitative. FTIR is most applicable to measuring the extent of demineralisation; however this is achieved more qualitatively by assessment of the relative amino acid content using RP-HPLC. In contrast, p-XRD reveals independent information on the HA crystallinity, which may be more useful as protein degradation is determined by amino acid analysis. p-XRD provides an overview of the bulk of the sample, in comparison to spectroscopic techniques, which focus on a very small area of a sample. This may be overcome by powdering and homogenising samples; however, several studies raise concerns over the effects of sample preparation techniques for FTIR (e.g. Surovell & Stiner, 2001). It was proposed that in this study p-XRD should be utilised as the major routine method of characterising the overall crystallinity of bone samples, with FTIR being applied in selected cases, for example to confirm the extent of bone demineralisation.

Microscopic methods have provided additional information, although the preparation methods can be time consuming and expensive. The value of that information can also be dependent on sample preparation techniques used (for example, thin-sectioning may cause cracking of delicate archaeological samples), and interpretations are user dependent. Throughout the study, SEM and TEM have been applied selectively when additional information is required, rather than being used as a primary means of analysis.

3.3 Analysis of wood deterioration

3.3.1 Introduction

Wood excavated from Star Carr (such as the extensive split-timber structure at the lake edge) has provided perhaps the earliest evidence for carpentry in Europe (e.g. Clark, 1954). Upon analysis of wood fragments excavated in 2010, it was found that wooden artefacts from different parts of the site were less well preserved. SEM analysis revealed a completely collapsed cell structure in several of the samples, possibly the result of cellulose loss, and standard decay assessment tests confirmed the poor preservation (Milner *et al.*, 2011a).

Wood is composed of a number of closely interlinked organic polymers: lignin, cellulose and hemi-cellulose (Hedges, 1990). Analysis of deterioration normally focuses on assessment of the relative composition, and applied techniques often consider both lignin and celluloses (e.g. Almkvist, 2011).

3.3.2 Experimental

For the MDE, an approximately 2 cm diameter branch was taken from a young birch tree and sliced into 3 mm thick sections using a band saw.

Solutions of pH 2, 3, and 5 sulfuric acid were made by diluting 12 M sulfuric acid (Fisher Scientific) with MilliQ water. Slices of wood were sealed into separate glass vials containing a solution of the appropriate pH, or MilliQ water (approximately pH 7) as a control. These were treated identically to the bone samples, as described in Section 3.2.2.

3.3.3 Bulk assessment

3.3.3.1 Methods

Visual assessment, mass loss and pH analysis was carried out as for bone during the MDE, using the methods described in Section 3.2.2.1.

3.3.3.1.1 *Maximum water content*

For wood, maximum water content (u_{\max}) provides additional assessment of the bulk condition of a sample and is commonly used prior to conservation of wood to assess its preservation (e.g. Panter & Spriggs, 1996). The method used here was adapted from that described by Hoffman (1981). Samples were immersed in water in an open glass vial. This was then put under vacuum for 30 seconds and then the vacuum slowly released. The process was repeated

a total of three times, ensuring maximum saturation. After drying the surface of the sample on a tissue, saturated mass was recorded immediately, and the sample left to dry at 105°C until a constant mass was reached. The dry mass was recorded and u_{\max} reported as a percentage of the dry mass.

3.3.3.2 Assessment of bulk analysis techniques

No visual alteration of the samples was observed in the MDE, although the surrounding solution darkened in all samples, with the less acidic samples appearing slightly darker. This is likely to be caused by water soluble 'extractives' such as tannins and humic acids leaching out of the wood (e.g. Hedges, 1990).

Mass losses in all of the method development samples were approximately 15%, which is possibly accounted for by the loss of non-structural components such as simple sugars and sap (Jane *et al.*, 1970). No significant difference in deterioration was observed at the different pH values. Similarly, u_{\max} was around 200 % for all samples, which is slightly higher than that of fresh wood (90-120 %, Hoffman, 1981). Hoffman (1986) defines degraded wood as having a higher u_{\max} than 300 %, suggesting that the experimental samples may have only lost non-structural components. However, it must be noted that as wood is a very porous material, obtaining an accurate dry mass is difficult, reducing the reliability of measurements both for mass loss and u_{\max} analysis (Jensen & Gregory, 2006). The pH of the surrounding solutions was found not to alter by more than ~ 0.5 pH units, signifying the much lower buffering ability of wood compared to bone. The implication of this is that the wood samples would have been exposed to low pH throughout the experiment.

3.3.3.2.1 Conclusions

Visual and mass loss analysis provides a fast and easy method of comparing deterioration between samples, although no alteration was observed for the method development samples. Whilst pH analysis of the surrounding solution did not show as much alteration as for bone, it is useful to monitor the conditions to which the wood samples are exposed compared to equivalent bone samples. u_{\max} should be used only as a rough guide of deterioration, and was not able to identify differences between the four experimental samples. Despite this, it is an established technique that has often been reported with regard to the assessment of archaeological wood. This means that it allows comparison with reported values for archaeological samples both from Star Carr and other sites.

3.3.4 FTIR spectroscopy

FTIR analysis of wood can provide molecular information regarding both the lignin and cellulose fractions of wood (e.g. Pandey, 1998; Gelbrich *et al.*, 2008). With the use of an ATR unit, where no sample preparation is required except for drying, it can also potentially be non-destructive. Direct analysis of the surface of the sample reveals a number of peaks characteristic of functional groups present in both polymers. In addition, the position of these peaks is often characteristic of the species of wood (Pandey & Pitman, 2003). A number of the characteristic absorption bands contains contribution from each of the two polymers; however, several key peaks can be identified as being the result of absorption of groups specific to cellulose (1375 and 1325 cm^{-1} , which relate to O-H and C-H bonds respectively) and lignin (1507 cm^{-1} , specific to the aromatic ring; 1240 cm^{-1} , specific to the C-O-CH₃ group) (Pandey, 1998). In this assessment, these four peaks have been focused upon.

3.3.4.1 Method

Minimum sample preparation is necessary for FTIR measurements, except for drying. A sub-sample of wood was sliced with a scalpel along the tangential plane. Analysis was carried out on a Vertex 70 FTIR spectrometer fitted with an ATR unit. A resolution of 4 cm^{-1} was used to scan between 600 and 3600 cm^{-1} using an averaged 16 scans (adapted from Gelbrich *et al.*, 2008).

3.3.4.2 Assessment of FTIR for the analysis of wood

Three readings were taken from each of the four MDE samples described in Section 1.3.2.1. Visually, little or no difference was seen between spectra. Intensities of the four key peaks (1507, 1375, 1325 and 1240 cm^{-1}) were calculated, as illustrated in Figure 3.13 (following the protocol of Gelbrich *et al.*, 2008).

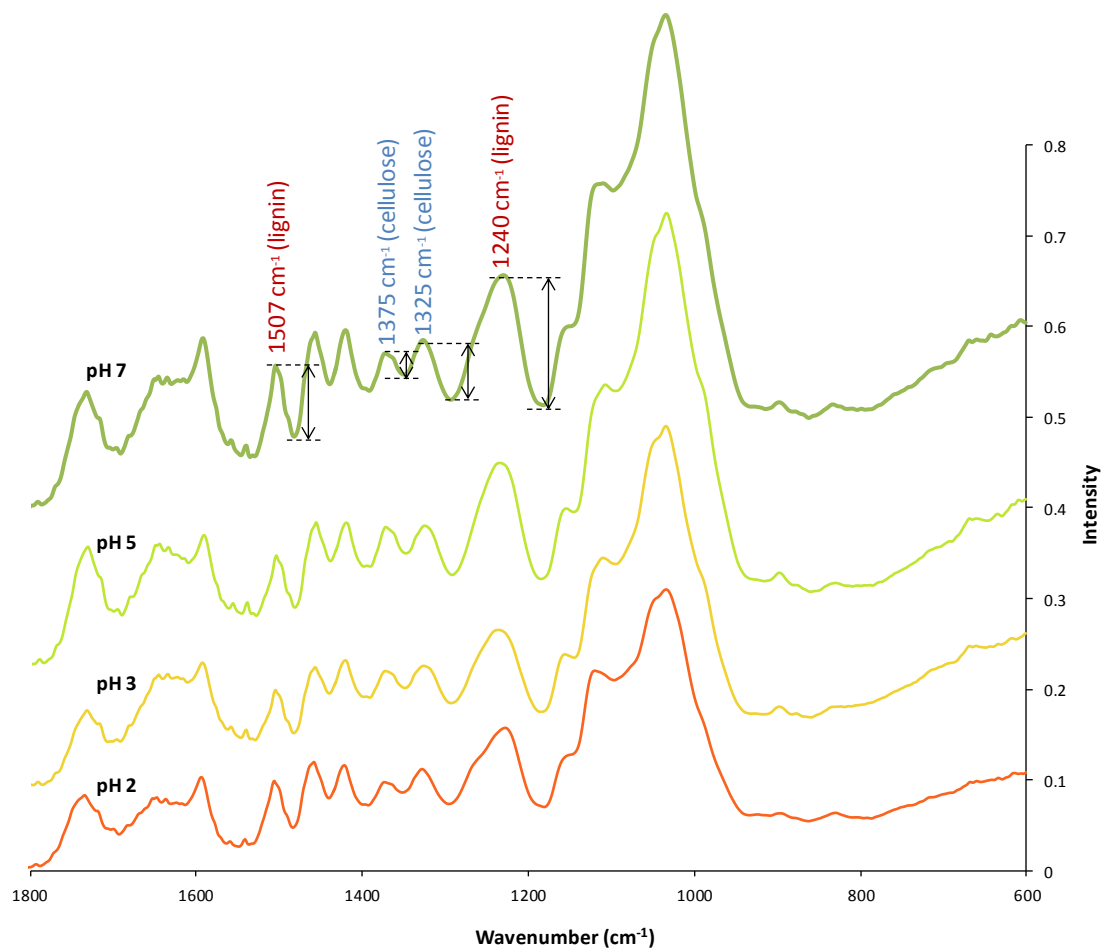


Figure 3.13: FTIR spectra for the four MDE wood samples, showing calculation of peak heights from the four key absorption peaks (following the protocol of Gelbrich *et al.*, 2008). (Originally in colour).

It has been suggested that an increase in the lignin: cellulose ratios derived from the FTIR spectra can be indicative of wood decay (Gelbrich *et al.*, 2008) as bacterial decay of cellulose often occurs before lignin loss in archaeological wood (e.g. Blanchette, 2000). However, Pandey & Pitman (2003) demonstrate that certain bacteria preferentially decay lignin, which may distort this ratio. As the phenolic group in lignin is also likely to be more resilient to decay than the functional methoxy group, comparison with only the phenolic absorption (1507 cm^{-1}) might also therefore be useful.

Peak height were calculated for the four key peaks indicated in Figure 3.14, by subtracting the minimum intensity to the right of the peak from the maximum intensity, according to Gelbrich *et al.* (2008). Based on the estimated order of decay (cellulose > methoxy lignin group > phenol lignin group) (Faix *et al.*, 1991; Pandey & Pitman, 2003), three ratios were then calculated from these peak heights. These were: total lignin: total cellulose (an increase in which indicates cellulose loss); 1507: total cellulose (again indicating cellulose loss, using only the most stable

lignin peak); and 1507: 1240 (an increase in which would indicate loss of the C-O-CH₃ functional group of lignin).

Although on initial inspection it appears that increased cellulose loss at low pH is indicated by an increase in the lignin: cellulose and 1507: cellulose ratios, consideration of the error in the results suggests that the differences are not significant. Mass loss and μ_{\max} analysis also showed that very little difference was seen between the four samples, and it is possible that degradation due to acid alone has simply not occurred in this short time-frame.

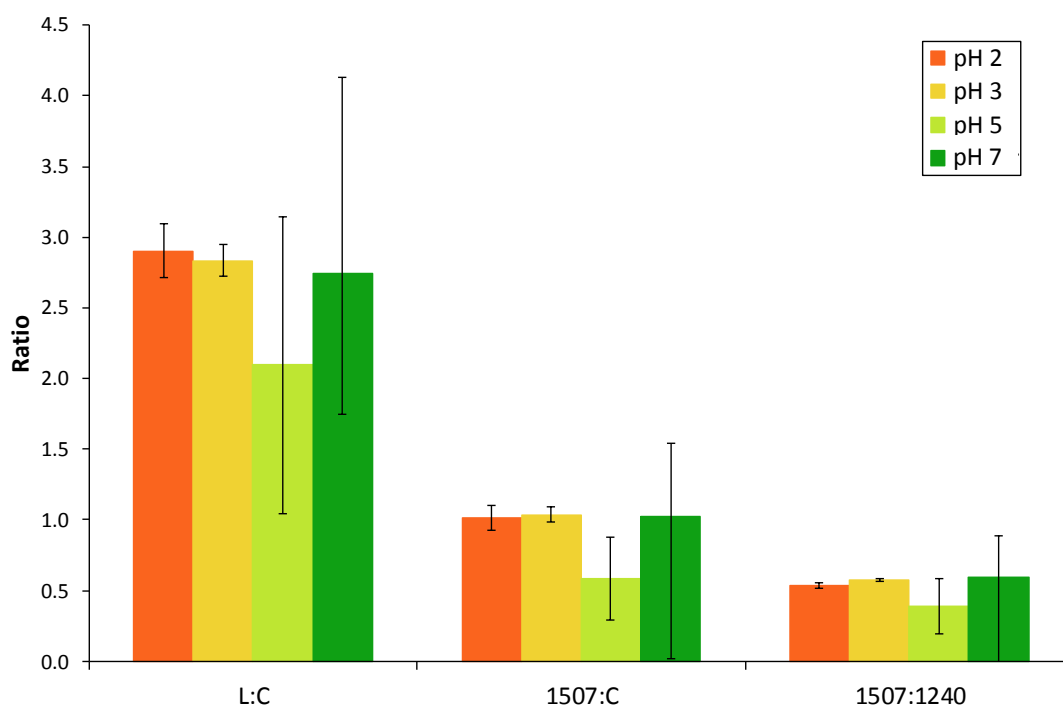


Figure 3.14: Comparison of ratios derived from FTIR peak heights for the four MDE wood samples. Error bars represent 1 standard deviation of three repeat readings for each sample. (Originally in colour).

In order to further test whether these ratios could be useful for directly comparing levels of degradation between wood samples, the analysis was expanded to include a number of archaeological samples. Further details of each of these are provided in Chapter 7, but in summary include:

- a sample from Star Carr excavated in 2007 and stored under aerobic conditions prior to analysis, visually assessed to be in an advanced state of decay
- an ash sample from the Bronze Age site of Must Farm, visually assessed as reasonably robust
- a sample from the Iron Age site of Fiskerton, also described as robust

Inspection of the FTIR spectrum from the Star Carr sample shows that the sample is degraded to such an extent that cellulose signals are very low and the peak at 1240 cm⁻¹ is not present

(Figure 3.31). This indicates that any lignin still present in the sample may be completely defunctionalised. As a result of this, the derived 1507: 1240 ratio is not comparable to the other samples and has therefore been omitted. Other ratios derived from FTIR spectra for the archaeological samples are compared to a fresh birch sample in Figure 3.32.

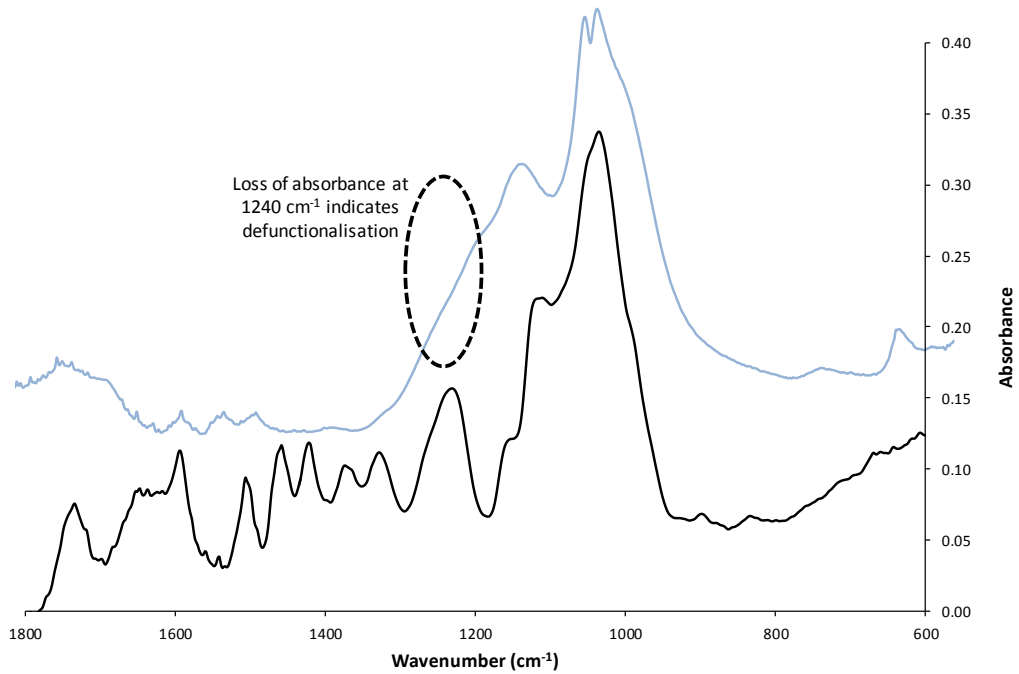


Figure 3.31: Comparison of FTIR spectra for untreated modern wood (bottom) and the wood sample excavated from Star Carr (top). (Originally in colour).

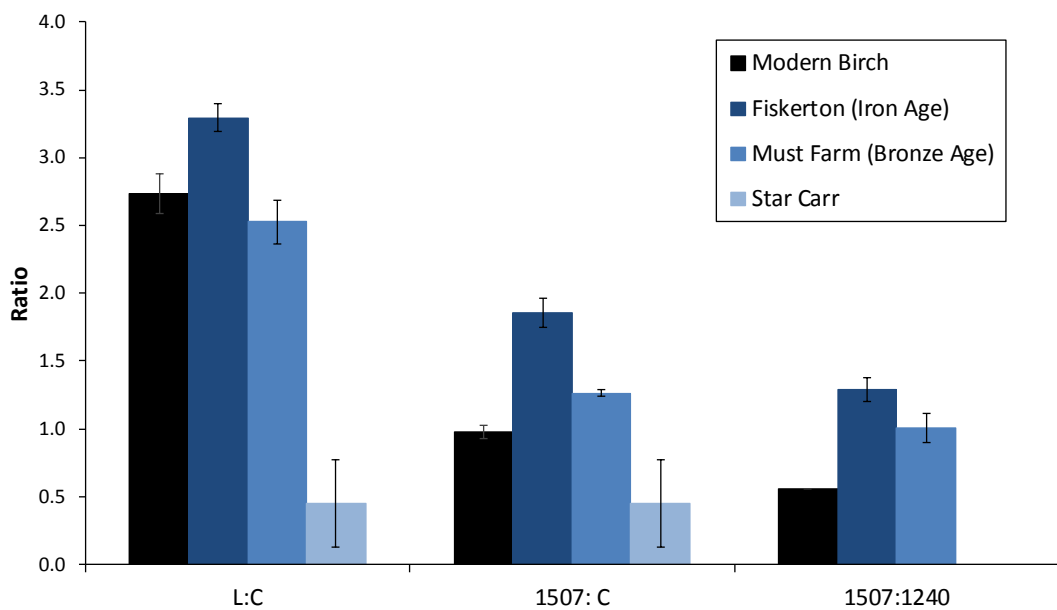


Figure 3.32: Ratios calculated for a series of archaeological samples compared to a modern birch sample. (Originally in colour).

As expected, both the Bronze Age and Iron Age samples have elevated 1507: C and 1507: 1240 ratios compared to the modern samples, indicating increased deterioration.

3.3.4.3 Conclusions of FTIR for the analysis of wood

Analysis of the four MDE samples showed very little difference between samples, with difference in the calculated ratios being within the margins of error (calculated by replicate analysis of an untreated sample). Whilst this supports analysis by bulk assessment methods, it is possible that FTIR analysis is not suitable for detecting very small chemical changes in wood.

FTIR analysis of archaeological wood showed that differences between archaeological samples could be more easily elucidated; in particular, the defunctionalisation of lignin in a sample excavated from Star Carr was detected by disappearance of the characteristic absorption at 1240 cm^{-1} (Figure 3.16). Analysis of the archaeological samples showed that by evaluation of three defined ratios, it is possible to compare samples directly although analysis must also be approached with caution. Ratios can be distorted by the absence of peaks, and therefore each spectrum should also be analysed individually. Alterations in the spectra such as peak splitting may also be indicative of decay (Pandey & Pitman, 2003).

3.3.5 Py-GC

FTIR analysis has been shown to be only semi-quantitative, with a relatively large degree of error between replicate readings of samples. Studies show that a more detailed analysis of polymer breakdown may be achieved by py-GC (e.g. Vinciguerra *et al.*, 2007; Colombini *et al.*, 2007).

The advantages of using py-GC analysis are primarily the small sample size (approximately 1 mg) and the lack of sample preparation required (Alves *et al.*, 2006). During pyrolysis, the major sub units of both lignin and cellulose are broken up into sub units, without fragmentation or alteration, due to the inert environment in which the sample is combusted. Studies using py-GC-MS have identified cellulose related products eluting first, followed by products relating to lignin (van Bergen *et al.*, 2000). The composition and relative abundance of these lignin related products reflect the chemical nature of the lignin prior to pyrolysis; for example, an increase in the number of lignin sub units containing double bonds on the side chain or complete loss of the methoxy substituents indicates that chemical alteration of the lignin has occurred (e.g. Faix *et al.*, 1991).

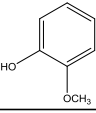
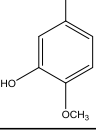
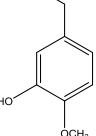
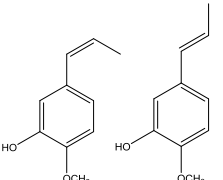
Py-GC has been assessed, as it is potentially more sensitive than FTIR for determining minor structural changes. Although FTIR is useful for determining parameters such as lignin: cellulose ratios, no differences between the four samples from the preliminary experiment were elucidated using FTIR. It is possible that this is because differences were very small over such a short time scale.

3.3.5.1 Method

Cross sections of the MDE wood samples were cut, dried and ground to a powder using an agate pestle and mortar. Approximately 1 mg sub samples were weighed into a quartz crucible and placed into a heated filament pyroprobe unit (CDS pyroprobe 5150, Chemical Data Systems). Samples were cleaned by heating to 290°C for 15 seconds in the presence of helium, to remove non-structural components (thermal desorption) followed by pyrolysis by heating at 610°C for 15 seconds. This was coupled to a trace GC Ultra gas chromatograph (Thermo Fisher) fitted with a flame ionisation detector and a fused silica capillary column (Thermo Trace TR-5; 30 m x 0.25 mm). The valve oven, transfer line and GC inlet were held at 310°C, and the oven temperature at 50°C for 5 minutes, and separation achieved using a ramp rate of 4°C/min to 320°C, with a helium carrier gas at 2 mL/min (adapted from van Bergen *et al.*, 2000).

Retention times of key structural compounds were confirmed by analysis of commercially purchased standards (Aldrich). Solutions of the standards were made by appropriate dilution in HPLC grade hexane (Fisher Scientific) and injected onto the quartz crucible whilst inside the pyroprobe, prior to pyrolysis. Approximate retention times are summarised in Table 3.1. These known standards were analysed periodically to confirm retention times, and these times used to assign chromatograms based on published mass spectrometry data (e.g. van Bergen *et al.*, 2000).

Table 3.1: Approximate retention times in applied GC method for important lignin related compounds.

Compound	Structure	Notation	Retention time (minutes)
Phenol		P	11
Guaiacol		G	15
2-Methoxy-4-methylphenol		1	19
4-Ethylguaiacol		2	22
Isoeugenol (cis/trans)		3/4	25/27

3.3.5.2 Assessment of py- GC technique

The four samples from the MDE were analysed by py-GC. Chromatograms from the samples treated at pH 2 and pH 7 (water) are shown in Figure 3.17. Identification of key lignin related peaks was carried out by comparison to the retention times of the standards listed in Table 3.1.

Bulk analysis and analysis by FTIR revealed only minimal differences between samples treated at different pH, and in the py-GC chromatograms, the intensity of cellulose and lignin peaks also appear similar in each sample (Figure 3.17). This confirms that degradation is minimal, or indeed absent.

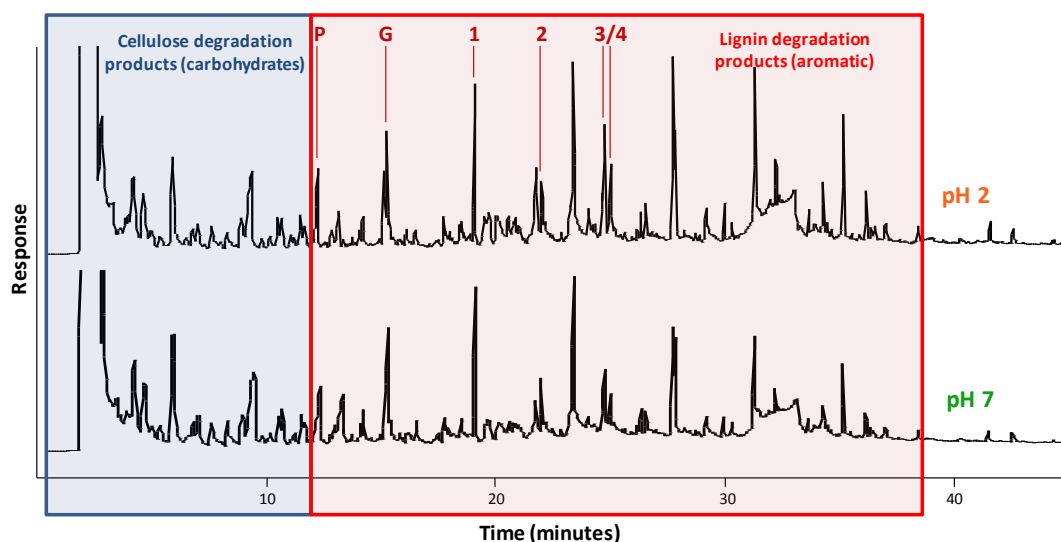


Figure 3.17: py-GC traces for MDE wood samples treated in pH 2 and pH 7 acid. Labelled peaks were identified by analysis of purchased standards, shown in Table 3.1. (Originally in colour).

An increase in phenol content of a sample is likely to be indicative of defunctionalisation of both syringol and guaiacol units of lignin, and may occur via either biological or chemical pathways (Hatcher, 1984; Martinez *et al.*, 2005). The phenol peak in each of the four MDE samples was identified using the approximate retention time in Table 3.1. Alves *et al.* (2006) show that quantification of peaks can be precise without the use of an internal standard, if the mass of that starting material is known. Therefore, the peak areas were divided by the mass of sample in mg, providing a measure of phenol peak area per mg. An increase in defunctionalisation also results in a higher P: G ratio, as more guaiacol type units are converted into phenol type sub-units. P: G ratios for all MDE samples were calculated using the peak areas as assigned using the retention times of the standards. These values are compared in Figure 3.18 along with an untreated birch sample. Each sample was analysed in duplicate and the average value shown.

Whilst these values do not provide an absolute measure of the phenol or guaiacol content, it allows an easy comparison between samples. However, the calculated error is high in all samples, and differences between the MDE samples were largely within the margins of error with the exception of the P: G ratio where an increase in defunctionalisation compared to the modern sample can tentatively be determined.

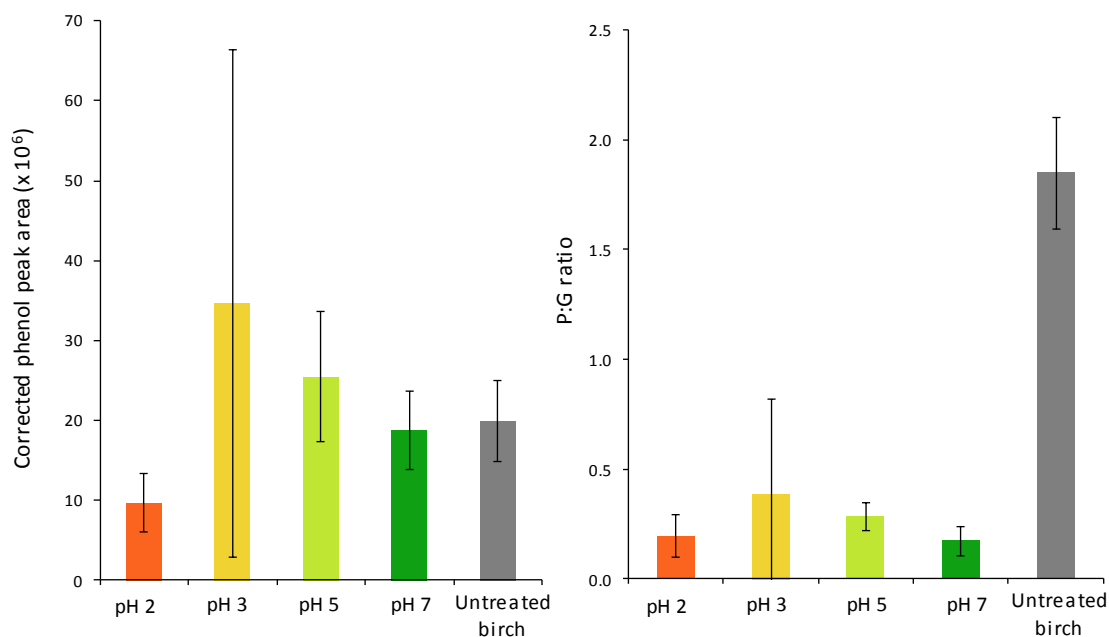


Figure 3.18: Peak areas of phenol corrected for mass (left) and P: G peak area ratios (right) for the four MDE samples preliminary samples compared to an untreated birch sample. Error bars are one standard deviation calculated from replicate analysis of the each sample. (Originally in colour).

In order to assess whether py-GC may be more informative for the analysis of archaeological material, where degradation may be more advanced, analysis was also carried out on a sample excavated from Star Carr in 2013 (sample SC13 93554; Figure 3.19). Further sample details are given in Chapter 7 where a comparison is made with other archaeological wood samples.

Analysis of the archaeological sample shows that where a sample is more degraded, alteration of the cellulose and lignin is easily identified by py-GC analysis. Loss of many of the cellulose related products at the start of the chromatogram indicates that the sample is severely depleted in cellulose. In addition, the phenol peak is more intense in the archaeological sample, indicating defunctionalisation of the lignin; this is also signified by a reduction in the intensity of the guaiacol peak (G) (Figure 3.19).

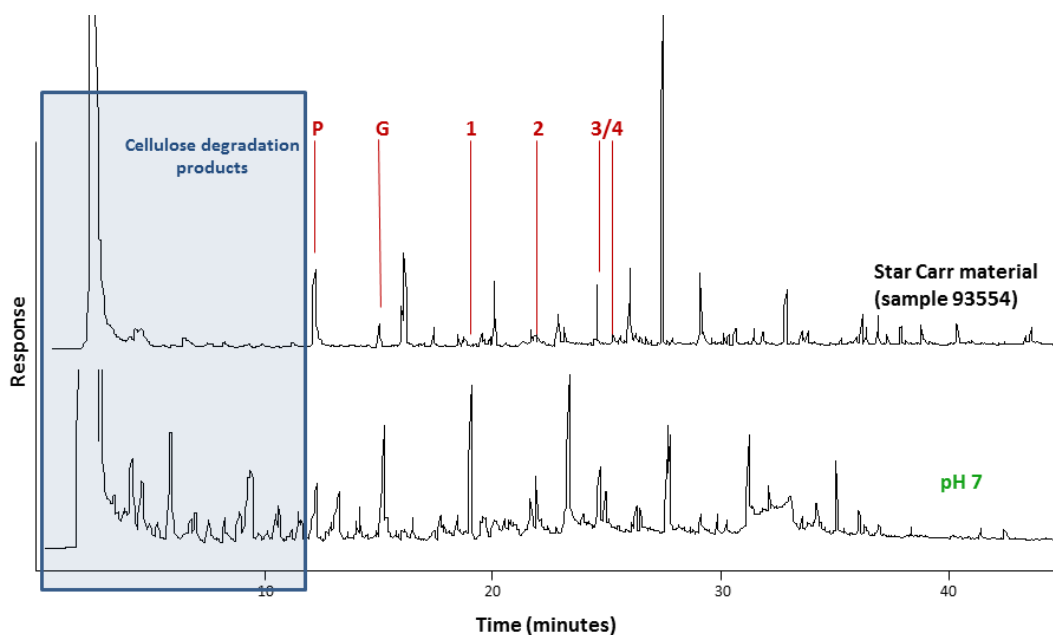


Figure 3.19: Comparison of py-GC traces between the MDE sample at pH 7 and an archaeological sample from Star Carr. Degradation of both lignin and cellulose is indicated in the archaeological sample by an increased intensity of the phenol peak (P) and a decreased intensity of other lignin components, labelled according to Table 3.1. (Originally in colour).

3.3.5.3 Conclusions of py-GC analysis of wood

Whilst FTIR reveals relative compositions of the wood samples, thus informing on the broad level of deterioration, py-GC gives a more detailed description of alteration of the major polymers, particularly lignin. An increase in the levels of defunctionalisation in lignin (due to chemical and biological attack: Martinez *et al.*, 2005) can be indicated by an increased concentration of non-methoxylated compounds in the GC trace, particularly phenol. In FTIR, such small-scale differences may be unobservable as long as the lignin is largely intact. Phenol concentrations measured by py-GC could therefore be a useful method of comparing samples. Although an increase in phenol was not observed in the method development samples, this is consistent with results from bulk and FTIR analysis that indicate that significant deterioration had not occurred. Comparison with an archaeological sample shows that py-GC can reveal changes to both the lignin and cellulose when degradation is more advanced.

Development of the py-GC method has not been fully investigated here. Ideally, more detailed interpretation of the lignin-related peaks would be carried out using mass spectrometry. Whilst peak ratios may allow direct comparisons between samples, the error has been shown to be significant, and the use of an internal standard would allow the technique to be more quantitative (Bocchini *et al.*, 1997). Py-GC has therefore been used primarily as a secondary technique throughout the study, applied to samples where additional information may be useful.

3.3.6 Microscopic techniques

Microscopic analysis of archaeological wood can reveal a great level of detail, as illustrated by studies such as those by Blanchette *et al.* (1990) and Bjordal & Nilsson (2007), where characteristic decay patterns are identified in different parts of the cells. Loss of structural parts of the wood may also be identified in both SEM and thin-section microscopy (e.g. Powell *et al.*, 2001).

3.3.6.1 Methodology

3.3.6.1.1 Optical microscopy

Two methods of preparing wood thin-sections for optical microscopy were tested.

Firstly, samples were set in resin similarly to as described in Section 3.2.7.1 Due to the porous nature of the material however, the resin did not fully set. This resulted in breaking up of the wood during polishing.

A more commonly used method for archaeological wood (e.g. Bjordal *et al.*, 1999) is to slice a thin-section with a razor blade, sometimes freezing the sample prior to sectioning. Although this is effective for soft archaeological wood, it is difficult to achieve thin enough slices of robust, modern samples for analysis.

Wood samples were viewed using plane polarised light with a Zeiss AxioScope binocular microscope with a motorised stage.

3.3.6.1.2 SEM

SEM analysis was carried out identically as for bone (Section 3.2.7.1).

3.3.6.2 Assessment of techniques

All four samples from the MDE were prepared in resin for thin-section analysis. Although structural components could be observed, differences between samples were not. It was not possible to analyse the samples optically using a sliced section.

The minimal preparation method used for SEM analysis did not result in cell wall collapse in the modern MDE samples, as is often seen for archaeological wood (M. Stark, pers. comm., 2011). Structural features of all samples were clearly visible, allowing the assessment of whether structural decay has occurred (Figure 3.20).

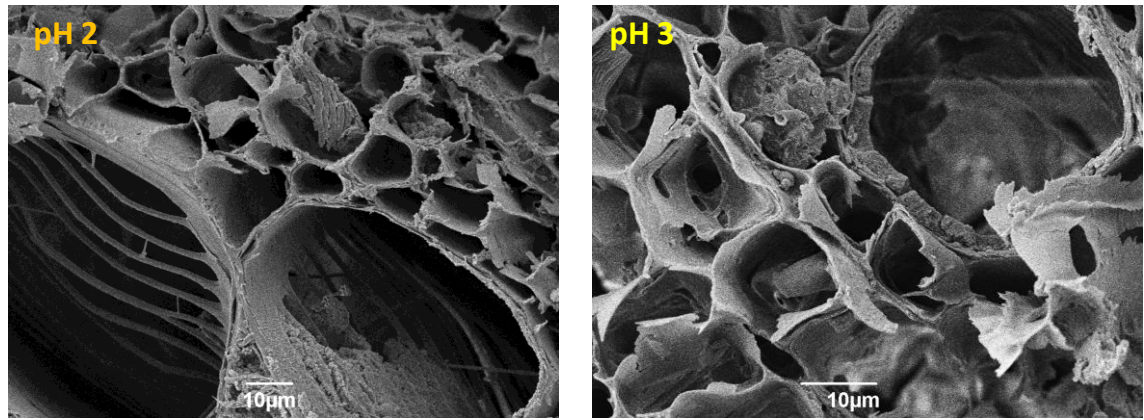


Figure 3.20: SEM images of wood samples treated at pH 2 (left) and pH 3 (right). Wood structure is clearly observed under SEM, and no damage is seen in either sample.

3.3.6.2.1 Conclusionsof microscopy methods

Both SEM and thin-section analysis of the four MDE samples revealed no structural differences; this agrees with results from other analytical methods, so does not suggest that microscopy is unsuitable for observing structural changes. Indeed, previous studies use it as a primary method of analysis (e.g. Blanchette *et al.*, 1999; Bjordal *et al.*, 1999).

Thin-section analysis of modern wood samples was not particularly successful and was not pursued as a primary method of analysis for this study. However, in softer archaeological samples it may be more appropriate, although it has not been applied here. A simple method of SEM analysis proved successful and has been used in preference to optical microscopy for the analysis of modern samples.

3.3.7 Conclusions on wood analysis methods

Analysis of a preliminary set of acid-treated wood samples has shown that over the short experimental time period used here, differences are minimal, and analytical techniques for the analysis of experimental wood deterioration are therefore required to be sensitive enough to detect small changes. Bulk assessment techniques are perhaps not as suitable for the analysis of wood as for bone; however, where they can be applied they allow both a direct comparison with bone treated at equivalent conditions and a quick comparison between samples. In addition, commonly used measurements such as u_{\max} may allow the direct comparison with reported data for archaeological samples.

Whilst a number of wet chemical methods for the chemical characterisation of wood exist and are widely reported (e.g. Alves *et al.*, 2006; Capretti *et al.*, 2008), all of these methods require large amounts of sample and complicated preparation (Kleen & Gellerstedt, 1991). For this reason, it was decided not to pursue these methods, as they would not be appropriate for the analysis of archaeological samples.

FTIR analysis is an alternative method of chemical characterisation and has been shown to give a reliable analysis of lignin: cellulose ratios in wood, as well as more detailed information, for example alteration of the lignin peaks upon lignin defunctionalisation (e.g. Pandey & Pitman, 2003; Gelbrich *et al.*, 2008). Due to its ease of use and potential to be applied non-destructively, it is highly appropriate for the analysis of archaeological wood. However, it was possibly not sensitive enough to detect changes in these experimentally altered samples. For this reason, py-GC was also investigated. Although in the early stages of development, the py-GC technique used provides complementary information to the FTIR analysis and has been used when additional information could be useful. In particular, by examining key degradation indicators, such as phenol content, lignin alteration could be more securely identified.

SEM analysis proved to be the most effective microscopic technique, considering that for the purposes of this study it needs to be appropriate for both archaeological and modern samples. Again, the technique is minimally destructive and provides complementary information, allowing the assessment of whether chemical changes have led to the loss of structural integrity. Visual analysis allows the comparison of samples with archaeological material reported in literature. SEM has also been applied selectively, providing additional information when necessary.

Table 3.2: Summary of all analytical techniques targeted for the analysis of organic materials throughout the rest of the study. The rationale for each technique has been previously detailed.

Technique	Material		Advantages	Disadvantages	Description of application
	Bone	Wood			
Visual analysis	✓	✓	<ul style="list-style-type: none"> Ease of application Direct comparison between samples 	<ul style="list-style-type: none"> Subjective 	Routinely applied to all samples throughout thesis
Mass loss analysis	✓	✓	<ul style="list-style-type: none"> Ease of application Direct comparison between samples 	<ul style="list-style-type: none"> Cannot be applied to archaeological material 	Routinely applied to experimental samples throughout thesis
pH analysis	✓	✓	<ul style="list-style-type: none"> Semi-quantitative Ease of application 	<ul style="list-style-type: none"> Cannot be applied to archaeological material 	Routinely applied to experimental samples throughout thesis
Maximum water content		✓	<ul style="list-style-type: none"> Ease of application Allows comparison with published archaeological data 	<ul style="list-style-type: none"> Subject to high levels of error 	Routinely applied to all wood samples throughout thesis
Amino acid analysis (concentration and racemisation)	✓		<ul style="list-style-type: none"> Fast; can routinely analyse large numbers of samples Allows comparison to literature data Minimally destructive 	<ul style="list-style-type: none"> Not widely available Concentration data is subject to high levels of error 	Routinely applied to all bone samples throughout thesis
Powder X-ray diffraction	✓		<ul style="list-style-type: none"> Potentially minimally destructive Ease of interpretation Allows comparison to literature data 	<ul style="list-style-type: none"> Not widely available Difficulty in powdering bone samples 	Applied to most bone samples throughout thesis
FT-Infrared spectroscopy	(✓)	✓	<ul style="list-style-type: none"> Widely available Ease of application Potentially non-destructive 	<ul style="list-style-type: none"> Non-quantitative Subjective 	Routinely applied to all wood samples and selected bone samples
Py-Gas chromatography		✓	<ul style="list-style-type: none"> Detailed analysis of lignin breakdown Allows comparison to literature data 	<ul style="list-style-type: none"> Slow analysis times Difficult to interpret without mass spectrometry 	Applied to selected wood samples
Optical microscopy		✓	<ul style="list-style-type: none"> Widely available Allows analysis of histological alteration 	<ul style="list-style-type: none"> Subjective Destructive 	Used only rarely due to difficulties in achieving thin sections
Scanning electron microscopy	✓	✓	<ul style="list-style-type: none"> Easy to interpret Minimal sample preparation 	<ul style="list-style-type: none"> Subjective Destructive 	Used on selected bone and wood samples
Transmission electron microscopy	(✓)		<ul style="list-style-type: none"> Provides high resolution visual analysis 	<ul style="list-style-type: none"> Not widely available Complicated and destructive sample preparation 	Applied minimally due to costs and destructive preparation

3.4 Summary of methods

A number of analytical methods suitable for the purpose of assessing organic preservation are reported. For the purposes of assessing the deterioration of organic materials at Star Carr, techniques that are minimally destructive, relatively cheap, and easily accessible have been focused on. It was important that the methods developed here could be applied to both modern and archaeological materials, providing a range of complementary information on the various structural components, both qualitative and quantitative.

Following analysis of MDE samples of both bone and wood, the techniques that have been routinely applied throughout this study are summarised in Table 3.2. In addition, some techniques have been applied only when additional information was deemed important. This was due to factors such as those techniques being not as readily available, costly or requiring large amount of sample to be destroyed, making them inappropriate for the routine analysis of archaeological materials.

CHAPTER 4

INVESTIGATING ORGANIC DETERIORATION IN ACID USING LAB-BASED EXPERIMENTS

4.1 Introduction

The following chapter is an adapted version of two papers; 1 currently in press and 1 currently under review:

1: Apatite for destruction: Investigating bone degradation due to high acidity at Star Carr. K. High, K.E.H. Penkman, N. Milner and I. Panter. Submitted to the Journal of Archaeological Science

2: Fading Star: Towards understanding the effects of acidification on organic remains (wood) at Star Carr. K. High, K. Penkman, N. Milner and I. Panter. Proceedings of the 12th ICOM-WOAM conference, 2013 (in press).

Results have been added to the second section (wood degradation) and therefore the two papers have been adapted and edited to fit in with the rest of the thesis.

The discovery of bone, antler and wooden artefacts in alarmingly advanced stages of deterioration during the 2006-2008 excavation phase at Star Carr raised concern for the future survival of any remaining organic archaeological material at the site (Milner *et al.*, 2011a; Chapter 1). The reasons for this accelerated decay were uncertain; factors contributing to organic degradation at wetland sites are many, and often interlinked. Examples include soil density, dissolved salts and soil water content (e.g. Pollard, 1996; Caple, 2004). An increase in oxygen content (for example caused by a reduction in the height of the water-table) is also likely to have a significant impact on the biological activity of the environment. Microbial and fungal activity in archaeological wood are major facilitators of both cellulose and lignin loss (e.g. Blanchette, 2000; Bjordal *et al.*, 1999). However, the most recent analysis of wood from Star Carr revealed no substantial evidence for levels of biological decay above those expected at a waterlogged site of this age (Milner *et al.*, 2011a).

Monitoring of the Star Carr site has suggested that the water-table may have recently fallen and begun to fluctuate through the archaeological layer, possibly due to the installation of a series of field drains in 2000. The time period of monitoring has not yet been sufficient to establish long term trends regarding the exact position of the water-table, but it is expected to lie close to the archaeology (Brown *et al.*, 2011). Geochemical analysis of the site in 2009 further suggested that the site is no longer permanently saturated; elevated redox values (suggesting high levels of dissolved oxygen) were reported across the site. The observation of soil pH values of < 2.5 in the archaeological zone, as well as high concentrations of dissolved sulfur and iron (attributed to the dissolution of minerals such as pyrite from underlying

Speeton clay deposits) has led to the hypothesis that these geochemical and hydrological factors have led to the formation of sulfuric acid at the Star Carr site (Boreham *et al.*, 2011; Chapter 2).

It has been assumed that this dramatic and presumably rapid increase in acidity is leading to accelerated decay of organic remains (Milner *et al.*, 2011a). However, few studies consider the effects of such high sediment acidity as that seen at Star Carr, although instances of similar pH levels in archaeological deposits are known. Examples include Yoxall Bridge, where a soil pH of 2 was thought to be caused by underlying sulfur-rich mineral deposits (Brown *et al.*, 2010), and areas of the Bronze Age site of Flag Fen where a pH of approximately 3.5 has been reported (Powell *et al.*, 2001). Despite this, studies at these sites have not fully investigated the preservation potential for organic materials (specifically bone and wood) in burial environments with as high acidity as Star Carr.

Previous research shows that high acidity has a detrimental effect on the survival of bone (Gordon & Buikstra, 1981). Other studies have taken an experimental approach to modelling bone diagenesis (e.g. Turner-Walker & Peacock, 2008; Karr & Outram, 2012). Research into the effects of the pH of the burial environment however, has been limited to environments with only mildly acidic sediment (e.g. pH > 3; Nicholson, 1996; 1998).

Studies on the degradation of archaeological wood often focus on biological contributions to diagenesis and tend to be focused on marine environments (e.g. Bjordal *et al.*, 1999). Although components of wood are known to be soluble in high concentrations of acid (e.g. Hoffman & Jones, 1990; TAPPI standard T 222 om-88), degradation of lignin and cellulose in acidic environments is more often researched outside of an archaeological context (for example in the paper and pulp, or coal industries) and therefore burial times do not often equate to the archaeological time scale (e.g. Adler, 1977; Xiang *et al.*, 2003).

This study aims to test how destructive high acidities equivalent to those found at the Star Carr site are to bone and wood, controlling for other site conditions. To this end, laboratory-based degradation experiments in sulfuric acid using a range of modern and archaeological bone were performed. This removes all other factors contributing to organic deterioration and allows the assessment of whether high acidity is the main contributor to the observed organic diagenesis at Star Carr.

4.2 Experimental

4.2.1 Materials

4.2.1.1 Bone

Bone originating from a range of different species has been recovered from Star Carr, and slight differences in deterioration have previously been observed when comparing different types of bone (e.g. Nicholson, 1996; Koon, 2006). Throughout this study, sheep bone has been used as a modern analogue to deer bone (the most commonly recovered species from Star Carr) as it is more readily available. Modern long bone and rib samples were obtained from a butcher and identified by the butcher as sheep, with long bone A being from a more mature animal than long bone B. All were de-fleshed by gentle warming in a mild solution of biological washing powder.

Modern analogues allow the comparison of different types of bone and range of conditions due to the greater quantity of material available, but archaeological bones will have already undergone a significant amount of deterioration in the burial environment (e.g. Jans *et al.*, 2002; Turner-Walker & Peacock, 2008). Therefore, a large mammal rib bone (likely to be red or roe deer) was obtained from Star Carr during excavations in 2010. This allowed the assessment of whether archaeological material is more at risk than modern material.

All bone samples were sliced into 3 mm cross sections using a water-cooled diamond edged band saw.

4.2.1.2 Wood

Wood has been discovered at Star Carr in abundance, and spans a wide range of species, primarily birch, willow and aspen (Clark, 1954; Milner *et al.*, 2013b). In addition, wood has been found as both round wood and split timbers. In order to compare differences between species, both willow and birch have been used throughout this study.

Modern samples of birch (approximately 3 mm cross sections of a young branch) and willow (approximately 1 cm³ pieces from the centre of a trunk), were cut into uniform sections using a band saw. Similarly as for bone, archaeological wood is likely to have undergone significant levels of biological and chemical decay during the burial period (e.g. Blanchette, 2000; Bjordal *et al.*, 2000). Archaeological wood samples were obtained from both the Bronze Age site of Must Farm (ash) and from Star Carr (unknown species, probably willow) during excavations in 2007 (SC07). Samples of approximately 3 cm³ were prepared using a scalpel.

4.2.2 Method

Stock solutions of sulfuric acid at pH values of 1, 2, 3 and 5 were made using MilliQ water and 12 M sulfuric acid (Fisher Scientific). The accurate pH of each stock solution was recorded using a glass pH probe calibrated between pH 4 and 7 (Denver instrument) and kept to within 0.1 pH units of the selected pH throughout the experiment. Each sample was placed in a sterile glass screw-top vial and filled with 50 mL / g of the relevant solution. Two hydrological regimes were mimicked: the first to replicate conditions where there is limited movement of solution ('stagnant' conditions; S), and a second where the solution was replenished, replicating a 'dynamic' site hydrology (D). Experiments were carried out at room temperature (RT) and at 80°C in order to accelerate decay under laboratory conditions. The experimental conditions are summarised in Table 4.1 (for bone) and Table 4.2 (for wood).

Periodically (approximately weekly) sub-samples of the supernatant liquid (aliquot samples) were taken from each sample and the pH of the remaining solution recorded. At these points, the solution was replaced in the "D" samples.

Table 4.1: Summary of time points (in weeks) and planned experimental conditions for each bone type. Where samples had to be removed early due to rapid dissolution, the actual time point is shown in brackets. "D" represents dynamic conditions, and "S" represents stagnant conditions. Long Bone A is from an older animal than Long Bone B.

		Time points (weeks)					
		Long Bone A		Long Bone B		Rib Bone	Arch. Rib
pH	T	D	S	D	S	D	D
1	Room temperature	6,8,16	6	6	6	6,16	6,16
2		6,8	6			6	6
3		6,8,16	6	6	6	6,16	6,16
5		6,8	6				
Water		6,8	6	6		6	6
1	Heated (80°C)	6,16(4)	6	6(3)	6	6(2),16(2)	6(1),16(2)
2		6	6			6	6
3		6,16	6	6	6	6,16	6,16
5		6	6				
Water		6	6	6		6	6

Table 4.2: Summary of time points (in weeks) and experimental conditions for each wood type. "D" represents dynamic conditions, and "S" represents stagnant conditions

		Time points (weeks)						
		Modern birch		Modern willow		Star Carr	Must Farm	
pH	T	D	S	D	S	D	D	S
1	Room temperature	6,16	6	6,16	6	6	6	6
2		6	6	6		6	6	6
3		6,16	6	6,16	6	6	6	6
5		6	6					
Water		6,16	6	6,16		6	6	6
1	Heated (80°C)	6,16	6	6,16	6	6	6	6
2		6	6	6		6	6	6
3		6,16	6	6,16	6	6	6	6
5		6	6					
Water		6,16	6	6,16		6	6	6

4.2.3 Analysis of bone deterioration

All analysis was carried out according to methods developed in Chapter 3. The key techniques applied are summarised.

4.2.3.1 Bulk assessment

All samples were assessed by visual and mass loss analysis according to Chapter 3 Section 3.2.2. Analysis of the pH of the reaction solution was carried out to provide a time-dependent analysis.

A selection of samples were analysed by SEM and TEM according to Chapter 3 Section 3.2.7.1.

4.2.3.2 Chemical analysis

Analysis of the HA fraction was carried out using p-XRD only Chapter 3, Section 3.2.4). In some cases, not enough of the sample remained for analysis following experimentation.

Total amino acid concentrations and amino acid racemisation was analysed for each bone sample based on the procedure outlined in Chapter 3 Section 3.2.3. Analysis of the supernatant aliquots taken at each sample point was also carried out.

Analysis of the starting materials was carried out prior to experimentation. Asx racemisation was slightly elevated in the archaeological samples compared to the modern bones (D/L = 0.1 vs 0.06).

1.1.1 Analysis of wood deterioration

1.1.1.1 Bulk assessment

Visual analysis, mass loss and maximum water content (u_{\max}) analysis were carried out on all wood samples as outlined in Chapter 3 Section 3.3.2. Analysis of the pH of the solution was also carried out at each sampling point.

A selection of samples were analysed by SEM according to Chapter 3 Section 3.3.5.1.

1.1.1.2 Chemical analysis

All samples were analysed using FTIR (Chapter 3, Section 3.3.3). Heights for the 4 major absorption peaks (cellulose at 1325 and 1375 cm^{-1} ; lignin at 1240 and 1507 cm^{-1}) were calculated and used to calculate 3 ratios that serve as a measure of diagenesis (lignin: cellulose, 1507: cellulose, and 1507: 1240).

Additional analysis by py-GC was carried out on selected samples in order to supplement FTIR analysis, according to Chapter 3 Section 3.3.4.

Analysis of the starting archaeological material was carried out using FTIR prior to the start of the experiment, and a reduction in the intensity of the peaks relating to cellulose indicate that wood from both Must Farm and, to a greater extent, Star Carr were depleted in cellulose prior to experimentation.

4.3 Investigation into bone deterioration

4.3.1 Results: Bulk analysis

It is expected that the dissolution of HA ($\text{Ca}_{10}(\text{PO}_4)_6(\text{OH})_2$) in sulfuric acid will ultimately result in the formation of phosphoric acid; a much weaker acid, thus reducing the acidity (Atkins *et al.*, 2006) (Equation 4.1).

Equation 4.1: Formation of phosphoric acid from dissolution of HA.



It is often assumed that in the burial environment, this buffering of acidity by HA dissolution prevents the breakdown of the highly stable collagen helix (Collins *et al.*, 1995). The capacity of the HA to buffer acidity is clearly demonstrated by analysis of the pH of the surrounding solution for bone samples at pH 2 and above, with a rapid increase in the pH of the supernatant in all bone samples (Figure 4.1, top). An increase in pH was maintained even after 16 weeks under D conditions.

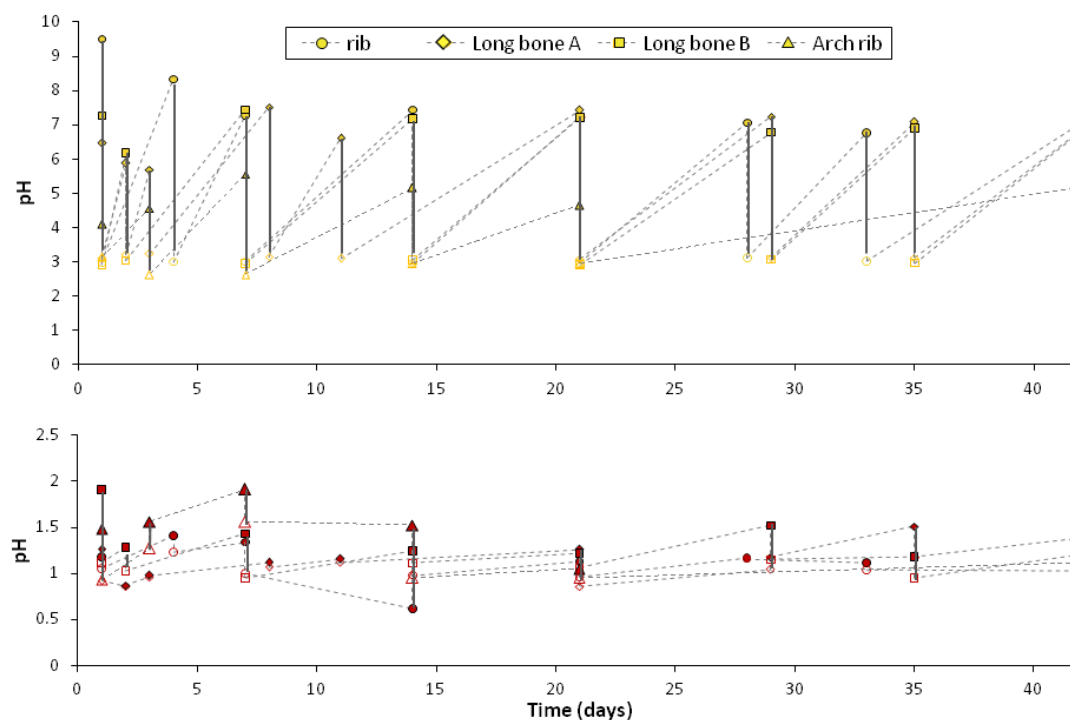


Figure 4.1: Measured pH for dynamic conditions at room temperature for all bone samples. Data is shown for the pH 1 experiment (bottom) and pH 3 experiment (top) for 6 weeks. Buffering continues at similar levels for the duration of the 16 week experiments. (Originally in colour).

At pH 1 this buffering ability is much weaker (Figure 4.1, lower), with a maximum pH of just under 2 being reached even in the S samples. Buffering is also significantly reduced in the

archaeological bone even at higher pHs, demonstrated by the data for pH 3 (Figure 4.1, upper); in contrast to the pH of 9.5 initially observed for the modern rib sample solution, the pH does not increase above 6.5 for the archaeological rib. It is likely that some mineral depletion has already occurred in the archaeological sample, leaving fewer phosphate and carbonate ions available to neutralise the acid.

At pH 1 and 80°C, disintegration began to occur after only three days for modern bones and one day for the archaeological bone, and so the experiment was stopped early in order to retain sample for analysis (indicated in Table 4.1). As the experiment progressed, severe distortion and a translucent texture was observed in both long bone A and long bone B at pH 1, RT by the 6 week time point. After 16 weeks, the same was seen in the bones at pH 2, RT (Figure 4.2).

Although no visible deterioration was seen during the experiment in the majority of other samples, upon drying all samples at pH 2 and 3, and those at pH 5 at 80°C, developed a chalky, brittle texture.

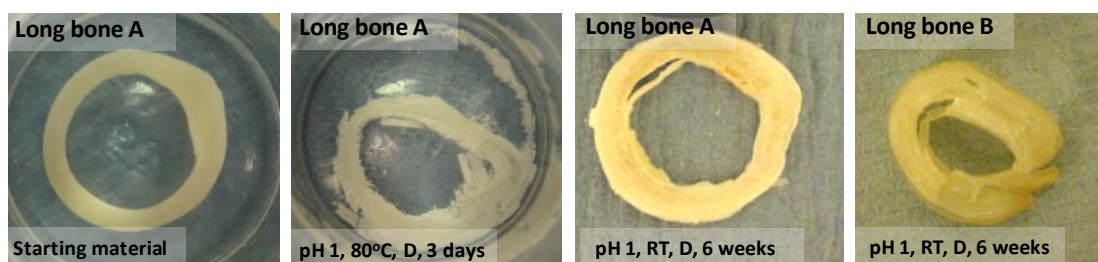


Figure 4.2 (Left to right): long bone A starting material; long bone A, pH1, 80°C, D after 3 days; long bone A, pH 1, RT, D after 6 weeks; long bone B, pH 1, RT, D after 6 weeks, illustrating differences between disintegrated, chalky and translucent samples. (Originally in colour).

Deterioration occurred far more rapidly in the archaeological samples. As early as seven days at pH 1, 80°C, the sample had completely disintegrated. Rapid deterioration or distortion of the archaeological sample was also visible at pH 1 and 2, RT, and most 80°C samples, including at pH 7.

Mass losses in all bone samples after 6 weeks are expressed as a percentage of the starting mass in Table 4.3. Approximately 5 % by mass of bone is made up of non-structural components, such as lipids and minor non-collagenous proteins that may be readily lost in an aqueous environment (Currey, 2002), and these may account for minor mass losses such as the ~2-3 % seen in water, RT. It is expected that these non-structural components would not still be present in archaeological bone at Star Carr.

Table 4.3: Mass loss in bone after 6 weeks and 16 weeks (in brackets) where relevant. Mass loss is presented as a percentage of the starting mass.

		Mass loss as a percentage of the starting mass at 6 and (16) weeks					
		Long Bone A		Long Bone B		Rib Bone	Arch. Rib
pH	T	D	S	D	S	D	D
1	Room temperature	46 (78)	4	54	8	50 (63)	79 (>90)
2		18	4			45	39
3		3 (4)	2	3		9 (16)	10 (3)
5		3	2				
Water		3	2	2		6	5
1	Heated (80°C)	>90 (>90)	5	>90		>90 (>90)	73 (>90)
2		32	7			73	67
3		9 (32)	5	28	28	36 (40)	34 (37)
5		5	5				
Water		5 (27)	5	31		36 (50)	30 (36)

Based on the buffering capacity observed (Figure 4.1), it is hypothesised that the majority of mass loss is due to dissolution of bone mineral. The mass of HA needed to change the pH from 1 to 1.25 is approximately 40 times greater than needed to change the pH from 3 to 5. This explains why much greater mass loss observed at pH 1, compared to pH 3 where buffering is much more easily achieved.

Mass loss was significantly lower in the S samples, even at low pH values: 3.5% compared to 45.8% loss at pH 1, RT; and 6.7% compared to an almost complete loss of sample at 80°C in long bone A. Slightly greater mass losses are also seen at high temperature, due to the expected acceleration of deterioration.

4.3.2 Results: Microscopy

4.3.2.1 SEM

In samples where significant visual changes were observed, SEM analysis was carried out. Analysis revealed that in samples that had developed a chalky texture, deep cracks in the bone surface could be identified (Figure 4.3, centre). In contrast, bones where distortion and a translucent appearance had occurred (mainly in samples treated in pH 1 acid), a smooth texture was seen under SEM (Figure 4.3, right), as well as the appearance of nodular formations. Collagen fibrils are approximately 0.5 μm in diameter (Rho *et al.*, 1998), meaning

that these nodules could potentially be collagen, visualised as a result of being exposed by HA loss.

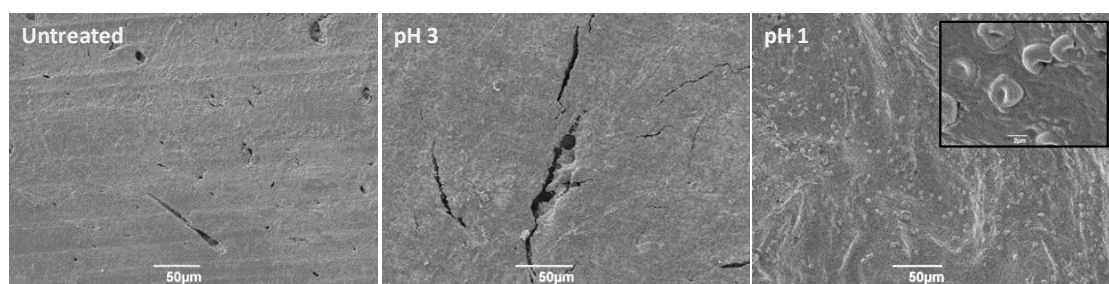


Figure 4.3: SEM images of bone at 400 x magnification. Left: untreated bone; Centre: long bone B treated at pH3, RT, D; Right: long bone B treated at pH 1, RT, D (inset, zoomed in section – scale bar reads 2 µm).

4.3.2.2 TEM

The number of samples analysed by TEM was limited by the fact that for heavily degraded samples, only a small sample size remained.

Many of the samples completely dissolved during the process of demineralisation in EDTA. The fact that any remaining collagen was soluble in EDTA indicates that it was heavily degraded, as fresh collagen is insoluble under most conditions (e.g. Glimcher & Katz, 1965). This solubility is likely to be due to loss of cross-linking between the collagen fibrils, or break up of the protein chains (Koon, 2006). Alternatively, no collagen was present in the samples and treatment in EDTA resulted in dissolution of any remaining HA.

A summary of the samples prepared for TEM is shown in Table 4.4, with those that dissolved indicated. The one sample successfully analysed is shown in Figure 4.4.

Table 4.4: Summary of samples treated for analysis by TEM.

Bone type	Conditions	TEM analysis
Long bone A	pH 1, RT, D	Dissolved
Long bone A	pH 2, RT, D	Analysed
Long bone A	pH 3, 80°C, D	Dissolved
Long bone B	pH 3, 80°C, D	Dissolved

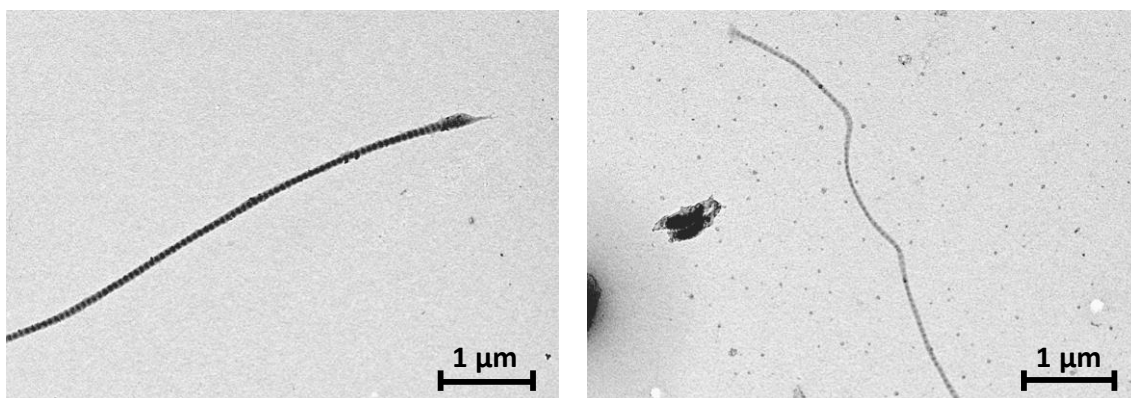


Figure 4.4: Images obtained using TEM of long bone A sample treated in pH 2, RT under dynamic conditions (left) compared to a modern sample (right).

Comparison of the pH 2 treated sample with a modern bone sample prepared using identical conditions shows no alteration of the collagen; characteristic banding is visible and no markers of collagen degradation, such as beading or swelling of the fibrils were identified (Koon *et al.*, 2003). This indicates that a significant increase in collagen diagenesis has occurred in the equivalent sample treated at pH 1, which dissolved in EDTA, compared that treated at pH 2 which displays little or no deterioration of the collagen (Table 4.4).

4.3.3 Results: Chemical analysis

4.3.3.1 Powder X-ray diffraction (p-XRD)

P-XRD was carried out on all samples where the size of the sample allowed. Analysis of both the modern and archaeological bone material prior to experimentation showed peaks characteristic of fresh bone (e.g. Bartsiokas & Middleton, 1992), and in the majority of samples treated at RT no alteration was observed. In heated samples however, sharpening or splitting of the HA peaks was seen, indicating an increase in HA crystallinity (e.g. Person *et al.*, 1995). For convenience and to allow comparison between large numbers of samples, these alterations have been characterised according to the degree to which the HA peak exhibits a slight shoulder or splitting. These characterisations have been termed 'peak with shoulder' (PS), mild splitting (MS) or splitting (S). These alterations are illustrated in Figure 4.5 and summarised for all samples in Table 4.5.

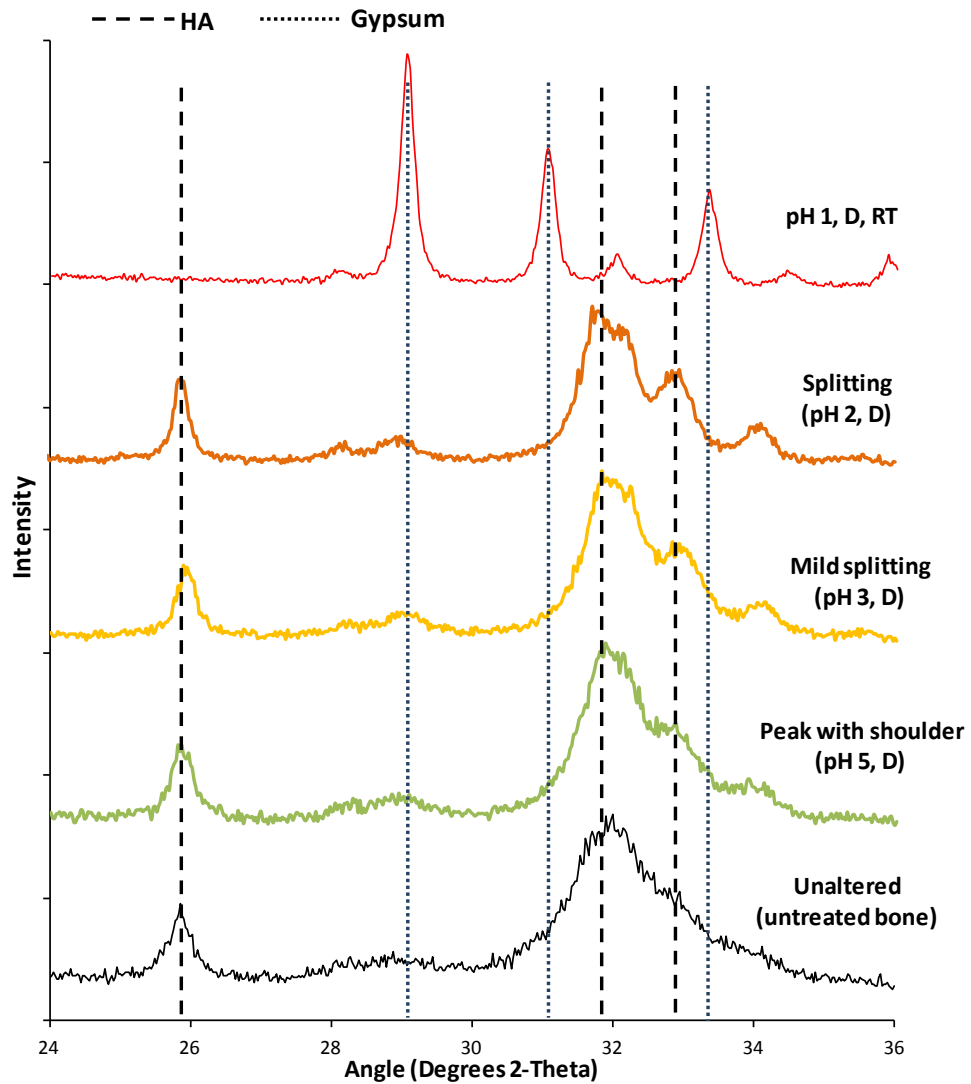


Figure 4.5: Example p-XRD patterns, illustrated by long bone A samples treated at 80°C at various pHs compared to an untreated modern bone (bottom), which displays the characteristic broad peaks of HA in fresh bone. Vertical lines indicate the positions of peaks characteristic of pure HA (dashed lines) and gypsum (dotted lines). (Originally in colour).

In all samples treated in pH 1 acid, even at RT, complete alteration of the crystal structure was observed and the characteristic hydroxyapatite peak at 32° 2θ lost. The positions of the peaks are consistent with a change to gypsum (CaSO₄·2H₂O) (e.g. Kontoyannis *et al.*, 1997). This suggests that complete dissolution and recrystallisation of the HA has occurred, incorporating the sulfur from the acid according to Equation 4.2.

Equation 4.2: Formation of gypsum via the dissolution of HA.



This was further confirmed by SEM analysis of the liquid removed after one day from the sample at pH 1, 80°C. Whereas HA crystals in bone are non-crystalline and measure on the

nano-scale (e.g. Rho *et al.*, 1998), crystalline ‘rosette’ formations characteristic of gypsum were observed (e.g. Shih *et al.*, 2005) (Figure 4.6).

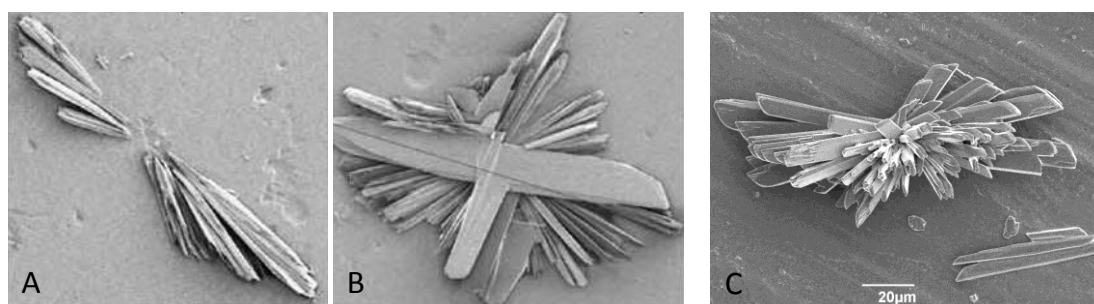


Figure 4.6: A and B show SEM images of gypsum rosette formation in different stages, reproduced with permission from Shih *et al.* (2005). Crystals pictured are in the 400-700 µm range. Image C is an SEM image of a crystal in the solution removed after 1 day from a bone sample displaying the X-ray diffraction pattern characteristic of gypsum (pH1, 80°C, D).

Table 4.5: Summary of changes to the p-XRD pattern for all analysed bones after 6 weeks, with characterisation after 16 weeks in brackets. (Originally in colour).

Key: **G** = gypsum structure; **S** = peak splitting; **MS** = mild splitting; **PS** = peak with shoulder; - = no alteration.

		p-XRD classification after 6 (16) weeks					
		Long Bone A		Long Bone B		Rib Bone	Arch. Rib
pH	T	D	S	D	S	D	D
1	Room temperature	G	G	G	-	G	
2		-	-				
3		-(-)	-	-	-	-(-)	-
5		-	-				
W		-	-	-		-	-
1	Heated (80°C)		G				G
2		S	MS			S	
3		MS (S)	MS	S	MS	S (S)	(-)
5		MS	PS				
W		PS (S)	PS	S	MS	MS (MS)	(-)

In long bone A after 16 weeks, RT pH 1, D no diffraction peaks were observed at all. This indicates that all crystalline inorganic material had been completely removed from the sample leaving behind only a protein matrix.

4.3.3.2 Amino acid racemisation analysis

4.3.3.2.1 Sample concentrations

Analysis of the starting materials showed that the total concentration of amino acids in the archaeological sample was not notably different to the modern material, agreeing with studies that show that collagen is relatively robust and can survive well in the archaeological record (e.g. Collins *et al.*, 1995). Slightly higher concentrations in the modern rib suggest that it is less densely mineralised, leading to a higher proportion of collagen.

A relative increase in total amino acid concentration in experimental samples compared to the starting materials can be caused by loss of HA, and was increasingly seen at lower pH in most samples at RT (Figure 4.7). The same is also seen after 16 weeks.

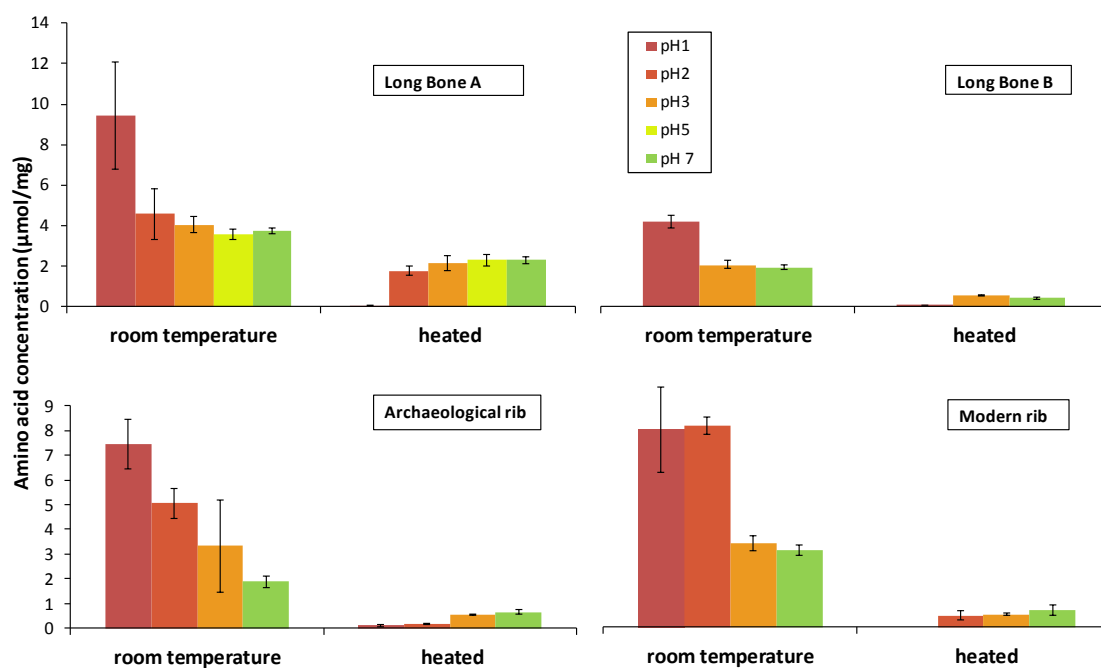


Figure 4.7: Total amino acid concentrations in all 4 bones under D conditions at RT and 80°C at 6 weeks. Water is given the description pH 7. Error bars are one standard deviation calculated from replicate analysis. (Originally in colour).

In the 80°C samples the reverse is seen. As significant mass loss has also occurred in these samples (Section 4.3.1) and analysis of the pH levels indicates the dissolution of HA, we can conclude that at high temperatures protein is simultaneously being lost. After 16 weeks, very few amino acids appear to remain in any of the 80°C bone samples, even at pH 7 (water). The concentrations decrease with increasing acidity, indicating increasing loss of the protein.

4.3.3.2.2 Sample racemisation

Analysis of the starting materials was carried out prior to experimentation. Asx racemisation was slightly elevated in the archaeological samples compared to the modern bones ($D/L = 0.1$ vs 0.06), although no racemisation of Ser was observed.

At RT, racemisation levels were consistently almost negligible, even after 16 weeks. Kinetic studies such as those by Bada (1972) have shown that racemisation rates are likely to be unobservable at RT over this short time-scale.

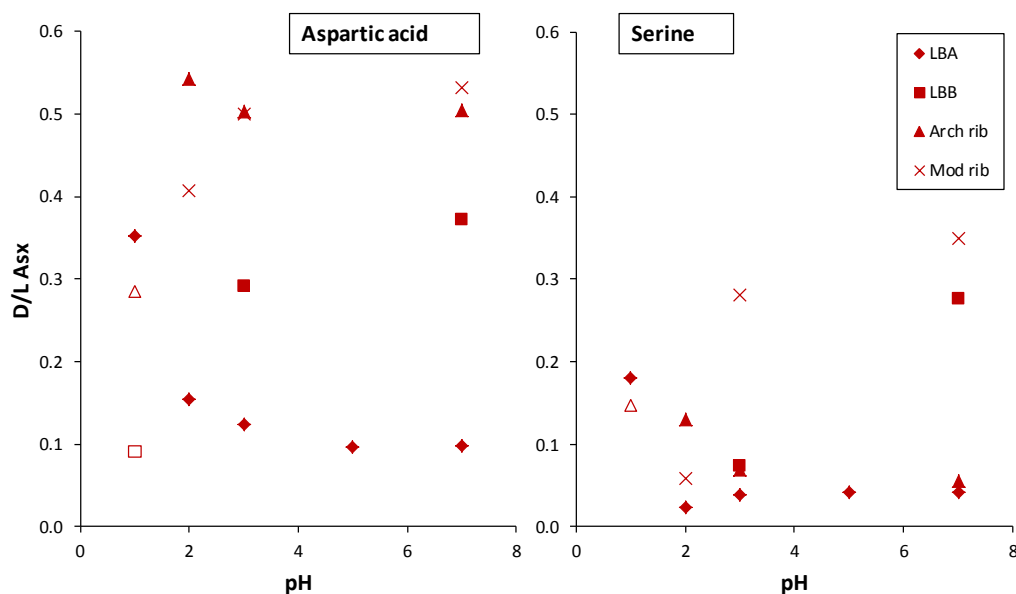


Figure 4.8: Aspartic acid (Asx; left) and serine (Ser; right) racemisation at 80°C , D for all 4 bone types after 6 weeks. Outlined data points represent samples which were removed early. Samples under dynamic conditions showed similar trends. Error bars were negligible and therefore not shown. (Originally in colour).

At 80°C however, Asx and Ser racemisation levels are elevated compared to the starting material in all samples, even those at pH 7 (water) (Figure 4.8) suggesting that the collagen structure is breaking apart within the bone. As both Asp and Ser can racemise in-chain, this could be due to an increase in conformational freedom in the collagen helix. In long bone A, this is pH dependent, with a very high D/L value observed in the bone sample at pH 1.

Although the same is not seen for other bone types, it must be noted that in these the samples at pH 1 disintegrated before the 6 week period and were removed from the experiment early. High levels of Asx racemisation are seen in the archaeological rib bone, despite being only slightly elevated in the starting material. This suggests that breakdown of the collagen proceeds more rapidly than in fresh bone, possibly due to damage already occurring during burial. This agrees with the slightly lower total concentrations in the final samples of the archaeological bone at 80°C .

4.3.3.2.3 Aliquot amino acid concentrations

Although it is difficult to quantify these results due to the potential evaporation of the solutions at 80°C, broad conclusions can be drawn. Amino acid concentrations in the supernatant solutions at RT throughout the experiments were very low; such low levels of amino acids present can be attributed to leaching of the small chain, non-structural proteins present in fresh bone. This suggests that only HA is dissolving, even at pH 1, RT where a high mass loss suggests that a significant proportion of the sample has disappeared. Alternatively, protein is also being lost, but the amino acids are broken down such that they cannot be detected. However, the high stability of amino acids has been widely reported, and suggests that this would be unlikely at such low temperatures over this short time-scale (e.g. Sato *et al.*, 2004; Yablokov *et al.*, 2009).

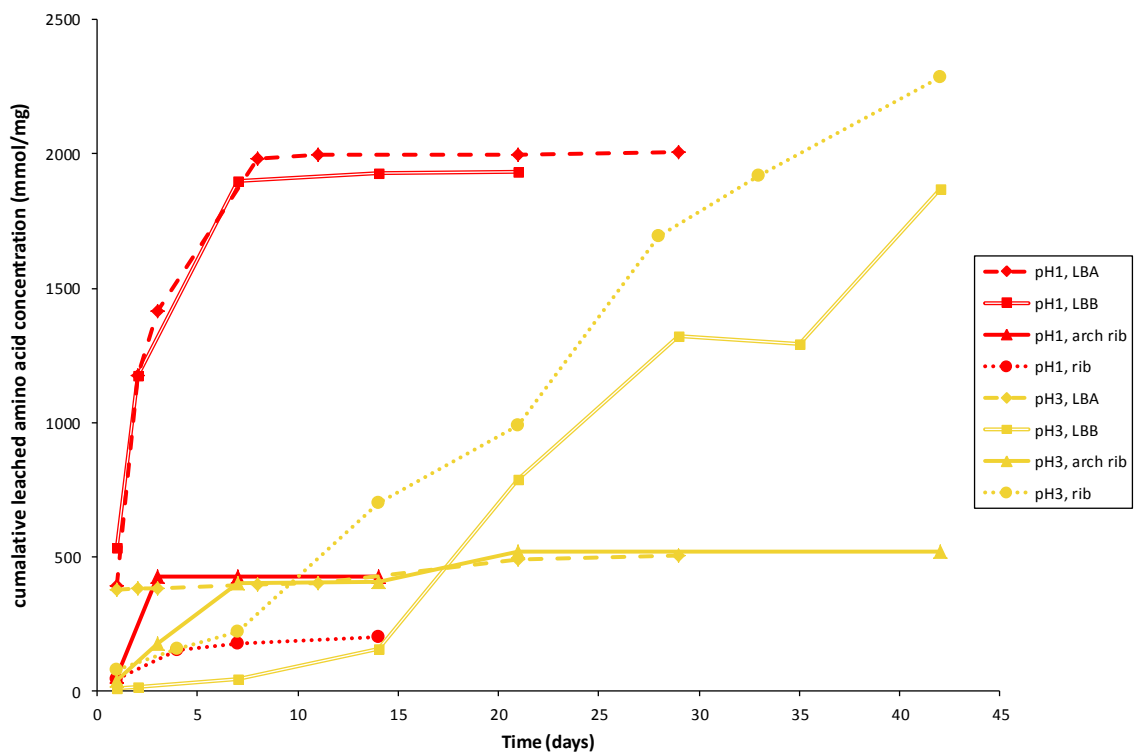


Figure 4.9: Aliquot solution amino acid concentrations over 6 week reaction period for all bone samples at 80°C for pH 3 and pH 1. (Originally in colour).

For the 80°C experiments, leaching is initially faster at pH 1, although large concentrations of amino acids are found in the solutions at pH 3 after the full 6 weeks (Figure 4.9). Leaching from the archaeological bone is also markedly faster than from the modern samples, resulting in an almost zero concentration of amino acids remaining in the bone itself by the end of the experiment (Figure 4.7), showing almost complete leaching of protein out of the bone.

Although much lower concentrations of amino acid are seen in solution at RT than at 80°C, it is possible that the reason for this is that when samples are heated short chains simply leach more readily out of the sample, rather than there being a larger number of short chains present in the bone. Collins *et al.* (1995) suggest that even free amino acids can be prevented from leaching out of the collagen matrix by hydrogen bonding, and this might be occurring at RT.

4.3.3.2.4 Aliquot amino acid racemisation

Racemisation values are consistently negligible in the samples at RT. At 80°C, Asx and Ser racemisation is observed, but is somewhat lower in solution than in the whole bone. For Asx this slightly increases towards neutrality (Figure 4.10). However, Smith & Evans (1980) suggest that racemisation, particularly of Ser, is faster in solution. Kinetic studies such as those by Bada and Shou (1980) also show that racemisation of free amino acids in solution is independent of pH between pH 3 – 9. A possible explanation for the observation here is that at low pH, rather than short peptide chains leaching into solution, collagen is leached out in a more stable form; either as a triple helix or in fibrils. In this case, lower racemisation may be explained by the inability of either Asx or Ser to racemise within the undisrupted helix.

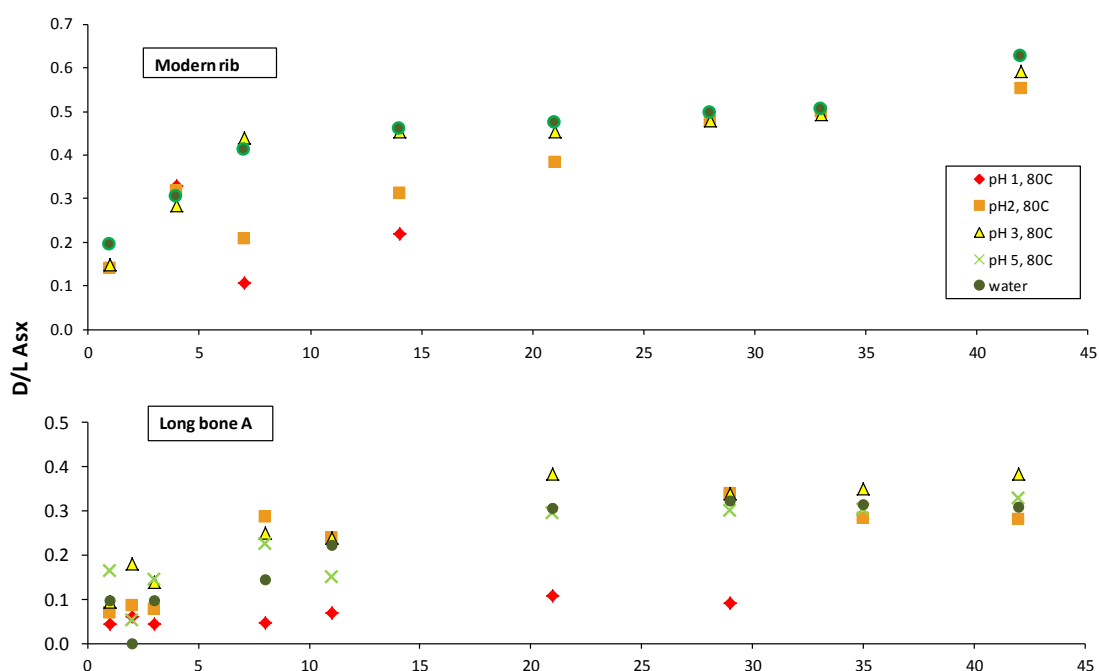


Figure 4.10: Racemisation values of Asx in solution at each sampling point during the experiment for modern rib and long bone A samples under dynamic conditions (the whole solution is replaced following each sampling point). Other bones show similar trends, with a slight increase in racemisation over time. (Originally in colour).

4.3.4 Discussion

Lab-based experiments have shown that at low pH, bone rapidly buffers the surrounding environment through loss of the HA (Section 4.3.1). In acidic environments, bone collagen may not, therefore, be exposed to this low acidity, particularly at pH values of > 3 . However, this study has demonstrated that this buffering capacity is severely limited at $\text{pH} \sim 1$ and is significantly reduced in archaeological samples. The implications for this are two-fold; firstly, more HA will continue to dissolve in order to establish equilibrium with the solution, and the bone itself (including the bone protein) will be exposed to low pH for longer. In a dynamic environment, where the water-table is fluctuating through the archaeological layer, this buffered zone would have to constantly be re-established, leading to more and more dissolution of bone mineral. Indeed, throughout the experiment, bones under stagnant conditions have been far less altered than those under dynamic conditions.

Alteration of the HA has been shown by p-XRD to occur within 6 weeks in the samples at 80°C , even in water. Hiller & Wess (2006) propose that in a situation where dissolution occurs and recrystallisation can proceed, it will do so by the formation of larger crystals. Indeed, alteration of the HA does occur even under S conditions, when mass loss is very low, and the transformation to gypsum at pH 1 shows that dissolution and recrystallisation is occurring. In an environment where recrystallisation is less likely (for example if groundwater fluctuates through the archaeological layer), increased crystallinity may be accounted for by the preferential dissolution of smaller crystals (Hedges & Millard, 1995).

Previous studies have shown that the association between collagen and HA lends a high degree of protection to the collagen (Roberts *et al.*, 2002; Koon, 2006). Therefore, this observed alteration of the inorganic HA structure is likely to have important consequences for the organic fraction. Racemisation values in the whole bone samples suggest that collagen breakdown within the bone is more progressed at pH 1, where HA alteration is also more advanced. This may be due to either complete collagen breakdown, or an increased degree of conformational freedom, for example by loss of the HA resulting in in-chain racemisation of Asp (e.g. Dobberstein *et al.*, 2008; Collins *et al.*, 2009). Complete collagen breakdown is supported by the high concentration of leached amino acids present in the surrounding solution. Bada & Shou (1980) show that free amino acid racemisation both in solution and in bone is independent of pH between pH 3 and 9 and only acid-catalysed at pH values of less than 1. It is possible therefore, that the increase in racemisation (i.e. increase in collagen damage) is not dependent on the pH, but is a secondary effect of HA dissolution, which is pH dependent. Covington *et al.* (2008) show that the stability of collagen is enhanced when

prevented from shrinkage by a tightly bound matrix – in the case of bone, this is hydroxyapatite.

The low levels of racemisation but high amino acid concentrations observed in the supernatant solutions at low pH could suggest that collagen could be dispersing into solution whilst remaining relatively intact. This is supported by SEM and visual analysis of the samples. Whilst a chalky and cracked texture was observed in bone exposed to pH > 2, bones treated at pH 1 developed a translucent, smooth texture. This could be the result of complete demineralisation leading to an exposed collagen matrix after rapid HA dissolution. The small ‘nodules’ observed on the surface of the bone under SEM (Figure 4.3) are potentially consistent with the size of a collection of collagen fibrils, supporting the hypothesis that they might be exposed by HA loss (Rho *et al.*, 1998). P-XRD analysis of the bone treated for 16 weeks at pH 1, RT revealed little or no inorganic fraction remaining, yet high levels of amino acids were present supporting this hypothesis of initial HA loss, with subsequent protein leaching (Section 4.3.3.2). This may explain the formation of the Star Carr ‘jellybones’, but would indicate that their demineralised state is not stable over the longer term.

The proposed mechanisms by which bone deteriorated under different strength sulfuric acid are simplified and summarised in Figure 4.11, showing that the rate at which HA dissolves appears to dictate the speed at which collagen degrades.

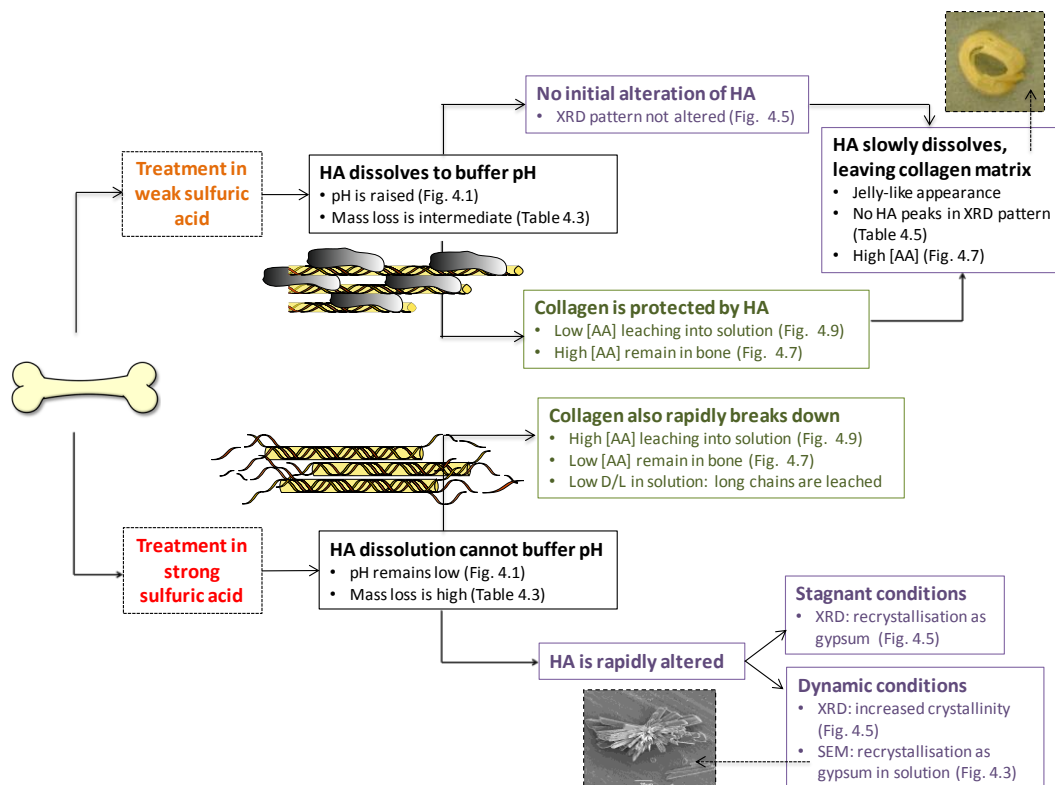


Figure 4.11: Schematic showing the proposed degradation mechanism of bone in different strength sulfuric acid solutions. (Originally in colour).

4.4 Investigation into wood deterioration

4.4.1 Results: Bulk assessment

All wood samples displayed much lower ability to buffer the acidity of the surrounding solution at all pH values (Figure 4.12), in comparison to the equivalent experiments using bone, where at pH 3 the dissolution of HA in modern bone caused the pH to rise by approximately 4 - 5 pH units.

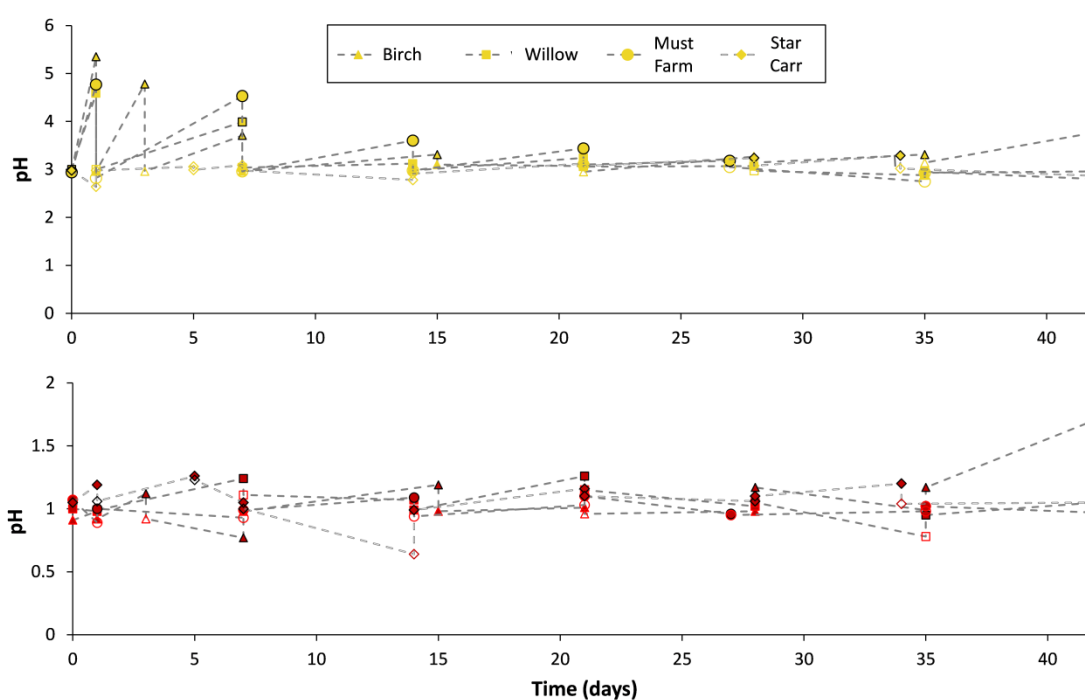


Figure 4.12: Measured pH for D conditions at 80°C for all 4 wood samples at pH 1(bottom) and pH 3 (top). A similar trend continues for the 16 week experiments. (Originally in colour).

In contrast to bone, when wood degrades it is more likely to release acidic compounds such as formic and acetic acids than ions with the ability to raise the pH (e.g. Shaw *et al.*, 1967). This may explain why in fact a slight increase in acidity is seen, particularly in the Star Carr sample. Whilst the lack of buffering ability is to be expected, analysis of the pH of the surrounding solution confirms that the wood samples are exposed to much lower pH throughout the experiment than the equivalent bone samples.

Visual changes after 6 weeks were minimal, aside from a slight darkening of the wood observed at 80°C, pH 1 (Figure 4.13). In addition, the surrounding solution also became darkened; this was more pronounced at higher (more neutral) pH. This darkening of the solution is likely to be due to the leaching out of components such as tannins, which are water-

soluble (Scalbert *et al.*, 1989). No change in texture or macroscopic alteration could be discerned after 6 weeks.

After treatment at pH 1, 80°C for 16 weeks however, both birch and willow samples appeared extremely dark and developed a brittle texture similar to charcoal upon drying. In the birch sample, this change had occurred throughout the sample whereas in the willow sample only the surface was affected. At pH 3, a slight darkening was observed but no change seen at pH 7 (water), indicating that this change is pH dependent. Whilst charring of wood is most often associated with exposure to high temperature, it occurs due to the decomposition of both cellulose and lignin into carbon (Di Blasi, 2008). It is possible that after 16 weeks in acid, similar processes have resulted in the complete breakdown of structural polymers and led to this darkening of the wood surface. Further analysis would be required to confirm this.

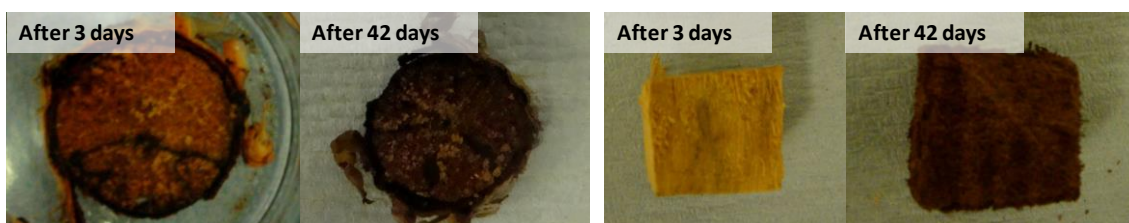


Figure 4.13: Images showing the darkening occurring in samples of birch (left) and willow (right) after 3 and 42 days at pH 1, 80°C and D conditions. (Originally in colour).

Mass losses in all wood samples after 6 and 16 (in brackets) weeks are expressed as a percentage of the starting mass in Table 4.6. Mass losses of approximately 10 %, as observed for the majority of samples at RT, can be explained by the loss of non-structural, water-soluble components such as sap, lipids and non-structural carbohydrates and sugars (Piispanen & Saranpaa, 2001), indicating that loss of structural polymers is not occurring at RT even at the 16 week time point. This would also explain a lower mass loss in the Must Farm samples, as it is likely that these water-soluble components would have been lost in the archaeological burial environment (e.g. Hedges, 1995).

Table 4.6: Mass loss in wood after 6 weeks and 16 weeks (in brackets) where relevant. Mass loss is presented as a percentage of the starting mass.

		Mass loss as a percentage of the starting mass at 6 and (16) weeks						
		Modern birch		Modern willow		Star Carr	Must Farm	
pH	T	D	S	D	S	D	D	S
1	Room temperature	10 (15)	8	5 (9)	5	10	0	0
2		10	7	4	-	10	1	2
3		10 (10)	7	4 (5)	4	12	0	0
5		8	8	-	-	-	-	-
Water		10 (11)	8	4 (5)	-	15	0	0
1	Heated (80°C)	40 (63)	32	29 (41)	24	30	16	9
2		40	29	26	-	37	16	13
3		33 (40)	19	25 (31)	16	29	15	13
5		26	14	-	-	-	-	-
Water		32 (39)	14	21 (30)	-	31	13	10

Whilst higher mass loss is seen at 80°C, similar losses are seen at all pH values suggesting that decay is largely temperature, rather than pH, dependent. After 16 weeks at pH 1 and 80°C, visual alteration of both birch and willow indicated that decay was progressed. However, even in these samples the mass loss in modern samples does not represent the total stripping of cellulose, which accounts for approximately 70 – 80 % by mass of wood (Hoffman, 1981). It is possible that degradation is occurring, but leaching out of the degradation products is limited by the complexity of the wood macro-structure resulting in a lower mass loss than expected.

Differences between types of wood are likely to be caused in part by differences in the relative composition (soluble components: cellulose: lignin) of the starting materials. In particular, it is likely that archaeological wood would have already been depleted in cellulose, which is readily lost due to microbial decomposition in an archaeological environment (e.g. Blanchette *et al.*, 1990; Jones & Eaton, 2006). This potentially explains the much lower mass loss in archaeological samples, indicating that remaining components are not as susceptible to decay due to acidic conditions. Another consideration is the difference in sample size and shape used; birch samples were smaller than willow which would lead to a higher proportion of the sample being exposed to acid.

Similarly to bone, mass loss data suggest that ‘dynamic’ conditions, regardless of the pH value, are more damaging than ‘stagnant’ conditions. This is unsurprising, as experimental studies

such as those by Nicholson (1996) and Crowther (2002) show how the rate at which degraded components of bone are washed away from the sample dictate the rate at which more of it degrades. It is very likely that the same is true for wood.

Maximum water content (u_{\max}) values for all samples at the end of the experiment are shown in Table 4.7. Variable u_{\max} data may be obtained depending on the method of analysis, and as such needs to be approached with caution (Panter & Spriggs, 1996). The size of samples used in these experiments was much smaller than would ordinarily be used for u_{\max} analysis; therefore procedural errors, for example in removing excess surface water, may contribute to a high level of inaccuracy (e.g. Jenson & Gregory, 2006).

Table 4.7: Maximum water content as a percentage of the end mass for all wood samples after 6 and 16 (in brackets) weeks.

		U_{\max} as a percentage of the end mass at 6 and (16) weeks						
		Modern birch		Modern willow		Star Carr	Must Farm	
pH	T	D	S	D	S	D	D	S
1	Room temperature	536 (246)	337	272 (309)	235	422	122	121
2		571	352	263		603	120	65
3		399 (216)	337	194 (305)	198	632	144	69
5		548	370					
Water		412 (254)	379	230 (329)		467	145	139
1	Heated (80°C)	775 (554)	552	300 (538)	303	533	155	107
2		795	493	254		396	159	161
3		652 (363)	447	320 (470)	252	448	164	164
5		695	350					
Water		630 (384)	423	247 (473)		500	191	168

Typical u_{\max} values for fresh, modern wood range from around 90-120 %, depending on the species (Hoffman, 1981) and wood with a u_{\max} value of approximately 300 % can be defined as severely degraded (Hoffman, 1986). Elevated values are seen in most of the experimental samples, particularly those under dynamic conditions, suggesting high levels of deterioration allowing a greater uptake of water; this is inconsistent with mass loss data.

Previously, analysis of wood excavated from Star Carr in 2010 had yielded values averaging 514%, suggesting that the level of decay in most of the experimental samples is equivalent to the level of degradation in wood at Star Carr (Panter, 2009). However, a lower u_{\max} after 16 weeks compared to 6 weeks (as seen in the modern birch sample) is very unlikely to be true, potentially suggesting that measurements are not accurately describing degradation; this may

be due to the high level of error incurred due to the small sample size. Excess water on the surface of such a small sample is likely to lead to an increased measured u_{\max} . If this is considered, and it is assumed that all results are too high, results are more consistent with mass loss data, in suggesting that degradation is not pH dependent although more degradation is seen at higher temperature.

4.4.2 Results: Microscopy (SEM)

Analysis of samples after 6 weeks by SEM revealed little or no histological difference between samples treated at different pH levels. Comparison between the untreated starting material of willow and birch wood however, revealed that differences are evident in the starting materials (Figure 4.14, top). Differences in chemical composition between wood samples may not be solely due to degradation, but may also exist due to factors such as the age, species and growth location of the tree (Jane, 1970; Pandey & Pitman, 2003). The cell walls in the birch sample appear to be much thinner, which may indicate the presence of less cellulose (Blanchette *et al.*, 1990). This is likely to be due to differences in age between the two types of wood sample, emphasising that care needs to be taken when comparing two different materials and potentially explaining the differences in mass loss between the two types of wood.

SEM analysis of the samples treated for 16 weeks showed that cell walls appeared to be of the same thickness as in the starting material in both willow and birch (Figure 4.14, bottom). This indicates that all of the cell walls still remain, suggesting that complete loss of cellulose has not occurred (Blanchette *et al.*, 1990). This is in agreement with the mass loss data; however on closer inspection, slight collapse of the cell walls can be observed, particularly in the willow sample. This is indicative that some loss of structural polymers (cellulose and/or lignin) has occurred (Blanchette *et al.*, 1990) and is consistent with the mass loss of ~ 40 % mass loss observed (Table 4.6).

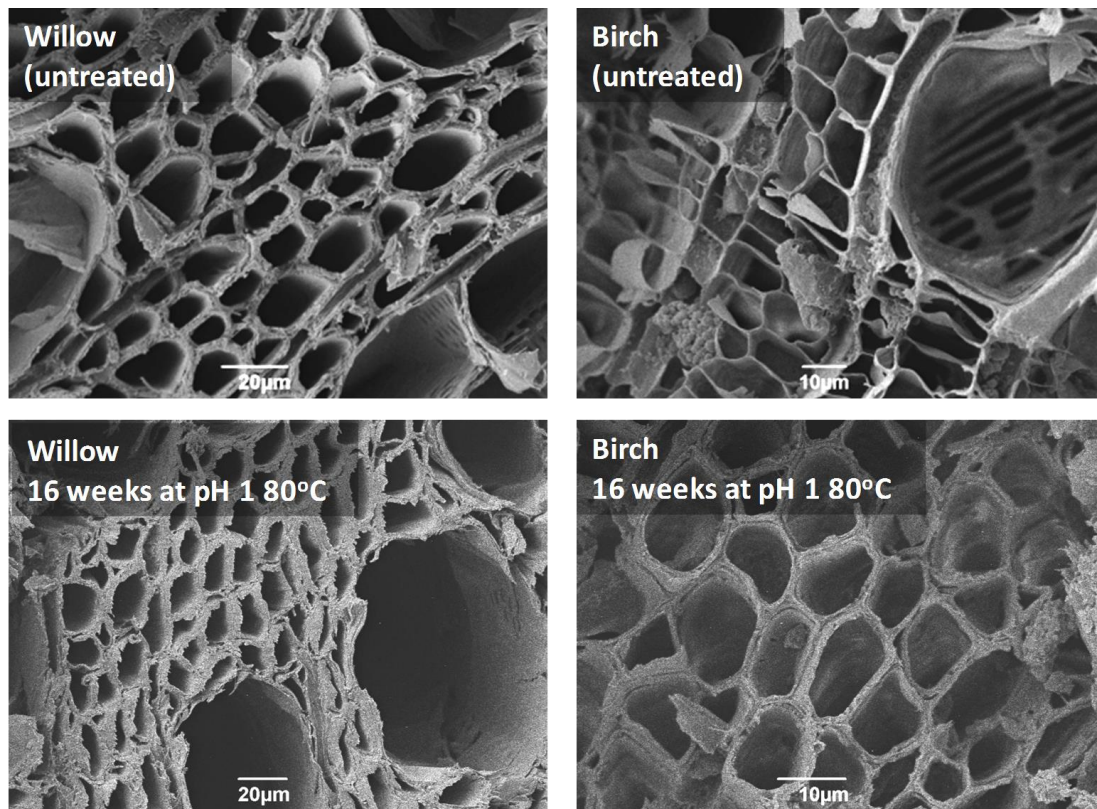


Figure 4.14: SEM images of modern willow and birch prior to the experiment (top) and after treatment for 16 weeks at pH 1 at 80°C, D conditions (bottom).

It is possible that polymeric material has broken down but the degradation products not leached away from the cell walls, explaining why the cell walls still appear thick under SEM. A study by Crestini *et al.* (2009) shows how the percentage mass of archaeological wood that can be extracted with mild solvents increases with increasing degradation. This was attributed to the short chain sugars resulting from hydrolysis of the long cellulose chains being more soluble than cellulose and showed how these short sugars can remain *in situ* even in archaeological material. This further illustrates why a 'dynamic' environment would be more damaging than one that is 'stagnant' as movement of water through buried archaeological wood may result in the removal of these soluble sugars.

4.4.3 Results: Chemical analysis

4.4.3.1 FTIR spectroscopy

All experimental samples were analysed by FTIR, with 3 spectra taken from the surface of each sample. FTIR spectra obtained from modern birch samples treated at a range of pH values, at 80°C under “D” conditions are shown in Figure 4.15. Very little difference in the fingerprint region is observed between spectra, even at 80°C. The same was seen in modern willow samples.

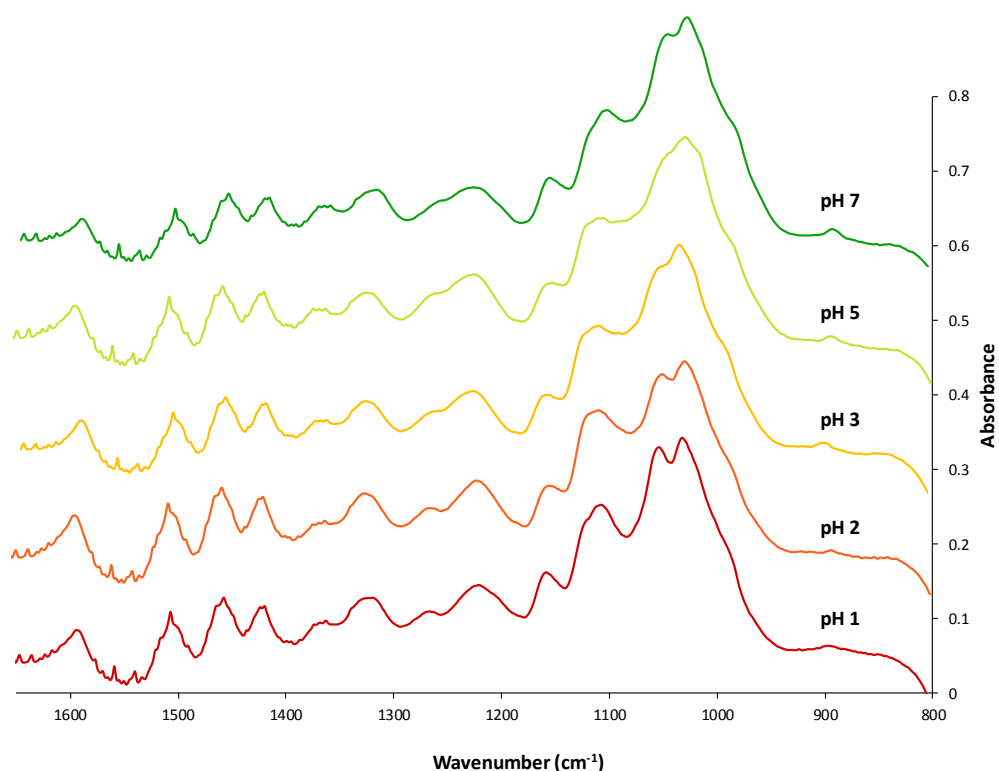


Figure 4.15: FTIR spectra for birch samples treated at different pH at 80°C and under “D” conditions. Little difference is seen between spectra; this is illustrative of all samples treated for 6 weeks. (Originally in colour).

Peak heights for key absorption peaks relating to lignin (1240 cm^{-1} and 1507 cm^{-1}) and cellulose (doublet at 1300-1375 cm^{-1}) were measured, and lignin: cellulose, 1507: cellulose and 1507: 1240 ratios calculated as outlined in Chapter 3 (Section 3.3.3). Differences in these ratios between samples were found to lie within the range of error (calculated by three repeat readings taken from each sample) (Figure 4.16). FTIR analysis further supports bulk assessment of the samples: wood deterioration over this short time frame does not appear to be pH dependent and even cellulose, which is susceptible to acid hydrolysis, is not completely removed. This is the same at 80°C, where degradation is expected to proceed more quickly.

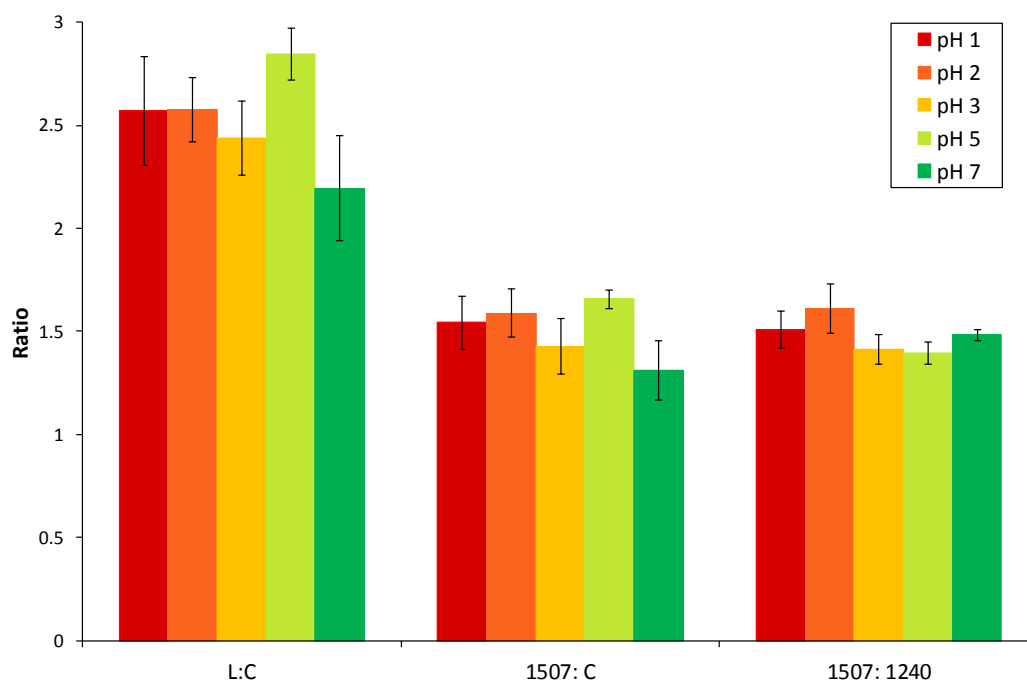
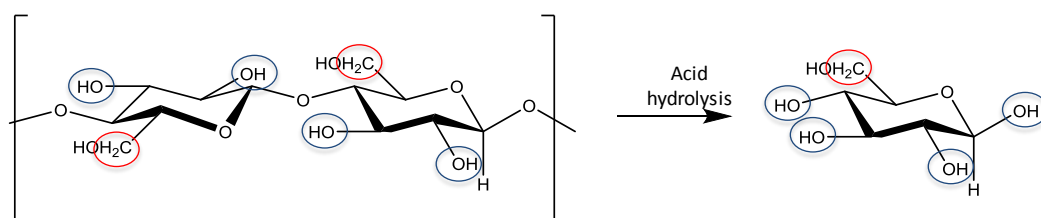


Figure 4.16: Key ratios determined as markers of degradation for birch samples treated at 80°C for 6 weeks. An increase in L: C and 1507: C ratios is indicative of cellulose loss, and an increase in the 1507: 1240 ratio is indicative of lignin defunctionalisation. (Originally in colour).

Despite the high abundance of both lignin and cellulose being indicated by intense peaks in the FTIR spectra, mass losses of up to 40 % were recorded in these birch samples at 80°C for 6 weeks (Table 4.6). This cannot be attributed to the removal of only non-structural components, as these compose only approximately 15 % by mass of wood (Hedges, 1990). As cellulose is composed of weakly bonded carbohydrate polymers, it is often quickly degraded by both chemical and biological processes (e.g. Blanchette, 2000). There is evidence in the literature suggesting that cellulose is susceptible to acid hydrolysis even at low temperatures, leading to degradation of the polymer by cleavage of the glycosidic bonds (e.g. Xiang *et al.*, 2003). Indeed, chemical characterisation of archaeological woods often utilises the relative ease by which cellulose can be extracted using strong sulfuric acid (Hoffman, 1981). If cellulose has broken down but remained *in situ* (as also indicated by SEM analysis), it is possible that the resultant short chain sugars contribute to the same absorption peaks as longer chain cellulose, and therefore chemical alteration of cellulose cannot be confirmed by FTIR analysis. Indeed, the peaks at 1325 and 1375 cm⁻¹ relate to the C-OH and CH₂ groups in cellulose respectively (Pandey, 1998), and these would still be present if hydrolysis of the glycosidic bond has occurred (Equation 4.3). Indeed, more OH groups are formed which may in fact result in an increase in the intensity of the peak at 1325 cm⁻¹.

Equation 4.3: Hydrolysis of cellulose to sugars, showing that the CH₂ group (red) is retained and there is an increased abundance of OH groups (blue) (from Li & Zhao, 2007). (Originally in colour).



These results suggest that FTIR is not suitable for assessing wood deterioration over the 6 week time frame; however after 16 weeks in modern samples, a high degree of visual alteration had occurred at 80°C and pH 1. Higher mass losses after 16 weeks compared to 6 weeks also suggest that degradation was more advanced. FTIR analysis of these samples provides conclusive evidence that alteration of both the lignin and cellulose had occurred in both birch and, to a lesser extent, willow (Figure 4.17).

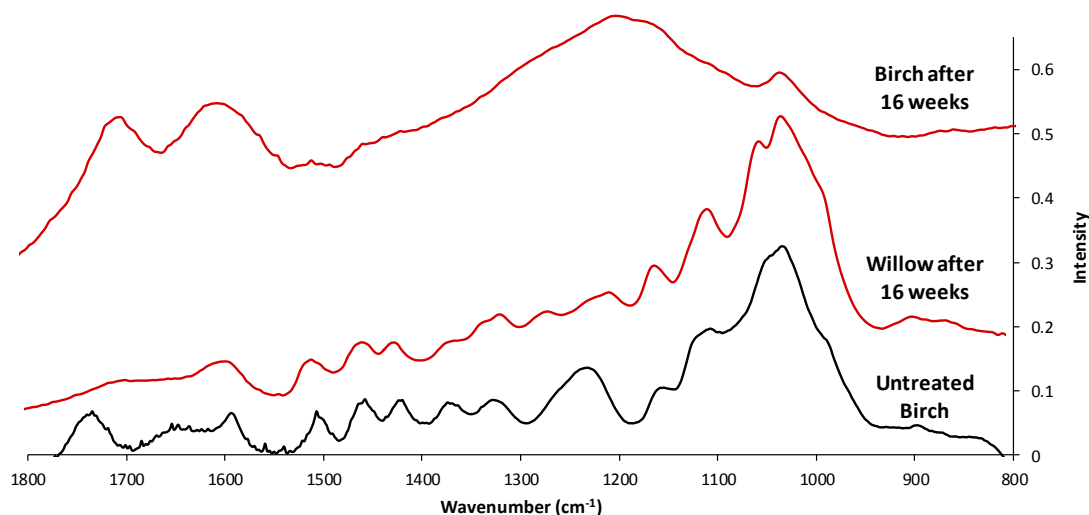


Figure 4.17: FTIR spectra of willow and birch following 16 weeks treatment in pH 1 sulfuric acid at 80°C, D conditions. (Originally in colour).

The complete loss of peaks relating to the absorption of cellulose as well as the peak characteristic of the methoxy group in lignin indicates that alteration of the birch sample has occurred. In the willow sample, a reduction in intensity of these peaks signifies that similar alteration has occurred, although to a lesser degree; although the peak relating to the aromatic ring in lignin is still present, a reduction in intensity and splitting of the peak at 1240 cm⁻¹ (relating to the methoxy groups on guaiacol and syringol) indicates that defunctionalisation of the lignin has occurred. These chemical changes are in agreement with the drastic visual alteration of the samples. A greater extent of alteration in the birch sample is possibly due to the smaller sample size resulting in more complete degradation of the

polymers compared to the modern willow sample, as degradation proceeds from the outside of the sample inwards.

Defunctionalisation of lignin is more often attributed to biological deterioration (Martinez *et al.*, 2005). This occurs by means of oxidative enzymes (Tuomela *et al.*, 2000). Biological deterioration is unlikely to have occurred to such an extent under lab conditions, particularly taking account the low pH and high temperatures, and instead similar mechanisms may have proceeded by chemical hydrolysis.

In both archaeological samples, no alteration of the FTIR spectra was seen after treatment for 6 weeks and peak ratios were within the margin of error, similarly to modern samples; this is consistent with bulk analysis. FTIR analysis of the starting materials however, illustrates that there are similarities between archaeological material and the modern willow sample after 16 weeks (Figure 4.18). A depletion of cellulose and splitting of the methoxy absorption (1507 cm^{-1}) is also evident in both the Must Farm and Star Carr starting material (Figure 4.18).

In the archaeological materials, degradation of polymeric material in the untreated starting materials is evident from analysis by FTIR. Analysis also shows similarities between the Must Farm and Star Carr samples although the Must Farm sample was visually assessed as 'robust' in comparison to the more degraded Star Carr sample.

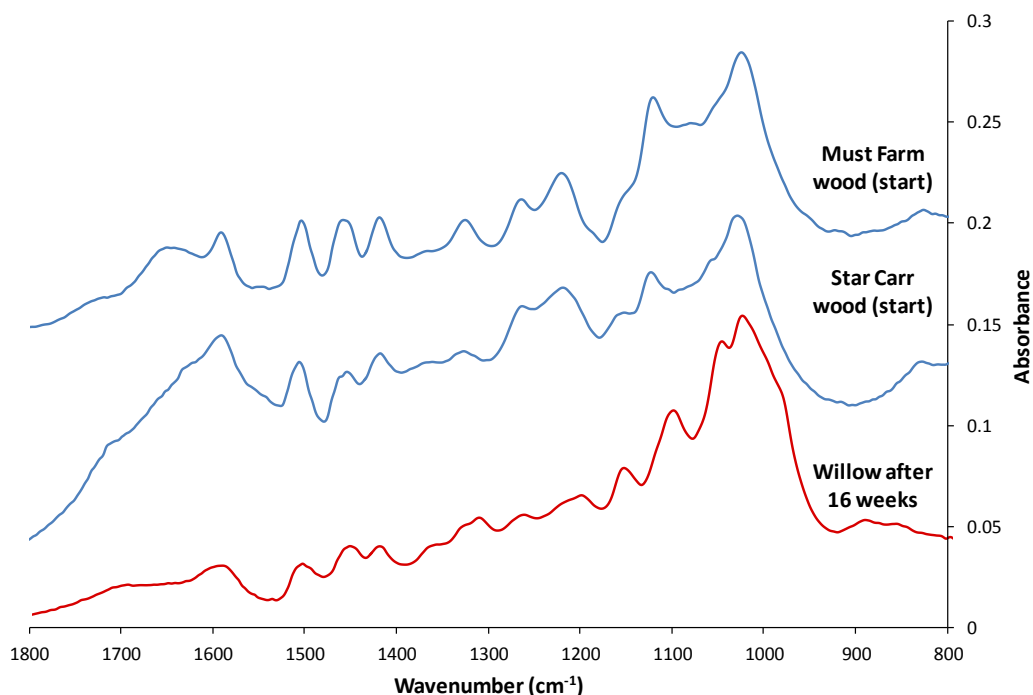


Figure 4.18: Comparison of FTIR spectra for willow treated at 80°C in pH 1 sulfuric acid for 16 weeks with wood from Star Carr and Must Farm, illustrating the similarities observed between the archaeological materials. (Originally in colour).

4.4.3.2 Py-GC

Py-GC, when combined with mass spectrometry, has been shown to provide detailed information regarding wood polymer degradation (e.g. Vinciguerra *et al.*, 2007). Breakdown of the lignin polymer can be indicated by the presence of defunctionalised repeating sub-units from the lignin polymer (syringol and guaiacol). An increase in phenol content indicates complete defunctionalisation. The presence of smaller, carbohydrate derived molecules can confirm the presence of cellulose (e.g. van Bergen *et al.*, 2000). Analysis of wood degradation products using py-GC has been carried out with FID detection, using published mass spectrometry data to assign retention times to degradation products (e.g. Faix *et al.*, 1991; van Bergen *et al.*, 2000; Alves *et al.*, 2006).

Comparison of the chromatograms for birch samples treated at the range of pH values for 6 weeks at 80°C, “D” conditions is shown in Figure 4.19.

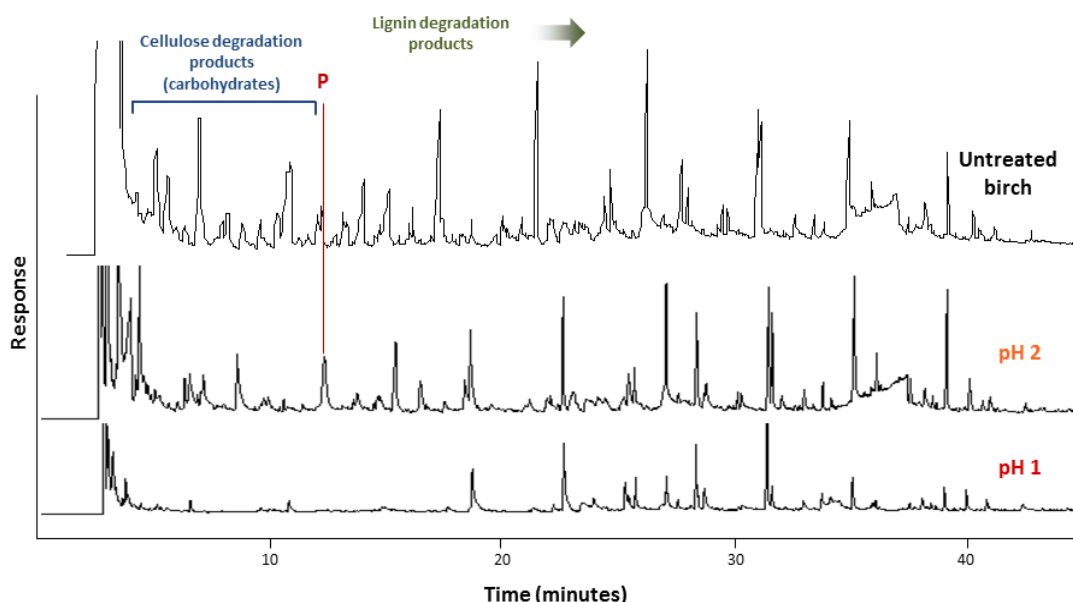


Figure 4.19: py-GC chromatograms for birch samples treated in various strength sulfuric acid solutions for 6 weeks at 80°C, D conditions. (Originally in colour).

In contrast to FTIR analysis, analysis of the samples by py-GC reveals that in fact there are clear differences in composition of the samples treated at lower pH; in particular, a reduction in carbohydrate related compounds eluting at the beginning of the chromatogram at pH 1 and 2, when compared to an untreated sample suggests that cellulose is in fact heavily depleted in the sample (Figure 4.19). This is perhaps unsurprising as cellulose is known to undergo acid hydrolysis (Hoffman, 1981; Li & Zhao, 2007), but contradicts observations made using FTIR. This could indicate that polymeric material has been broken down but remains *in situ*; whilst in FTIR these breakdown product also contribute to the spectrum, as the sample is first cleaned

by heating to 290°C prior to py-GC analysis, it is expected that any volatile degradation products would be removed. This is consistent with microscopic analysis (Section 4.4.2).

Breakdown of lignin at low pH is also indicated by a slightly more intense signal attributed to phenol in the py-GC trace, suggesting that some syringol and guaiacol-type sub-units have been completely defunctionalised. A decrease in intensity of the later signals, assigned to larger lignin polymer units, is also indicative of degradation of the polymers prior to analysis. Again, this appears to be pH dependent, although the high intensity of the majority of lignin related products shows that lignin degradation is only minimal after treatment for 6 weeks.

Analysis of the birch sample treated at pH 1 for 16 weeks was also carried out, and an absence of any peaks relating to either cellulose or lignin present in the 16 week sample further supports the FTIR data that there is no polymeric material remaining in the sample.

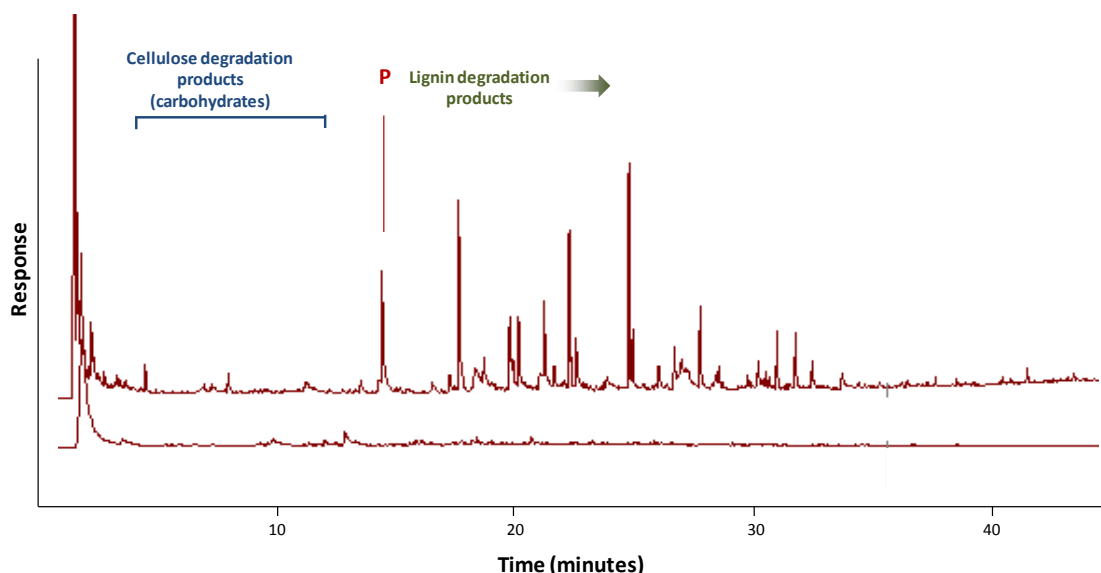


Figure 4.20: Comparison of py-GC traces for birch sample treated for 6 (top) and 16 (bottom) weeks in pH 1 sulfuric acid at, 80°C, D conditions. (Originally in colour).

Similarly, py-GC analysis of the two archaeological starting materials (Figure 4.21) shows very low intensity peaks within the first 10 minutes of the chromatograms, confirming an absence of cellulose in both samples. In addition, py-GC analysis of the Star Carr samples yields no peaks relating to lignin. In contrast, in the Must Farm sample large numbers of peaks present in the chromatogram after 10 minutes indicate that lignin is present in abundance. This shows disagreement with FTIR analysis, where similarities in the spectra indicate that both archaeological samples were at a similar stage of degradation. This discrepancy could again be due to lignin degradation products remaining *in situ* and being detected using FTIR, whilst they are removed prior to analysis by py-GC. A further discussion of archaeological material is carried out in Chapter 7.

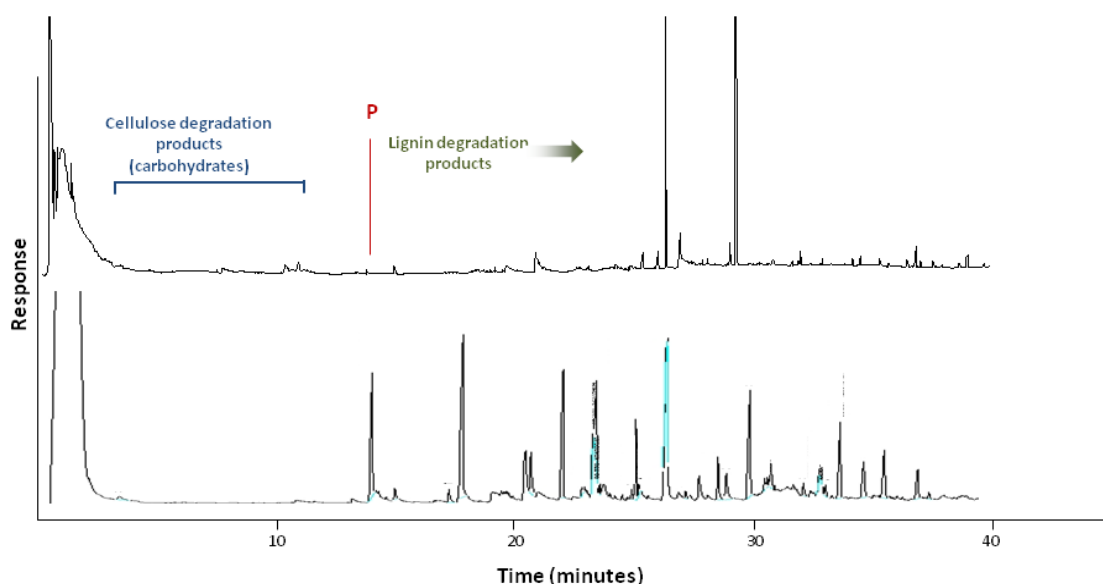


Figure 4.21: Comparison of py-GC traces for archaeological starting material; Star Carr (top) and Must Farm (bottom). (Originally in colour).

4.4.4 Discussion

This study has shown that the use of complementary analytical techniques is fundamental for the accurate assessment of degradation in archaeological wood. It has been shown that whilst fast, easily accessible methods such as mass loss and visual analysis provide an initial indication of diagenesis, more in-depth chemical characterisation is required alongside these. The use of FTIR spectroscopy for the analysis of archaeological woods can be highly informative, and its non-destructive application and fast analysis time makes it ideal for the analysis of precious cultural objects (e.g. Gelbrich *et al.*, 2008). However, comparison with results obtained by py-GC analysis suggest that the use of one technique in isolation may give an inaccurate or incomplete view of the deterioration occurring, particularly when looking at very low levels of deterioration. Results suggest that degradation of polymers, particularly cellulose, do occur upon treatment in acid, but that the degradation products are held within the porous wood structure. This affects bulk assessment analysis and FTIR analysis. Whilst this may not be so important for archaeological materials, where degradation products have time to be removed, it has important implications for experimental studies.

Analysis of modern wood samples treated in sulfuric acid indicates that increasing acidity does have some effect on wood degradation, suggesting that organic material may be at risk by site acidification to the extent of that seen at Star Carr. Despite this, both lignin and cellulose do appear to remain in the experimental wood samples treated at pH values above 2 after 6 weeks, suggesting that the effects are limited. In addition to this, low mass losses in

archaeological wood samples, where only a lignin skeleton is expected to remain, suggest that lignin is relatively stable to acidification. Although some increase in the intensity of the peak related to phenol in py-GC indicates that defunctionalisation of lignin has occurred in acid, the overall structure is retained, signified by intense peaks throughout the lignin region.

After 16 weeks however, modern wood treated at pH 1 underwent significant degradation of polymeric material, indicated by both FTIR and py-GC. Kirk & Farrell (1987) show how lignin degradation occurs primarily via demethylation or demethoxylation of the sub-units, leading to an increased phenol content; this was observed by py-GC analysis. As biological deterioration of the polymers is unlikely to have occurred (for example, the conditions would have been anaerobic), this has been attributed to chemical hydrolysis, showing how high levels of acidity could result in chemical alteration of the lignin.

Analysis by SEM and bulk assessment initially indicated that little change had occurred; in particular, no apparent change in the thickness of the cell walls was seen under SEM. This indicates that even though polymeric material is being chemically altered, the macroscopic structure of the wood can be retained.

4.5 Conclusions

This study has shown that bone degradation is pH dependent, primarily due to the speed at which HA is altered at low pH. Bone that is already damaged (for example archaeological material) is at far greater risk than modern analogues. Bones present in a dynamic environment are at much greater risk from acidification. This is an important consideration for Star Carr, where changing water-levels have resulted in groundwater fluctuating through the archaeological horizon (Brown *et al.*, 2011), and illustrates the importance of monitoring water-levels at wetland archaeological sites. The complete degradation of the archaeological sample at pH 1, 80°C within 7 days is particular cause for concern, suggesting that bone yet uncovered at the Star Carr site is at severe risk and unlikely to survive under present site conditions for much longer. As this study has indicated that there is a threshold pH at which bone mineral becomes sufficiently damaged that collagen breakdown soon follows, it is vital that sediment pH at Star Carr and other vulnerable sites is monitored where possible. Where high acidity is identified at an archaeological site, recovery of any bone artefacts should be considered. As experiments at different pH values show that bone can readily establish a buffered zone, it is possible that in the less acidic areas of the site, bones could remain in a relatively well-preserved state; however, these would be highly susceptible to any increase in acidity.

Lab-based experiments have also highlighted that different levels of degradation are seen in bone of different ages and different types (e.g. racemisation was much higher in the modern rib bone than long bones). This is likely to be due to differences in bone mineral density between animal ages and types of bone (e.g. Green & Kleeman, 1991). From an archaeological point of view this is a very important consideration; preferential preservation of more densely mineralised bones is likely to occur where there is high acidity.

Equivalent experiments on wood samples have shown that deterioration is also pH dependent, but that degradation of structural polymers occurs a lot more slowly than for bone (extensive alteration was only seen after 16 weeks at pH 1 and 80°C, in comparison to bone where complete dissolution of most bones occurred within 6 weeks). Once chemical alteration has occurred, wood can retain its macroscopic appearance. For these reasons, it is likely that wood material is not as at risk from acidification at Star Carr as bone is. Even if chemical deterioration occurs, information such as species and age of the wood may still be obtained from the artefacts. Importantly, analysis of experimental wood samples has shown that employing a multi-analytical approach to determining levels of degradation in organic materials is critical in obtaining an accurate measure of deterioration.

Although high acidity may be the major contributor to the deterioration of bone observed at Star Carr, it seems likely that the deterioration of wood observed at the site is driven primarily by other factors. Wood recently excavated from the site is undoubtedly heavily deteriorated, with py-GC analysis showing a lack of both cellulose and lignin (Figure 4.21), and the experiments in sulfuric acid have shown that lignin in particular is relatively stable to acidification. Although defunctionalisation was observed under extreme conditions, this did not result in the loss of macroscopic structure. As previously discussed, further factors likely to be contributing to organic degradation are biological activity (possibly this is increased at Star Carr due to a lowering of the water-table; Blanchette *et al.*, 1990; Jones & Eaton, 2006) and a fluctuating hydrology (Schwarzel *et al.*, 2002). Overall, the experimental study has demonstrated that both bone and wood are more at risk in 'dynamic' hydrological environment than 'stagnant'. As it is hypothesised that at Star Carr the water-table is fluctuating through the archaeology (Brown *et al.*, 2011; Chapter 2), this illustrates that organic archaeological material (particularly wood) still buried at the site is at risk from factors aside from high acidity.

CHAPTER 5

LAB-BASED BURIAL EXPERIMENTS (MICROCOSMS)

5.1 Introduction

Lab-based experiments (Chapter 4) have shown that whilst bone is severely deteriorated in the presence of acid, the effects on wood are less clear. However, the experiments were designed to assess only the effects of high acidity at Star Carr, and as such did not account for factors such as microbial activity, site hydrology and soil geochemistry, which are all known to have an important contribution to organic deterioration in archaeological sites and cannot be disregarded (e.g. Caple, 1994; Blanchette, 2000; Child, 1995; Nicholson, 1996). Indeed, high levels of deterioration have been seen in wood excavated from Star Carr (Milner *et al.*, 2011a), suggesting that factors aside from high acidity are playing an important role in the deterioration of organic materials at the site.

Biological (fungal and microbial) activity is often acknowledged as the primary mode of deterioration of both lignin and cellulose in wood (e.g. Blanchette *et al.*, 1990; Kim & Singh, 2000). In addition, although bone is often considered protected from biological degradation by the hydroxyapatite (HA) (e.g. Collins *et al.*, 1995), lab-based experiments (Chapter 4) have shown that in the presence of high acidity, this is rapidly removed and as such the collagen component may be exposed to biological degradation by collagenase producing bacteria (Child *et al.*, 1993). Biological activity is intrinsically linked to oxygen content, and therefore degree of waterlogging, or hydrological regime of a burial location (e.g. Lillie & Smith, 2007). Studies such as those by Nicholson (1996; 1998) and Bartlett *et al.* (2010) illustrate how important other environmental conditions, such as water movement and soil density, are in influencing this. As such, specific soil types and burial locations contribute to organic deterioration in very specific ways; each burial location is unique, and as such difficult to characterise (Caple, 1994).

Due to the abundance of variables contributing to preservation *in situ*, studies into specific factors have often utilised 'microcosms,' or lab-based burial experiments. These offer the opportunity to conduct burial experiments in a semi-controlled manner. Examples include an investigation into the effects of short-term fluctuations in water levels on the decay of oak samples, conducted by Lillie & Smith (2007). Using a series of large fermentation containers where the water levels were altered periodically, wood decay in different zones of saturation was monitored. Gelbrich *et al.* (2012) demonstrate the success of using microcosms in a study where bacteria were purposely introduced into the vessel, and biological activity in different zones of aeration monitored.

At Star Carr, very specific and unusual site conditions have been recorded (Chapter 2); full characterisation of the burial environment is difficult, but it is likely that the phenomenon of

high acidity is not the sole factor facilitating the decay of bone and wood. Lab-based burial experiments were therefore set up in order to enhance data obtained from experiments in sulfuric acid only, by introducing other burial conditions. By conducting burial experiments in soil excavated from the site itself, and comparing this to decay observed in different soil types, the aim was to more fully understand the unique burial environment at the site. In addition, different degrees of aeration in various zones of each soil were created in order to form zones that were expected to be more or less conducive to biological activity, thus providing data regarding the extent to which microbial and fungal decay may be contributing to deterioration at Star Carr.

5.2 Experimental

5.2.1 Method

5.2.1.1 Experimental set up

Three separate microcosms were initially set-up using 25 L fermentation vessels measuring approximately 37 cm in height, based on the method described by Lillie & Smith (2007). Microcosms were set up for a period of 12 months, and contained three different sediment types; peat from Star Carr, and two very different sediments (sand and compost) with which to compare this (Section 2.2.2). These were nominally divided into 3 zones with the aim of obtaining a dry, fluctuating and saturated zone for each soil type. This was achieved by first covering the base of the vessel with a 2 cm layer of gravel to aid in the drainage of water and then installing a tap into the side of each vessel and sealing this with epoxy resin. A clear plastic tube was similarly attached to the outside of the vessel in order to allow the water level to be viewed (Figure 5.1).

Due to experimental difficulties, some later adaptations were necessary, and an additional Star Carr peat zone was added (C4). These adaptations are detailed in Section 2.1.2 and all zones summarised in Table 1. A set of the materials listed in Section 2.2 was accurately weighed and spaced within each zone of each microcosm. Plastic tubes were also buried as 'dipwells' to allow the sampling of water during the experiment if necessary (Figure 5.2, left).

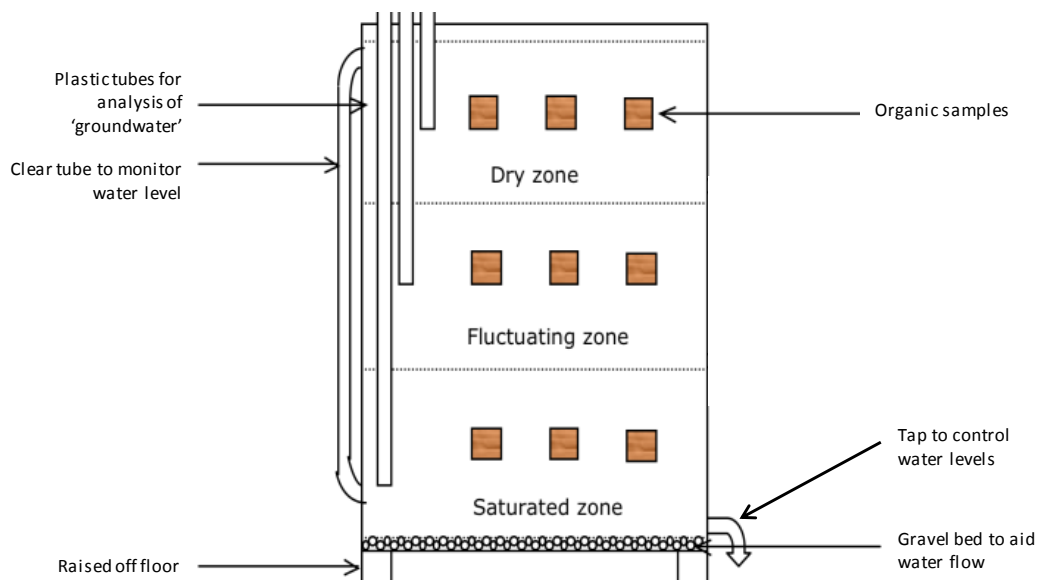


Figure 5.1: Schematic of the initial microcosm set up. Additional containers were also later set up.



Figure 5.2: Photos of materials laid out in the microcosms, showing the dipwells in the centre and the material spaced around the edge(left), and the outside of the microcosms (right). (Originally in colour).

Initially, enough deionised water was added to raise the water level to the top of the saturated zone. After 2 weeks, 500 ml of deionised water was added to the top of the microcosm to raise the water level, which was then slowly drained back down using the tap, to the top of the saturated zone over a 2-week period. This process was repeated every month for 12 months.

5.2.1.2 Sediment types

The aim of the experiment was to obtain three distinct zones in the fermentation vessel for each sediment type. However, problems were encountered with defining the water level, as well as issues with leaking from microcosm C. In order to account for this, several adaptations were made to the experiment, resulting in zones that were broadly 'dry,' 'saturated' or 'damp.' 'Dry' zones were set up in separate containers, and assumptions made about the levels of aeration in each of the other zones (see descriptions of sediment types). Table 5.1 summarises each of the 10 environments set up in the microcosm experiment.

Table 5.1: Summary of all conditions, or zones.

Description of each of the 10 'zones' in the microcosm experiment			
Label	Sediment	Hydrology	Detailed description
A3	Sand	Dry	Set up separately; completely dry and open to the air. Aerobic
A2		Fluctuating	Relatively aerated compared to A1. Kept damp
A1		Saturated	Expected to be anaerobic as it is at the base of the microcosm and waterlogged. However, water level difficult to define
B3	Compost	Dry	Set up in separate container. Dry
B2		Fluctuating	Relatively aerated compared to B1. Kept damp, with water regularly flushed through
B1		Saturated	Set up in separate container. Permanently saturated, expected to be anaerobic
C4	Star Carr	Dry	Set up in separate container. Dry. (No Tanner Row bone available)
C3		Damp	Relatively dry as it is the top of the microcosm, but some water washing through
C2		Fluctuating	Relatively aerated compared to C1. Kept damp
C1		Saturated	Expected to be anaerobic as it is at the base of the microcosm and waterlogged

5.2.1.2.1 Microcosm A: Sand

Sand provides an environment where groundwater can percolate very readily, due to its high permeability (e.g. Wilson *et al.*, 2008). For this reason, bone in sandy sites is often badly preserved and low in organic content; the bone can act as a 'trap' for ions in water moving through it, resulting in crystallisation following cracking, giving the bone a brittle texture (e.g. Grupe, 1995). In addition, the high porosity of sand allows microbial colonies to flourish due to the ease with which nutrients and oxygen are transported (e.g. Bartlett *et al.*, 2010).

The disadvantage of this permeability from an experimental perspective is that a clear water level could not be defined within the microcosm due to the high wicking ability of sand. The 'dry' zone for sand was kept separate to avoid this problem, resulting in only two layers in the main fermentation vessel, although all three zones will be referred to as 'microcosm A' for convenience. It has been assumed that the lowest level in the fermentation vessel was less aerated than the top, although both layers were kept damp throughout. Sand was obtained from a building merchant, and left untreated as to allow any natural microbial colonies to remain undisturbed.

5.2.1.2.2 *Microcosm B: Compost*

Organic rich sediments such as compost tend to be very conducive to the preservation of organic materials if waterlogged and anaerobic (e.g. Kenwood & Hall, 2000). Due to the high organic content they can also support large amounts of biological activity when they become aerobic (i.e. no longer waterlogged); indeed, large numbers of micro-fauna are involved in the composting process itself (e.g. Tiquia *et al.*, 2002). Therefore, the use of ordinary garden compost serves as a microbially rich control environment.

Two distinct layers were achieved in the compost microcosm: permanently saturated, and damp. As the water content of compost increases, the air permeability decreases, meaning that waterlogged compost at the base of the microcosm has been considered anaerobic (e.g. Das & Keener, 1997). To ensure comparability to the two other microcosms, where it was necessary to set up a 'dry' zone in a separate container, this was also done for microcosm B using air-dried sediment (see Table 5.1). Again, all three zones are referred to as 'microcosm B'.

5.2.1.2.3 *Microcosm C: Peat from Star Carr*

The majority of archaeological materials at Star Carr have been recovered from a thick layer of reed and woody peat (Boreham *et al.*, 2011; Chapter 1). Although this has a high organic content (similarly to compost), the low pH and high sulfur content at Star Carr make it unusual. The very low permeability of the peat also means that groundwater is slow to fluctuate through the sediments (Brown *et al.*, 2011).

To replicate the burial environment at Star Carr most accurately, peat taken directly from the site was used to fill the microcosm. As excavations had not recently taken place at the site, and therefore fresh sediment was not available, a number of soil samples excavated in 2007 from the wetland area of Trench SC23 were combined for this purpose.

Possibly due to the exposure to oxygen since excavation 4 years previously, the pH of the peat recorded at the time of setting up the experiment was 1.63; this is lower than observed in much of the Star Carr site when analysed in field (pH 2-3; Chapter 2). Due to the high acidity, the epoxy resin seals leaked continually throughout the experiment. Therefore, the 'permanently saturated' zone cannot confidently be described as always waterlogged, although the low permeability of the peat combined with the thick layers of peat on top of the zone indicate that it would have been highly anaerobic. To ensure that the 'dry' zone was properly achieved, a separate vessel was again set up containing air-dried peat (see Table 5.1).

5.2.1.3 Analysis

Analysis of organic deterioration was carried out according to methods described in Chapter 3 unless otherwise stated.

Analysis of sediments was carried out as described in Chapter 2 (Section 2.3.2).

5.2.2 Materials

Both bone and wood were buried in each microcosm. The material was selected to be comparable to the lab-based study (Chapter 4) as well as later *in situ* burial experiments (Chapter 6). However, in some cases the amount of available material limited this. Both modern and archaeological materials were included, as archaeological material can be expected to have already undergone some degradation prior to excavation (e.g. Child, 1995; Blanchette, 2000). Further discussion of the archaeological materials used is carried out in Chapter 7.

An asterisk denotes samples that are directly comparable to in situ burial experiments (Chapter 6).

5.2.2.1 Bone (3 modern, 2 archaeological)

*Modern sheep rib bone, obtained from a butcher. Cleaned in biological washing powder and sliced into approximately 4-5 mm pieces using a water-cooled band saw. Marrow not removed

*Modern artificial 'jellybone': sheep long bone obtained from a butcher. De-fleshed and sliced using a water-cooled band saw. Demineralised in 0.6 M HCl for 1 week, sewn into netlon bag

*Modern sheep long bone, obtained from a butcher, cleaned in biological washing powder Sliced into approximately 4-5 mm pieces using a water-cooled band saw and the marrow removed

Archaeological cow metatarsal from the early medieval site of Tanner Row, York. Sliced into approximately 4-5 mm sections using a water-cooled bone saw

*Star Carr rib bone excavated in 2010 (sample number 92419) 'robust' in appearance. Sliced into approximately 5 cm lengths using a water-cooled band saw

5.2.2.2 Wood (3 modern, 2 archaeological)

*Modern oak, approximately 3 cm³ pieces of trunk, cut using a band saw

*Modern willow, approximately 3 cm³ pieces of trunk, cut using a band saw

*Modern birch, branch of approximately 2 cm diameter, cut into 10 cm lengths using a band saw

*Must Farm (Bronze Age) wood (ash), approximately 5 cm³ section, dried

*Star Carr wood (unidentified, likely to be willow), approximately 3 cm³ piece from a split timber plank excavated in 2007. Dried and sewn into netlon bag.

5.3 Results and discussion

5.3.1 Sediment analysis

5.3.1.1 pH and redox analysis

'Dipwells' were inserted at each depth in the microcosms with the aim of periodically removing water for analysis. In the majority of zones however, insufficient water was available for this to be feasible. Therefore, pH and redox values are reported only from analysis at the end of the experiment, as well as after 1 day and 6 months in a few cases (Table 5.2).

Table 5.2: Summary of geochemical data for each of the 10 experimental zones. Where data was not recorded, the box is left blank.

pH and Redox measurements of each microcosm								
Zone	Hydrology		After 1 day		After 6 months		End (12 months)	
			pH	Redox (mV)	pH	Redox (mV)	pH	Redox (mV)
A3	Dry	Sand					7.26	188
A2	Fluctuating						7.40	173
A1	Saturated						7.35	54
B3	Dry	Compost					5.00	435
B2	Fluctuating		4.88	187			5.58	194
B1	Saturated		5.53	149	6.15	474	3.58	176
C4	Dry	Star Carr					0.85	487
C3	Damp		0.66				1.58	571
C2	Fluctuating		0.60	524			1.84	559
C1	Saturated		1.98	481	1.05	475	1.63	501

Microcosm C (Star Carr) remained highly acidic through the experiment, in all 4 zones. In the aerated, dry zone (C4) pH is even lower; this is possibly due to the presence of oxygen which may cause an increased level of sulfuric acid via the oxidation of sulfides, which have been identified in high abundance in the peat at Star Carr (e.g. Boreham *et al.*, 2011; Chapter 2).

In addition, redox potential is very high in all zones in microcosm C, suggesting a highly oxidising environment (Patrick & Mahapatra, 1968). A high redox potential is often interpreted as indicating the potential for high levels of microbial activity and by proxy, little propensity for organic material to survive (e.g. Lillie & Smith, 2007). High redox potential can however also be indicative of high concentrations of acid, which also cause oxidation (Caple, 1994; Atkins *et al.*,

2006). At such low pH values it is possible that microbial activity is in fact suppressed in spite of this oxidising environment; although a few groups of bacteria can adapt to and even thrive in such extreme environments (e.g. Brock *et al.*, 1972; Cotter & Hill, 2003), low pH is likely to severely limit the growth of most aerobic colonies (e.g. Russel & Dombrowski, 1980; Beales, 2004).

In other microcosms, where pH is not as high, redox potential is more likely to serve as a proxy indicator for microbial activity. In most regions redox potential is moderate; however in the aerated zone of the compost microcosm an elevated redox potential (> 400 mV, indicating aerobic conditions) and almost neutral pH may provide ideal conditions for extensive microbial colonisation (Beales, 2004).

In microcosm A (sand), a neutral pH is maintained and the low redox potential in the saturated (or least aerobic) zone confirms the absence of oxygen. This is likely to prohibit aerobic microbial activity, although anaerobic bacteria and fungi may still be active (e.g. Lillie & Smith, 2007).

5.3.2 Bone analysis

5.3.2.1 Mass loss and visual analysis

All buried bone samples were recovered from each microcosm except for the 'jellybone' samples in 'anaerobic' zones B1 and A1 where they had completely disappeared, leaving only the netlon bag behind. Other 'jellybone' samples from microcosms A and B had become discoloured and displayed high mass loss, although small fragments were recovered. However, in all mineralised bone retrieved from microcosms A and B, no real difference in appearance was seen in comparison to the starting materials except some slight staining visible in the modern samples (Figure 5.3).

In contrast, all samples from waterlogged or damp zones in microcosm C had developed a very chalky and deformed texture, appearing almost swollen in appearance and barely recognisable as bone. In C4 this change had not occurred, with recovered material appearing little altered from the starting material. All 'jellybone' samples were still present in microcosm C, although they had become darkened and distorted.

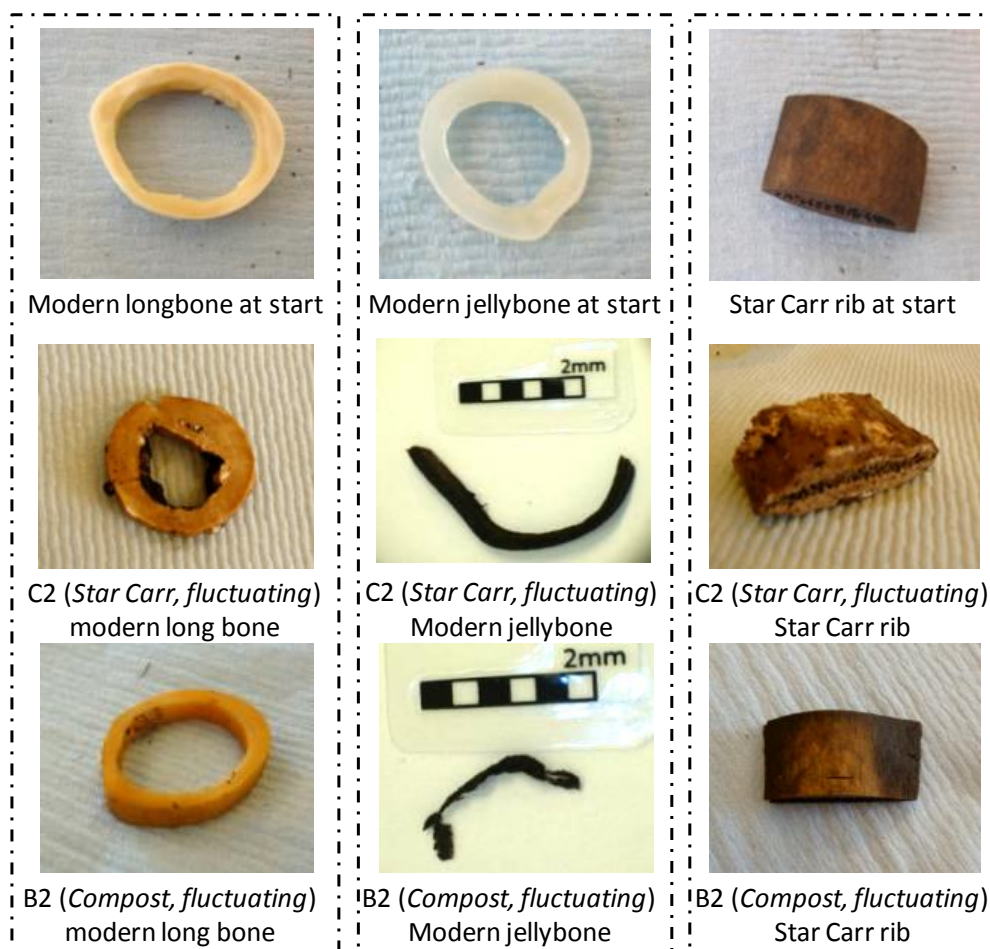


Figure 5.3: Image of buried bones before (top) and after burial in zone C2 (centre) and B2 (bottom). Note that C2 modern 'jellybone' is pictured after sub-sampling for analysis, and was in fact retrieved intact. (Originally in colour).

Mass loss is reported as a percentage of the starting mass in Table 5.3. Mass loss is likely to be subject to quite a high level of error, due to the difficulty in ensuring samples are completely dry, and the possible inclusion in the measurement of soil adhering to the samples. Despite this, some broad observations can be made. An increase in mass is seen in many of the samples in microcosm C (negative mass loss), which must be the result of uptake from the soil environment; this could be moisture or other species present in the sediment. This is in accordance with the 'swollen' appearance of the samples.

Mass losses are high in the modern rib samples, although this is possibly explained by loss of bone marrow, which was still present prior to burial, rather than structural components. In microcosms A and B, this is supported by the negligible mass loss observed in all archaeological samples, where these non-structural components are likely to have been removed over their long period of deposition prior to the experiment (Currey, 2002). As such, this is suggestive that very little structural alteration has occurred in mineralised bone in microcosms A and B.

Table 5.3: Mass loss data for all bones from each of the 10 microcosm zones. No Tanner Row bone was buried in environment C4. (Originally in colour).

Mass loss as a percentage of the starting mass							
Zone	Hydrology		Material				
			Modern rib	Modern longbone	Jellybone	Star Carr rib	Tanner Row bone
A3	Dry	Sand	31	-6	23	0	0
A2	Fluctuating		21	1	21	0	0
A1	Saturated		48	0	100	0	0
B3	Dry	Compost	42	4	17	0	0
B2	Fluctuating		35	6	35	0	0
B1	Saturated		30	3	100	0	0
C4	Dry	Star Carr	4	0	28	-1	
C3	Damp		27	-154	16	4	-15
C2	Fluctuating		15	-12	17	-16	-15
C1	Saturated		3	-22	14	-22	-24

The fact that the ‘jellybone’ samples, where all HA had been removed, underwent high mass loss compared to other samples highlights the important role that the HA plays in protecting the bone protein; a fact also highlighted by other studies (e.g. Child, 1995; Collins *et al.*, 2002). In particular, it has been acknowledged that HA contributes to preventing microbial degradation of the collagen by enzymatic attack, as the close packing of the mineral phase excludes the large collagen degrading enzymes (collagenases) (Child *et al.*, 1993; Child, 1995). The rapidity at which ‘jellybones’ were lost in zones A1 and B1 may therefore indicate that this was due to a large amount of biological activity, as opposed to chemical degradation; low mass loss and a lack of visual changes suggest that chemical deterioration of HA has not occurred in the mineralised bones (e.g. Collins *et al.*, 2002; Hedges, 2002). If this is the case, the fact that all ‘jellybones’ survived in microcosm C (a highly acidic environment) is tentatively indicative of the fact that microbial activity was actually suppressed.

5.3.2.2 Amino acid analysis

Amino acid analysis of bone samples retrieved from the microcosm experiments was partly carried out by Lucy Dawson as part of a summer placement project. Very little alteration of the total amino acid content is observed in the majority of samples from microcosms A and B with the exception of 'jellybone' samples (where recovered) where much lower total amino acid concentrations were recorded (Figure 5.4, right). No HA was present in these samples prior to burial, meaning that loss of collagen would not alter the relative composition. Instead, this reduction is more likely to be due to the inclusion of material from the burial environment in the sample.

In addition, a small reduction in total amino acid concentration was observed in the Star Carr rib buried in all zone A and B environments. This suggests that some loss of collagen may have occurred. This could potentially be attributed to the same microbial activity that degraded the 'jellybone' samples. In the modern samples, HA will prevent access of microbes to the collagen, but in an archaeological sample the low levels of diagenesis already present may have already increased the porosity of the bone (e.g. Child, 1995; Hedges, 2002).

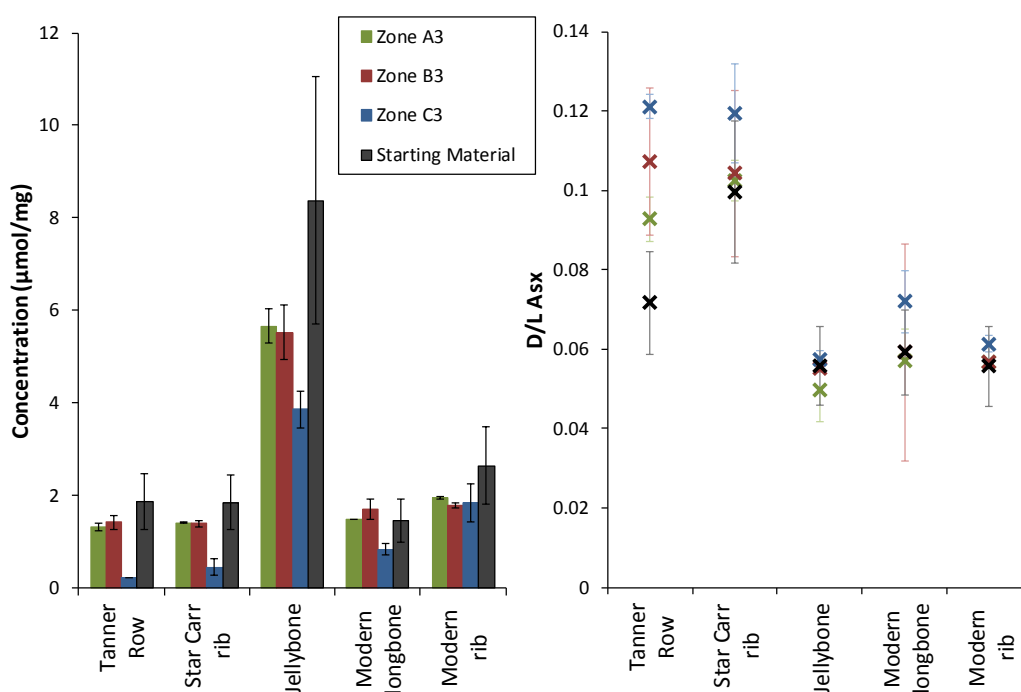


Figure 5.4: Comparison of total amino acid concentrations in buried material compared to the starting material (left) and Asx racemisation in the same samples (right). (Originally in colour).

In all microcosm C samples with the exception of the modern rib, total amino acid content is decreased to a greater extent than in microcosms A and B (Figure 5.4, left). This could also be attributed to collagen loss, similarly to that seen in zones A and B, although mass loss analysis contradicts this; in the majority of cases, a mass gain was actually seen in samples buried in

peat from Star Carr. It is possible that this mass gain is the result of uptake of material from the sediment, additionally resulting in a reduced relative concentration of amino acids.

Racemisation of Asx can serve as an indicator of collagen damage, as it is more likely to occur when there is a loss of conformational freedom in the collagen chain (Chapter 3). Asx racemisation is little altered from the degree of racemisation in the starting material for most modern samples, suggesting that collagen has remained intact (Figure 5.4, righttt). As racemisation is normally very slow to occur this is not unexpected over only 12 months at room temperature (e.g. Smith & Evans, 1980). It is however slightly elevated in some of the archaeological bones. This may be because low levels of collagen breakdown and unravelling of the fibrils have already occurred in the starting material, by processes such as hydrolysis, which may allow further breakdown to proceed more readily (Koon, 2006).

In all recovered 'jellybone' samples, even those displaying high mass loss, racemisation is lower than archaeological samples. This may corroborate conclusions drawn from the lab-based experiments, where it appeared that racemised fragments may be readily leaching from the most deteriorated bones, reducing their observed degree of racemisation. However, not enough data is available here to fully confirm this.

Differences between different zones of each microcosm are difficult to elucidate and this may be a result of the experiment being carried out over such a short time-scale; very little alteration of degree of racemisation is observed. Despite this, some initial observations from microcosm C, zones 1, 2 & 3, show a decrease of total amino acid content in all samples compared to that starting material (Figure 5.5); this is much less significant for zone 4 (dry). This is in agreement with mass loss data and visual analysis, which suggested that alteration was much less advanced in the dry zone. This further indicates the important role that groundwater movement is likely to play in facilitating diagenesis, as it enables chemical reactions to occur (Hedges & Millard, 1995; see discussion in Chapters 1 & 2).

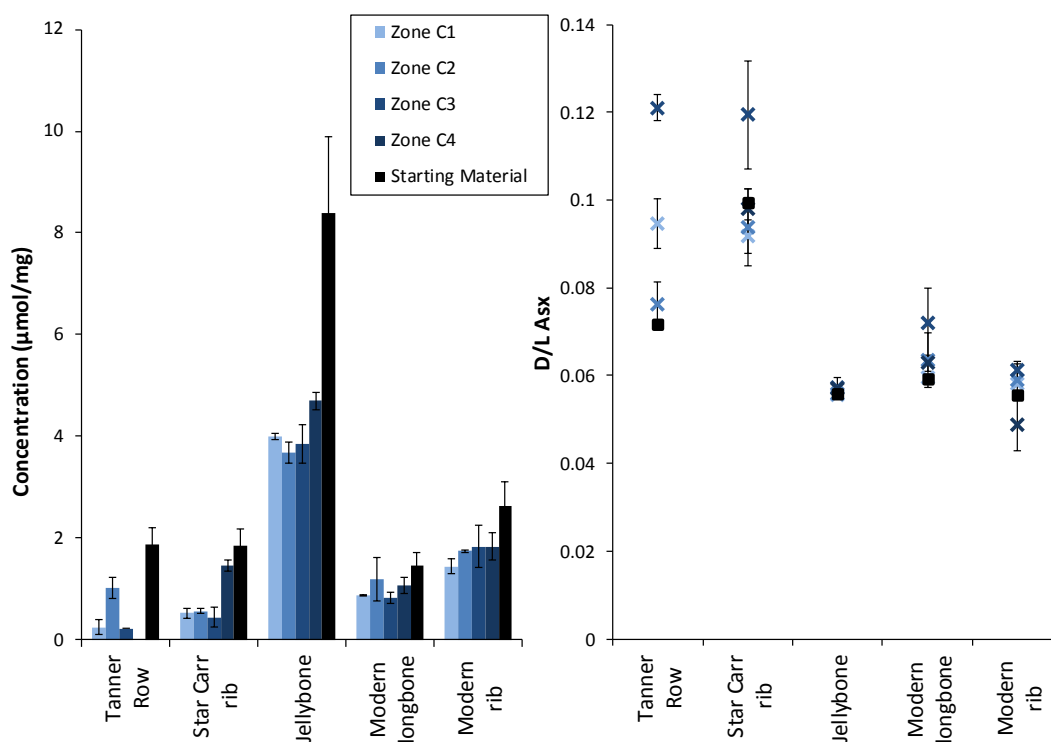


Figure 5.5: Comparison of total amino acid concentration (left) and Asx racemisation (right) in all bone samples excavated from microcosm C compared to the starting material. Error bars are calculated as the standard deviation of replicate measurements, except for the starting material where the error calculated in Chapter 3 is applied. (Originally in colour).

5.3.2.3 Powder X-ray diffraction

The shape of the diffraction pattern for each sample has been classified according to the definitions outlined in Chapter 4 and summarised in Table 5.4. One 'jellybone' sample from microcosm C was analysed and found to contain no HA peaks, as expected as this was removed by treatment in acid prior to the experiment. Further 'jellybone' samples are therefore not included in the analysis.

No alteration of the diffraction pattern is observed in any of the A and B samples. The appearance of a small shoulder in analysis of the Star Carr rib bone and Tanner Row bone in each case is attributed to alteration of the sample prior to burial rather than during the experiment. This lack of alteration further confirms that in both sand and compost, diagenetic processes were not sufficiently fast to cause bulk alteration of the mineral fraction within the time-scale of the experiment; in comparison to an archaeological time scale, the duration of the burial experiment was negligible. Whilst splitting of the HA peaks in fossil bones has been reported, it is often very minor in much younger archaeological bones (e.g. Person *et al.*, 1995). This is in agreement with analysis of the amino acid content, where again little alteration of the organic fraction is indicated.

Table 5.4: Summary of p-XRD patterns for all analysed bone sample, characterised according to classifications defined in Chapter 4 (Section 4.3.3.1). (Originally in colour).

Key: **G** = gypsum structure; **S** = peak splitting; **MS** = mild splitting; **PS** = peak has shoulder; - = no alteration.

Characterisation for all bones samples analysed by p-XRD						
Zone	Hydrology		Material			
			Modern rib	Modern longbone	Star Carr rib	Tanner Row bone
A3	Dry	Sand			PS	PS
A2	Fluctuating		-	-	PS	PS
A1	Saturated		-	-		PS
B3	Dry	Compost	-	-	PS	
B2	Fluctuating		-			PS
B1	Saturated		-		PS	PS
C4	Dry	Star Carr		-	MS	
C3	Damp			G	G	G
C2	Fluctuating			G	G	G
C1	Saturated			G	G	G

In stark contrast to the lack of alteration of the HA in microcosms A and B, all samples analysed from damp or wet environments in microcosm C displayed the diffraction pattern characteristic of gypsum (Figure 5.6). This was also seen in lab-based experiments in Chapter 4, and there was attributed to high concentrations of sulfur causing dissolved HA to recrystallise as gypsum (calcium sulfate) according to Equation 5.1.

Equation 5.1: Reaction of HA with sulfuric acid to form gypsum.



Gypsum has been reported as inclusions in bones from archaeological sites of various ages (e.g. Zapata *et al.*, 2006; Turner-Walker & Peacock, 2008). However, analysis of the 'jellybone' sample showed no gypsum peaks, suggesting that gypsum has resulted from interaction with the HA rather than uptake from the sediment. In addition, p-XRD analysis of mineralised bones from microcosm C reveal no peaks related to HA at all, suggesting that almost total transformation to gypsum has occurred. This may account for the increase in mass, as the change to gypsum according to Equation 5.1 would account for an approximately 230 % increase in mass of the mineral fraction, which accounts for approximately two thirds the total

mass of bone (Green & Kleeman, 1991). Further analysis would be required to confirm the extent of this transformation.

In order for such an alteration of the mineral fraction to proceed, it must be assumed that sufficient interaction with the burial environment has occurred (e.g. Wilson & Pollard, 2002). Indeed, the fact that the change does not occur in the dry environment (C4) highlights the important role that groundwater interactions play in this transformation. In addition, in lab-based experiments it was observed that the transformation was more likely to occur under 'stagnant' conditions; assumedly as a result of the dissolved ions from the HA not being washed away, allowing recrystallisation to occur. The rate at which groundwater is replenished is often cited as an important factor in the preservation of bone (e.g. Hedges & Millard, 1995; Crowther, 2002).

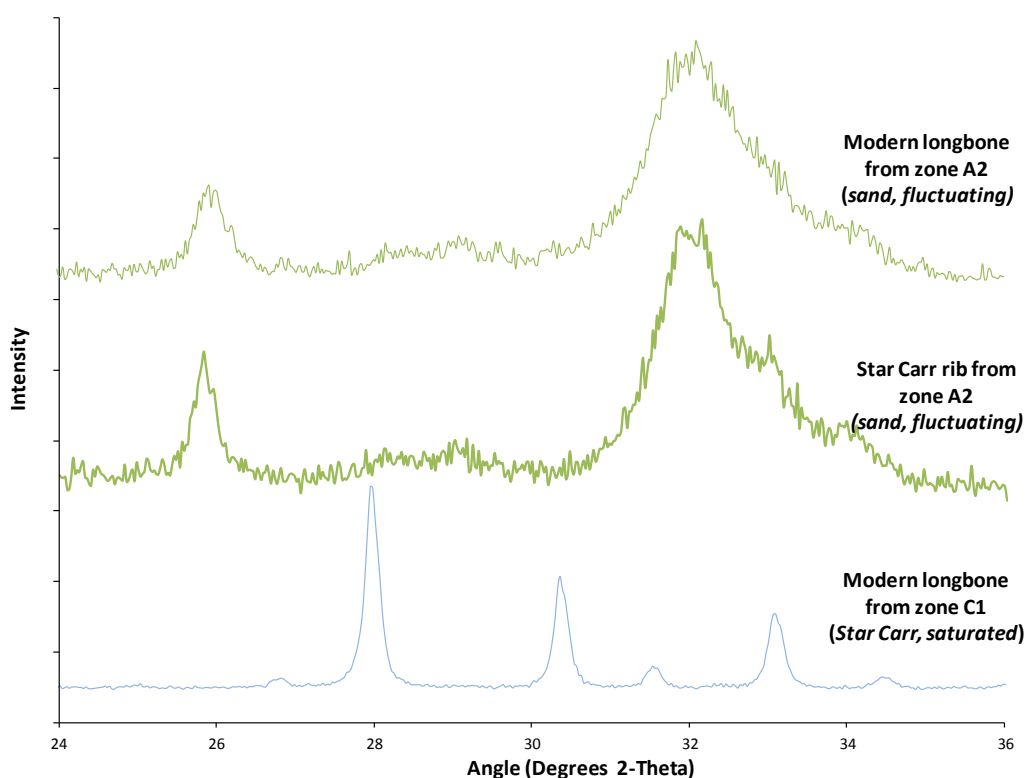


Figure 5.6: Comparison of diffraction patterns for the modern long bone and Star Carr rib samples from zone A2, where no alteration is seen (note that a small shoulder on the HA peak in the Star Carr rib pattern was present prior to burial), compared to the distinctive gypsum diffraction pattern in the modern long bone sample from zone C1. All analysed samples from zones C1, C2 and C3 displayed this pattern. (Originally in colour).

In part, this transformation is likely to be due to the increased speed at which HA will dissolve at low pH, in order to buffer the surrounding environment, as demonstrated by lab-based experiments (Chapter 4) as well as studies on the solubility of HA, such as those by Berna *et al.* (2004). HA normally re-precipitates as HA as this is one of the most stable forms of calcium

phosphate (Turner-Walker, 2008). Berna *et al.* (2004) show that there is only a small window of pH (around pH 7) within which this recrystallisation as apatite occurs. This may suggest that the low pH of the peat at Star Carr is not only causing dissolution of bone, but restricting the way in which it recrystallises, even in a completely stagnant environment.

5.3.2.4 Microscopy

In previous studies, the presence of gypsum crystals in bones has been identified using microscopic techniques (Turner-Walker & Jans, 2008). For this reason, one sample from microcosm C (modern long bone from zone 3) was analysed by SEM according to procedure outlined in Chapter 3.

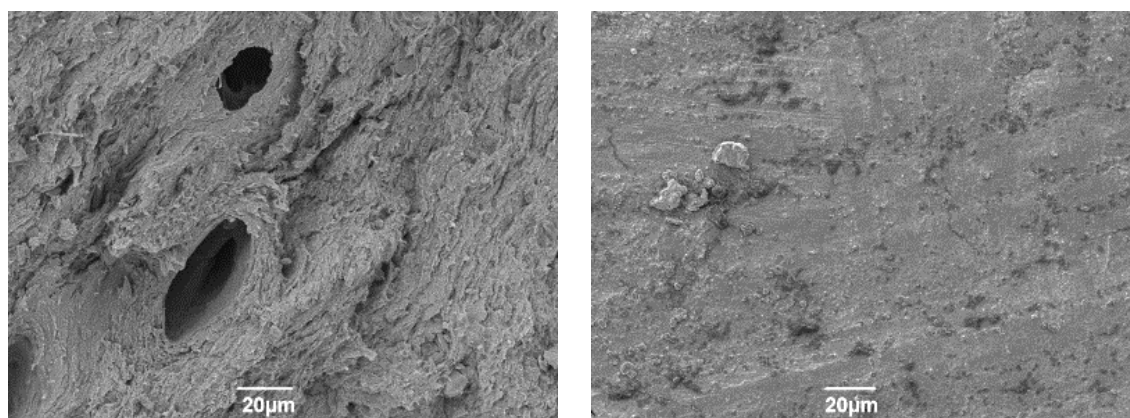


Figure 5.7: SEM image of modern long bone excavated from zone C3 (left), compared to untreated long bone (right).

The surface of the bone excavated from zone C3 appeared 'spongy' in texture when compared to fresh bone. This is comparable to the appearance of bones analysed after incubation in sulfuric acid, and could therefore be the result of dissolution of the bone mineral (Chapter 4). Using SEM it was not possible to make a definitive conclusion about whether gypsum crystals were present, as their characteristic shape was not observed. In order to further investigate the extent of the transformation to gypsum in the bones from microcosm C, it may be necessary to employ a technique such as trace element analysis (e.g. Zapata *et al.*, 2006). Alternatively, use of SEM with backscattered electron (BSE) function, for example as used by Turner-Walker & Jans (2008), may reveal changes in density of the bone mineral, which relates to chemical transformations.

5.3.2.5 Summary of bone analysis

Deterioration of all mineralised bone samples recovered from microcosms A and B was minimal, with analysis revealing little alteration of both the HA and collagen in the majority of samples. This is unsurprising on this timescale; bone can be well preserved in archaeological contexts for millions of years (e.g. San Antonio *et al.*, 2011). The complete loss of two 'jellybone' samples and a high mass loss in others however, shows that demineralised bone has the potential to be rapidly lost in certain types of soil. It is hypothesised that the primary mode of this rapid deterioration was biological; both compost and sand have the potential to support large microbial colonies, and displayed mild pH and positive redox values, conducive to microbial activity (Lillie & Smith, 2007). Without the protection of the HA it is possible that microbial decay of collagen can occur with little difficulty (Child, 1995).

The mode of deterioration in microcosm C (Star Carr peat) appears to be completely different. Whereas drastic alteration of the HA has been revealed by p-XRD in mineralised bone samples, the 'jellybone' samples survived well, aside from some discoloration. The seemingly complete alteration of the HA to gypsum in all samples analysed by p-XRD demonstrates the rapidity with which bone can potentially undergo chemical changes under the conditions present at Star Carr. The reasons for the rapid change are likely to be due to both the high acidity and high sulfur content, which combine to cause the alteration from apatite to gypsum. Over such a short time scale, no subsequent alteration of the collagen in these mineralised samples was seen. However, it is well established that the HA in bone ordinarily protects the collagen from both microbial and chemical attack (e.g. Child, 1995; Collins *et al.*, 2002). Furthermore, lab-based studies carried out at 80°C showed that upon alteration of the bone mineral, collagen breakdown is quick to proceed (Chapter 4). Further lab-based experiments using only collagen have shown that collagen completely dissolved within hours in pH 2 sulfuric acid and 65°C (Rhodes, 2014). It is therefore hypothesised that this rapid alteration of the HA would be detrimental to the long-term survival of any remaining collagen in archaeological samples.

As HA is known to protect the collagen, the fact that 'jellybone' samples did not completely disappear in any of the C environments, in contrast to in microcosms A and B, may suggest that microbial activity is suppressed at such low pH. At such low pH, chemical hydrolysis of the collagen is likely to occur in the absence of HA, and as such loss of collagen may have been expected (Collins *et al.*, 2002). In such a short-term experiment as the one reported here however, this may not be observed.

5.3.3 Wood analysis

5.3.3.1 Mass loss and visual analysis

All wood samples were retrieved from all zones of the study, and all samples retained the appearance and texture of fresh or archaeological wood, with some slight darkening in microcosms B and C attributed to high levels of tannins present in peaty sediments (e.g. Nicholson, 1998). In microcosm A long, fibrous formations, similar in appearance to fine plant roots, were observed adhering to the surface of the both the modern oak and willow samples from zone A1 (waterlogged/ anaerobic). These have not been definitively identified but are likely to be evidence of biological activity, for example fungal hyphae or filamentous bacteria such as actinomyces; both have the potential to degrade cellulose and lignin in wood (Buscot & Varma, 2005). In addition, when the oak sample was excavated from the top layer of microcosm A, the surrounding sand was darkened. This could potentially be the result of water soluble tannins leaching out of the wood (Bjordal & Nilsson, 2007).

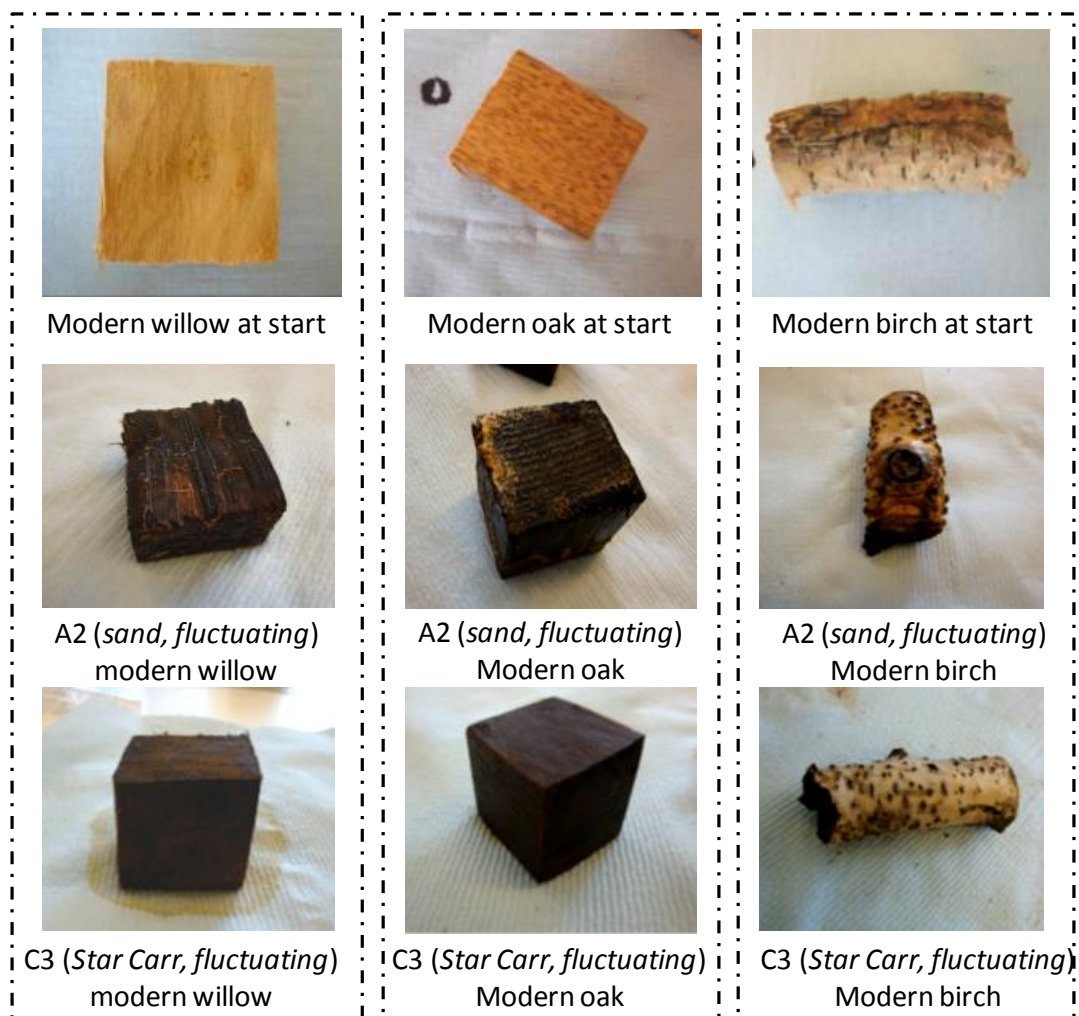


Figure 5.8: Images of wood material before burial (top) compared to burial in zone A2 (centre) and C3 (bottom). (Originally in colour).

Table 5.5: Mass loss data for all wood samples from each of the 10 microcosm zones. (Originally in colour).

Mass loss as a percentage of the starting mass							
Zone	Hydrology		Material				
			Modern oak	Modern willow	Modern birch	Star Carr wood	Must Farm wood
A3	Dry	Sand	-2	-8	-2	16	-2
A2	Fluctuating		6	25	44	27	1
A1	Saturated		2	-4	10	38	1
B3	Dry	Compost	1	2	4	25	6
B2	Fluctuating		3	1	6	44	11
B1	Saturated		1	1	11	38	3
C3	Damp	Star Carr	-4	-37	-26	26	-9
C2	Fluctuating		-8	-31	-42	23	-13
C1	Saturated		-8	-54	-39	13	-16

Mass loss data was obtained for all samples except those from zone C4, as masses were not recorded prior to burial (Table 5.5). Negative mass losses are indicative of mass gain. Similarly to bone buried in Star Carr peat, many of the modern wood sample have gained mass. This could be a result of taking up ions from the sediment. Whilst in bone samples this manifested as swelling of the samples, wood (particularly archaeological wood) is much more porous which may readily allow extraneous material to become incorporated into the voids within the structure (Hoffman & Jones, 1990).

Whilst mass loss analysis in wood is subject to a degree of error due to this porosity, it appears that higher mass loss occurred in microcosm A than B for modern samples, whilst the reverse was seen for archaeological material. It is possible that the greater mass loss in modern samples is due to cellulose loss, as analysis of both the Must Farm and Star Carr samples prior to burial revealed low cellulose content. The differences between the two microcosms may be linked to the potential presence of fungi indicated by the fibrous formations observed in microcosm A, as fungal attack is widely recognised as a major contributor to deterioration of both cellulose and lignin (e.g. Blanchette *et al.*, 1990; Kim & Singh, 2000).

Mass loss is also high in the Star Carr wood in all microcosms, and particularly so in microcosm C, in contrast to other samples where a mass gain is seen. It must be noted that this sample was extremely crumbly and some parts of it may not have been recovered in all cases. Despite

this, further analysis of this sample prior to burial showed that it was extremely degraded and contained a large abundance of crystals that have been interpreted as gypsum (Chapter 7). This may result in it being degraded much more readily than other samples, by both chemical and biological means.

5.3.3.2 FTIR spectroscopy

Analysis of all wood samples was carried out by FTIR. Analysis of the starting materials by FTIR showed that cellulose was already heavily depleted in both the Must Farm and Star Carr wood samples prior to burial. In the Star Carr starting material, splitting of the signal at 1240 cm^{-1} , (which relates to the C-O bond in the methoxy groups on the lignin sub-units) indicated defunctionalisation of the lignin, resulting in alteration of the methoxy environments (see Chapter 3 for further discussion). In the Must Farm sample prior to burial this peak was broadened with some slight splitting, which could also indicate some defunctionalisation, or could be due to slight differences in the FTIR spectra for different wood species (Pandey & Pitman, 2003). After burial in microcosms A and B, this peak is little altered in both modern and archaeological samples, signifying that deterioration of the lignin has not occurred to an extent that is observable by FTIR spectroscopy.

In all excavated modern wood samples, strong absorption peaks remain at both 1325 and 1375 cm^{-1} confirming the continued presence of cellulose. Excavated archaeological samples also still retain small peaks relating to cellulose, indicating that cellulose loss has been minimal over the 12 month burial period, in all zones (Figure 5.9). However, in lab-based experiments (Chapter 4), it was proposed that polymer degradation could have occurred but not been identified by FTIR as the degradation products remain *in situ* in the porous wood structure. This must therefore also be accepted as a possibility here.

In contrast, in the majority of both modern and archaeological samples from microcosm C zones 1, 2 and 3 (Star Carr), the complete disappearance of the peak at 1240 cm^{-1} indicates that methoxy groups have been completely removed from the phenolic units in lignin (Figure 5.9, top spectrum).

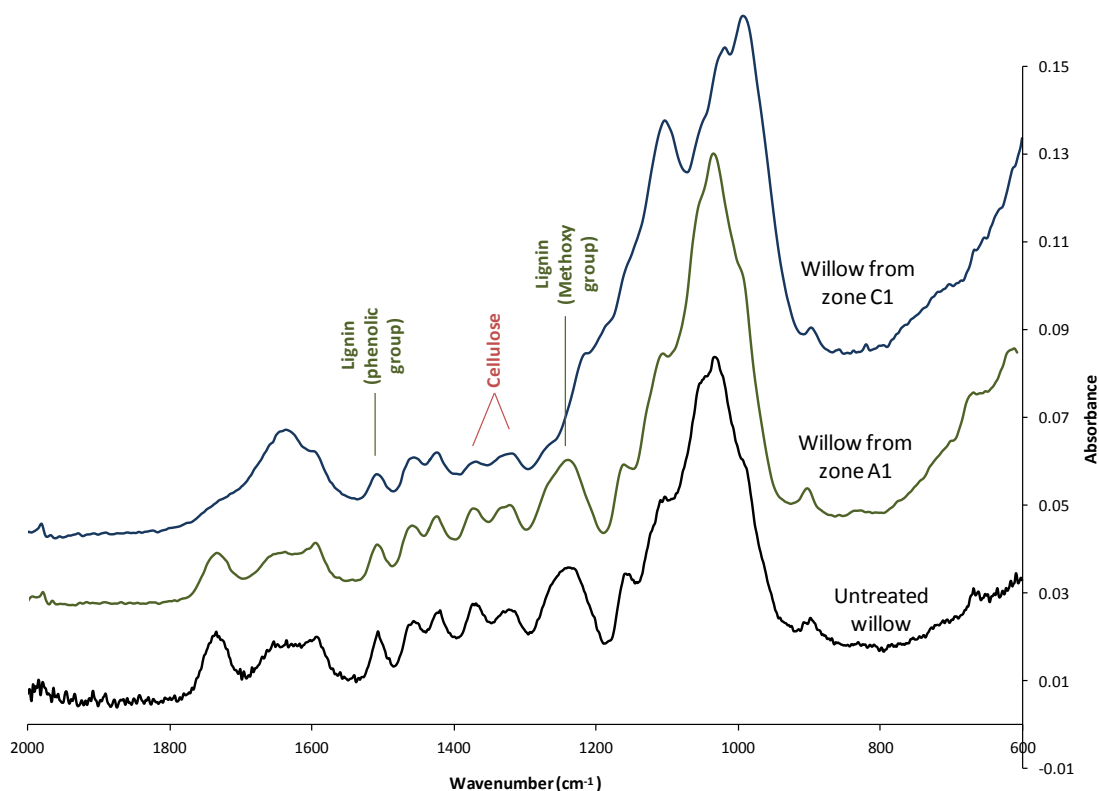


Figure 5.9: Comparison of FTIR spectra from untreated willow (bottom) and willow samples buried in zones A1 and C1. Note the complete loss of the methoxy signal at 1240 cm^{-1} in zone C1, although small cellulose peaks remain at 1325 and 1375 cm^{-1} . (Originally in colour).

Such alteration of the IR spectrum was also seen in the lab-based experiments, but only after 16 weeks incubation at 80°C in pH 1 sulfuric acid (Figure 4.15). This is in accordance with the measured pH of microcosm C ($< \text{pH } 1$). Cellulose is more easily degraded by biological attack than lignin; it is more accessible and more easily broken down by enzymatic activity, and this is the reason that increased lignin: cellulose ratios are often seen in archaeological woods (Hoffman & Jones, 1990; Gelbrich *et al.*, 2008). In microcosm C, where this defunctionalisation of lignin has occurred however, cellulose peaks are still detected, suggesting that biological activity has not been sufficient to result in complete loss of cellulose. This agrees with observations made regarding bone decay; ‘jellybone’ samples survived in microcosm C, suggesting little biological activity. It is therefore likely that this defunctionalisation is driven instead by chemical hydrolysis; this has been shown to occur with intense treatment in acid or alkali due to oxidation (Adler, 1977).

Alternatively, decay could have been caused by white-rot fungi, which is rarely found in waterlogged environments, but preferentially decays lignin rather than cellulose (Hedges, 1990; Pandey & Pitman, 2003). Physical evidence for white-rot fungi was potentially seen in the form of fibrous strands adhering to the surface in several samples from microcosm A (Section 3.3.1).

A number of ratios have been determined as indicators of decay. These are, an increase in lignin: cellulose and 1507: cellulose ratios can indicate cellulose loss, whereas an increase in the ratio of the two lignin peaks, 1507: 1240, signifies lignin defunctionalisation (Figure 5.10). For the microcosm C samples, this final ratio cannot be determined due to the loss of the peak at 1240 cm^{-1} . In addition, the lignin: cellulose value will be distorted by the absence of the 1240 cm^{-1} peak. Comparison of the 1507: cellulose ratio confirms that cellulose loss in microcosm C samples is within the expected error, corroborating the hypothesis that lignin defunctionalisation is occurring without significant cellulose depletion.

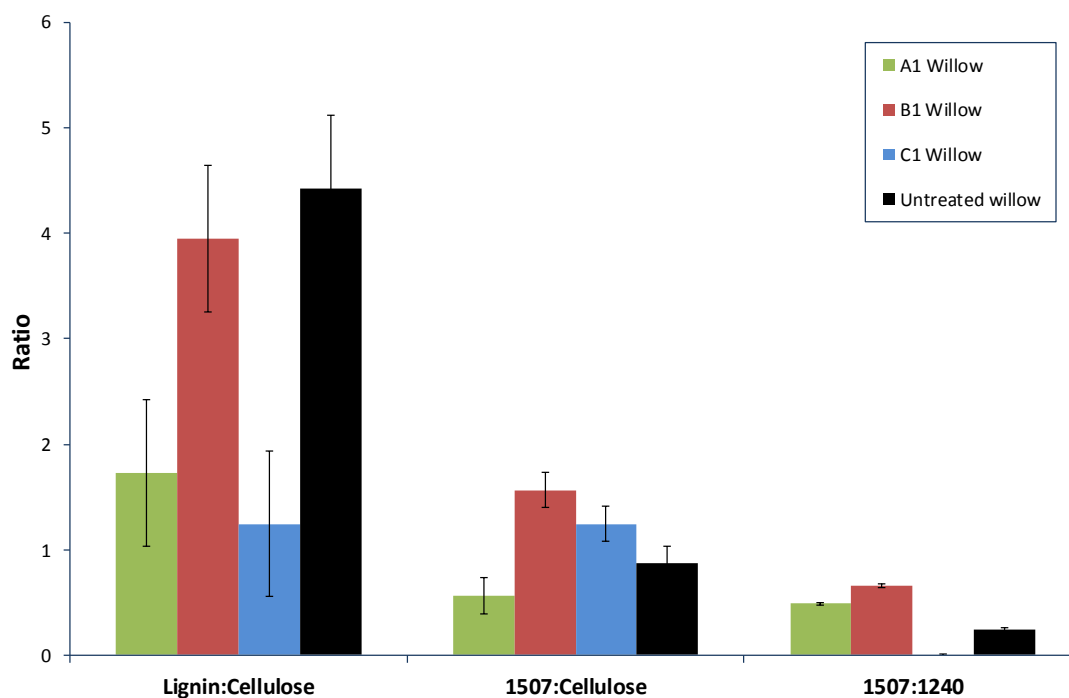


Figure 5.10: Plot of peak height ratios indicating degradation parameters for willow samples excavated from zones A1, B1 and C1 compared to an untreated willow sample. Error bars are the standard deviation of three measurements of a modern willow sample. An increase in Lignin: Cellulose and 1507: cellulose ratios is indicative of cellulose loss, and an increase in 1507: 1240 ratio suggests lignin defunctionalisation. (Originally in colour).

In contrast, the 1507: cellulose ratio in the A1 samples is low; this suggests that lignin is being preferentially degraded in microcosm A1 and lends further evidence to the presence of white-rot fungi (Hedges, 1990).

5.3.3.3 Py-GC

FTIR analysis of the samples from microcosm C indicated that defunctionalisation of the lignin had occurred in all of the wet or damp zones. In order to investigate this further, py-GC was carried out on all willow samples from zones C1 – 4 (Figure 5.11). Due to the short time-scale of the experiment, analysis was carried out on sub-samples taken from the surface of the samples (rather than through a cross section) and therefore represents surface degradation.

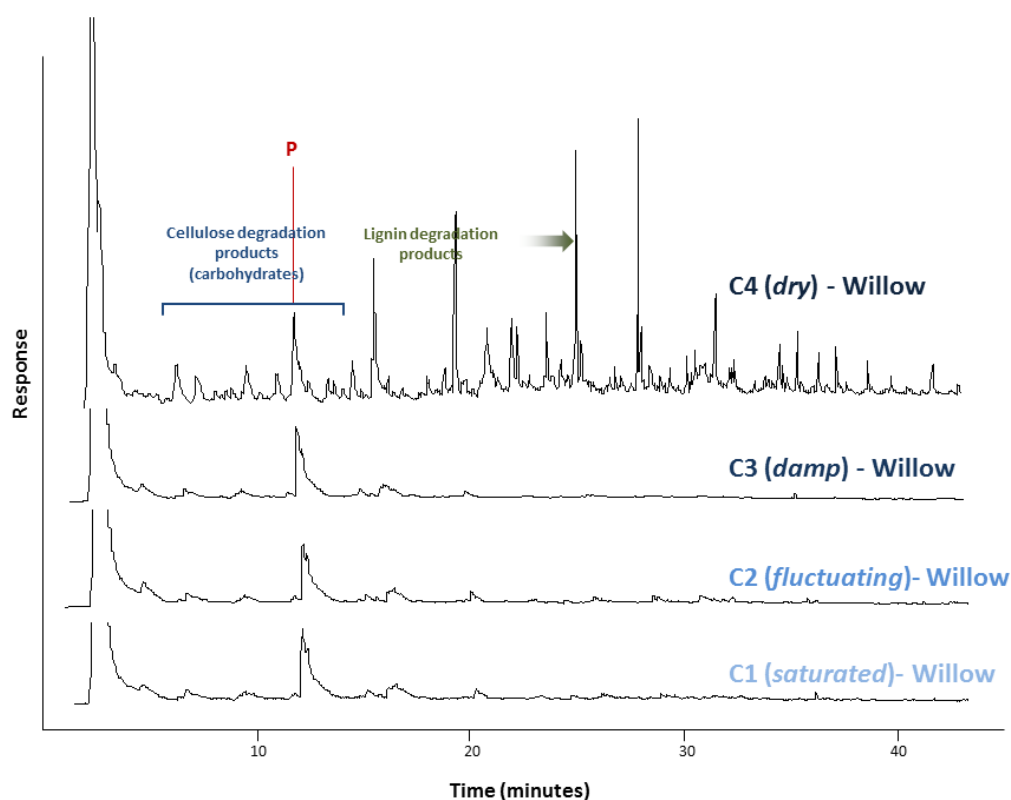


Figure 5.11: Py-GC traces from all four zone C (Star Carr) willow samples, showing extensive degradation of all samples in damp or wet zones. (Originally in colour).

The lack of peaks eluting later in the chromatograms confirm extensive degradation of lignin in those samples retrieved from zones that were wet or damp; this confirms FTIR analysis where loss of the absorption peak at 1240 cm^{-1} indicated that lignin had been completely defunctionalised. The relatively intense peak at approximately 11 minutes has been assigned with the use of standards as phenol. This indicates that although lignin has been chemically altered, the main phenolic structure remains, probably explaining why no loss of macroscopic structure was observed as lignin is the main source of mechanical strength in wood (Martinez *et al.*, 2005). In addition analysis was carried out only on the surface and it is likely that lignin remains in the rest of the sample.

In contrast to FTIR analysis, py-GC analysis also indicates that cellulose is no longer present in the surface of samples C1 – 3. This is in agreement with results from lab-based experiments (Chapter 4), where cellulose was also visible under SEM and by analysis by FTIR but shown to be depleted upon analysis by py-GC. A possible explanation is that cellulose is being broken down but remaining *in situ*; as FTIR is carried out with no sample preparation degraded cellulose may still be observed, as opposed to in py-GC where non-structural components are first removed by heating at 290°C. Phenol content and P: G ratios were not calculated for the lab-based burial experiments, as no guaiacol peak could be found in the traces for zone C1-3 samples and an increase in phenol content was obvious.

The survival of both polymers in the C4 willow sample, as well as willow samples analysed from zones A1 and B1, was indicated by py-GC. This is in agreement with FTIR analysis and visual assessment of the samples, where little change was observed. The traces from willow samples C4, B1 and A1 are shown in Figure 5.12.

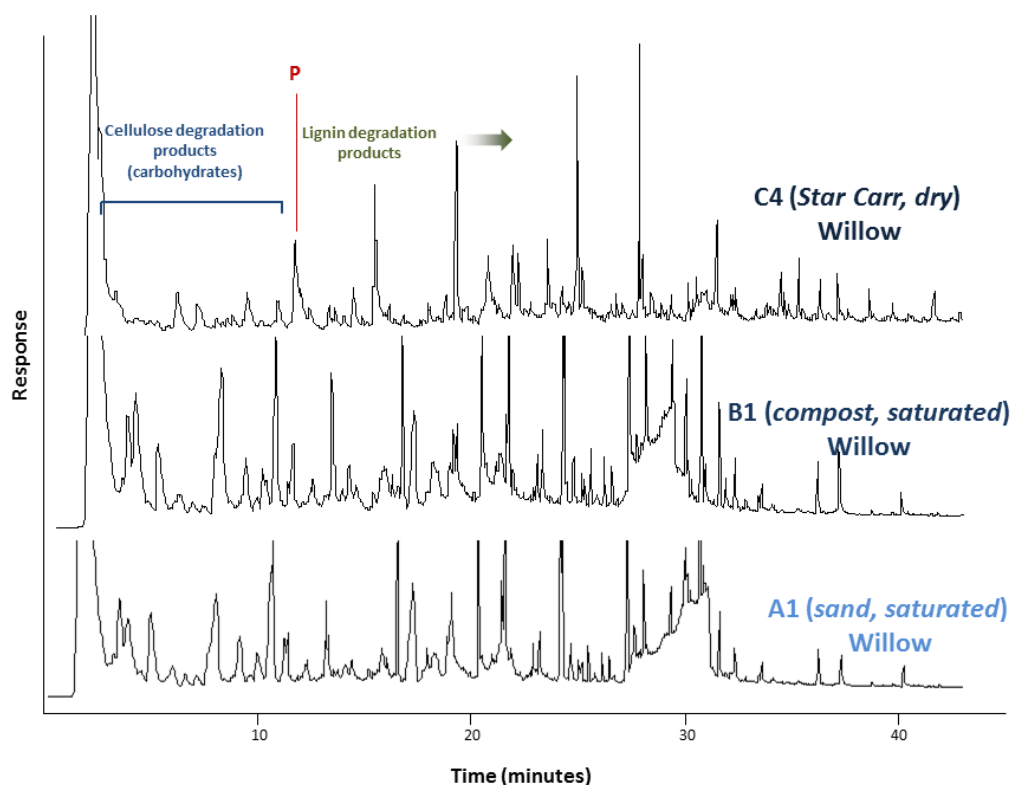


Figure 5.12: Comparison of py-GC traces for willow samples recovered from zones A1, B1 and C4. (Originally in colour).

In sample C4, cellulose loss and a relative increase in phenol is apparent, suggesting chemical alteration of the lignin, although it has not occurred to the same extent as in samples from wet or damp environments. This again highlights the important role that groundwater plays in aiding chemical reactions in burial environments (e.g. Hedges & Millard, 1995).

5.3.3.4 Microscopy

SEM imaging was carried out on several wood samples with the aim of identifying any extensive evidence of fungal activity and obvious histological alteration. Again, analysis was carried out on the outermost surface of the samples.

Evidence of fungal activity was observed in several of the samples analysed, including those from zones C1 and C2 (Figure 5.13, right), where it had been hypothesised that the low oxygen content and low pH may suppress biological activity. However, some studies do show that certain types of fungi can adapt to extreme conditions (e.g. Highley & Kirk, 1979; Blanchette *et al.*, 1990). It is also possible that this activity developed post-excavation, as samples were analysed several weeks post-excavation, to allow for air drying of the samples.

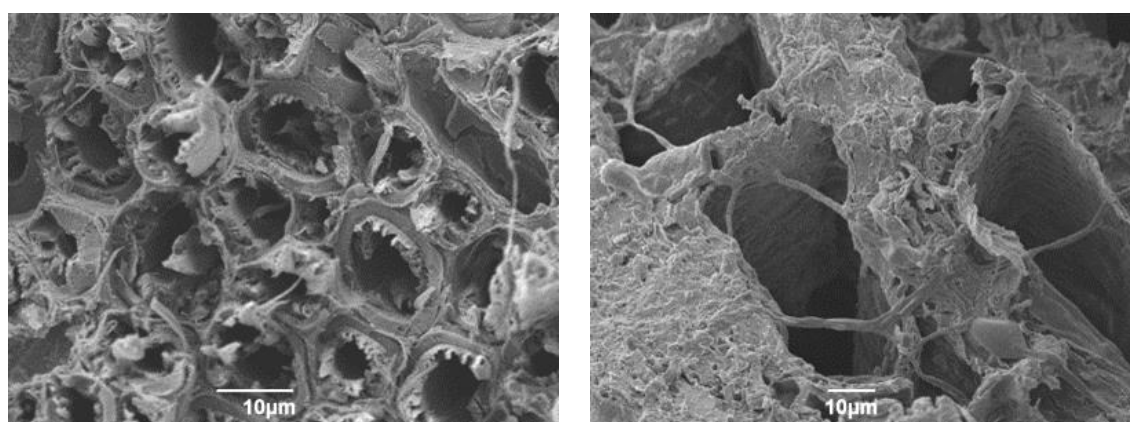


Figure 5.13: SEM images of wood samples retrieved from microcosm C. Oak from zone 1 shows potential degradation of the inner cell walls (left) and Must Farm wood from zone 2 shows evidence for fungal activity (right).

In the C1 oak sample (Figure 5.13, left) cell walls still appeared thick, suggesting that the cellulose rich secondary cell walls are still present; however, in places it appears that the cell walls may be coming away from the outer, lignin-rich cell walls. This is suggestive of early stages of degradation (e.g. Blanchette *et al.*, 1990). A similar appearance in an archaeological wood sample is reported by Florian (1990), where it has been interpreted as swelling of the secondary cell walls due to early stages of degradation, resulting in the separation from the primary cell walls. This was also observed in lab-based experiments in acid only (Chapter 4), where it was interpreted as degraded cellulose remaining *in situ*. Indeed, the fact that cellulose could be detected by FTIR, where no samples preparation was carried out, but not by py-GC, where samples were cleaned prior to analysis, is supportive of this hypothesis.

5.3.3.5 Summary of wood analysis

Analysis of wood samples from the microcosm experiments shows primarily that wood deterioration in sand and compost was only in very early stages within the 12 month period; both FTIR and py-GC analysis showed that deterioration of the polymeric structure was not advanced, and samples retained the morphological characteristics of wood. In contrast, in microcosm C (Star Carr peat) zones 1-3 and, to a lesser extent, zone 4, lignin had been defunctionalised and cellulose depleted. This indicates either that biological activity had occurred or that degradation had occurred due to chemical processes. Lignin defunctionalisation occurs primarily by fungal activity (Martinez *et al.*, 2005); however, at the low pH and expected anaerobic conditions in the wet zones of microcosm C, fungal activity would be expected to be severely suppressed (e.g. Blanchette, 2000; Kim & Singh, 2000). In addition, no conclusive evidence for biological activity was seen in microcosm C, in contrast to microcosm A where long fibrils adhering to the surface of wood samples is suggestive of fungal activity. Therefore, chemical deterioration offers the most likely explanation. That these processes occurred within 12 months highlights that the conditions at Star Carr are not conducive to the preservation of archaeological wood. This is in contrast to assessment using lab-based experiments where it was concluded that wood was at much lower risk from acidification than bone.

5.4 Discussion and conclusions

Conducting burial experiments under lab controlled conditions aimed to introduce a number of variables that are potential factors contributing to diagenesis, which were not accounted for in the lab-based experiments reported in Chapter 4. Primarily, this experiment aimed to achieve regions in different soils with different levels of oxygen content, which is likely to be related to microbial activity. Unfortunately, a number of practical difficulties resulted in a failure to confidently establish three distinct zones in each microcosm. In addition, the experiment was carried out over a relatively short period in comparison to the archaeological time-scale. Despite this, several observations were made from analysis of the material that has furthered our understanding of organic deterioration in the unique geochemical conditions at Star Carr.

Biological activity was indicated by the presence of long fibres (potentially fungal hyphae or filamentous bacteria; Buscot & Varma, 2005) in several wood samples in microcosm A, and possibly confirmed by the complete loss of demineralised bone ('jellybone') samples in aerated zones of microcosms A and B. However, visual evidence for biological deterioration of both wood and bone was not identified in microcosm C. This is not surprising, as few micro-organisms can thrive at such harsh pH (e.g. Russell & Dombrowski, 1980; Beales, 2004). This tentatively indicates that, although it is likely to occur at low levels, biological activity is not a major influence on the rate of deterioration of organic artefacts at Star Carr.

Despite the apparent absence of biological activity, alteration of both the cellulose and lignin in wood were detected by FTIR and py-GC analysis in microcosm C (Star Carr peat). This indicates that chemical deterioration is more of a factor in wood degradation than estimated by lab-based experiments in acid only (Chapter 4). The low pH at the Star Carr site may therefore contribute to accelerated decay of wood, particularly if the acidity were to increase.

Evidently, chemical decay of both bone and wood proceeded rapidly in microcosm C where conditions were damp or wet; the transformation of HA to gypsum and the defunctionalisation of lignin within the 12-month period illustrates how destructive the geochemical conditions at Star Carr are. This demonstrates that any remaining archaeological material still buried at the Star Carr site is at risk of rapid deterioration, primarily due to the high acidity.

Aside from the acidity, results indicate that the water content of the sediments plays an important role in facilitating organic deterioration. In the dry zone in microcosm C, neither bone nor wood deterioration was as advanced. This is likely to be because the presence of groundwater allows faster exchange between the burial environment and organic remains

(Hedges & Millard, 1995). The absence of deterioration in the dry zone is also further evidence that deterioration was driven primarily by chemical rather than biological processes; in the most aerated zone, more biological activity may be expected.

Microcosm experiments have added considerably to the lab-based experiments, showing that whilst site acidity may be a major factor in causing deterioration of organic material (particularly bone), other factors such as interaction with the groundwater and biological activity need to be considered. However, both lab-based approaches have considered conditions that do not fully represent conditions at the Star Carr site. In particular, hydrological effects (the movement of water through the archaeological zone) are likely to have a major impact on the rate of deterioration; analysis of wood has shown that cellulose may degrade but remain *in situ*. In a stagnant environment therefore, degradation may not be as advanced as in one with a dynamic hydrology which may wash out degradation products. In addition, transformation of the HA in bone to gypsum may not have the opportunity to proceed in a real burial environment, where recrystallization does not have chance to occur. Therefore, further burial experiments have been carried out *in situ*, providing the best possible representation of actual burial conditions at the Star Carr site (Chapter 6).

CHAPTER 6

IN SITU BURIAL EXPERIMENTS

6.1 Introduction

Lab-based experiments, such as those carried out in sulfuric acid (Chapter 4) and microcosms (Chapter 5), provide a controlled environment in which to investigate selected factors contributing to degradation. In reality however, a large number of biological and chemical factors will combine to contribute to diagenesis in an archaeological context (e.g. Gordon & Buikstra, 1981; Hopkins, 1996; Caple, 2004).

In situ burial experiments aim to replicate diagenesis in an environment that is as close to the archaeological environment as possible, and the benefits of such experiments are demonstrated by a number of published studies. Notable long term examples include 'The taphonomic bog-body project': carried out in Scandinavian peat bogs (e.g. Turner-Walker & Peacock, 2008), and a 33 year burial experiment to study bone degradation at regular intervals at Wareham, Dorset (Crowther, 2002). Both have widened our understanding of the rate at which bone deteriorates in an archaeological context.

Burial experiments are often also carried out alongside conservation projects in order to monitor organic deterioration. One example is an *in situ* experiment carried out during re-watering of the Iron Age site of Fiskerton, where a series of both modern and archaeological bone samples were buried at varying depths (Williams *et al.*, 2006; Chapter 1 Section 1.4.5.3). The aim of this was to assess whether raising the water-table would impact positively on organic preservation at the site. Similarly, whilst assessing the practicality of preservation *in situ* of Bronze Age wood at Flag Fen, a series of modern wood samples were buried and re-excavated periodically (Powell *et al.*, 2001). Assessment of microbial deterioration in those samples served as an indicator for potential risks from biological activity to the rest of the site.

A 7-year study by Nicholson (1996; 1998) aimed to further understand the contribution of the nature of the burial environment to bone deterioration, and included sites at a range of different acidities (the lowest being measured at pH 3.2 - 4.5). It was concluded that bone diagenesis is not solely dependent on soil pH and can differ greatly depending on the specific conditions of the burial environment, which can vary very locally. Crowther (2002) also concluded from long term burial experiments in different soil types, that factors which have an influence on the rate of leaching of phosphate from buried bone (such as soil type and groundwater percolation) contribute significantly to the rate of diagenesis, along with pH. Hedges & Millard (1995) also discuss how site hydrology is a key factor in bone diagenesis.

Whilst these previous studies have provided a large amount of data and greatly advanced our understanding of the effects of the burial environment on organic preservation, they have also

highlighted the fact that burial conditions must be considered on a site-by-site basis (e.g. Caple, 1994; Nicholson, 1998). In this study, site hydrology has been accounted for in part by the use of 'dynamic' and 'stagnant' conditions in lab-based burial experiments (Chapter 4). Without thorough monitoring data it is impossible to accurately replicate exact site hydrology without conducting an in-field burial experiment. The occurrence of two successive field seasons at Star Carr provided the opportunity to conduct *in situ* burial experiments for a period of 12 months at the site, as well as at another site located around prehistoric Lake Flixton (Flixton Island site 2).

The burial period used here represents only a very short time in comparison to the majority of burial experiments described in literature, and it is unlikely that environmental conditions in only 12 months would have been representative of the average conditions to which archaeological materials have been exposed. However, it was hoped that by applying the analytical techniques described in Chapter 3, it would be possible to identify any small changes evident in the early stages of diagenesis. Data obtained from *in situ* burial experiments can also be correlated with lab-based studies in order to further understand the specific nature of the organic diagenesis at the Star Carr site. In addition, burial experiments allow an assessment of whether lab-based studies appropriately address the preservation problems seen at the site.

6.2 Experimental

6.2.1 Materials

6.2.1.1 Pilot study

Prior to this research studentship, a pilot burial study was initiated in the summer of 2007, in a test pit located to the north of Star Carr (SC29; Section 6.2.2.1). Pig rib bone and chicken legs were buried at varying depths into the excavated wall of the trench (Needham, pers. comm.). Unfortunately, no record exists as to how each bone was treated, but it is thought that most of these were cooked, and that both fleshed and de-fleshed samples were included in the study. No wood samples were included. Permission was granted for this material to be analysed part of this PhD studentship. Samples were re-excavated and analysed in 2012, and the results reported here.

6.2.1.2 Main study

In the 12-month burial experiments conducted as part of this study, both bone and wood samples were buried. The experiment was designed to be comparable to the lab-based burial experiments (Chapter 5), although some limitations were imposed due to the availability of materials. Cooked bone was included in order to allow a comparison with the pilot study, as well as to enable a preliminary assessment of the differing behaviour of cooked and uncooked bone. Due to the short time-scale, all bones were de-fleshed by scraping as much as possible, although the uncooked sheep rib did have some flesh adhering to the surface on burial.

6.2.1.2.1 Material buried in SC29 (4 wood types, 6 bone types)

An asterisk denotes samples that are directly comparable to the lab-based burial experiments (Chapter 5)

*Modern oak and willow, approximately 5 cm³ pieces of trunk, cut using a band saw

*Must Farm (Bronze Age) wood (ash), approximately 5 cm³ section, dried

*Star Carr wood (unidentified, probably willow), approximately 3 cm³ piece from a split timber plank excavated in 2007. Dried and sewn into netlon bag

*Star Carr rib bone excavated in 2010 (sample number 92424) 'robust' in appearance. Sliced into approximately 5 cm lengths using a water-cooled band saw, sewn into netlon bag

*Modern artificial 'jellybones': sheep long bone and rib, obtained from a butcher. De-fleshed and sliced using a water-cooled band saw. Demineralised in 0.6 M HCl for 1 week, sewn into netlon bags

Roasted pig tibia and rib, kept whole and de-fleshed

*Raw sheep rib, obtained from butcher, kept whole and slightly de-fleshed

6.2.1.2.2 Material buried at Flixton Island (4 wood types, 6 bone types)

*Modern oak and willow, approximately 5 cm³ pieces of trunk, cut using a band saw

*Modern birch, branch of approximately 2 cm diameter, cut into approximately 10 cm lengths

*Star Carr wood (unidentified, probably willow), approximately 3 cm³ piece from a split timber plank excavated in 2007. Dried and sewn into netlon bag

*Star Carr rib bone excavated in 2010 (sample number 92373) 'robust' in appearance. Sliced into approximately 5 cm lengths using a water-cooled band saw, sewn into netlon bag

*Modern artificial 'jellybones': sheep long bone and rib, obtained from a butcher. De-fleshed and sliced using a water-cooled band saw. Demineralised in 0.6 M HCl for 1 week, sewn into netlon bags

Roasted pig tibia and rib, kept whole and de-fleshed

*Raw sheep rib, obtained from butcher, kept whole and slightly de-fleshed

6.2.2 Burial locations

6.2.2.1 SC29

The 'jellybone' excavated in 2007 (described by Milner *et al.*, 2011a) was discovered in a small test pit known as SC29 located in a field to the north of the Star Carr site (Figure 6.1; National Grid Reference: 502912 4881161). SC29 was also the location of the pilot burial experiment carried out in 2007 by Needham (2007). Sediment analysis at the time of the pilot burial indicated that the pH of this test pit was around 3.5, similar to that of parts of the Star Carr site (A. Needham, *pers. comm.*). The deposits in SC29 consist of a peat layer up to a metre thick, overlying pre-Holocene sediments of gravel and sand (Boreham *et al.*, 2011). In SC29, as well as parts of the Star Carr site, a grey clay lens lies between the peat and the gravel at a depth of approximately 80 cm below ground level. Higher pH has been observed in this clay, indicating buffering of acidity (Boreham *et al.*, 2011). SC29 is waterlogged from a depth of approximately 70 cm below ground level, and therefore 3 different horizons were identified: dry, possibly fluctuating, and waterlogged (Figure 6.3).

6.2.2.2 Flixton Island

Flixton Island site 2, located to the east of Star Carr (Figure 6.1; National Grid Reference: 503575 481170) was used as a control site. Previous excavations at the site are largely unpublished, but site reports show that poorly preserved, crumbly bone has been recorded (Milner & Taylor, 2012). Similarly to Star Carr, deposits consist of peat overlaying gravel, although the peat layer is much thinner and much of the archaeology is contained within the

gravel rather than the peat. No clay layer separates the two (Figure 6.2 & Figure 6.3). Measured pH values at the time of burial were approximately neutral (Figure 6.3). The water level at Flixton Island site 2 was not reached during excavations, and therefore only two hydrological zones were identified: dry, and possibly fluctuating.

In the absence of extensive hydrological data for both burial sites, the defined hydrological zones are an estimate. However, the weather over the 12-month period (September 2012 – September 2013) was characterised by heavier rainfall as well as slightly warmer temperatures (approximately 0.6°C warmer) than usual for the North East of England (metoffice.gov.uk). This suggests that the height of the water-table would have been similar to (or higher than) observed during burial, for much of the experimental burial period.



Figure 6.1: Map showing approximate geographical location of both burial sites in relation to Star Carr. National Grid locations are shown. (Originally in colour).

6.2.3 Method

6.2.3.1 Burial

Turner-Walker & Peacock (2008) emphasise the problems regarding the introduction of the burial samples into the burial environment; this should be achieved with minimum disturbance. At Star Carr, this is even more critical, as highly reactive sediments have been identified at the site, and pH has been shown to alter rapidly upon exposure to oxygen (Boreham *et al.*, 2011; Chapter 2 Section 2.3.3.1). A few studies have reported a method where the samples are contained in a plastic tube and pushed vertically into the ground (e.g. Turner-Walker & Peacock, 2008; Williams *et al.*, 2006). However, it was decided that due to the short time-scale of the experiment, samples should be in direct contact with the soil to maximise degradation.

For both the pilot and main study, samples were pushed directly into the face of the excavated trench at intervals of approximately 10 cm (Figure 6.2). The aim of this was to minimise exposure of the sediments, thus reducing oxidation.



Figure 6.2: Photographs of material buried during the pilot study at varying depths in SC29 (left) and at two levels at Flixton Island for the 12 month study (right). Note the water-table visible at the base of SC29. Depths are approximate. (Originally in colour).

In the pilot study, two columns of samples were buried at various depths. For the main study, three sets of material were buried into the wall of the re-excavated test-pit SC29 at depths of 92 cm, 50 cm and 30 cm below the ground surface. At Flixton Island site 2, two sets were buried, at 60 cm and 30 cm into the face of a trench already excavated. Small or vulnerable samples were sewn into netlon bags prior to burial to aid with retrieval. During burial, pH analysis of the sediments was carried out according to as outlined in Chapter 2 (Section 2.3.2.1) and shown in Figure 6.3.

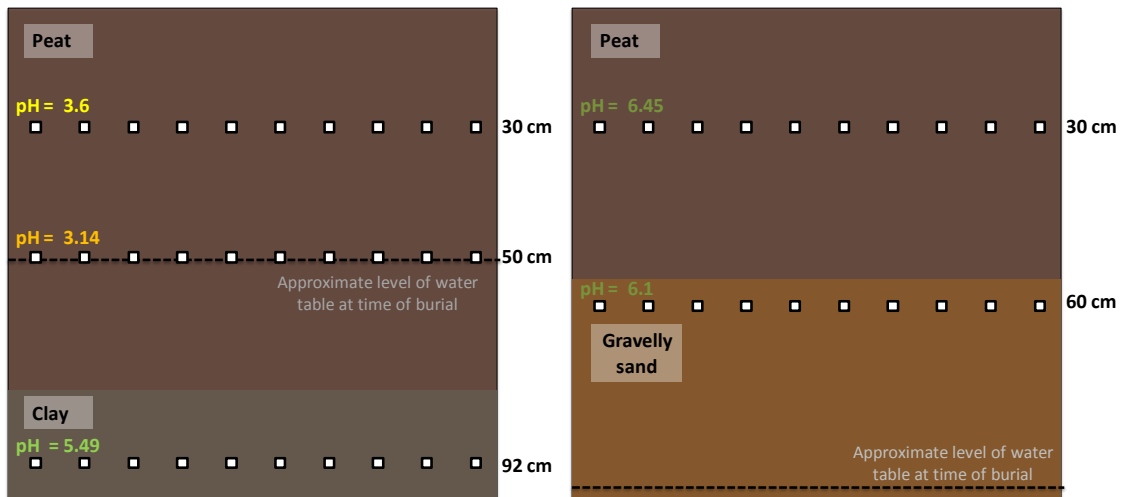


Figure 6.3: Schematic showing location of samples buried for the 12 month study at SC29 (left) and Flixton Island (right). pH values recorded at time of burial are indicated. (Originally in colour).

6.2.3.2 Excavation

All samples were retrieved by hand by re-excavating a portion of the trench and carefully digging into the trench wall. All samples were kept at 4°C until required for analysis.

Upon excavation, sediment pH and redox was again recorded adjacent to the samples.

6.2.3.3 Analysis

All samples were accurately weighed and photographed prior to burial to allow mass loss and visual analysis. Analysis of the organic materials was carried out according to methods outlined in Chapter 3.

6.3 Results and discussion

6.3.1 Sediment analysis

6.3.1.1 pH and redox analysis

Held field probes (HI-98121 pH and ORP pocket probe, Hanna Instrument) were used to measure both soil pH and redox potential on site prior to burial of material, according to the method described in Chapter 2 (Section 2.3.2.1). The pH was recorded adjacent to the burial material at both sites and in additional locations in SC29, and then measured on the same samples after 24 hours storage at 4°C using a calibrated glass pH probe (Denver Instrument) (Table 6.1). Although the sediments at SC29 are very acidic in comparison to those from Flixton Island, the lowest pH recorded at SC29 (2.86) does not reach quite as high acidities as some areas of Star Carr, which have been reported to have a pH as low as 2.5 (Boreham *et al.*, 2011; Chapter 2).

Table 6.1: Measured pH and redox values at both burial locations at the time of burial.

Depth (cm)	Flixton Island			SC29		
	pH in field	pH + 24 hours	Redox (mV)	pH in field	pH + 24 hours	Redox (mV)
30	6.45	6.67	167	3.60	3.38	220
50				3.14	3.01	229
60	6.10	6.19	168	3.27	3.36	259
70				2.86	2.76	283
80				3.74	3.67	236
90				5.49	5.52	17

The reasons for the high acidity at Star Carr are discussed in more detail elsewhere (Chapter 2). In brief, it is believed to arise via oxidation of sulfide according to Equation 6.1 (Dent & Pons, 1995; Boreham *et al.*, 2011).

Equation 6.1: Oxidation of iron sulfide (pyrite) to acid sulfates.



Boreham *et al.* (2011) reported a change in pH in soil samples from Star Carr analysed both in field and after 24 hours. Samples here were analysed with a different pH probe after 24 hours, which may account for some discrepancies. However, similar trends were seen to those reported by Boreham *et al.* (2011); a slight decrease in pH after exposure to oxygen was observed in the most acidic samples from SC29, thought to be due to the continued oxidation of remaining sulfides upon exposure. Boreham *et al.* (2011) suggested that such a small decrease may be indicative that almost complete oxidation to sulfates had already occurred. In contrast, sediments from the upper, more neutral layer, undergo a slight increase in pH after 24 hours. A potential explanation for this was proposed by Boreham *et al.* (2011); 'liming' of the soils in agricultural processes could lead to the neutralisation of acidic sulfates by gypsum formation (Chapter 2, Section 2.4.1.1).

Studies where redox readings have been taken alongside water-level monitoring suggest that it serves as a good indicator for waterlogging (e.g. Brunning *et al.*, 2000). Patrick & Mahaptra (1968) define sediments with a redox potential < 100 mV as reducing and > 400 mV as oxidising. In between these values the higher the redox value the more oxidising, or aerobic, the sediments. However, in acidic soils the redox potential is also increased by the presence of acids, which are also highly oxidising (Atkins *et al.*, 2006), and as such does not necessarily equate to oxygen content.

All redox measurements at both SC29 and Flixton Island suggest that the sediments are moderately oxidising, indicating that both burial locations are aerobic. An exception is the base of SC29 (90 cm) where low redox potential implies that oxygen levels are low, possibly due to extended periods of waterlogging. Due to the rate at which the sediments at Star Carr have been observed to oxidise on exposure to oxygen, this may explain the high acidity in the upper regions of SC29 (Equation 6.1). Redox values measured at Star Carr in 2009 were often > 400 mV, implying that sediments across the site may be more oxidising, and therefore more acidic, than represented by SC29 (Boreham *et al.*, 2011).

6.3.1.2 Sulfur content analysis

Soil samples adjacent to each set of burial material, as well as in additional locations in SC29, were collected upon burial of the material, and analysis of carbon, nitrogen, hydrogen, and sulfur content performed as outlined in Chapter 2 (Section 2.3.2.2). Percentage compositions are presented in Table 6.2.

Table 6.2: Percentage values of sulfur and carbon in sediment samples from varying depths at Flixton Island and Test pit SC29.

Flixton Island			SC29		
Depth (cm)	% Sulfur	% Carbon	Depth (cm)	% Sulfur	% Carbon
30	0.2	34.8	30		
45			45	5.8	40.3
60	0.5	36.9	50	1.6	41.4
70			70	9.9	21.1
80			80	15.0	23.6
92			92	4.1	5.8

As the formation of sulfuric acid is hypothesised to be the cause of high acidity at Star Carr, it was expected that high sulfur concentrations would be found, and this is the case in SC29. Typically, soils have a sulfur content of 0.005 – 0.05 % (50 – 500 ppm) (Steinburgs *et al.*, 1961). Sulfur content of peat is often elevated, but considered high when around 1% (1000 ppm) (Brown, 1985). Based on this, it is clear that sulfur content in SC29 is high throughout the profile, particularly in comparison to Flixton Island, despite its geographical proximity.

The increasing concentration with depth (up to 80 cm) may suggest that the source of sulfur is from underlying deposits rather than sources from above, such as rainwater or agricultural activities. This is consistent with the hypothesis presented by Boreham *et al.* (2011) of a “sulfur pump” system where sulfur from underlying mineral deposits rises and gets trapped above the underlying clay lenses. This may also explain why concentrations of sulfur are lower in the bottom layer, as the clay-like consistency could mean that sulfur-rich groundwater is trapped above it. The difference between the two sites also supports the theory that these mineral

deposits occur in small outcrops around the Star Carr site and do not underlie the Flixton Island site (Boreham *et al.*, 2011; Brown *et al.*, 2011).

6.3.2 Bone analysis

6.3.2.1 Pilot study in SC29

6.3.2.1.1 Visual analysis

Six bones were retrieved in total after approximately five years of burial, out of an estimated initial 10. The visual appearance of each is summarised in Table 6.3 and Figure 6.4. The first sample was found at a depth of 50 cm, at which point groundwater also appeared in the trench, indicating waterlogging. It is believed that another layer of samples were buried above this, but these were not retrieved. It is not possible to say whether this is due to complete degradation of the samples or a failure to locate them, although the high acidity of the soil suggests that complete loss of the bone could have occurred. The sample at 50 cm was barely recognisable as bone and only fragments of material were retrieved by sieving in a 400 µm metal mesh. Other samples from the top and middle of the trench were easily bent, suggesting HA has been lost. Bones retrieved from the lower layers were fairly robust in contrast, potentially because of the more neutral recorded pH leading to the loss of less HA due to buffering.

Table 6.3: Visual analysis of samples retrieved from Test pit SC29 after five years burial.

Sample	Description	pH
Column A, 50 cm depth	Only very small fragments recovered by sieving – not certain to be bone	3.12
Column A, 70 cm depth	Very bad preservation, easy to bend suggesting high mineral loss. Stained dark brown	3.27
Column A, 92 cm depth	Good preservation upon excavation, although an orangey colour appeared soon after recovery	5.49
Column C, 45 cm depth	Discolouration, very easy to bend suggesting mineral loss	3.12
Column C, 68 cm depth	Less discolouration but also easy to bend	3.27
Column C, 85 cm depth	Excellent preservation, almost no visual deterioration other than discolouration. Very robust	5.49



Figure 6.4: Photographs of six samples retrieved from pilot study in 2007 after approximately 5 years burial. (Originally in colour).

6.3.2.1.2 Amino acid analysis

Analysis was carried out as described in Chapter 3. Where the retrieved samples were big enough to do so, sub-samples were taken from both the outermost, exposed surface of the bone and the inside,.

The relative amino acid compositions of all samples are characteristic of collagen, confirming that they are bone. In the two samples recovered from the base of the trench (A 92 cm and C 85 cm) as well as column C at 45 cm, a slight increase in relative concentration in the outer section (when compared to the untreated chicken bone) indicates that HA has been lost (Figure 6.5). However, in samples A at 50 cm and C at 68 cm, a significant reduction in the amino acid concentration indicates that collagen may have broken down and been leached from the bone.

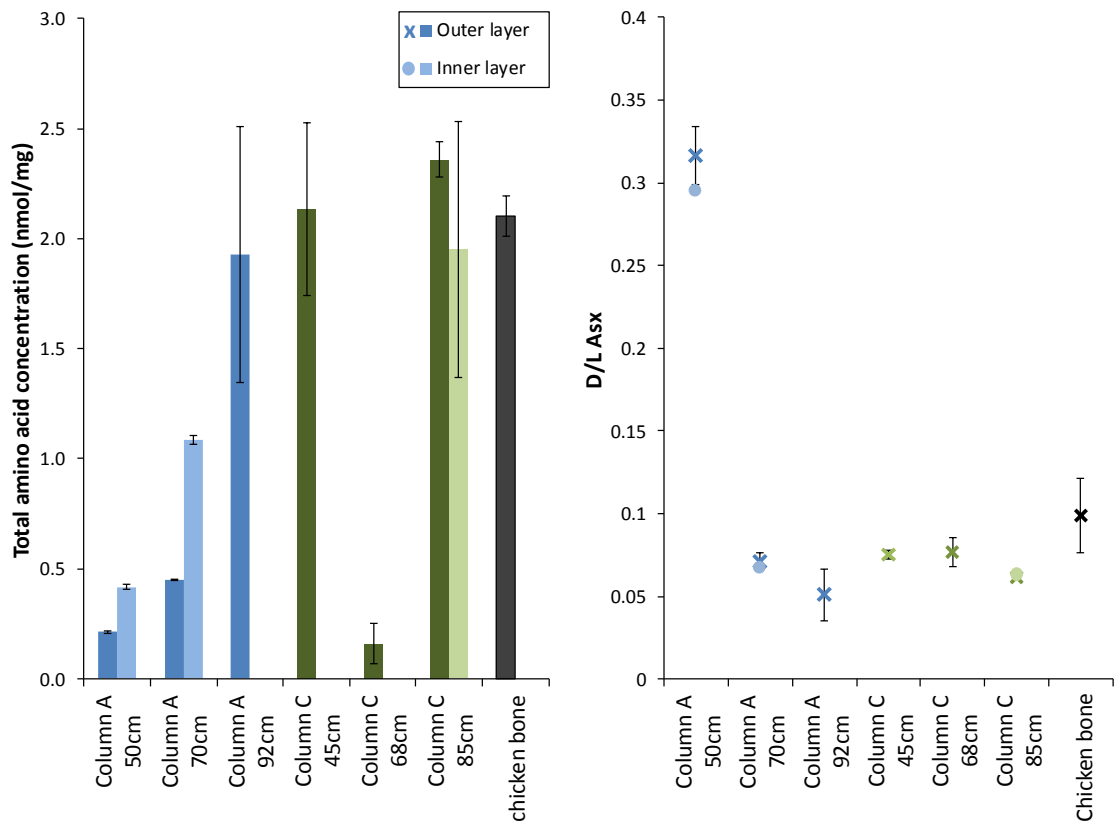


Figure 6.5: Comparison of total amino acid content for all excavated bones, compared to a modern cooked chicken leg bone (left) and Asx racemisation values in all excavated bones (right). Error bars are one standard deviation calculated from replicate analysis. (Originally in colour).

Despite the reduction in total amino acid concentrations seen for most of the bones in the uppermost, acidic zones of the trench, Asx racemisation is only elevated outside the margin of error of the modern reference sample (chicken bone) in the one sample: A at 50 cm. This corroborates the hypothesis that a reduction in total amino acid concentration has occurred, and suggests that the collagen triple helices have broken down to some extent. Due to their jelly-like appearance and reduced total concentrations, we may have expected to also see an increase in Asx racemisation for C at 68 cm and A at 70 cm, whereas despite a clear reduction in amino acid concentration, no racemisation is observed in the sample. In lab-based experiments (Chapter 4) however, samples that developed a translucent, jelly-like texture also had only slightly elevated racemisation levels at room temperature despite having D/L values of over 0.5 at 80°C. This suggests that racemisation is too slow to observe on this timescale at these low temperatures. An alternative explanation for the low observed D/L in Asx is that as the samples were located in the region of the water-table, fluctuating water may have resulted in degraded fragments of collagen leaching away from the samples. As these small fragments are likely to have the highest levels of racemisation, this would reduce the observed racemisation in the bone (e.g. Dobberstein *et al.*, 2008).

Low racemisation values in the bones at the base of the trench, combined with minimal alteration of the relative amino acid concentration of the centre of the bone suggest that the damage in the waterlogged zone is only superficial and the loss of HA in the outer surface of the bones has not led to significant collagen damage.

6.3.2.1.3 Powder X-ray diffraction

p-XRD was carried out on all bones where the sample size allowed in order to assess the HA crystallinity. Both bones recovered from the lower, neutral zone displayed diffraction patterns characteristic of modern bone, indicating minimal alteration of the bone mineral (Figure 6.6, bottom).

Sharp peaks appearing close to the HA diffraction peaks may be due to mineral impurities, such as quartz, that are commonly present in archaeological and fossil samples and originate from the burial environment (e.g. Bonar *et al.*, 1983; Person *et al.*, 1995).

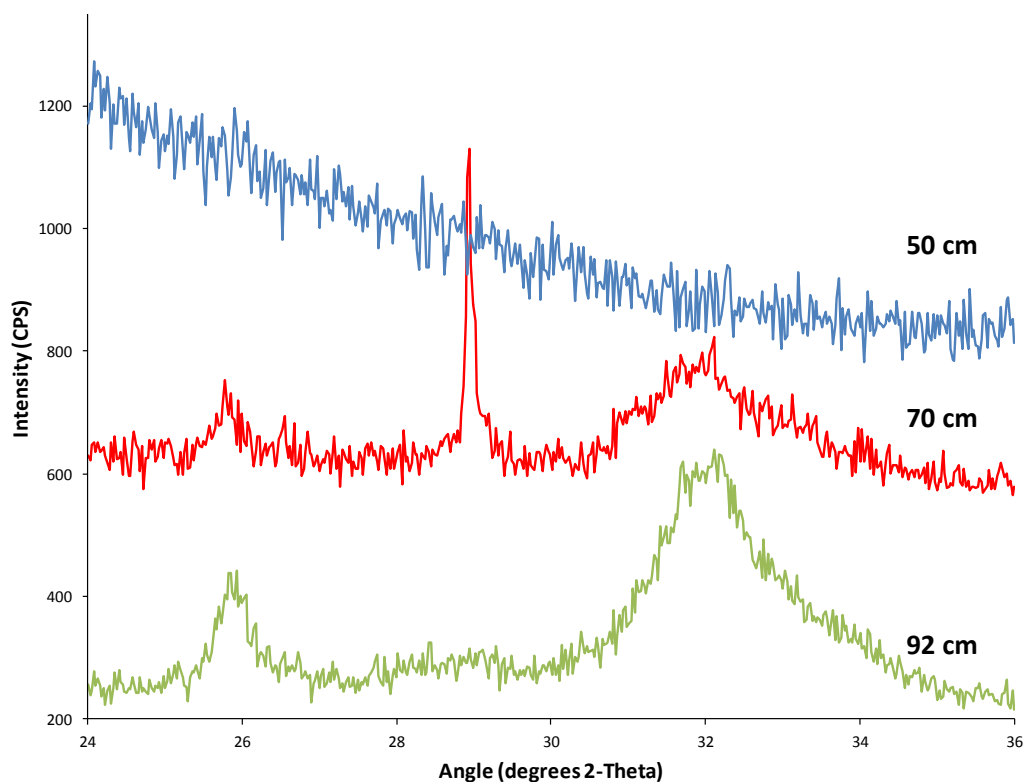


Figure 6.6: p-XRD patterns for all 3 samples retrieved from column A. The sharp peak at $28.5^{\circ}2\theta$ is probably due to a quartz impurity (e.g. Person *et al.*, 1995). (Originally in colour).

Minimal alteration of the HA, as indicated by p-XRD, is in agreement with total amino acid analysis, where little diagenesis was indicated, particularly in the middle section of the bones. Similarly, those in the middle zone showed little alteration, although a reduction in the intensity of the HA signal was observed. As the intensity of a diffraction line is proportional to

the volume of the material irradiated, this reduction in intensity may be a result of mineral depletion (Cullity, 1978). In contrast, p-XRD analysis of the bones located near the surface of the trench (dry, acidic) lacked any peaks characteristic of HA, suggesting that all bone mineral has been removed. This would be expected to result in elevated levels of amino acids, but this is not seen (Figure 6.5), again indicating that collagen is either simultaneously or subsequently being lost. Loss of both the protein and mineral fraction combined with high oxygen content (as indicated by elevated redox potential) in this region suggests that water may have been fluctuating through the sample.

6.3.2.1.4 Microscopy

Due to the fragile nature of most retrieved samples, thin-section optical microscopy was not possible. Instead, SEM was carried out on all 6 samples.

Analysis by AAR and p-XRD has revealed both samples from approximately 50 cm to be heavily deteriorated, and SEM imaging revealed a cellular-like histological structure very unlike bone in appearance, with extensive deep cracking (Figure 6.7, left). The regular structure suggests that it is cortical bone and therefore likely to be pig rib (e.g. Bell, 1990). Osteons in cortical bones cannot often be viewed so clearly unless the bone has been acid treated, suggesting that degradation has occurred in these samples (Boyde, 2012). In this case, the spongy appearance may be the result of dissolution of the centre of the osteons from the Haversian canals outwards. This may occur by either chemical or microbial activity (Bell *et al.*, 1996). In contrast, the chicken bone (which is naturally formed of a more open network; Boyde, 2012) uncovered at depths of 70 cm (Figure 6.7, right) as well as at 92 cm both displayed no deep cracking and no obvious alteration of the surface. This corroborates AAR and XRD analysis which both suggested that deterioration was not as advanced.

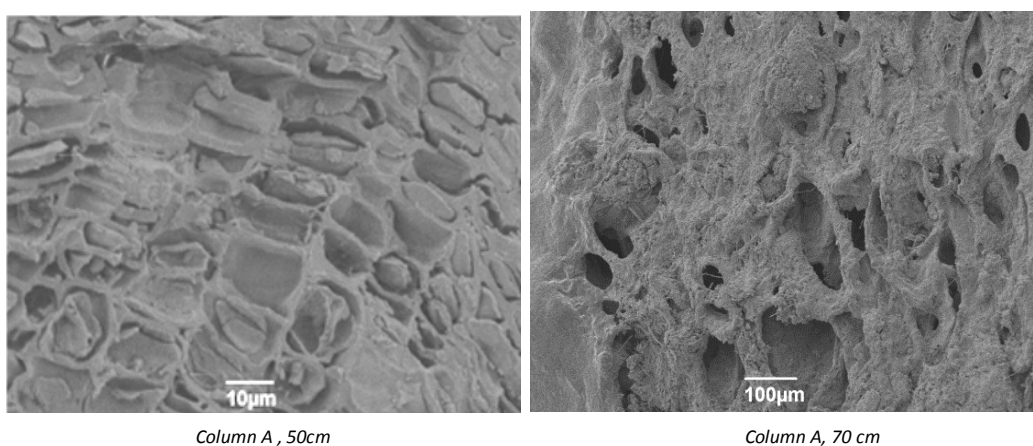


Figure 6.7: SEM images of bone excavated from the pilot study in SC29, showing cortical bone (left) which is similar in appearance to bone treated in acid (Chapter 4). The more porous network of trabecular bone (right) makes it more difficult to observe damage.

In all samples in the top two layers, ribbon-like formations were identified under SEM (Figure 6.8, left). The appearance of these suggests that they could be fungal hyphae, indicating the presence of biological activity (e.g. Blanchette *et al.*, 1990; Powell *et al.*, 2001). Evidence of fungal activity suggests that the soil is not permanently waterlogged, leading to aerated sediments (e.g. Nicholson, 1996; Kim & Singh, 2000). Indeed, this is also supported by the high redox values measured in the peat layers of SC29. This is likely to increase the risk of organic deterioration; microbial activity is more likely to occur in aerated zones (e.g. Caple, 1994; Lillie & Smith, 2007).

In other samples, such as that from column C at 70 cm (Figure 6.8, right), fibres adhering to the surface of the bone were less ribbon-like and could potentially be interpreted as collagen fibrils (Fantner *et al.*, 2004; Boyde, 2012). This is consistent with a loss of HA leading to exposure of the collagen matrix.

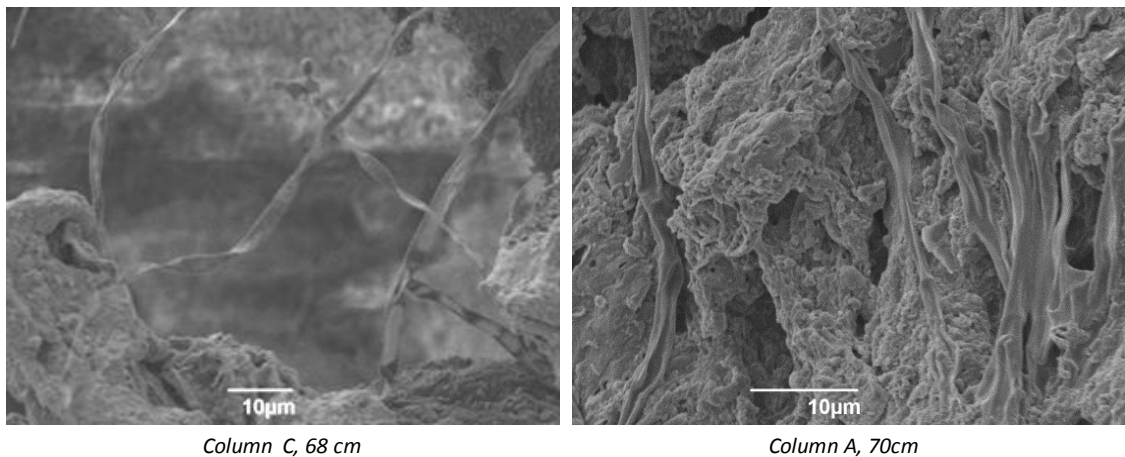


Figure 6.8: Features observed by SEM analysis of bone samples from SC29 which could be evidence for fungal activity (left). In other samples, fibres bear some resemblance to collagen fibrils (right) (Fantner *et al.*, 2004).

6.3.2.2 Main Study

6.3.2.2.1 Mass loss and visual analysis

Out of 18 bone samples buried in SC29, all 18 were recovered after one year. Visual alteration of most bone samples had occurred during the 12 months; in particular a darkening of the material which can be attributed to tannins present in the peat (e.g. Nicholson, 1998). Out of 12 bone samples buried at Flixton Island, all 12 were recovered. Visual analysis revealed little alteration, except in the artificial 'jellybones', where darkening and distortion had occurred (Figure 6.9, bottom right).

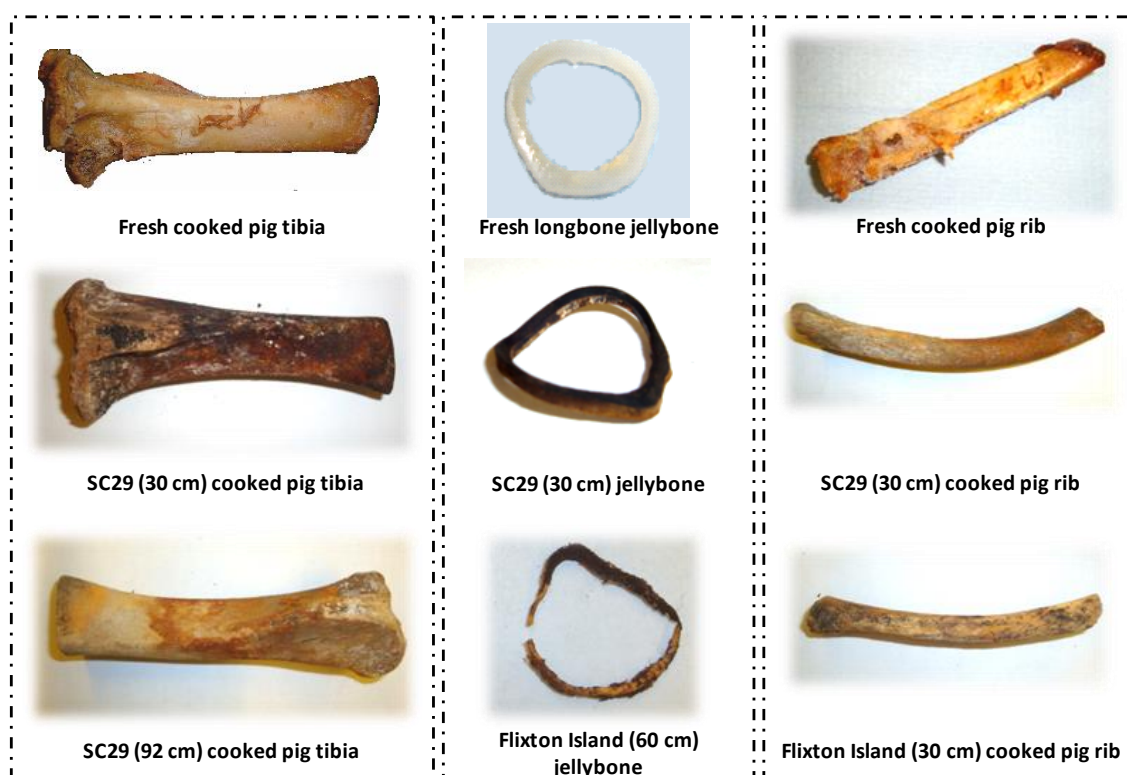


Figure 6.9: Images of the starting material (top) compared to after burial for 12 months at different locations. Orange deposits can be seen on the surface of bones from SC29, and the difference between material buried at 30 cm and 92 cm at SC29 is demonstrated by comparison of the cooked pig tibia (left). 'Jellybones' underwent discoloration and distortion at all burial locations (centre). (Originally in colour).

Orange deposits developed on the surface of several bones after a few days post-excavation, particularly those from SC29. A non-quantitative test was carried out on this based on theories outlined by Feigl & Anger (1972). A few milligrams of the deposit were scraped off and heated at 80°C with 2 M HCl for 1 hour. A few drops of 6 M potassium thiocyanate solution was added to this, and a colour change to blood red strongly indicated that these deposits contained iron.

Mass loss analysis was carried out where possible and is reported as a percentage of the starting mass in Table 6.4. In the modern sheep rib, mass loss may be due to the loss of flesh rather than bone and was therefore not carried out. Pig femurs were not weighed prior to burial in SC29 and therefore no data was obtained.

Table 6.4: Mass loss in samples buried for 12 months in Test pit SC29 and Flixton Island site 2.

Mass loss as a percentage of the starting mass					
Material	SC29 (depth)			Flixton Island (depth)	
	30 cm	50 cm	95 cm	30 cm	60 cm
Modern pig rib (cooked)	41	36	34	48	56
Modern pig femur (cooked)				42	38
Star Carr rib section	14	14	5	-1	0
Modern longbone 'jellybone'	9	22	26	23	16
Modern rib 'jellybone'	23	-7	14	14	14

Mass loss analysis must be approached with caution, due to the potential uptake of components from the burial environment; however, a few initial observations can be made. Mass loss in the 'jellybones' was comparatively low, even in the most acidic zones (30 and 50 cm at SC29). This indicates that the majority of mass loss in the mineralised bones does not come from the organic (collagen) fraction, and is more likely to be due to HA dissolution. This is in accordance with conclusions from lab-based experiments, described in Chapter 4.

Mass loss was seen to increase with increasing acidity in the Star Carr rib bone, suggesting that HA loss is pH dependent, again agreeing with results from experiments described in Chapter 4 as well as literature studies (e.g. Gordon & Buikstra, 1981; Margolis & Moreno, 1992).

Negligible mass loss was observed in the equivalent sample located at Flixton Island, further suggesting that HA loss is less severe at more neutral conditions.

The very high loss in the cooked modern samples compared to the archaeological samples is somewhat unexpected, as lab-based experiments have shown that modern uncooked material is less susceptible to degradation than archaeological analogues (Chapter 4). It is possible that some of this mass loss comes from the leaching out of non-structural components, such as fats and small proteins which are present in fresh bone (Currey, 2002). These are likely to have been removed from the archaeological sample shortly after its initial deposition. However, these are unlikely to account for mass losses of around 50 % such as seen at Flixton Island.

Cooking of bone can cause ‘melting’ of the collagen (Koon *et al.*, 2003) and it is possible that this accelerates the loss of the organic fraction, allowing it to occur before loss of the of HA.

6.3.2.2.2 Amino acid analysis

Samples were all analysed for total amino acid content and amino acid racemisation in duplicate, with mean values reported below.

Analysis of the starting materials showed that the artificial ‘jellybone’ samples have a much higher amino acid concentration than other starting materials as a result of the removal of the HA. However, racemisation was the same for untreated bone, suggesting that none was caused by the treatment with acid prior to burial. Analysis of the Star Carr rib revealed a higher total concentration and slightly elevated Asx racemisation relative to modern bone. Similarly, Asx racemisation in the cooked pig tibia was elevated to 0.18 suggesting that collagen damage has been caused by cooking.

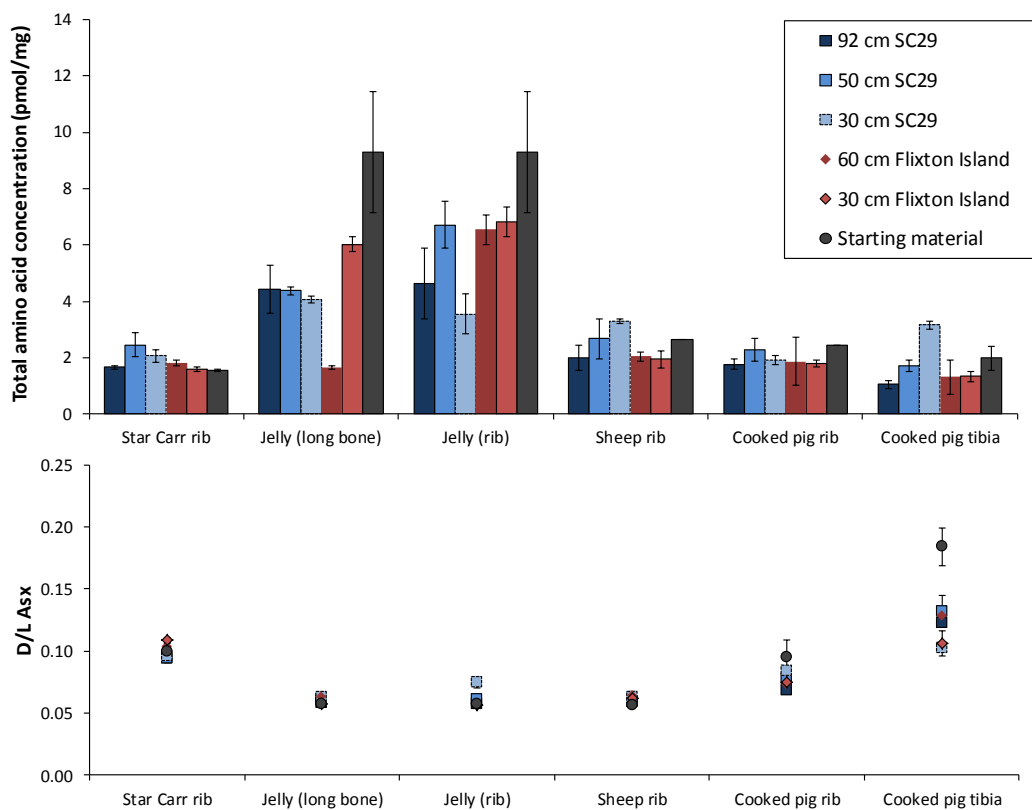


Figure 6.10: Total amino acid concentration (top) and Asx racemisation (bottom) in all excavated samples compared to the starting material. Error bars represent one standard deviation calculated from replicate analysis. (Originally in colour).

An increase in total amino acid concentration is seen with decreasing depth, or increasing acidity, in SC29 in both modern and archaeological rib samples and the cooked pig tibia (Figure 6.10, top). This indicates a loss of HA and supports results from the pilot study and lab-based

experiments, as well as mass loss analysis. Lower amino acid concentrations at high acidity in the 'jellybone' samples may indicate loss of collagen. However, as no HA is present it is more likely that uptake of surrounding material from the soil has contributed to the mass of the sample, thus altering the relative concentration of amino acids. At Flixton Island, little alteration of the total amino acid content is observed. This is also the case for the cooked bones, where a high mass loss was recorded, which could mean that HA and collagen are simultaneously being lost.

Racemisation of Ser is consistently low in all recovered samples, indicating that advanced collagen breakdown has not occurred. Asx racemisation is also similar to the starting material except for in the cooked pig tibia, where it is lowered (Figure 6.10, bottom). A possible explanation for this is that collagen has been broken down by the cooking and therefore smaller, more highly racemised peptide chains and amino acids can easily leach out, lowering the observed racemisation levels. In this case, lower values in samples buried nearer the surface in both locations could be indicative of increased water movement through the samples, which may also contribute to faster dissolution of HA (e.g. Hedges *et al.*, 1995).

6.3.2.2.3 Powder X-ray diffraction

As only small amounts of HA are expected to be present in the 'jellybone' samples, p-XRD analysis was limited to the Star Carr rib bones and cooked pig ribs. Analysis of the starting materials showed that the pig rib had a diffraction pattern characteristic of fresh bone whereas the Star Carr sample displayed a slight shoulder on the HA peak at 32-34 °2θ, signifying diagenesis (e.g. Bonar *et al.*, 1983; Bartsiokas & Middleton, 1992).

Alteration of the diffraction patterns for all bone samples was minimal; this is attributed largely to the short time-scale of the experiments. In all pig rib samples, no alteration of the HA was indicated by p-XRD except for perhaps the appearance of a small shoulder in the 50 cm sample (Figure 6.11). This is somewhat contrary to the high mass losses observed, which indicate that material is dissolving, indicating that HA is dissolving to a limited extent but is not able to recrystallize. This is supported by an increase in amino acid concentrations and is further evidence for the percolation of groundwater through the samples (e.g. Hedges *et al.*, 1995).

The shoulder in the HA peak at 50 cm indicates that HA dissolution is pH dependent, in agreement with the lab-based experiments (Chapter 4). In the analysed archaeological rib samples, no alteration was seen depending on depth and location of burial. Again, this is attributed to the short time-scale of the burial experiment.

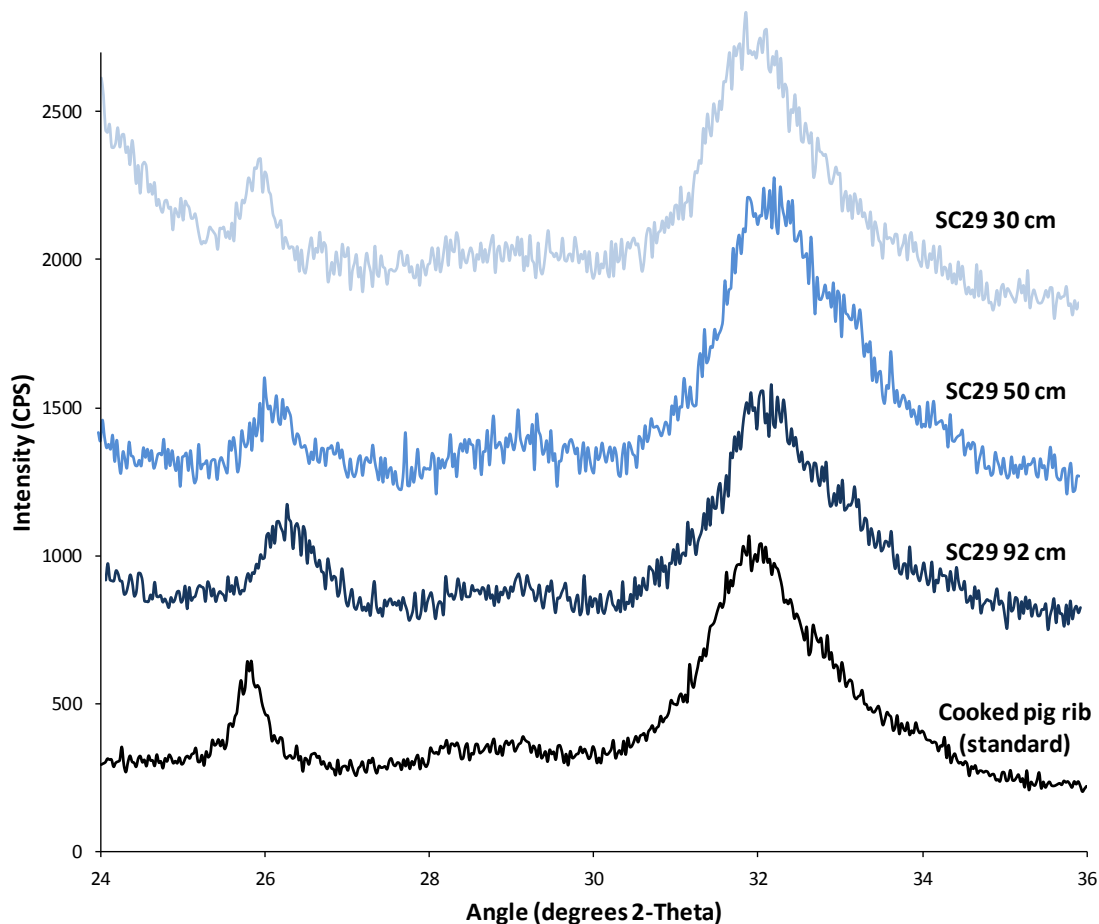


Figure 6.11: *p*-XRD patterns for the pig rib excavated from Test pit SC29 at all depths compared to an untreated cooked pig rib, showing no alteration of the HA. (Originally in colour).

6.3.2.2.4 Microscopy

Microscopic analysis of the burial samples was carried out using SEM in order to be comparable to the pilot study. Analysis was carried out on all 5 cooked pig ribs.

The porous structure of the trabecular bone in the centre of the rib was unaltered in all 5 samples (e.g. Figure 6.12, bottom left). However, in samples from SC29 crystalline deposits could be observed adhering to the surface (Figure 6.12, top left). These are possibly the orange formations that can be observed visually. The surface of the bones from 30 and 50 cm also appears pitted and smooth, in comparison to the rough texture seen in the samples retrieved from Flixton Island. This texture has also been seen in acid-treated samples in the lab (Chapter 4) and may be the result of dissolution of the HA, leaving a collagen rich matrix.

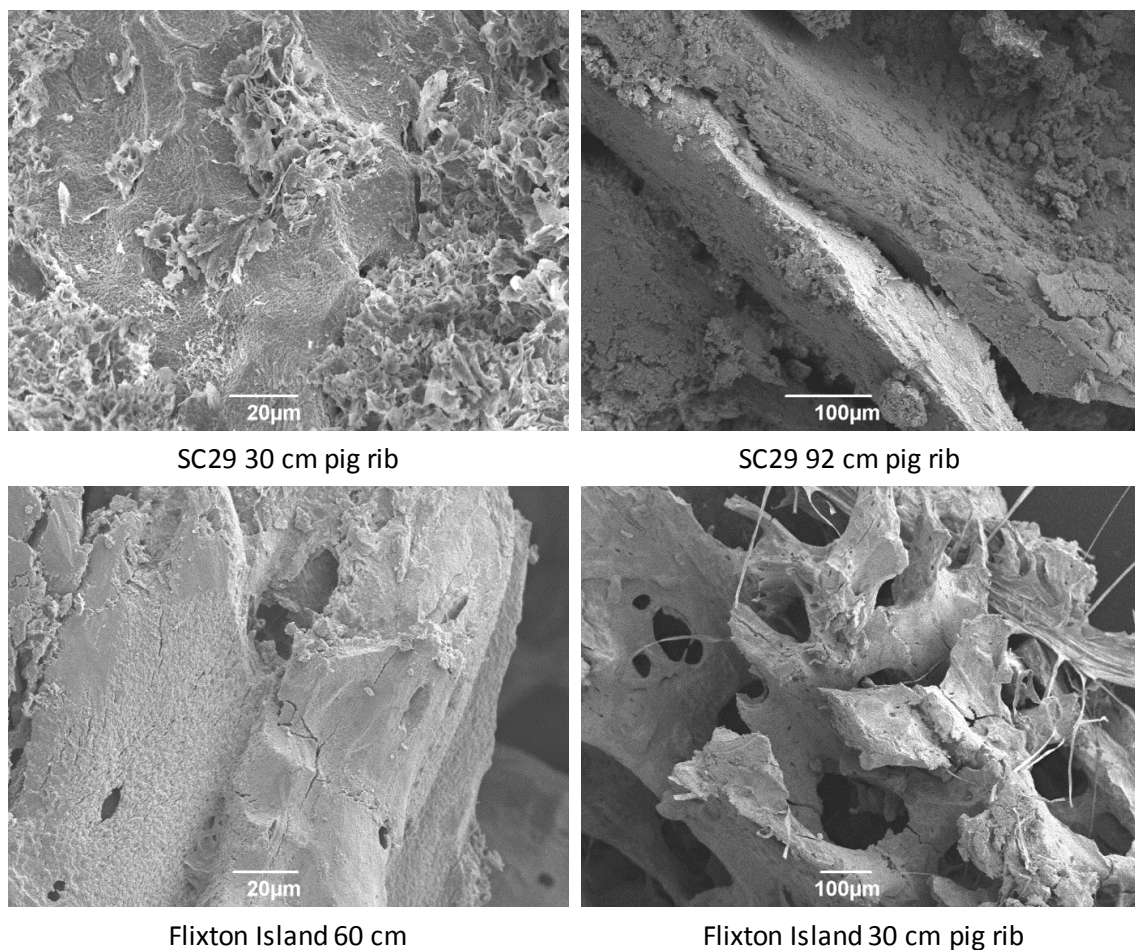


Figure 6.12: SEM images of pig ribs from SC29 (top) and Flixton Island (bottom) after 12 months. Different magnifications are used to highlight certain features, including crystals adhering to the bone surface (top left) and possible fungal activity (bottom right).

Cracks appearing on the surfaces may be the result of sample preparation. In most bones however, possible evidence for fungal activity was also identified (e.g. Blanchette *et al.*, 1990). This was not extensive, and could not be observed without microscopic techniques. However, potential fungal hyphae were most extensive in samples from SC29 92 cm and both samples from Flixton Island (Figure 6.12, bottom right). These were in the most neutral soils and this is suggestive that fungal activity may be suppressed in the more acidic conditions in the top of the trench. This supports observation made in the lab-based burial experiments (Chapter 5) where ‘jellybone’ samples were less degraded than in other soils, possibly due to a suppression of microbial activity.

6.3.2.3 Discussion

Analysis of bones buried *in situ* has revealed primarily that only low levels of diagenesis are seen within 12 months. In lab-based experiments at a similar pH to SC29 (pH 3) and room temperature, very low loss mass loss and minimal chemical alteration of samples was also seen (Chapter 4). Furthermore, although complete alteration of the HA was seen in Star Carr peat after 12 months in the lab-based burial experiments, the measured pH was much lower than that measured in SC29 (Chapter 5). It is therefore not surprising that only low levels of deterioration were seen in the majority of bone samples in the *in situ* experiments. Nevertheless, analysis by AAR and p-XRD has allowed some assessment on the impact of the burial environment.

Material buried for a 5-year period (pilot study) displayed alteration to the HA fraction, and a clear difference depending on depth of burial. This correlates to differences in soil pH, moisture content and redox potential (a proxy for oxygen content), all of which are intrinsically linked to bone preservation (e.g. Nicholson, 1996; Caple, 2004).

Both the 12-month and 5 year study provided a strong indication that HA loss is the primary initial mode of bone alteration at these sites, with collagen remaining relatively intact in the majority of samples. Analysis suggests that site acidity is a major contributing factor to this, as more HA appears to be lost at low pH, but differences in bone at the same pH suggest that that site hydrology may also have an important contribution. In particular, bones located in the middle of the burial experiment, where the water-table is likely to fluctuate, underwent the largest loss of HA. This is in agreement with studies such as those by Williams *et al.* (2006) and Crowther (2002) that show that a fluctuating hydrological regime is detrimental to the survival of archaeological material.

Cooked bone has not been included in any of the lab-based studies (Chapters 4 & 5). Research by Koon (2006) shows that there is a slight difference in collagen stability between pig and sheep bone, making direct comparisons between cooked and uncooked samples here slightly problematic. However, such a marked difference in racemisation between cooked and uncooked rib bones after burial indicates that leaching of collagen from cooked bone is faster than in uncooked bone. Indeed, Koon (2006) also shows how collagen that has been broken down, for example by cooking, leaches faster. It is possible that the same would be observed where collagen has been broken down due to acid-catalysed chemical hydrolysis.

6.3.3 Wood analysis

6.3.3.1 Main study

6.3.3.1.1 Mass loss and visual analysis

Out of 12 wood samples buried in SC29, nine were recovered after one year. Based on the good level of preservation observed in the recovered samples, it is unlikely that the lost three samples had completely degraded and it is concluded instead that they were just not found. All wood samples were visually unchanged except for some slight discolouration (Figure 6.13). Both modern and archaeological samples retained their structure, displaying no evidence of compression, as has been observed in wood excavated from Star Carr (Milner *et al.*, 2011a).



Figure 6.13: Willow samples after 12 months at all burial locations, compared to the starting material, showing little alteration apart from some slight discolouration and some orange staining in the sample from SC29, 50 cm. (Originally in colour).

Out of eight wood samples buried at Flixton Island, eight were recovered. Again, macroscopic appearance of the samples was largely unchanged. However, a small amount of white mould appeared on the surface of the birch sample at 60 cm a few days after excavation. Similarly as for bone, some evidence for iron-based compounds was also seen in the form of orange staining. This is likely to be iron oxide, determined by its distinctive colour (Schwertmann & Cornell, 2000).

Mass loss analysis is reported as a percentage of the starting mass in Table 6.5.

Table 6.5: Mass loss from wood samples buried for 12 months at both SC29 and Flixton Island site 2. Samples that were not recovered are indicated by a shaded box, and where there was no sample to begin with, this is indicated by a line through the box.

Mass loss as a percentage of the starting mass					
Material	SC29 (depth)			Flixton Island (depth)	
	30 cm	50 cm	95 cm	30 cm	60 cm
Modern birch	/	/	/	14	7
Modern willow	-1	-1	-4	18	5
Modern oak	19	-19		1	0
Bronze Age wood (Must Farm)		39		/	/
Star Carr wood	52	54	37	46	44

Mass loss analysis in wood can be variable, as the porosity of the wood makes it difficult to obtain an accurate dry mass (e.g. Panter & Spriggs, 1996; Jensen & Gregory, 2006). Negative mass losses are possibly explained by the inclusion of soil into these pores following burial. However, some broad trends can be identified. Mass loss appears to be greater in archaeological samples (from Star Carr and Must Farm, where recovered). Analysis of the starting materials by FTIR prior to burial suggested significant cellulose depletion had already occurred in the sample from Must Farm and some lignin alteration had occurred. In the sample from Star Carr, all cellulose had been removed and lignin was also depleted (see Chapter 7 for full analysis). This suggests therefore that lignin has been further degraded since burial, particularly in the Star Carr samples where little or no cellulose was left to be removed. Alternatively, the loss of cellulose has increased the porosity of the wood, making mass loss analysis even more prone to error. However, evidence of mould on the surface of the birch samples at Flixton Island suggests that fungal activity could be occurring. Fungal activity is known to be the major facilitator of lignin degradation (e.g. Kim & Singh, 2000).

The mass losses in modern samples are low enough to be explained by the loss of non-structural components such as starches and simple sugars (e.g. Jane *et al.*, 1970). The mass loss data therefore tentatively suggests that archaeological samples where lignin alteration has already occurred are more likely to undergo lignin diagenesis than modern samples.

As the samples were not fully waterlogged to begin with, u_{\max} analysis was not carried out due to the difficulty in ensuring that samples were fully saturated prior to recording initial masses, leading to high level of error (Jenson & Gregory, 2006).

6.3.3.1.2 FTIR spectroscopy

All excavated wood samples were analysed by FTIR as outlined in Chapter 3 (Section 3.3.3). Three readings were taken directly from the outer surface of the samples. Peak heights were read for each of the 4 major peaks relating to cellulose (1325 and 1375 cm^{-1}) and lignin (1240 and 1507 cm^{-1}), and heights averaged for all three readings. Analysis of the starting materials showed that only very small cellulose peaks were present in both the Star Carr and Must Farm samples, suggesting that cellulose was already heavily depleted.

Cellulose depletion results in a higher lignin: cellulose (L: C) ratio, calculated by summing the heights of the two major peaks for each polymer (e.g. Pandey & Pitman, 2003; Gelbrich *et al.*, 2008). Ferraz *et al.* (2000) suggest that only the phenolic signal at 1507 cm^{-1} can be solely attributed to lignin, and as this is highly stable it can therefore be used as a reference. A comparison of the height of this peak with the cellulose peaks was also made, to confirm that the L: C ratio is not distorted by simultaneous breakdown of lignin. Both ratios are shown for each of the recovered willow samples in Figure 6.14.

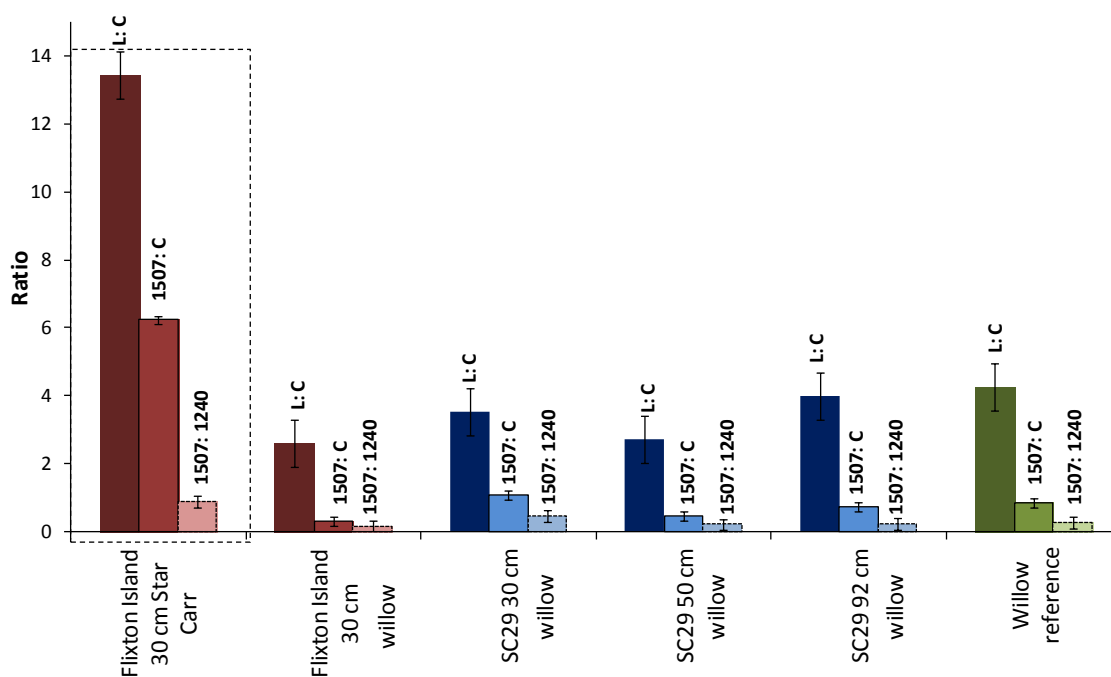


Figure 6.14: Comparison of several indicators of degradation for willow samples from the 12 month burial experiment, compared to the Star Carr wood used in the experiments and an untreated willow sample. An increase in L: C and 1507: C ratios indicate an increase in cellulose loss, and an increase in the 1507: 1240 ratio is indicative of lignin defunctionalisation. (Originally in colour).

Compared to the Star Carr sample retrieved from 60 cm at Flixton Island (dashed line), where all ratios are highly elevated, no real difference was seen between modern materials buried at different depths in SC29, taking the error calculated from the untreated sample into account.

As wood degradation via chemical hydrolysis occurs primarily by loss of the cellulose (Hoffman & Jones, 1990; Pandey & Pitman, 2003) followed by defunctionalisation of the lignin (Martinez *et al.*, 2005), this suggests that hydrolysis is not occurring at a level that is detectable by FTIR, even in the most acidic parts of the trench.

Breakdown of the lignin structure by hydrolysis is likely to initially occur by defunctionalisation of the phenol rings, resulting in a decrease in the height of the peak at 1240 cm^{-1} relative to the stable phenol peak at 1507 cm^{-1} . No differences in this ratio were observed between modern samples (Figure 6.14), although it is elevated in the archaeological samples.

Splitting of the peak at 1240 cm^{-1} was not seen in any of the modern samples, suggesting that lignin is undergoing only minimal deterioration (Pandey & Pitman, 2003).

One exception to the lack of observed degradation using FTIR was in the sample where mould had developed (birch from Flixton Island, 60 cm; Figure 6.15). The phenolic lignin peak at 1507 cm^{-1} was not detected in analysis of the sample close to the fungal activity, although it was seen in a measurement taken from elsewhere on the sample. This indicates loss of the aromatic ring and is in accordance with the observation that lignin is primarily degraded by fungal activity (e.g. Blanchette, 2000; Kim & Singh, 2000).

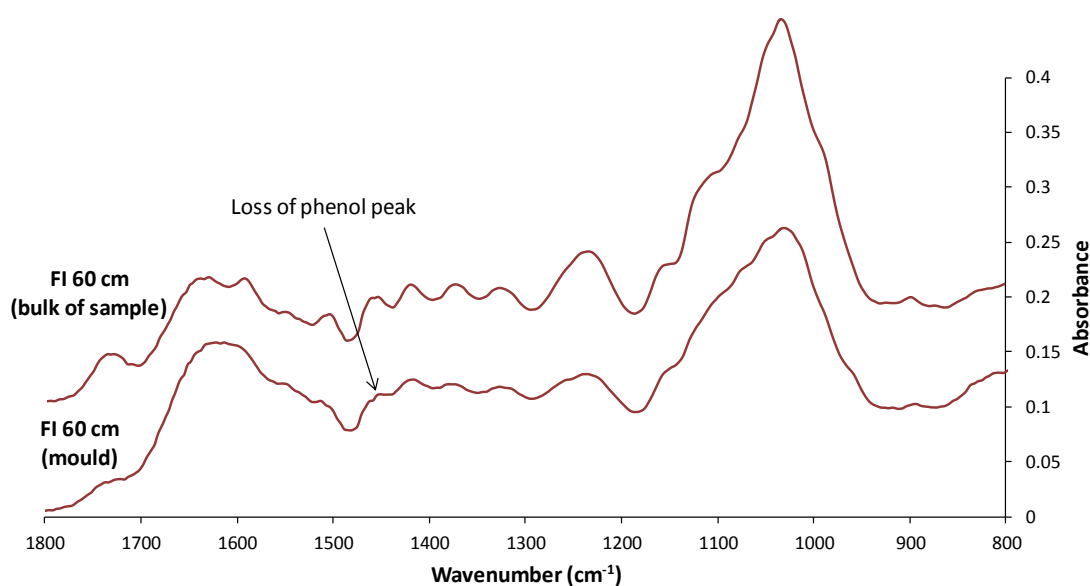


Figure 6.15: Comparison of FTIR spectra of the birch samples excavated from Flixton Island, 60 cm where mould was present (bottom) and the bulk of the sample, showing loss of the phenol absorption.

6.3.3.1.3 Py-GC

Visual, mass loss and FTIR analysis of the wood samples from both burial sites indicate that diagenesis has not occurred significantly within the 12 month burial period, particularly in modern wood samples. However, py-GC provides a more detailed analysis of polymer breakdown (Chapter 3). In addition, lab-based experiments (Chapters 4 & 5) have indicated that degradation products may remain *in situ* in wood samples, leading to inaccurate mass loss and FTIR measurements. In order to supplement the FTIR data, 2 willow samples were therefore analysed by py-GC, according to the protocol outlined in Chapter 3 (Section 3.3.4).

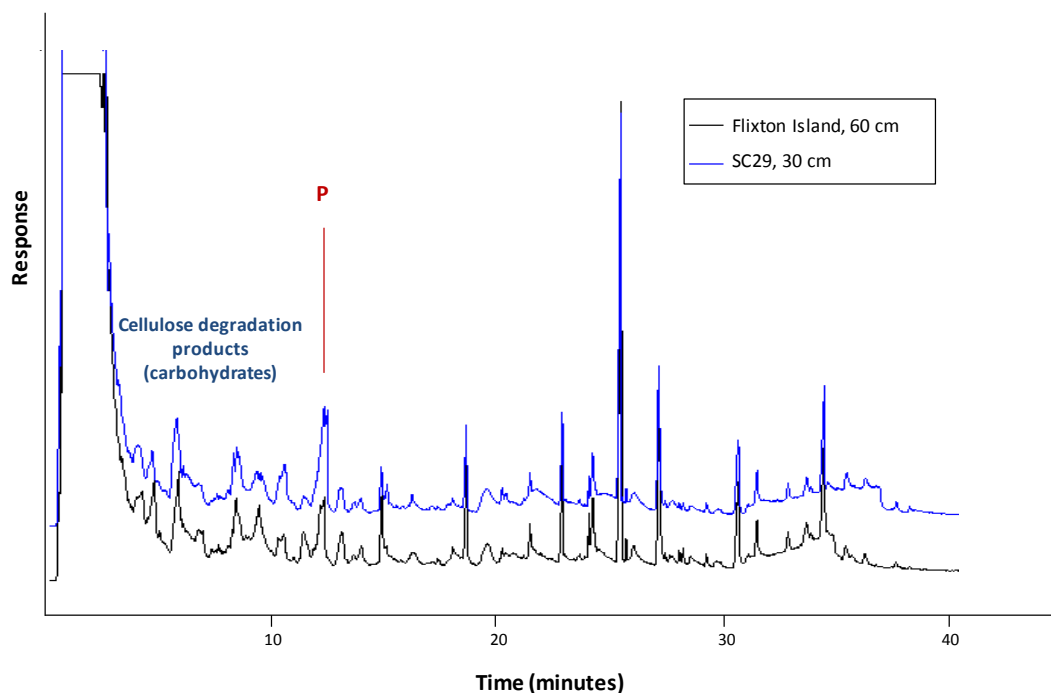


Figure 6.16: py-GC chromatograms for willow samples from Flixton Island, 60 cm and SC29, 30 cm.

Chromatograms from both samples contained significant peaks relating to celluloses and lignin, confirming results from FTIR analysis (Figure 6.16).

Due to the high levels of error involved (Chapter 3, Section 3.3.4) combined with the fact that only subtle changes are observed in the chromatograms, no peak ratios have been calculated. Visual comparison of the chromatograms potentially indicates an elevated level of phenol in the sample from SC29 compared to that from Flixton Island, indicating defunctionalisation of the lignin. Although this data is currently only qualitative, and therefore this interpretation should be considered only alongside other evidence, this is in agreement with data from lab-based experiments in acid (Chapter 4) where defunctionalisation of lignin in acidic solutions was more conclusively determined by both py-GC and FTIR.

6.3.3.1.4 Microscopy

Willow samples retrieved from each of the five burial sites were analysed. Fungal hyphae were identified in all samples, but were far more extensive in wood from Flixton Island, and at a depth of 92 cm in SC29 (Figure 6.17).

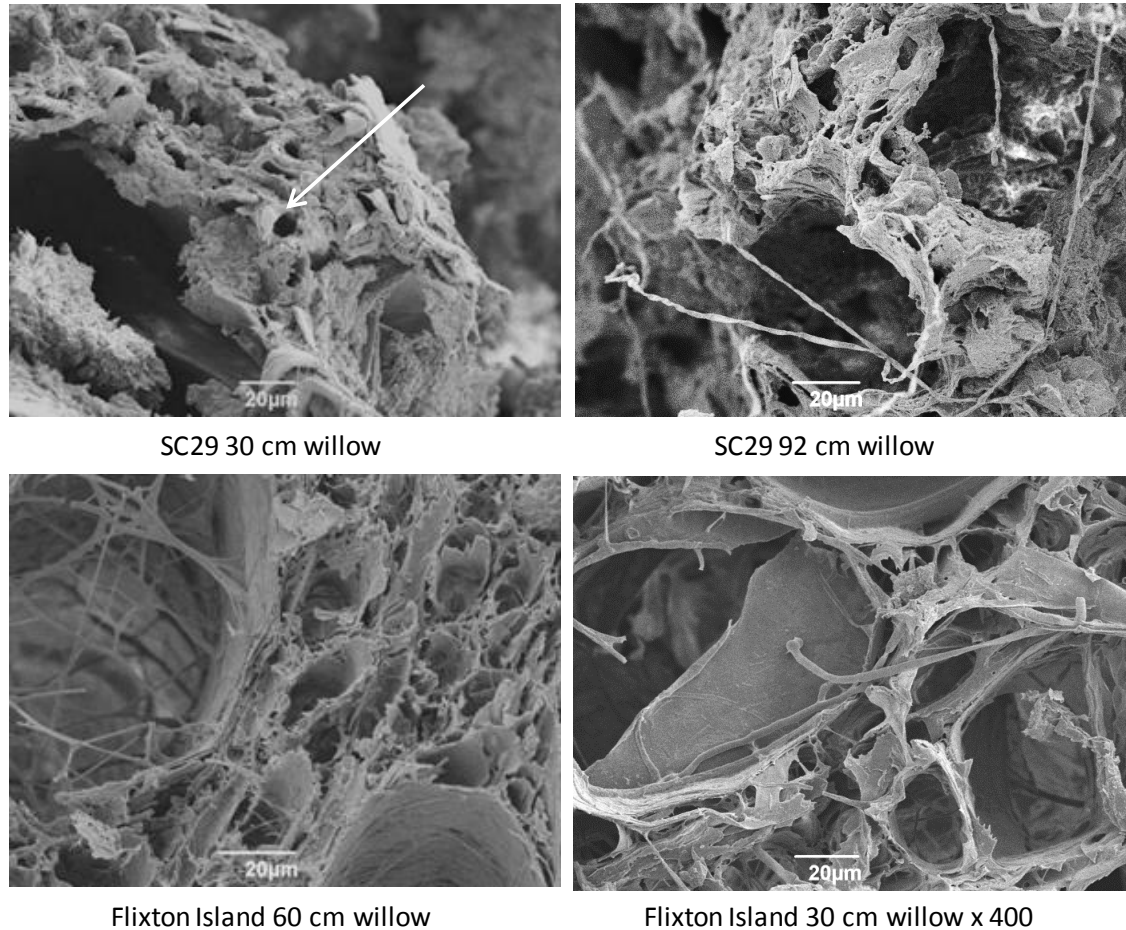


Figure 6.17: SEM images of wood samples excavated at both site, illustrating the extent of fungal activity.

Similar observations regarding fungal activity were observed in bone samples (i.e. lower abundance in samples located in the top of SC29) again suggesting that the acidic conditions in the upper levels of SC29 may be slowing biological activity. For wood, this is an important consideration, as biological activity is often identified as the major cause of wood deterioration (e.g. Hedges, 1990; Blanchette *et al.*, 1990; Kim & Singh, 2000). If biological activity is suppressed under the conditions at Star Carr then this would suggest that any deterioration observed in wood at the site occurs primarily due to chemical processes.

The thick cell walls viewed under SEM (indicated by an arrow in Figure 6.17, top left) also confirms that cellulose is still present, whereas in lab-based burial experiments (Chapter 5)

cells walls appeared shrunken and collapsed. This indicates that degradation of cellulose is not advanced, even in Test pit SC29 where conditions were slightly acidic.

6.3.3.2 Discussion

Chemical analysis (FTIR and py-GC) of wood samples retrieved from the burial experiments indicates that diagenesis is minimal over the 12 months studied, including in the acidic regions of Test pit SC29. Lab-based experiments have indicated that low pH does not have as detrimental an effect on wood survival as bone, and that deterioration was only detectable after 16 weeks in pH 1 acid for 16 weeks. Even in SC29, the pH was almost 2 pH units greater than this. In addition, the time-scale of the experiments was only short, meaning that any degradation that did occur may be too minimal to observe. After a similar time-frame in the lab-based burial experiments, deterioration was observed only on the surface of samples buried in Star Carr peat, and again the measured pH was much lower than that in the *in situ* burial locations. Such low levels of deterioration are therefore not unexpected.

Evidence for fungal activity has been observed, both visually and by SEM imaging throughout the trench at Flixton Island and in the more neutral regions of SC29 (92 cm). The destructive effect of this biological activity is demonstrated by FTIR analysis of the willow samples from 60 cm at Flixton Island, where mould was observed on the surface of the sample. Absorption peaks relating to both lignin and cellulose were heavily depleted (Figure 6.15). In contrast, wood buried in more acidic regions of SC29, which is more comparable to parts of the Star Carr site, displayed little evidence for fungal activity, suggesting that it is suppressed. As this relates to the top layer of the trench, it seems more likely that this suppression is due to the high acidity than low levels of oxygen; indeed, redox potential measurements indicate that these layers are the most oxygenated.

Levels of deterioration are low in all samples; however, an increased phenol content (identified by py-GC; Figure 6.16) and high mass loss (Table 6.5) tentatively suggest that despite the absence of biological activity, deterioration of the wood is more advanced in the acidic regions of SC29 than the control site. This indicates that chemical deterioration is a major factor in facilitating degradation of both lignin and cellulose in acidic environments. This supports data from lab-based experiments (Chapter 4) where deterioration was advanced after 16 weeks at pH 1 and 80°C. In addition, the outer layer of wood samples buried in highly acidic Star Carr peat in lab-based burial experiments (Chapter 5) were found to contain defunctionalised lignin, further indicating that defunctionalisation occurs at low pH.

6.4 Discussion and conclusions

It was anticipated that a 12 month *in situ* burial experiment would reveal only the very early stages of diagenesis, and this has been shown to be the case. All material was recovered except for three wood samples, which has been attributed to a failure to locate the buried samples rather than total degradation of the material. For most materials, no significant visual alteration was observed except for some darkening, attributed to staining by tannins (e.g. Nicholson, 1998). The exceptions are distortion and high mass loss in the 'jellybone' samples buried at Flixton Island, and the appearance of fungal hyphae on wood samples at Flixton Island. In addition, orange deposits developing on the surface of many of the SC29 samples have been interpreted as iron oxide formation (Schwertmann & Cornell, 2000).

It is assumed that in waterlogged sites, microbial and fungal activity is suppressed (e.g. Hedges, 1990; Bjordal *et al.*, 1999). However, fungal hyphae are visible under SEM in material excavated from the lower levels at both sites, although these had been assumed waterlogged. In contrast, little evidence was observed in the upper regions of SC29, where acidic pH was recorded (pH 3.6 for 30 cm; pH 3.14 for 50 cm). This suggests that biological activity was suppressed at low pH. Despite this, deterioration of wood samples was detected by FTIR and py-GC in these regions, indicating that chemical activity was a factor in the deterioration of both lignin and cellulose. The pH dependence of bone deterioration is even more obvious; an increase in relative amino acid concentrations at lower pH signifies a greater loss of HA. These results are in agreement with lab-based experiments (Chapter 4) which demonstrated that bone degradation was greatly accelerated by low pH, and that after 16 weeks at 80°C wood deterioration also appeared to be pH dependent.

Lab-based burial experiments (Chapter 5) led to the hypothesis that site hydrology was a major factor facilitating organic degradation; a theory also backed up by previous experimental studies (e.g. Crowther, 2002; Williams *et al.*, 2006). Further assessing the impact of site hydrology was a key aim of these *in situ* burial experiments. Analysis of material from the pilot study shows that bone deterioration was more advanced in the middle regions of the trench compared to the top (pH 3.27 at 70 cm compared to pH 3.12 at 50 cm). This was indicated by both amino acid analysis and p-XRD. Deterioration in the main study for both bone and wood was too low to definitively assess a difference between different depths and assumed hydrological regimes; however, a slight shoulder appeared on the HA peak in p-XRD in the middle sample from SC29 (50 cm; likely to be fluctuating) was seen. This tentatively confirms that water was fluctuating through the samples, and that this has caused increased deterioration.

Although deterioration in the main burial experiments was minimal, the analysis of material from the 2007 pilot study provided additional data over a longer time period and suggested that bones buried in SC29 were highly vulnerable to deterioration. Samples in the top layer of the trench were barely identifiable, and it is believed that further samples were buried in the trench that were not recovered (A. Needham, pers. comm., 2012). Whilst it cannot be ascertained whether this is due to a failure to locate the sample or their complete disintegration, the fragmentary nature of the bone uncovered at 50 cm depth suggests that complete disappearance of the bones is possible. This further agrees with data obtained in Chapters 4 & 5 that suggests that bone present in acidic conditions such as those at Star Carr is likely to deteriorate rapidly. Bone present that is already deteriorated (e.g. archaeological bone) is unlikely to survive for much longer at the low pH at Star Carr.

Flixton Island acted as a control site in this experiment. However, neither bone nor wood were much better preserved there. This is probably because the site was not waterlogged or acidic and as such biological activity could rapidly proceed. The high mass loss in the 'jellybone' samples at Flixton Island supports observation made in Chapter 5 that biological activity may be the major mode of deterioration of exposed collagen. Evidence of fungal activity on samples buried at 60 cm depth at Flixton Island indicates that biological factors could be contributing to organic diagenesis. This highlights that although low pH is highly detrimental to the survival of bone, drying out of the site, or fluctuations in the water-table should be another major cause for concern at the Star Carr site (e.g. Bartlett *et al.*, 2010; Hedges & Millard, 1995; Caple 2004).

Data obtained from lab-based experimental studies have demonstrated that low pH is likely to be highly detrimental to the survival of both bone and wood. *In situ* burial studies have shown that if this is combined with a lowered water-table, decay of both bone and wood is likely to be accelerated. This is likely to be due both to the washing away of dissolved material and an increase in biological activity. Deterioration of material at Flixton Island in particular demonstrates that although low site pH may be a major factor facilitating organic decay at Star Carr, the negative effects of the presence of biological activity needs to also be considered.

The information gained from *in situ* burial experiments re-enforces data obtained from the lab-based experiments (Chapter 4 & 5), showing how controlled experiments can replicate site conditions effectively. However, in order to fully assess the effects that these conditions have on archaeological material remaining at Star Carr, an assessment of excavated material has also been carried out.

CHAPTER 7

ANALYSIS OF ORGANIC ARCHAEOLOGICAL MATERIALS FROM STAR CARR

7.1 Introduction

Lab-based experiments (Chapters 4 & 5) and field-based burial experiments (Chapter 6) have shown that high sediment acidity at Star Carr is likely to be playing a major role in the deterioration of bone at the site. Those experimental studies have shown that bone deterioration at low pH occurs initially by loss of the bone mineral (HA) to buffer the acidity, followed by degradation of the collagen once it is unprotected.

Although high acidity seems to be less detrimental to the survival of wood, FTIR and py-GC analysis of experimental samples that have been exposed to high levels of acidity (pH 1) for a long period of time (16 weeks), has indicated both loss of cellulose and defunctionalisation of lignin. This suggests that both major polymeric components of wood can undergo chemical hydrolysis in highly acidic conditions.

It has been hypothesised that the burial conditions at Star Carr have only recently become acidic (Boreham *et al.*, 2011). Even if this is the case, Mesolithic material buried at the site will have already undergone low levels of diagenesis, as interaction between buried artefacts and the burial environment is continually taking place (e.g. Caple, 1994; Hedges & Millard, 1995; Pollard, 1996). Transfer of chemical species such as heavy metals from the burial environment can lead to changes in the composition of both bone (Turner-Walker, 2008) and wood (Hedges, 1990). It is likely that even in a neutral environment some loss of HA from bone will have occurred due to dissolution (Dixon *et al.*, 2008). In addition, low levels of biological attack following loss of the HA may have caused some deterioration of the collagen (Child *et al.*, 1993). Even in a waterlogged environment where fungal activity is likely to be suppressed (Blanchette, 2000), low levels of microbial activity, for example from erosion bacteria, may contribute to the loss of cellulose from buried wood (e.g. Gelbrich *et al.*, 2008).

Archaeological materials have been included in the experiments described in Chapters 4, 5 & 6 in order to assess whether they undergo diagenesis faster than modern analogues. Lab-based experiments have shown that archaeological bone is less able to buffer surrounding acidity; this may result in faster subsequent degradation of the collagen. For wood, differences in the rates of degradation between modern and archaeological material is less clear. However, analysis of the Must Farm and Star Carr materials used in experiments has shown that it is depleted in cellulose, illustrating the compositional differences between modern and archaeological materials.

Literature studies, as well as field and burial experiments carried out as part of this study have shown that the specific site chemistry plays an important role in the mechanisms by which both bone (e.g. Nicholson, 1996; 1998) and wood (e.g. Powell *et al.*, 2001) decay in an archaeological site. An extensive geochemical survey carried out in 2009-2010 revealed areas of the Star Carr site containing highly oxidative, acidic sediments (Boreham *et al.*, 2011). However, further analysis also revealed that acidity was highly variable across the site (Chapter 2, Section 2.3.3.1). It is likely that this variability impacts upon the preservation of organic artefacts locally, and there may be areas of the site where organic materials remain in good states of preservation, for example where acidity is buffered by the presence of clay. Although this variability has been accounted for in part by the experimental approaches, it is likely that conditions will have fluctuated over the period of burial. Along with the 11,000 year time-frame, this makes it difficult to replicate the exact burial conditions at the site through lab-based studies.

In this Chapter, an assessment of the current state of organic materials recovered from Star Carr is made, using analytical techniques developed in Chapter 3. Comparison of these samples with experimental data and material from other archaeological sites was expected to allow an assessment of whether deterioration seen at the site is unusual, or simply what could be expected from a site of this age. In addition, the state of preservation can be related to the geochemistry of the burial location where possible.

7.2 Materials and burial locations

All samples analysed from Star Carr are listed in Table 7.1 (bone) or Table 7.2 (wood). The locations of all samples within the site are indicated in Figure 7.1 (bone) or Figure 7.3 (wood).

7.2.1 Bone from Star Carr

7.2.1.1 Early excavations

Only one bone was available for analysis from the original excavations in 1948. This was reportedly recovered from the spoil heap and is the rib bone of a large mammal. This is referred to as '1948 – spoilheap'. Geochemical data from the site is not available for this sample.

In addition, visual observation of several bones from the original excavations (now located at the British Museum) was made, although no destructive analysis was possible.

No material from the 1985 and 1989 excavations was available for analysis.

7.2.1.2 2007/2008 excavations

A number of chalky and brittle bone fragments of unidentified species were excavated from Trench SC23 in 2007 and 2008 and a selection of these provided for analysis. Trench SC23 is contained on the dryland area of Star Carr and all bone recovered from here was reported to be "poorly preserved" (Milner *et al.*, 2011a, pg 2819). Based on original site reports (Clark, 1954), it has been suggested that although it is now dry (Milner *et al.*, 2011a), this trench may have been previously waterlogged. No pH measurements are recorded from SC23, although the investigation by Boreham *et al.* (2011) suggests that the dryland parts of the site are less acidic than the wetland, ranging from pH 4 - 5.5.

7.2.1.3 2010 excavations

Re-excavation of Cutting 2 (Clark's original trench) in 2010 uncovered a large array of bone material in the backfill from the 1952 excavations. These were mainly classified as 'robust' upon excavation (B. Knight, pers. comm., 2010). Several of these bones were used in lab and field-based experiments in this study (Chapters 4, 5 & 6). Again, no geochemical data exists for these samples, although the backfill was fairly dry on excavation (various excavators, pers. comm., 2010).

On extension of Cutting 2 (Context 234), a number of more badly preserved bones were uncovered and two of these analysed. Similarly, in SC33, a new trench located only in the wetland area, a number of heavily demineralised bones (termed 'jellybones') were uncovered and analysed.

7.2.1.4 2013 excavations

The most recent excavations allowed for a more comprehensive geochemical study to take place. A series of bones from both wetland and dryland areas of Trench SC34 were sampled, with preservation varying greatly between samples. In several cases soil samples were taken from directly underneath the artefacts, and extensive pH measurements were taken across the site according to the procedure in Chapter 2 (Section 2.3.2.3). These were found to vary significantly across the trench, with differences of several pH units within metres (Chapter 2, Section 2.3.3.1). In some cases, the pH was recorded directly underneath the bone, and when this was not possible the pH was estimated based on nearby readings. The results are discussed alongside chemical analysis of the bone samples (Sections 7.3.2.2.1 and 7.3.2.3).

7.2.2 Comparative material (bone)

Amino acid analysis data from the bone from Star Carr has been compared to archive data obtained using the same method by the NEaar laboratory at York. Samples include a rhino bone from the cave site of Kirkdale, Yorkshire (grid reference: SE 76781 8561), estimated to date from around 112 ka BP (McFarlane & Ford, 1998; Buckley & Collins, 2011), and a range of cow bones from the Viking site of Coppergate, York (grid reference: SE 6042 5172) estimated to date from the mid-9th to 10th century AD (O'Connor, 1989).

For p-XRD comparison, a cow metatarsal from the site of Tanner Row, York (grid reference: SE 6002 5180) was analysed. The sample was from unstratified contexts, but is estimated to date from the early medieval period (obtained from T. O'Connor). Bone from Tanner Row is generally considered very well preserved (e.g. Carrott *et al.*, 1997).

Table 7.1: Summary of all bone samples analysed from Star Carr. Where the species is known this is listed.

Sample Information				
Sample Name	Year of excavation	Trench (context)	Description	
Spoilheap	1948	Unknown	Very robust. Rib bone of large mammal	
86063	2007	SC23 (48)	Chalky, brittle. Fragment.	
86253			Chalky, brittle. Fragment.	
86634		SC24 (93)	Chalky, brittle. Fragment.	
87093		SC24 (85)	Jellybone	
89508	2008	SC23 (125)	Chalky, brittle. Fragment.	
90027			Chalky, brittle. Fragment.	
90243			Chalky, brittle. Fragment.	
91782			Chalky, brittle. Fragment.	
92105		SC23 (155)	Chalky, brittle. Fragment.	
92310	2010	Cutting 2 (backfill)	Robust but with longitudinal splitting. Large mammal rib	
92315			Robust but with longitudinal splitting. Large mammal rib	
92339			Robust, large mammal tibia	
92373			Robust, no flaking. Large mammal rib	
92383			Robust large mammal metapodial. No flaking.	
92404			Robust, large mammal tibia	
92418			Robust. Large mammal rib	
92419			Robust. Large mammal rib	
92420			Fragment of large mammal skull. Fairly robust	
92423			Robust but flaking. Orange deposits on surface. Large mammal	
92424			Robust, some surface flaking. Large mammal rib	
92434			Robust but flaking. Large mammal scapula	
92436			Robust, no splitting. Large mammal rib	
92471			Cutting 2 (234)	Tibia, possibly squashed, badly preserved
92509				Scapula? Fragment
92745 A		SC33 (240)	Jellybone	
92753			Jellybone, end of large mamma humerus	
92811			Jellybone, small fragments	
98144		2013	SC34 (wetland)	Jellybone. Orange flakes in bag
98930	Jellybone. White powder in centre			
99342	Jellybone, dark in colour			
99762	Almost translucent, white powder in centre. Coming apart			
99871	Scapula; firm in centre but jelly texture towards thin part			
103426	Scapula; firm in centre but jelly texture towards thin part			
103610	Robust. Small fragment taken from bag			
94647	SC34 (dryland)		Chalky, brittle. Fragment.	
94825			Chalky, brittle. Fragment.	
95290			Chalky, brittle. Fragment.	
95430			Chalky, brittle. Fragment.	
102869			Chalky, brittle. Fragment.	

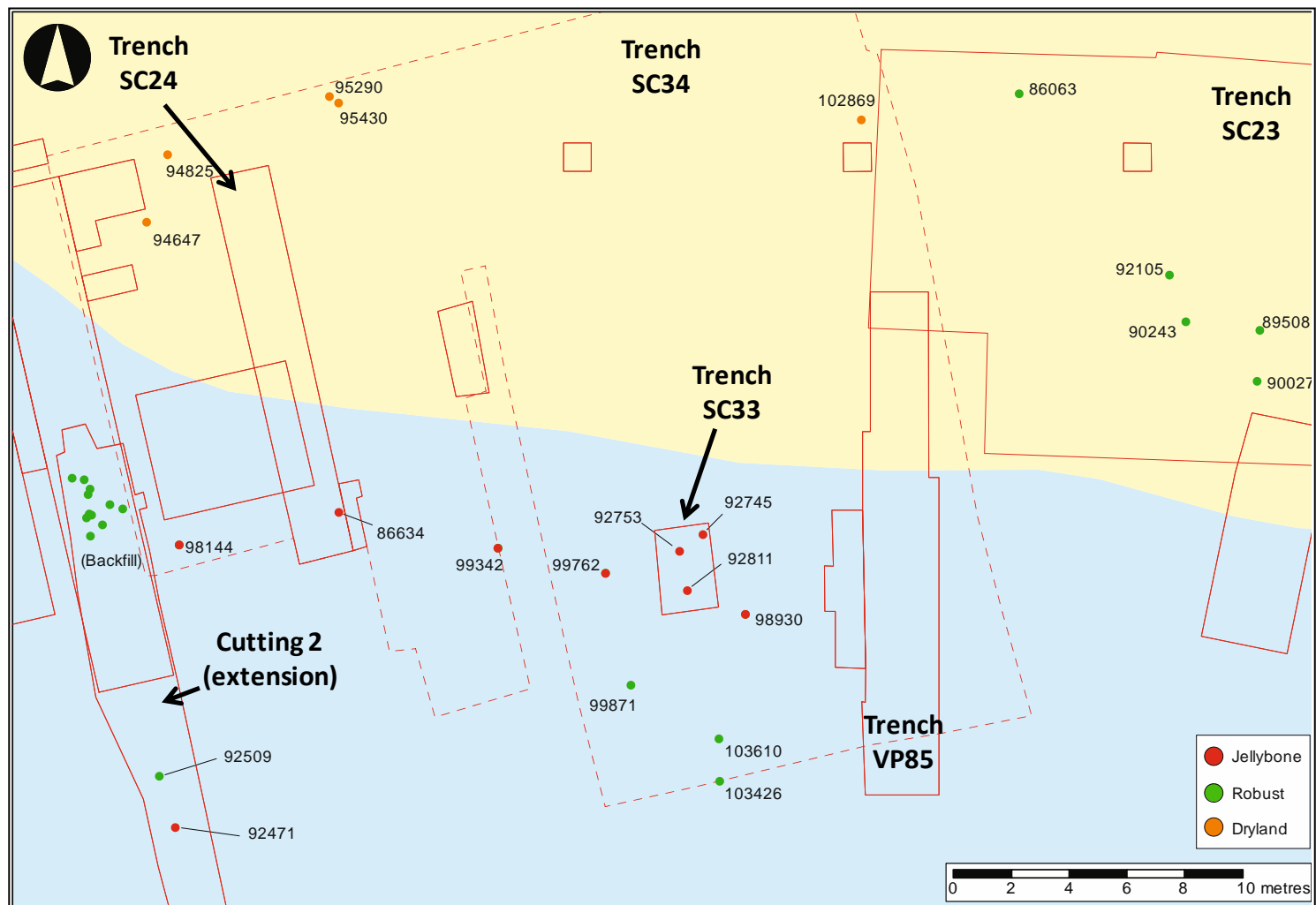


Figure 7.1: Location of all analysed bone samples from the 2013 excavations at Star Carr. (Originally in colour).

7.2.3 Wood from Star Carr

7.2.3.1 Early excavations

No material was available for analysis from the early excavations at Star Carr as the majority has been conserved. However, visual comparisons have been attempted using photos from the original site reports.

7.2.3.2 2007/2008 excavations

Analysis was carried out on one section from a split timber plank excavated from Trench SC24 in 2007, which was also used for the lab-based and burial experiments (Chapters 4, 5 & 6). It must be noted that this sample had been excavated approximately four years prior to analysis and had not been stored under anaerobic conditions. It is possible therefore that preservation of the timber when analysed was not representative of the condition upon excavation.

Archive condition assessment data for seven wood samples analysed shortly after excavation in 2007 and 2008 has also been provided (Panter, 2009). These samples were all willow, poplar or birch and came from either Trench SC24 or Test pit SC29 (both of which waterlogged and estimated to be acidic; Chapter 2).

7.2.3.3 2013 excavations

Almost all wood samples from the Star Carr site analysed as part of this study were collected during excavations in 2013. The majority of the samples were only fragmentary and for this reason, an assessment of condition through the sample was not possible. During re-excavation of Trench VP85 in 2013, pH measurements were taken at different depths down the profile of the trench (Chapter 2, Section 2.3.3.1) and non-archaeological wood samples were recovered directly from the peat adjacent to these measurements (series SC13-MA1-7; indicated by a yellow box in Figure 7.3). In addition, a number of samples were taken alongside pH measurements across the surface of Trench SC34 (series SC13-JA1-4). These are shown on Figure 7.3 and summarised in Table 7.2. The species of these samples have not been identified.

Ten fragmentary samples were also provided from within the extensive split timber platform indicated in the southern end of Trench SC34, uncovered during the 2013 excavations. These were all located within a brushwood 'trackway', indicated in Figure 7.3 and were either willow or poplar (M. Bamforth, pers.comm., 2013).

7.2.4 Comparative material (wood)

All wood analysed for comparison is summarised in Table 7.3.

7.2.4.1 Flag Fen (National Grid Reference: TL 22841 991144)

Flag Fen, a Bronze Age site located on the East Anglian Fens, has yielded vast amounts of archaeological wood (mainly oak) during excavations over the past 30-40 years (Taylor, 1992). The area has suffered from drainage and peat shrinkage over past decades (Pryor, 1991) and as such may provide a comparable site to Star Carr, where drainage is also known to be occurring (Boreham *et al.*, 2011; Bradley *et al.*, 2012). It has been noted that the extensive drainage of Flag Fen has caused visible deterioration of the archaeological timbers in certain areas of the site (Powell *et al.*, 2001).

Wood samples, mainly of oak, were analysed from four different trenches with different site hydrology (I Panter, pers. comm., 2012). In summary, those samples from Test pits 1 and 3 had been waterlogged upon excavation whereas those from Trench 1 were dry. Test pit 2 had been previously excavated; a section of a stake from this trench (sample D00128) was sampled in three places as shown in Figure 7.2, spanning parts of the sample that had been previously exposed and the permanently waterlogged base.

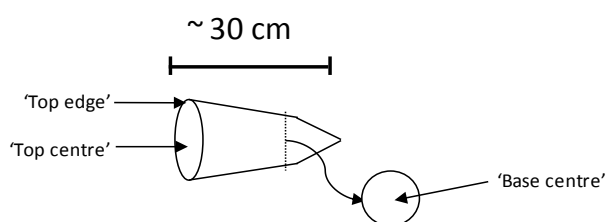


Figure 7.2: Illustration of where samples from stake D00128 were taken (not drawn to scale).

7.2.4.2 Must Farm boats (National Grid Reference: TL 235 968)

Eight Bronze Age log-boats were uncovered at Must Farm near Flag Fen in 2011-2012. All 8 log boats appear to have been purposefully sunk, and therefore it is assumed that they had been continuously waterlogged (Panter, 2013). The boats have been classified only as 'oak' and 'non-oak'.

Table 7.2: Summary of all wood samples analysed from Star Carr. Where the wood species is known, this is listed.

		Sample Information			
		Sample Name	Year of excavation	Trench (depth)	Description
Archive data from YAT		2007 plank	2007	SC24	Heavily deteriorated, stored damp. Acidic
		YAT-45		SC24	Fragment of willow/poplar
		YAT-B0025		SC24	Fragment of willow, top of sequence
		YAT-B0325		SC24	Fragment of willow, middle of sequence
		YAT-B0371		SC24	Fragment of willow, base of sequence
		YAT-111	2008	SC29	Fragment of birch, close to lake edge
		YAT-118		SC29	Fragment of poplar, close to lake edge
		YAT-119		SC29	Fragment of birch, close to lake edge
		SC13 – MA1	2013	VP85 (surface)	Fragment
	SC13 – MA2	VP85 (10 cm)		Fragment	
	SC13 – MA3	VP85 (20 cm)		Fragment	
	SC13 – MA4	VP85 (30 cm)		Fragment	
	SC13 – MA5	VP85 (40 cm)		Fragment	
	SC13 – MA6	VP85 (50 cm)		Fragment	
	SC13 – MA7	VP85 (60 cm)		Fragment	
	SC13 – JA1	SC34 (surface)		Fragment	
	SC13 – JA2	SC34 (surface)		Fragment	
	SC13 – JA3	SC34 (surface)		Fragment	
	SC13 – JA4	SC34 (surface)		Fragment	
	SC13 – JC4	SC34 (surface)		Fragment	
	94023	SC34 (timber platform)			Willow, robust
	94009				Willow, robust
	94004				Willow, robust
	98005				Poplar, robust
	94018				Poplar, robust
	93556				Poplar, very crumbly
	93554				Willow or poplar. Robust
	94006				Willow or poplar. Robust
	94025			Willow or poplar. Robust	
	94010			Willow or poplar. Robust	

Table 7.3: Summary of all wood samples analysed for comparison.

Sample Information				
Sample Name	Year of excavation	Trench (depth)	Description	
FF - D0003	2011/2012	Trench 1	Crumbly, oak timber	
FF - D0007			Crumbly, oak timber	
FF - D0053		Test pit 1	Robust, some compression. Oak timber	
FF - D0052			Robust, some compression. Oak timber	
FF - D0128 Top		Test pit 2	Crumbly, top part of exposed stake	
FF - D0128 Centre			Centre of stake, underneath ground	
FF - D0128 Base			Edge of base of stake, underneath ground	
FF - D0149		Test pit 3	Robust, some compression. Oak timber	
FF - D0155			Robust, some compression. Oak timber	
Must Farm boat 1		Must Farm - Unknown		Good condition, waterlogged. Oak
Must Farm boat 2				Good condition, waterlogged. Oak
Must Farm boat 3				Good condition, waterlogged. Oak
Must Farm boat 4				Good condition, waterlogged. Oak
Must Farm boat 5				Good condition, waterlogged. Non-oak
Must Farm boat 6	Good condition, waterlogged. Oak			
Must Farm boat 7	Good condition, waterlogged. Oak			
Must Farm boat 8	Good condition, waterlogged. Non-oak			

Flag Fen

Must Farm

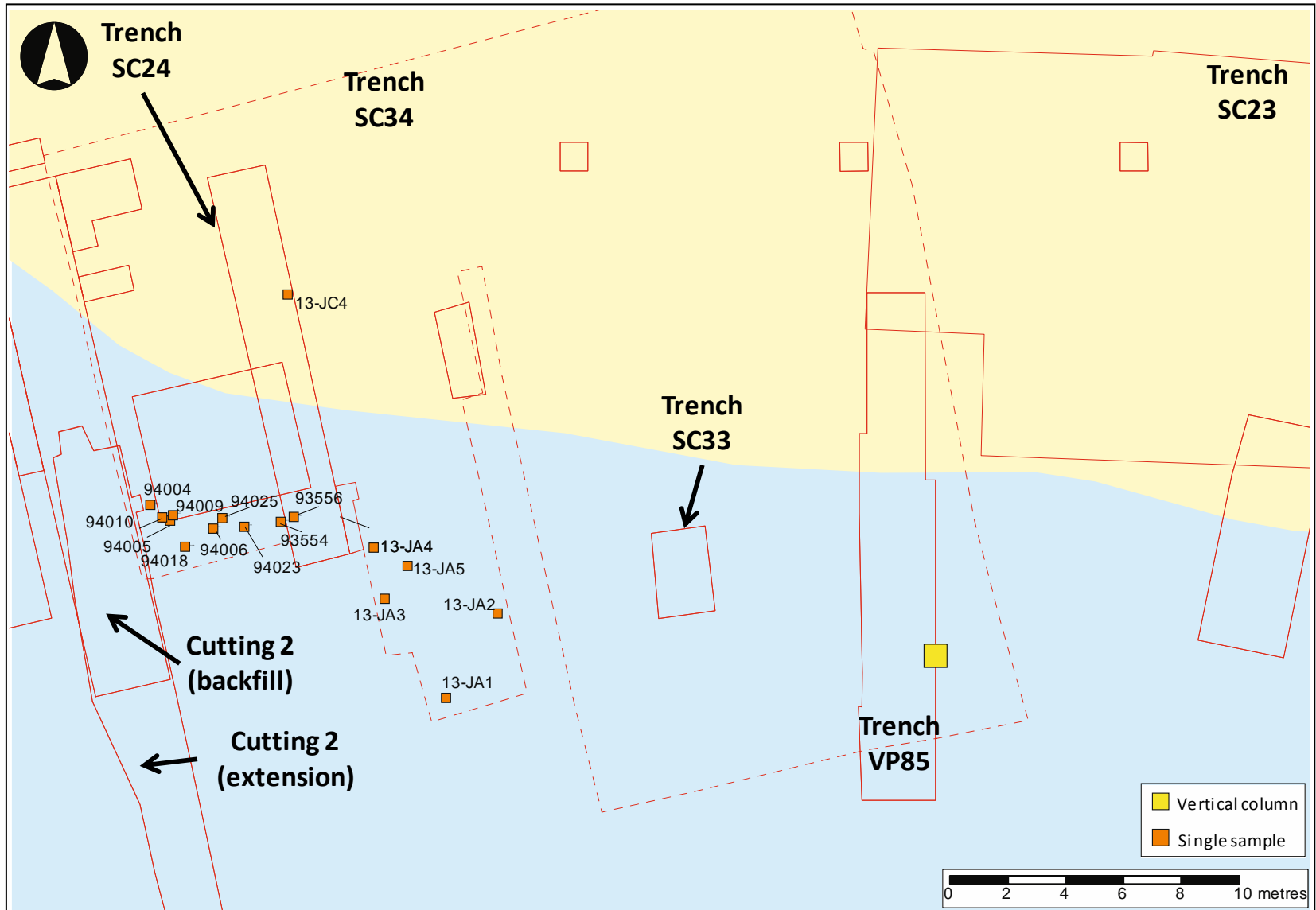


Figure 7.3: Location of all analysed wood samples from most recent excavations (2013) at Star Carr. (Originally in colour).

7.3 Results and discussion: Bone

7.3.1 A review of previous analysis

Assessment of bone preservation carried out during excavations in the 1950s and 1980s was limited to visual analysis. A difference in preservation between areas of the site was acknowledged even by Clark (1954); although the majority of both bone and antler are understood to have been robust and described as “firm” (Clark, 1954, pg 7), some pieces found further away from the lake edge were described as “dark in colour and soft as leather” (Clark, 1954, pg 1).

Excavations in 1985 and 1989 uncovered a large array of well-preserved faunal material, although a number of fragments of bone were assessed to be in a poor state of preservation (Rowley-Conwy, 1998). Further detail was not recorded.

Two ‘jellybone’ samples were discovered in 2007 and 2008 (Milner *et al.*, 2011a). Sample SC07 – 86634 was located in the lower, waterlogged end of SC24: a trench extending into the wetland area of the site (see Figure 7.1). Geochemical analysis by Boreham *et al.* (2011) revealed pH values of between 2.5- 3 in the lower end of SC24. The 2008 ‘jellybone’ was discovered in Test pit SC29 located north of the site (see Chapter 6). Geochemical analysis of SC29 revealed the pH to be approximately 3.4 (A. Needham, pers. comm., 2011).



Figure 7.4: 2007 ‘jellybone’ sample showing its flexibility, probably due to extensive demineralisation (reproduced with permission from Milner *et al.*, 2011a). (Originally in colour).

Analysis of the two ‘jellybones’ was carried out shortly after excavation (Milner *et al.*, 2011a). Histological integrity was determined by optical microscopy and TEM according to the protocol outlined in Chapter 3. Both bones were found to be almost completely demineralised, and elevated total amino acid concentrations further confirmed the extent of this demineralisation. However, the low levels of amino acid racemisation indicated that deterioration may either have occurred very rapidly, or that broken down protein chains and

amino acids had leached out of the bone, reducing the observed racemisation. A difference in total amino acid concentration between the inner and outer parts of the bones also indicated that HA was more heavily depleted on the outside of the bone (Milner *et al.*, 2011a).

Analysis of the more robust bones from excavations between 2007 and 2010 had not been carried out prior to this study, beyond visual observation. However, visual observations have suggested that much deterioration observed in the more robust bones, such as longitudinal splitting of rib bones, occurs rapidly after excavation and drying out (B. Knight, pers. comm., 2010).

7.3.2 Further analysis

All analysis of archaeological bone undertaken as part of this study was carried out as described in Chapter 3 unless otherwise stated. Analysis of geochemical samples was carried out as described in Chapter 2, Section 2.3.3.1.

7.3.2.1 Visual analysis

7.3.2.1.1 Early excavations

The bone retrieved from the spoil heap in 1948 was incredibly well preserved and displayed very little discolouration. Similarly, most of the bones seen from the collection at the British Museum were robust in appearance; although these were dark in colour, most of the bones had been treated for conservation and discolouration may be a result of this (Figure 7.5, bottom two pictures).

However, in several of the bones in the British Museum collection, a slight 'chalkiness' could be identified and parts of the surface had flaked away (Figure 7.5, top right). This further suggests that even in the original excavations at Star Carr, parts of the site may have been less conducive to good preservation of bone than others. This is in agreement with the original site report, where Clark identified that bone preservation was less good away from the lake edge (Clark, 1954), although the exact location of the observed finds cannot be determined.



Figure 7.5: Bone retrieved from the spoil heap in 1948 (top left) and bones held in the British Museum collection from original excavations at Star Carr. Site locations are unknown. Many were observed to be robust (bottom), but some bones show advanced degradation, with chalky deposits and severe cracking (top right). (Originally in colour).

7.3.2.1.2 2007/2008 excavations

All samples analysed from Trench SC23 from the 2007 and 2008 excavations were yellow in colour, brittle and chalky. They could easily be ground to a powder using an agate pestle and mortar. This brittleness indicates that collagen has been depleted, as collagen lends bone its elasticity (Currey, 2002) and is in contrast to the often 'leathery' bones that were reported uncovered from the lake edge deposits (Milner *et al.*, 2011a). The 'jellybone' samples from 2007 and 2008 (analysed immediately post excavation and reported by Milner *et al.*, 2011a), were recovered from Trench SC24 which is partly in the wetland area of the site.



Figure 7.6: Chalky and brittle bone fragments, typical of all those found located in the dryland part of the site in 2007 and 2008. (Originally in colour).

7.3.2.1.3 2010 excavations

Upon excavation, the bones recovered from the backfill of Cutting 2 in 2010 were determined to be relatively robust (B. Knight, pers. comm., 2010). However, alteration was observed after 2-3 months of storage. In many of the bones (particularly rib bones) small crystals had formed, presumably following drying. In some cases this resulted in the longitudinal splitting of the bones. Orange formations were also observed on the surface of several bones (Figure 7.7, centre). This was also observed in the field burial experiments (Chapter 6). A test using potassium thiocyanate as an indicator on these deposits from sample number 92423 confirmed them to be iron based (Feigl & Anger, 1972; Chapter 6 Section 6.3.2.2).

Samples excavated from below the backfill of Cutting 2 (Context 234) were more leathery in appearance and slightly bendable. The three samples excavated from SC33 (a wetland trench; Figure 7.1) were far more discoloured and soft, and have been classified as 'jellybones'.



Figure 7.7: Bone excavated in 2010, showing splitting of rib bones (top), and a flaky surface on scapula (bottom left). Orange deposits formed post excavation. The 'jellybone' samples from SC33 (bottom right) are much darker in colour, and bendable. (Originally in colour).

7.3.2.1.4 2013 excavations

A large number of bone artefacts were discovered during the excavation of Trench SC34 in 2013, and preservation varied greatly. Those excavated from the dryland were reported to be crumbly, and of those excavated from the wetland trenches several were reported as

appearing to be in the process of turning to 'jellybone'. In particular, in bone such as scapula (where parts of the bone are thinner than others) a distinction could be made between 'jelly' regions in the dorsal surface and a more robust spine. However, many others from the wetland area were classified as being in a good state of preservation, particularly those recovered from the mud layers below the peat (Knight in Milner *et al.*, 2013; Figure 7.8, top).



Figure 7.8: Examples of bones recovered in 2013, showing grey concretions adhering to the surface (top), white chalky deposits in the centre of the bones (bottom left) and translucent 'jelly' on the surface (bottom right). (Originally in colour).

In several of the samples analysed here, grey concretions formed on the surface of the more robust bones following drying that were difficult to remove (Knight, pers. comm., 2013; Figure 7.8, top). Tests using the potassium thiocyanate method showed these not to contain iron. Total amino acid analysis was also carried out on the concretions and amino acids were present in the relative concentrations characteristic of collagen. This indicates that the

concretions originate from collagen, although no further analysis has been carried out to confirm this.

A number of bones excavated from the wetland area of the site were so ‘jellyfied’ that they were almost translucent in appearance, and layers of this jelly appeared to be peeling away. Within the jelly, white powdery deposits were often found (Figure 7.8, bottom two pictures).

7.3.2.2 AAR analysis

All samples listed in Table 7.1 were analysed by HPLC to determine the total amino acid content and aspartic acid racemisation (D/L Asx).

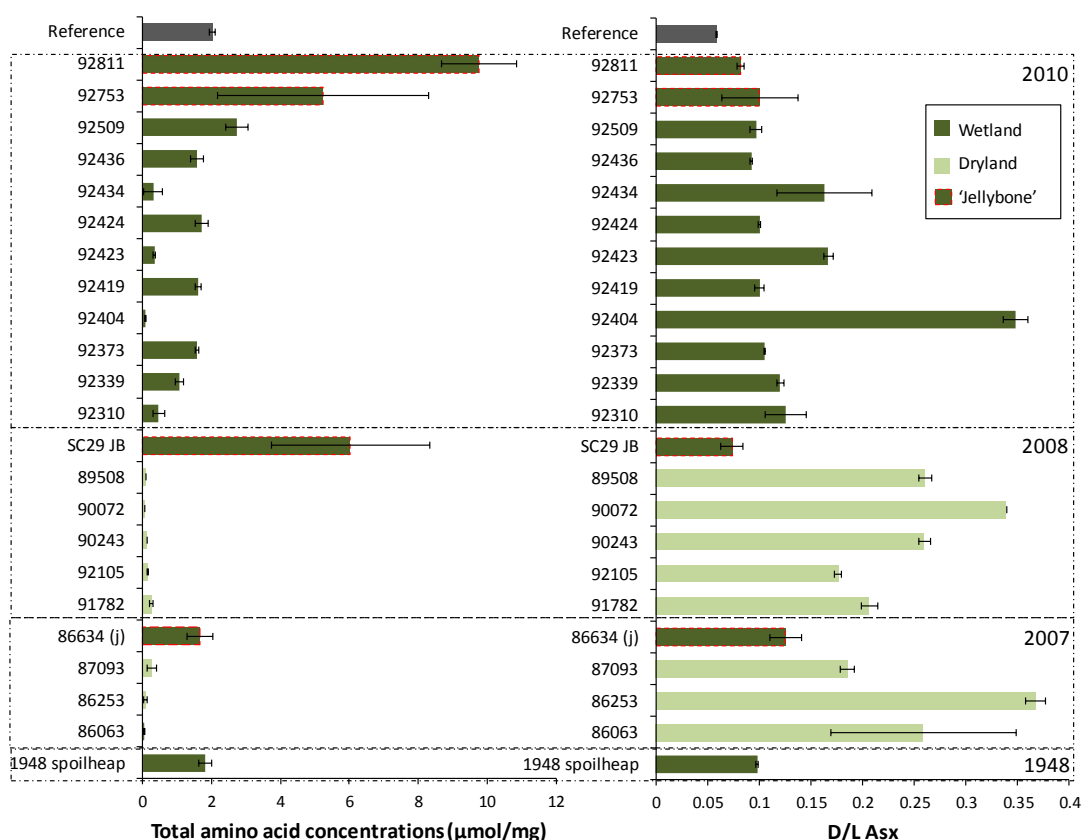


Figure 7.9: Total amino acid concentrations (left) and Asx racemisation (right) measured in a number of samples excavated from Star Carr compared to a fresh untreated bone (‘reference’). Those samples categorised as ‘jellybone’ following visual analysis are indicated. Full sample details are shown in Table 7.1. (Originally in colour).

As expected, most of the bones categorised as ‘jellybone’ have a much higher amino acid content than a control sample, indicating loss of HA (Figure 7.9, left). In contrast, very low amino acid concentrations are seen in samples recovered from the dryland part of the site (as low as 0.03 µmol/mg, compared to 2 µmol/mg in fresh bone). While in the wetland regions, bones have been identified as turning to ‘jelly’ via the loss of HA, an alternative mode of

diagenesis seems to be occurring in the dryland part of the site, leaving a mineral shell with very little collagen remaining.

The conspicuous difference in composition between bones from the wetland compared to dryland areas is likely to be related to the difference in pH, which has been measured as only mildly acidic in the dryland parts of the site (approximately pH 4 – 5.5; Boreham *et al.*, 2011). Lab-based experiments (Chapter 4) have shown how this would result in less loss of HA, as buffering of the acidity is much more rapidly achieved.

However, the reasons that collagen has been lost is less clear, as collagen can survive very well in an archaeological context under normal conditions (e.g. Collins *et al.*, 2002). It is possible that percolation of groundwater through the archaeological zone in the dryland areas would accelerate the loss of collagen as dissolved components are quickly washed away (Hedges & Millard, 1995). Alternatively, the aerobic and neutral conditions have allowed biological deterioration of the collagen to occur (e.g. Child *et al.*, 1993).

Data from lab-based experiments suggest that collagen is fast to break down following loss of HA (Chapter 4). This can be indicated by increased racemisation of amino acids, either due to more terminal positions becoming available, or an increased level of conformational freedom allowing the in-chain racemisation of Asx (e.g. Collins *et al.*, 1999). Elevated levels of Asx racemisation are seen in samples recovered from the dryland areas, further indicating that collagen has been heavily degraded (Figure 7.9, right). Racemisation exceeds that observed in a 112 ka rhino bone from Kirkdale (D/L = 0.13; Buckley & Collins, 2011), indicating that collagen is heavily deteriorated.

In contrast, many of the bones defined as 'jellybone' display a similar Asx D/L value to modern untreated bone (approximately 0.06) despite the fact that HA has been removed. This may be the result of a fluctuating water-table, as if small fragments of collagen are washed away this would reduce the observed racemisation (Dobberstein *et al.*, 2008). Evidence for a fluctuating water-table has been reported by both Boreham *et al.* (2011) and Brown *et al.* (2011).

Furthermore, during excavation of the wetland trenches it appeared that the majority of archaeological material was located above the water-table (various excavators, pers. comm., 2010). Alternatively, low racemisation in 'jellybones' could be the result of such rapid and recent loss of HA that the collagen has not yet had chance to racemise (Milner *et al.*, 2011b). This is supported by the observation of low levels of Asx racemisation in samples that became rapidly demineralised when treated in pH 1 sulfuric acid in lab-based experiments (Chapter 4).

The '1948 spoilheap' sample has both a total amino acid concentration and D/L Asx that is very similar to fresh modern bone, suggesting that minimal deterioration has occurred. This is in

agreement with visual analysis of the sample. Similarly, in some of the more 'robust' bones from the 2010 excavations (i.e. those from the backfill of Cutting 2), similar concentrations of amino acids were detected as in fresh bone. This indicates that little loss of HA has occurred. Geochemical data was not recorded near these samples. However, the investigation by Boreham *et al.* (2011) revealed evidence to suggest that pH was considerably higher in previously excavated trenches. This was attributed to the mixing up of calcium-rich topsoil with the acidic sediments resulting in gypsum formation, thus neutralising the acidic sulfates (see Chapter 2). A much lower acidity in Cutting 2 would explain the good preservation observed in these bones. Asx D/L values in the region of 0.07-0.08 are comparable to racemisation measured in cow bones from both Tanner Row (D/L = 0.073) and Coppergate (D/L = 0.08). This further suggests that deterioration of collagen is not unusual in the robust bones from Star Carr.

Analysis of both the outer layer and inner layer was carried out on a number of bones excavated in 2010 where the sample size allowed (Figure 7.10). Concentrations in the outer layer are not consistently lower than the inside of the sample in bones analysed from 2010 excavations and differences are mainly within the margin of error (one standard deviation calculated from replicate analysis), indicating that HA loss is similar throughout the bone.

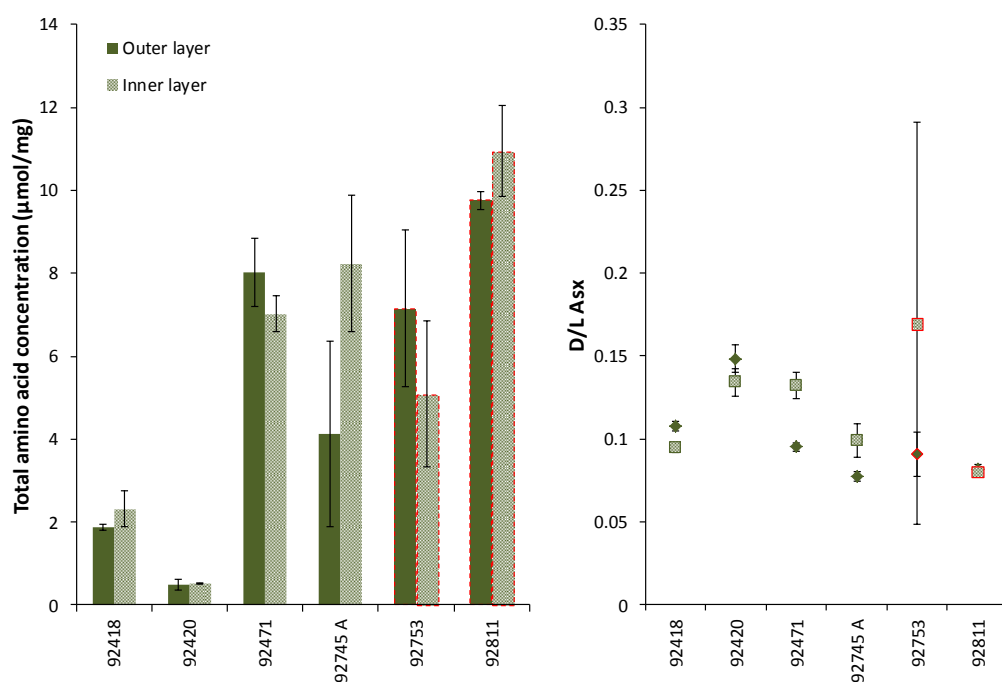


Figure 7.10: Comparison of total amino acid content (left) and Asx racemisation (right) for inner and outer sub samples for a number of samples from 2010 excavations. Those bones identified as 'jellybone' are outlined in red (samples 92753 and 92811). (Originally in colour).

Ordinarily, we may expect higher levels of racemisation on the outer layer of the bones where the collagen is more exposed to chemical and biological influences, leading to its breakdown and subsequent racemisation. Indeed, this is seen in all bones characterised as 'robust' (Figure 7.10, right). However, the reverse is true for the 'jellybone' samples. The lower observed racemisation towards the outside of the bones suggests that small chain proteins and amino acids are readily leaching out of and away from the bone; this would be more effective in the outer layers of the sample. This further evidences that a dynamic hydrological environment in parts of the Star Carr site may be leading to greater damage of bone material due to the continuous flushing away of dissolved components.

7.3.2.2.1 2013 excavations

Excavation in 2013 allowed a more comprehensive geochemical survey to be carried out (Chapter 2). Therefore, bone samples can be related to the measured pH at the location that they were discovered. 2013 samples were prepared and analysed by Becky Rhodes as part of her MChem research project (Rhodes, 2014).

Total amino acid content and Asx racemisation is shown for the bones analysed along with the measured pH where this is known, in Figure 7.11. For dryland samples, it has been assumed that the pH is mildly acidic – neutral, based on analysis reported by Boreham *et al.* (2011). For bones excavated from wetland areas, if a distinction could be made between parts of the bone that were 'jelly-like' (J) compared to 'firm' (F), both have been analysed. In others, the white chalky deposits in the centre of the bones (Ch) (Figure 7.8, bottom left) have been analysed in addition to the jelly outer layers.

Similarly as for previous excavations, dryland bones display a much lower total concentration than both a modern untreated bone and wetland bones (Figure 7.11, left). Again, Asx racemisation is comparable to that seen in the 112 ka bone from Kirkdale (D/L = 0.13; Buckley & Collins, 2011) indicating that collagen is breaking down, allowing racemisation to occur either by a higher concentration of short chain amino acids or due to conformational freedom in the protein chains as a result of breakdown of the triple helix (Smith & Evans, 1980; Orgel *et al.*, 2001). An alternative explanation is that this racemisation is due to contamination from soil microbes (Child *et al.*, 1993).

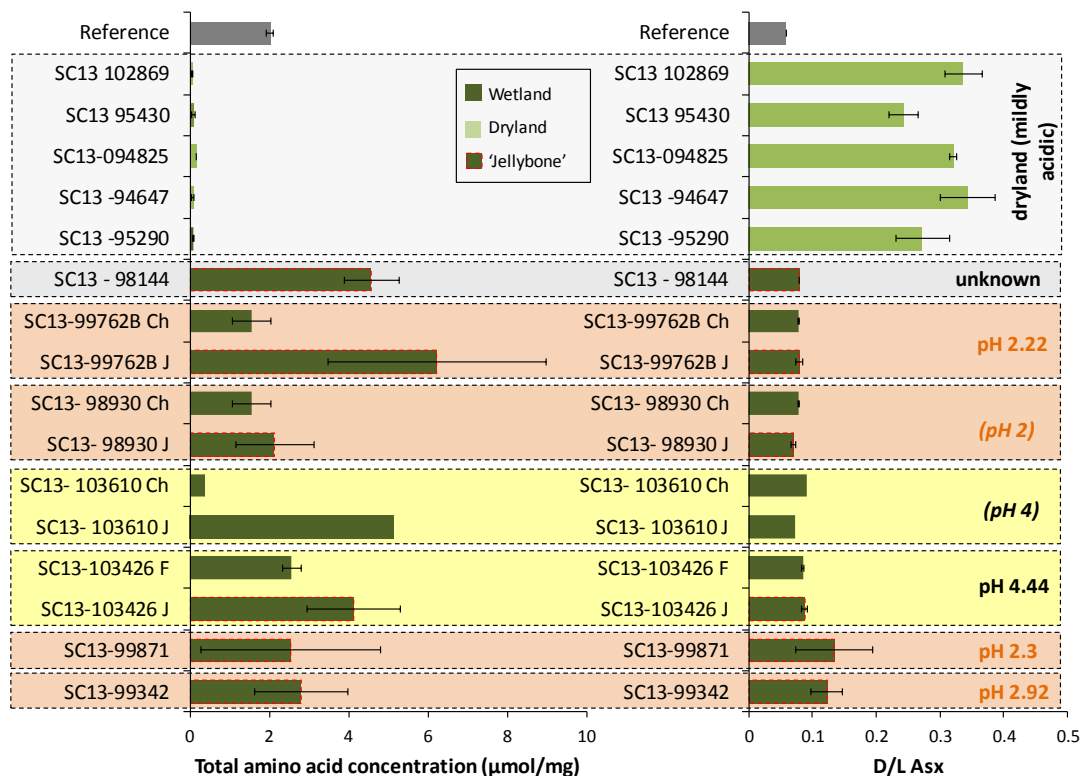


Figure 7.11: Total amino acid concentrations (left) and Asx racemisation (right) for bones excavated from Star Carr in 2013. Where known, the adjacent sediments pH is indicated, or estimated based on nearby sediments pH (in brackets). Where relevant, values for the jelly-like (J), chalky deposits (Ch) and firm (F) parts of the bone are shown. (Originally in colour).

All 'jellybone' samples have elevated total amino acid concentrations (indicative of HA loss) as expected. In the white chalky deposits however, low concentrations were detected in comparison to a modern sample. This suggests that this substance could be mainly HA.

Asx racemisation is low in all wetland bones, and there are no significant differences between the 'jelly' and 'chalky' fractions. The low levels of racemisation observed could be the result of the leaching away of short chain proteins, resulting in a lower observed racemisation and corroborates analysis of other 'jellybones' from 2007, 2008 and 2010.

The pH of the adjacent sediments does not appear to be a factor in determining either racemisation or HA loss. In particular, for one 'jellybone' (sample 103426), the measured pH was only mildly acidic. Lab-based experiments have shown that low levels of HA are lost even at pH of approximately pH 5 if the environment is dynamic. However, for bones to have lost enough HA for the bones to become translucent, it is likely that this process of dissolution and washing away of the HA would have had to occur for a prolonged period. An alternative explanation for the discovery of a 'jellybone' in mildly acidic sediment is that the pH has been fluctuating, and the pH has been lower than measured at the time of excavation. Furthermore, the pH of the adjacent sediments could also have been raised by dissolution of the HA itself.

7.3.2.3 Powder X-ray diffraction

A selection of archaeological samples were analysed using p-XRD in order to investigate alteration of the mineral fraction. The diffraction patterns of each have been characterised according to the definitions described in Chapter 4, and are summarised in Table 7.4.

Table 7.4: Summary of p-XRD patterns for analysed bones from Star Carr, described according to classifications defined in Chapter 4 (Section 4.3.3.1). (Originally in colour).

Key: **G** = gypsum structure; **S** = peak splitting; **MS** = mild splitting; **PS** = peak has shoulder; **LI** = low intensity peaks; **0** = no peaks; - = no alteration.

Sample Information				Sample analysis	
Sample Name	Year of excavation	Trench (context)	Description	p-XRD description	
Spoilheap	1948	Unknown	Very robust	PS	
86063	2007	SC23 (48)	Chalky, brittle	MS	
86253			Chalky, brittle	PS	
86634		SC24 (93)	Jellybone	0	
87093		SC24 (85)	Jellybone	PS	
89508	2008	SC23 (125)	Chalky, brittle	PS	
90027			Chalky, brittle	MS	
90243			Chalky, brittle	MS	
91782			Chalky, brittle	PS	
92105		SC23 (155)	Chalky, brittle	MS	
92310	2010	Cutting 2 (backfill)	Robust but splitting	PS	
92315			Robust but splitting	LI	
92339			Robust	LI	
92404			Robust	PS	
92419			Robust	PS	
92420			Robust	-	
92423			Robust but flaking	MS	
92424			Robust but flaking	PS	
92434			Robust but flaking	G	
92509			Cutting 2 (234)	Slightly jelly like	PS
92753			SC33	Jellybone	0
98144	2013	SC34 (wetland)	Jellybone	0	
98930			Jellybone	G	
103426			Firm in centre jelly at edges	MS	
94647	SC34 (dryland)	Chalky, brittle	LI		
95290		Chalky, brittle	LI		
102869		Chalky, brittle	S		

Many samples analysed that had been categorised as 'jellybone' yield a diffraction pattern with no peaks present that are characteristic of HA (indicated by '0' in Table 7.4). This signifies that all of the HA has been removed from the bone, which is in accordance with amino acid analysis, where elevated total concentrations were detected. FTIR analysis was carried out as outlined in Chapter 3, and the absence of any phosphate peaks confirmed the absence of any HA. In other samples, very low intensity (LI) HA peaks suggest that HA is highly depleted, although still present (Cullity, 1978).

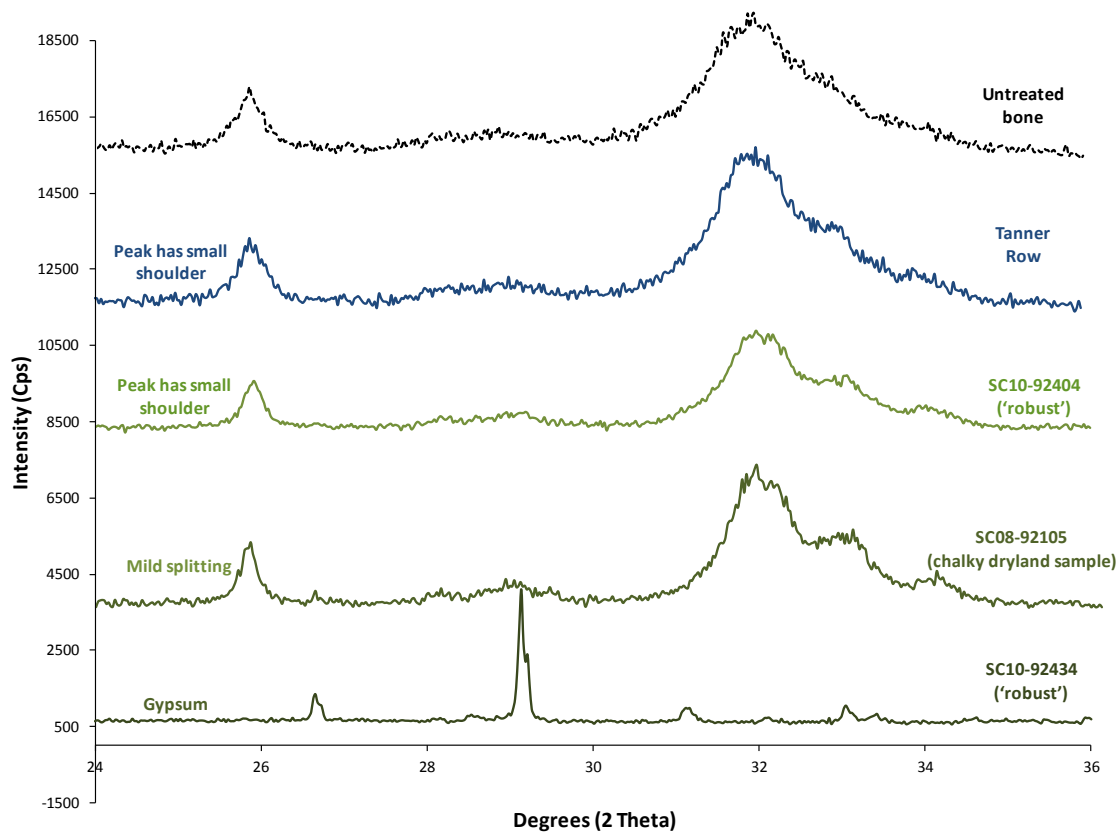


Figure 7.12: Diffraction patterns for a number of Star Carr samples, compared to an untreated modern bone sample. Patterns have been classified according to as outlined in Chapter 4 (Section 4.3.3.1). (Originally in colour).

Many of the chalky samples recovered from the dryland areas during 2007, 2008 and 2013 excavations display the greatest amount of splitting (Figure 7.12). This shows that although it has been suggested by amino acid analysis that these samples consist of a HA-rich shell, the HA has undergone alteration. Whether this occurred before or after loss of the collagen cannot be determined.

In order to assess what may be expected from p-XRD analysis of a robust archaeological sample, a cow metatarsal from the early medieval site of Tanner Row was also analysed. The HA peaks were only mildly shouldered, suggesting that little or no alteration of the mineral had occurred (Figure 7.12). A comparison with literature data for heavily degraded bones from an archaeological site in Western France was also made (approximately 2300 years BP) (Person *et al.*, 1995). Diffraction patterns obtained from these bones using similar experimental parameters tended to yield slightly shouldered or even split HA peaks, similar to the chalky, dryland samples from the 2007 and 2008 excavations at Star Carr, despite their much younger age (Person *et al.*, 1995). This suggests that many of the bones from areas of the Star Carr site

that are not defined as 'jellybone' are not unusually deteriorated (particularly those from the backfill of Cutting 2 and the '1948 spoilheap' bone).

One sample from 2010 (sample 92434) displays a diffraction pattern that is characteristic of gypsum (Kontoyannis *et al.*, 1997). This was also seen in several samples treated in pH 1 sulfuric acid in the lab-based experiments (Chapter 4) and indicates that dissolution and recrystallisation of the HA has occurred to such an extent that sulfur has been incorporated, forming calcium sulfate (gypsum), according to Equation 7.1.

Equation 7.1: Reaction of HA with sulfuric acid to form gypsum.



The white powdery deposits found inside some of the 'jellybones' excavated in 2013 were also found to have this same pattern (Figure 7.13). For this to occur, sufficient time would have to pass following dissolution and flushing away of the dissolved components for recrystallisation to occur. However, the transformation was also observed in 'dynamic' samples in the lab-based experiments, suggesting that this time period could be short.

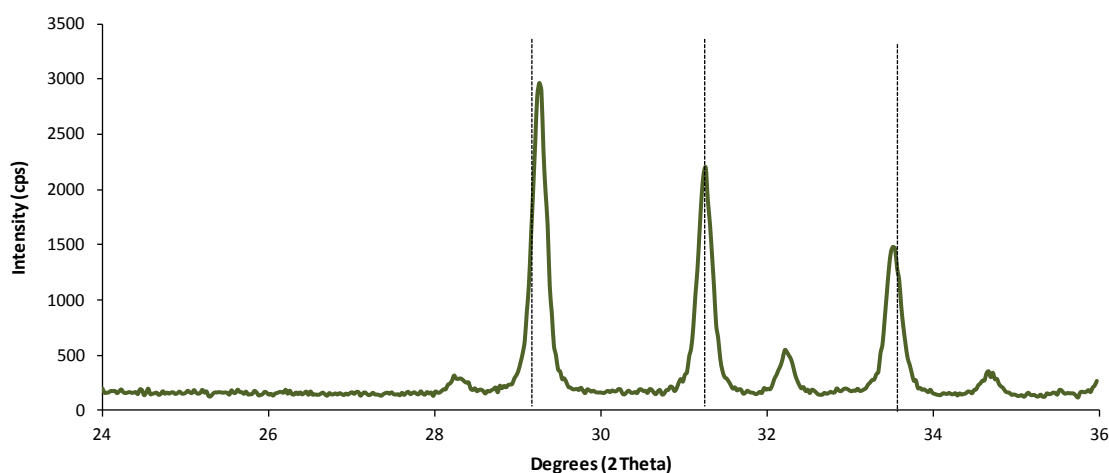


Figure 7.13: Diffraction pattern of the white powder present in several of the 2013 bones. Dotted lines indicate the typical position of peaks in pure gypsum (calcium sulfate).

7.3.2.4 Microscopy

7.3.2.4.1 SEM

A small selection of bones excavated from Star Carr in 2010 and 2013 were analysed by SEM as described in Chapter 3.

Deep cracks were seen throughout the 'robust' bones excavated from the backfill of Cutting 2 in 2010 (Figure 7.14). However, analysis of bones treated in acid (Chapter 4) showed that dissolution of the HA due to acidity occurs around the osteons, following the form of the histological structure, whereas in the 2010 robust samples they are more random. It is more likely that these cracks are due to compression from burial. However, nearer the surface of the sample, much deeper cracks were seen, causing splitting away of the outer surface.

The surface of the robust bones excavated from dryland deposits (chalky, brittle bones) in 2013 appeared much more porous in comparison to the 'robust' bones from the backfill of cutting 2 (Figure 7.14, bottom). In the wetland bones, this porosity appears to have followed the histological pattern of the bone, following the outline of the osteons, as opposed to the compression cracks seen in those excavated in 2010.

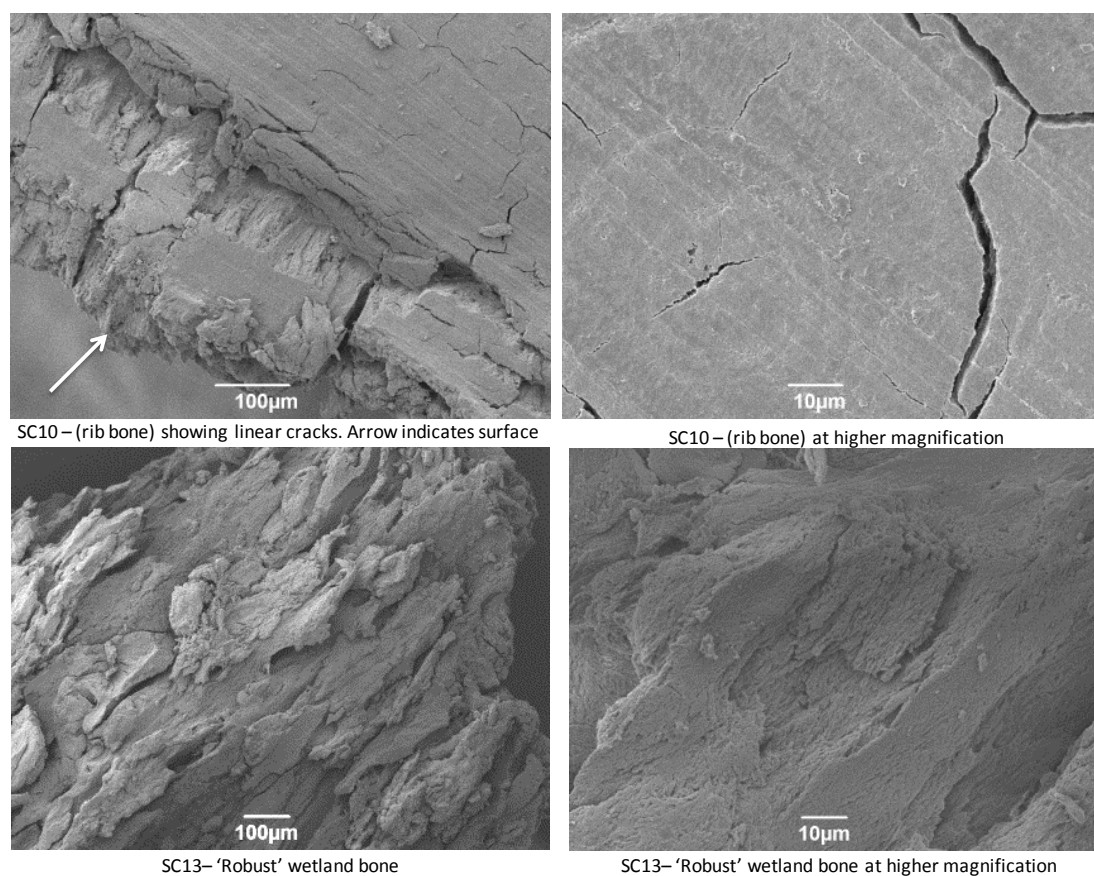


Figure 7.14: SEM images of 'robust' rib bone excavated from the backfill of Cutting 2 in 2010; cracking is likely to be due to compression (top), compared to the chalky, brittle bones excavated from the dryland areas of the site (bottom).

SEM analysis of 'jellybone' samples revealed large numbers of cracks and inclusions of particulate matter from the soil. Cracks were deep and longitudinal, giving the bone a fibrous appearance (e.g. Figure 7.15, top left). In addition, small fibrils were present that are very similar in size and appearance to those viewed in 'jellybones' made under lab conditions (Chapter 4). These are illustrated in Figure 7.15, bottom left, where these long fibrils can be seen in the background (circled). It is possible that these fibrils are large collections of collagen fibres, exposed due to the loss of HA. Comparison with an SEM image from Fantner *et al.* (2004), where collagen was exposed when bone was mechanically fractured, supports this.

In several of the 'jellybones' excavated in 2013, an extensive filamentous network was observed under SEM (Figure 7.15, top right). These have not been identified, but can be distinguished from the potential collagen fibres by their regular size and the presence of spores which that these are microbial or fungal (e.g. Buscot & Varma, 2005). It is impossible to tell whether these developed before or after excavation.

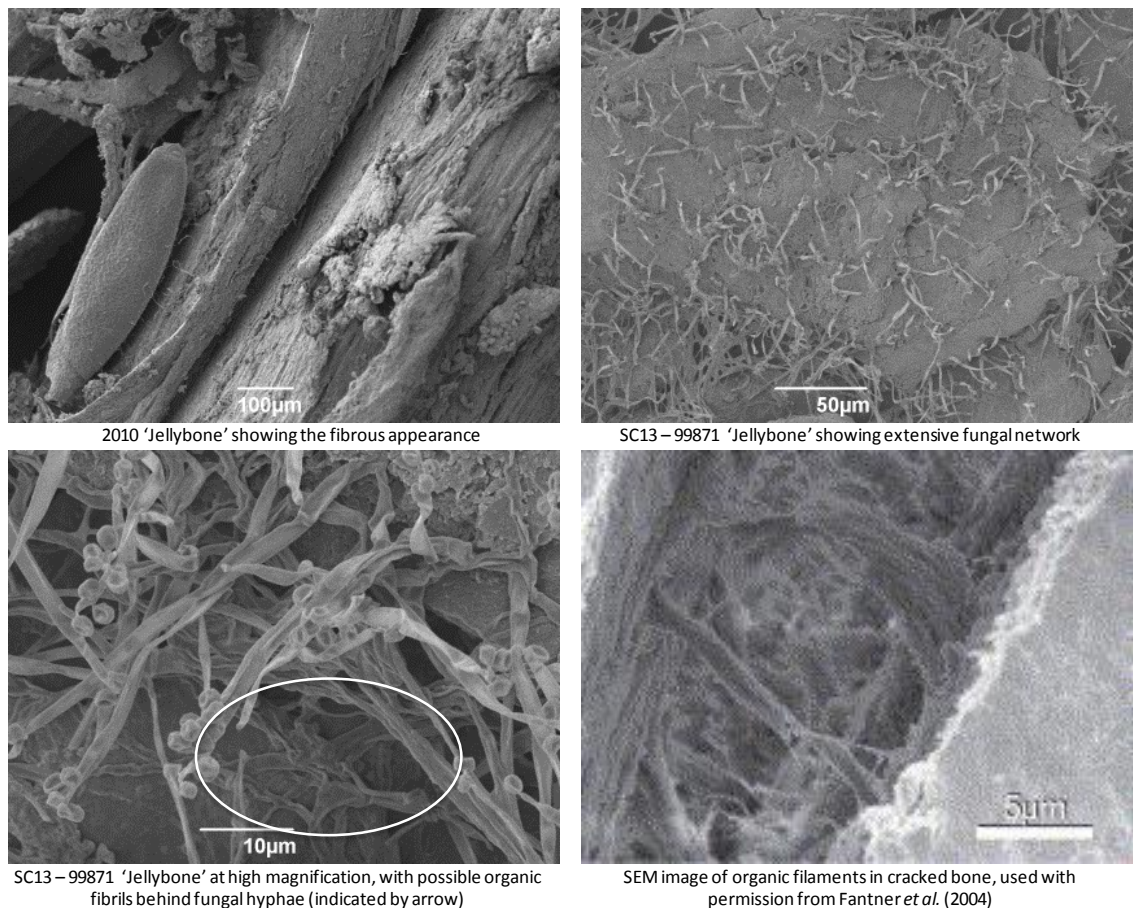


Figure 7.15: SEM images of 'jellybone' samples excavated in 2010 (top left) and 2013 (top right and bottom left), showing extensive fungal network. Comparison is made to an image taken from Fantner *et al.* (2004).

7.3.2.4.2 Thin-sectioning

Thin-sectioning was largely unsuccessful on archaeological samples due to their fragile nature, resulting in difficulties obtaining a thin-section. However, a number of bones from the 2010 excavations were analysed according to procedure outlined in Chapter 3.

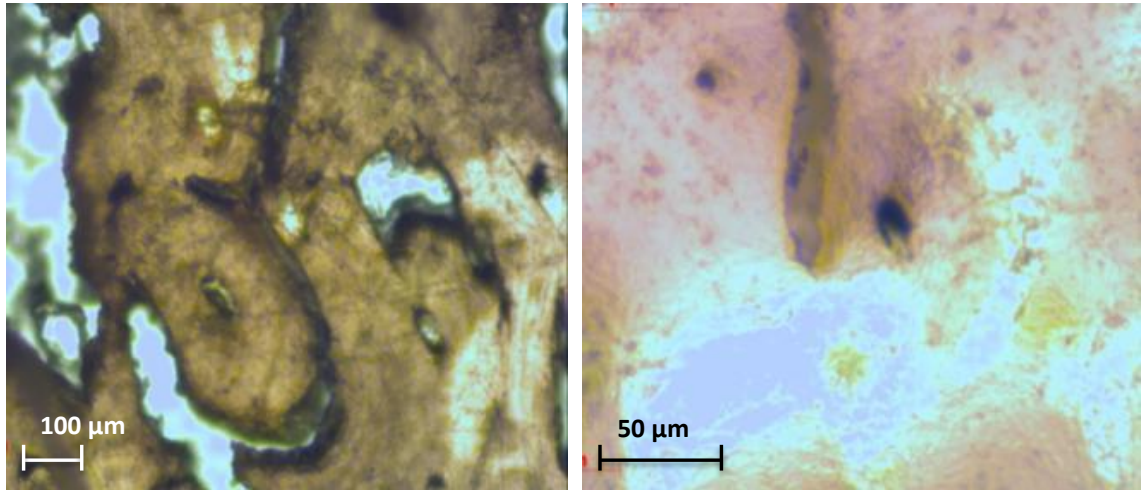


Figure 7.16: Optical microscopy images of thin-sections of a 'robust' rib bone (left) compared to a 'jellybone' from the 2010 excavations (right). (Originally in colour).

Comparison between the more 'robust' bones from the backfill of Cutting 2 and the 'jellybones' (Figure 7.16) reveals the complete loss of histological structure in the demineralised bones; osteons can barely be recognised.

Thin-section microscopy also aimed to confirm that no specific evidence for microbial activity could be seen, as often characteristic tunnelling patterns can be observed (Child *et al.*, 1993; Child, 1995; Jans 2005). However, no clear evidence of microbial colonisation was identified.

7.3.2.5 Summary of bone analysis

Analysis of both the amino acid content and HA of bone from Star Carr has shown primarily that the state of deterioration in bone artefacts differs greatly across the site. Bone from the dryland areas of Star Carr contain barely any collagen, yet HA is still present. A potential explanation for this is that HA has been sufficiently altered to allow biological degradation of collagen to proceed (Child *et al.*, 1993; Dixon *et al.*, 2008). The time frame in which this may have occurred could not be assessed, although Hedges *et al.* (1995) suggest that complete biological deterioration of collagen can occur within hundreds of years. Comparison with a 112 ka bone from Kirkdale (Buckley & Collins, 2011) demonstrated that in many of the bones excavated from the dryland areas of the site racemisation of Asx is elevated, indicating that collagen is relatively highly degraded.

In contrast, the discovery of large numbers of 'jellybones' during the 2013 excavation season, which contain almost no HA, suggest an alternative mode of deterioration. The low D/L Asx values in the majority of wetland bones suggest either that degraded fragments of collagen are quickly leached away or that loss of HA has occurred so recently that collagen breakdown has not yet had chance to occur. The significant difference in racemisation values across the Star Carr site indicate that localised geochemical conditions may be causing accelerated deterioration of the bone collagen only in very specific areas.

The p-XRD patterns of chalky deposits within some of the wetland bones revealed them to be gypsum. This was also seen in all mineralised bone samples buried in Star Carr peat in the lab-based burial experiments (Chapter 5) and indicates that complete dissolution and recrystallization of the HA has occurred. This both further highlights the extent to which the HA dissolves in an acidic environments, and indicates that the site hydrology could be sufficiently stagnant to allow recrystallization to occur. However, in lab-based experiments recrystallization as gypsum was observed even in a 'dynamic' environment (Chapter 4), indicating that this may occur in a very short space of time (days to weeks).

7.4 Results and discussion: Wood

7.4.1 A review of previous analysis

Descriptions of wood from the original excavations suggest that it was soft; roots had grown through the artefacts, although visual records show that it retained the macroscopic appearance of wood (Clark, 1954). Similarly, images of the excavations in 1985 and 1989 show the wood in the wetland parts of the site to be macroscopically identifiable as wood.

Wood excavated in 2006 and 2007 was visually observed to be well preserved, but on handling was found to be extremely delicate (Milner *et al.*, 2011a). The peat-wood interface was often very difficult to define and as a result wood was difficult to analyse (M. Taylor, pers. comm., 2010) Where possible, the condition of the wood was further assessed using SEM imaging and standard decay tests such as density and maximum water content (u_{\max}) (Milner *et al.*, 2011a). It was concluded that little or no cellulose was remaining in much of the wood, leaving only a lignin-rich skeleton.

7.4.2 Further analysis

7.4.2.1 Visual analysis

7.4.2.1.1 2007/2008 excavations

The sample stored for 4 years prior to analysis ('2007 plank') was incredibly crumbly and barely distinguishable from the surrounding peat. This may be a result of drying out as a result of exposure to air post-excavation. The sample had been stored damp rather than waterlogged.

The samples analysed by York Archaeological Trust in 2009 from the 2007/2008 excavations were described as 'soft and spongy' and described to be in much better conditions than the 2007 plank. Compression damage was possibly identified (Panter, 2009).

7.4.2.1.2 2013 excavations

All wood samples obtained directly from the site in 2013 were also soft and spongy, although they retained the appearance of wood.

7.4.2.1.3 Flag Fen/Must Farm

Although some compression was seen in the timber planks from Flag Fen, and the wood was slightly spongy, the samples retained the visual appearance of wood. An exception was the top of the exposed stake, D0128 and samples from Trench 1 (not waterlogged). This is likely to be

a result of oxygen being introduced into the burial environment, facilitating biological degradation.



Figure 7.17: Images of Must Farm log boat 1, and detail on log boat 3 (right), showing the excellent condition of the boat.

All samples from the log-boats deliberately sunk at Must Farm were also observed visually to be in very good condition (Panter, 2013). The boats all broadly retain their original structure (Figure 7.17) and tests such as drill decay profiles (Seaby, 1991) showed them to be robust, particularly in the centre.

7.4.2.2 Surface pH analysis

Following excavation (approximately 1 month), the pH of the water in which samples had been stored was recorded using a calibrated glass pH probe. This was carried out on the archaeological samples taken from the wooden platform during the 2013 excavations and those analysed by YAT from 2007 and 2008 excavations. Results are shown in Table 7.5. The plank from Trench SC24 that was stored for 4 years prior to analysis was not stored in water and therefore this was not possible. However, the pH was taken using pH indicator paper and found to be less than pH 1.

Geochemical analysis carried out in the field showed that sediment in Trench SC34 reached as low as pH 1.83 (Chapter 2, Section 2.3.3.1). The pH of the surface of many of the wood samples is much lower than this, particularly the '2007 plank'. This indicates that continued acidification could occur post excavation. This is in agreement with geochemical analysis carried out by Boreham *et al.* (2011) that showed that sediments rapidly increased in acidity post excavation. It is possible that the low pH observed in excavated wood is the result of these reactive sulfides being present within the highly porous structure of the wood. Indeed, chemical species present in a burial environment can often easily become incorporated into the wood structure (Hedges, 1990). Similar processes have been observed in wood excavated from a number of archaeological sites, particularly marine environments. Examples include the Vasa shipwreck (Almkvist, 2008) and the Mary Rose shipwreck (Sandström *et al.*, 2005).

Table 7.5: pH measured from the water in which wood samples were stored or the surface of the sample where this was not possible.

Sample Information					
	Sample Name	Year of excavation	Trench	Description	pH (surface or storage water)
	2007 plank	2007	SC24	Heavily deteriorated, stored damp. Acidic	< 1.00
Archive data (YAT)	YAT-45		SC24	Fragment of willow/poplar	1.70
	YAT-B0025		SC24	Fragment of willow, top of sequence	2.20
	YAT-B0325		SC24	Fragment of willow, middle of sequence	1.80
	YAT-B0371		SC24	Fragment of willow, base of sequence	2.00
	YAT-111	2008	SC29	Fragment of birch, close to lake edge	3.00
	YAT-118		SC29	Fragment of poplar, close to lake edge	2.70
	YAT-119		SC29	Fragment of birch, close to lake edge	2.50
		94023	SC34 (timber platform)	Willow, robust	1.53
		94009		Willow, robust	1.41
		94004		Willow, robust	1.31
	98005	Poplar, robust		1.43	
	94018	Poplar, robust		2.22	
	93556	Poplar, very crumbly		1.44	
	93554	Willow or poplar. Robust		1.48	
	94006	Willow or poplar. Robust		1.81	
	94025	Willow or poplar. Robust		1.33	
	94010	Willow or poplar. Robust		1.58	

7.4.2.3 Maximum water content (u_{\max})

Data from the 2007/2008 samples analysed by Ian Panter showed an average u_{\max} of 514 %, compared to 90-120 % expected for undecayed fresh wood. This suggests a relatively high level of decay, allowing increased water into the pores due to the removal of structural components (e.g. Hoffman, 1981; Panter & Spriggs, 1996). The majority of samples analysed from the 2013 excavations had values slightly higher than this (Table 7.6), suggesting that decay could be more advanced. Although samples were all analysed using a vacuum method adapted from Hoffman (1981), it must be noted that levels of error in u_{\max} measurements may differ depending on factors such as size of the sample and species. In addition, the inclusion of minerals and other species from the environment may reduce the u_{\max} value, and therefore may depend on the nature of the burial environment (Panter & Spriggs, 1996).

Comparison with u_{\max} values from the material analysed from Flag Fen suggests that decay is comparable; the highest value from Flag Fen is very close to the highest values from Star Carr in 2013. The majority of the Must Farm log boats have been identified as well-preserved and this is reflected in the u_{\max} data.

Table 7.6: u_{max} data for a number of samples from Star Carr as well as comparative material from Flag Fen and the Must Farm log boats (provided by Ian Panter).

	Sample Name	Year of excavation	Trench (depth)	Description	uMax (%)
Archive data (YAT)	2007 plank	2007	SC24	Heavily deteriorated, stored damp. Acidic	-
	YAT-45		SC24	Fragment of willow/poplar	442
	YAT-B0025		SC24	Fragment of willow, top of sequence	521
	YAT-B0325		SC24	Fragment of willow, middle of sequence	521
	YAT-B0371		SC24	Fragment of willow, base of sequence	652
	YAT-111	2008	SC29	Fragment of birch, close to lake edge	404
	YAT-118		SC29	Fragment of poplar, close to lake edge	550
	YAT-119		SC29	Fragment of birch, close to lake edge	652
		94023	SC34 (timber platform)	Willow, robust	858
	94009	Willow, robust		561	
	94004	Willow, robust		572	
	98005	Poplar, robust		594	
	94018	Poplar, robust		611	
	93556	Poplar, very crumbly		682	
	93554	Willow or poplar. Robust		640	
	94006	Willow or poplar. Robust		719	
	94025	Willow or poplar. Robust		506	
	94010	Willow or poplar. Robust		355	
Analysed by I. Panter	FF - D0003	2011/2012		Trench 1	Crumbly, oak timber
	FF - D0007		Crumbly, oak timber		250
	FF - D0053		Test pit 1	Robust, some compression. Oak timber	598
	FF - D0128 Top		Test pit 2	Crumbly, top part of exposed stake	510
	FF - D0128 Centre			Centre of stake, underneath ground	414
	FF - D0128 Base		Test pit 3	Edge of base of stake, underneath ground	707
	FF - D0149			Robust, some compression. Oak timber	387
	Must Farm boat 1			Must Farm - Unknown	Good condition, waterlogged
	Must Farm boat 2		Good condition, waterlogged		260
	Must Farm boat 3		Good condition, waterlogged		344
	Must Farm boat 4		Good condition, waterlogged		367
	Must Farm boat 5		Good condition, waterlogged		727
	Must Farm boat 6		Good condition, waterlogged		476
	Must Farm boat 7		Good condition, waterlogged		544
	Must Farm boat 8		Good condition, waterlogged		705

Wood from other waterlogged sites, for example the Viking site of Coppergate in York, also yields u_{max} values in the region of 400-700 % (Spriggs, 1981) despite being generally regarded as in a good state of preservation and suitable for conservation. This suggests that although wood is certainly deteriorated at Star Carr, at least from parts of the site this degradation is not particularly unusual for a waterlogged site of this age.

7.4.2.4 FTIR spectroscopy

For FTIR analysis, readings were taken directly from the outer surface of the dried samples and average peak heights calculated.

In all samples from the 2013 excavations, the cellulose peak at 1375 cm^{-1} (relating to absorption by the C-H bonds in cellulose; Pandey, 1998), is very low or completely absent, indicating that breakdown of the cellulose polymers has occurred. However, the 1325 cm^{-1} peak, (characteristic of the C-OH groups), is often still present although at very low intensity (Figure 7.18). This indicates that some cellulose remains, although it may be chemically altered. The same is seen in samples from Flag Fen, again suggesting that deterioration in wood at Star Carr is not significantly more advanced than may be expected for an archaeological site of this age. Some level of cellulose or hemi-cellulose loss would be expected to occur through slow chemical hydrolysis over the period of burial even in a neutral waterlogged environment (Hoffman & Jones, 1990).

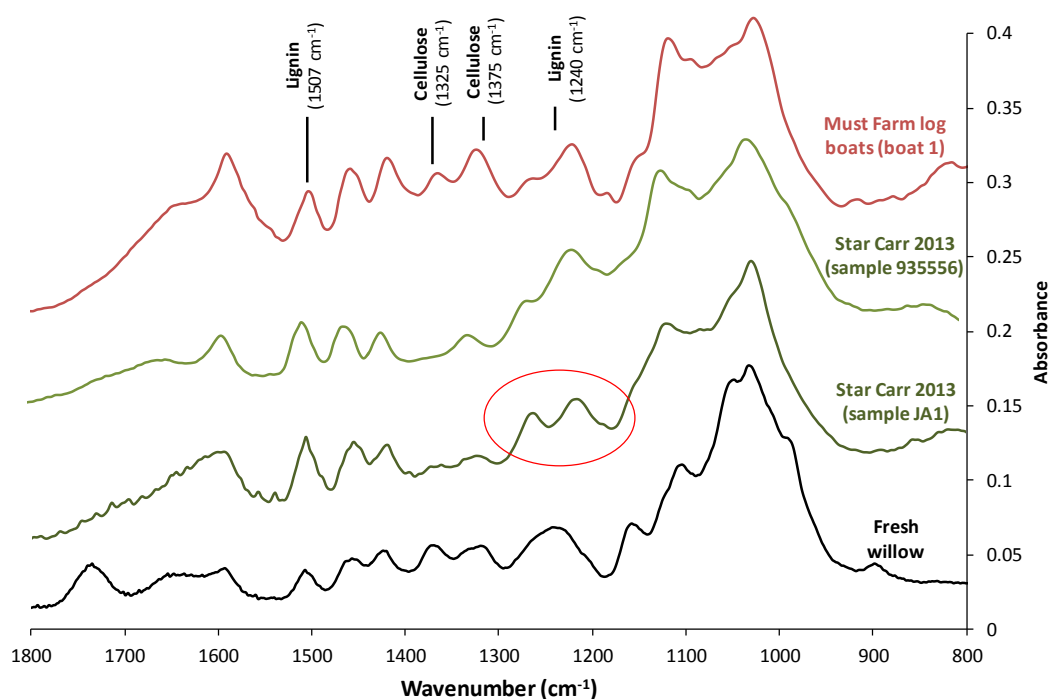


Figure 7.18: FTIR spectra for two samples from Star Carr compared to a fresh willow sample and a log boat from Must Farm. Important features are a reduction in the relative height of the cellulose peaks and splitting of the peak at 1240 cm^{-1} in archaeological samples (circled). These changes are slightly more significant in samples from Star Carr than the Must Farm boat. (Originally in colour).

In contrast, in several of the boats from Must Farm, the C-H peak at 1325 cm^{-1} does remain, suggesting that celluloses are much better preserved. This may be because the boats are from a much younger archaeological site than Star Carr, and that the boats were permanently waterlogged. This would slow down biological deterioration of both lignin and cellulose (e.g.

Blanchette, 1990). It is possible that an increased level of oxygen is the major factor causing cellulose depletion at both Star Carr and Flag Fen, where drying out of the site is known to be occurring. This may lead to increased biological activity and subsequent depletion of carbohydrates (e.g. Bjordal *et al.*, 1999; Blanchette, 2000; Gelbrich *et al.*, 2008).

In order to compare samples more comprehensively, L: C, 1507: C and 1507: 1240 ratios were plotted for all samples (see Chapter 3 for further discussion of these ratios; Figure 7.19). An increase in the L: C and 1507: TC ratios can be indicative of cellulose decay. For many of the Star Carr samples, these ratios are higher than for the Flag Fen and Must Farm boats, suggesting that cellulose loss is greater at Star Carr. The lowest ratio in Star Carr material is seen in sample 94010, which also showed the lowest u_{\max} value.

As the 1507 cm^{-1} peak is more stable than the 1240 cm^{-1} lignin peak (which relates to absorption by the C-O-CH₃ group), an increase in the 1507: 1240 ratio is indicative of lignin defunctionalisation (Pandey & Pitman, 2003), and in all samples this is elevated compared to the untreated willow sample (Figure 7.19). However, the increase does appear to be greater in the Star Carr samples, particularly when compared to the Must Farm boats.

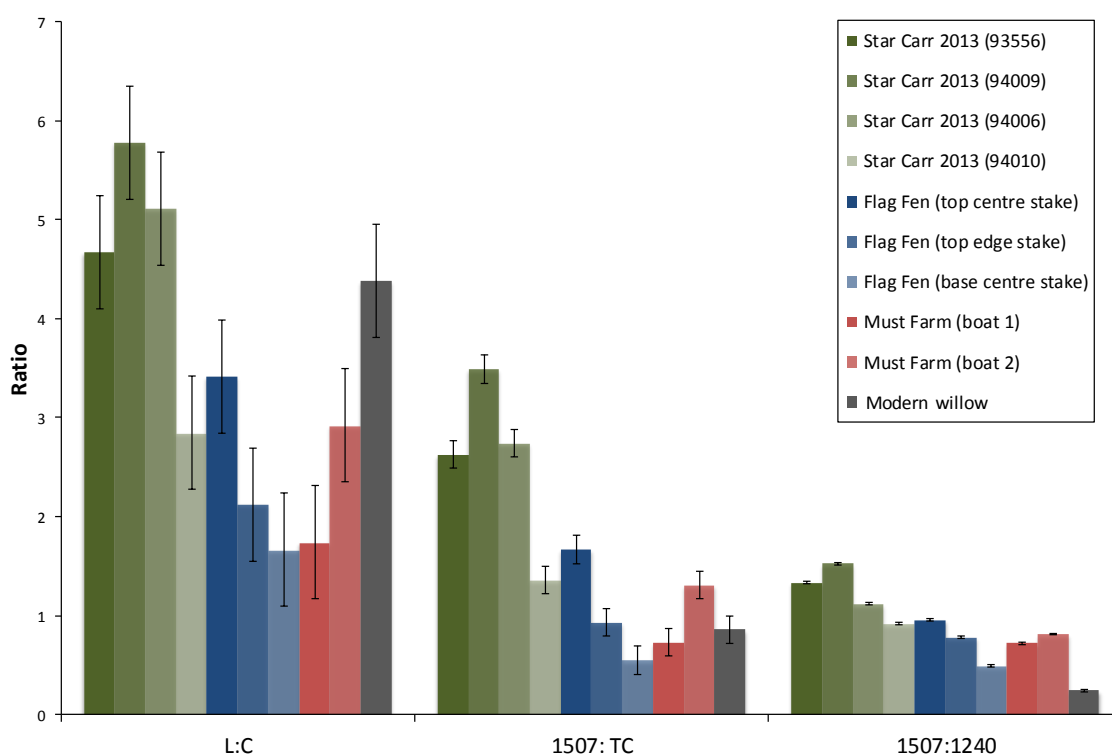


Figure 7.19: Plot of ratios derived from FTIR analysis of samples from Star Carr (green), Flag Fen (blue) and Must Farm (red) compared to a willow standard. Error bars are one standard deviation of 3 readings from the willow standard. An increase in the L: C and 1507: Total Cellulose (TC) peaks indicates loss of cellulose, and an increase in the 1507: 1240 peak indicates lignin defunctionalisation. (Originally in colour).

In addition, although in the majority of samples from Star Carr the peak at 1240 cm^{-1} was still intense, it was observed to have split, indicating that the chemical environment of the methoxy groups may have changed (Martinez *et al.*, 2005; Figure 7.18). This could indicate defunctionalisation of the syringol and guaiacol type units, even though the lignin may still be largely intact. A similar observation was made in samples buried in highly acidic peat from Star Carr in the lab-based burial experiments (Chapter 5). The absence of microbial activity there suggested that the process is chemically driven. However, similar changes could also occur due to microbial activity over time.

In the few samples where both the inner and outer parts were analysed, a distinction could be seen; the cellulose peaks were considerably lower. This is unsurprising as often the inner part of large artefacts has been more protected from the burial environment and chemical hydrolysis will proceed from the outer layers inwards (e.g. Hoffman & Jones, 1990; Almkvist 2008). This is demonstrated most clearly by a lower L: C ratio in the 'base centre' sample of D0128 from Flag Fen (Figure 7.19).

No FTIR analysis was carried out on samples analysed by YAT from the 2007 and 2008 excavations at Star Carr. However, analysis of the wooden plank stored prior to analysis revealed almost no characteristic peaks (Figure 7.20). When compared to the analysis of material excavated in 2013, which is fairly robust, it is evident that degradation of both cellulose and lignin is far more advanced. It is possible that this deterioration occurred post excavation, as the sample had been stored damp. This would be likely to increase biological activity, which can result in deterioration of both of the polymers (Hoffman & Jones, 1990; Blanchette, 2000).

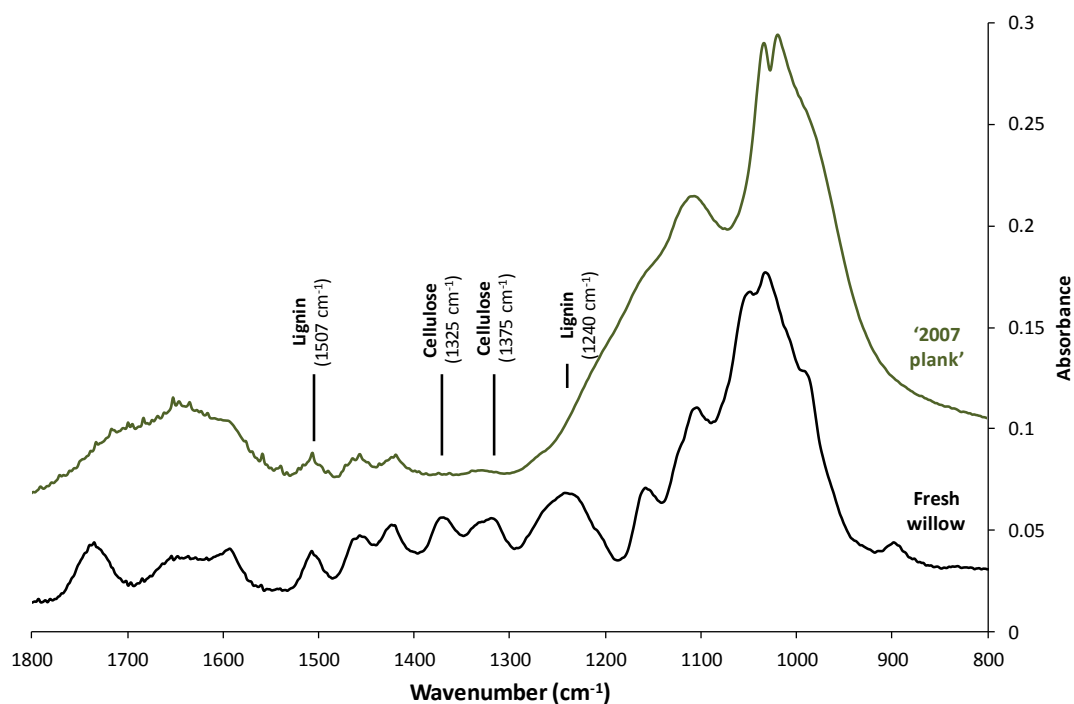


Figure 7.20: Samples from Star Carr 2007 excavations that had been stored for several years prior to analysis, compared to an untreated willow sample. Cellulose is indicated to have completely depleted, and loss of the 1240 cm^{-1} peak indicates extensive defunctionalisation of the lignin. (Originally in colour).

7.4.2.5 Py-GC

All archaeological samples listed in Table 7.2 and Table 7.3 were analysed by py-GC as outlined in Chapter 3.

In many samples from the 2013 excavations at Star Carr, peaks relating to cellulose were detected (before around 10 minutes retention time), although these were significantly reduced compared to a modern willow sample (Figure 7.21). This is in agreement with analysis by FTIR, where in the majority of samples very small peaks relating to cellulose were present, suggesting that although heavily depleted and chemically altered, cellulose has not been completely removed. In comparison to samples from both Must Farm and Flag Fen, these cellulose peaks were slightly lower in intensity. However, it must be noted that the concentrations of cellulose has not been quantified in this method, and therefore peak intensities can only be taken as a guide.

Peaks relating to lignin, eluting later in the chromatogram, are significant in all samples from Star Carr, confirming observations by FTIR that lignin is likely to remain in the samples. However, some differences are seen when compared to a modern sample, indicating that chemical alteration of the lignin has occurred. An increase in phenol indicates increased defunctionalisation of sub-units in lignin (Martinez *et al.*, 2005; Chapter 4 Section 4.4.4), and can be identified by a characteristic peak appearing at approximately 11 minutes retention

time. In several of the Star Carr samples (see sample 93554, Figure 7.21) the phenol peak is very high, particularly in comparison to one of the Must Farm boats. Again, this is in agreement with FTIR analysis, where alteration of the methoxy absorption (1240 cm^{-1}) was observed in all samples.

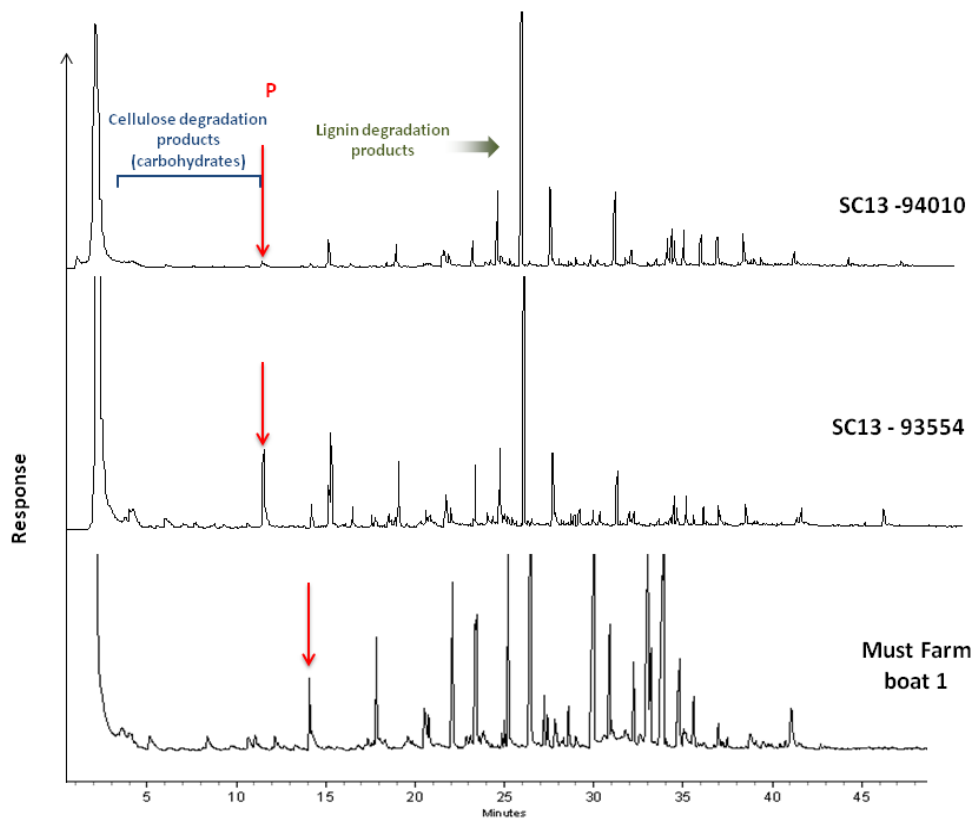


Figure 7.21: py-GC traces for 2 samples from Trench SC34 excavated in 2013 compared to a log boat excavated from the Bronze Age site of Must Farm (note that this sample was analysed using a longer GC column and as a result the peaks have slightly shifted). Whilst cellulose peaks are present, these are small, and an increase in the intensity of the phenol peak (indicated with an arrow for each sample) suggests lignin defunctionalisation. (Originally in colour).

Without applying a detection method such as mass spectrometry, the assignment of the peaks in the lignin region is problematic. However, by using commercially bought standards, the retention time for phenol was confidently assigned for each of the samples from Trench SC34. The phenol concentrations were corrected for the mass of sample analysed in order to determine relative phenol content for each sample, and compared to samples from Must Farm boats 1 and 2.

Replicate analysis of preliminary samples showed the calculations of phenol content to have a large degree of error (Chapter 3, Section 3.3.4.2). The potential reasons for include incomplete transfer of the sample from the pyrolysis unit to the GC and errors due to the small sample size. As such results need to be interpreted with caution. However, most samples from the 2013 excavations at Star Carr appear to have an increase in phenol content compared to the

modern willow sample and the Must Farm log boats. An exception is seen in sample 94010, where a low lignin: cellulose ratio as measured by FTIR also suggests that this sample is the least deteriorated. This indicates that defunctionalisation of lignin has occurred, and corroborates results by FTIR.

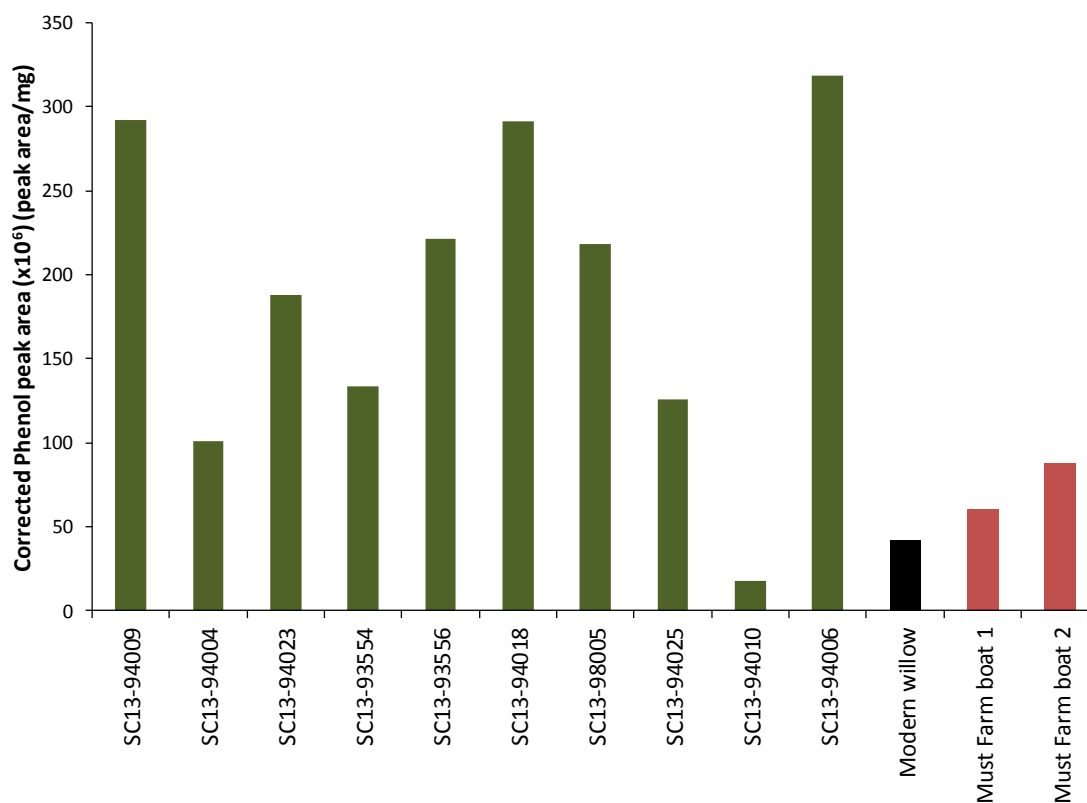


Figure 7.22: Comparison of corrected peak areas for phenol in a number of samples excavated from Star Carr in 2013 compared to an untreated willow sample and two of the Must Farm log boats. (Originally in colour).

Analysis by py-GC was also carried out on the 2007 sample that had been kept in storage since excavation (approximately four years) (Figure 7.23). In contrast to the samples from 2013 excavations, almost no structural components were identified. This suggests that in addition to the expected loss of cellulose, even the lignin is severely degraded in this sample. This is in contrast to samples analysed soon after excavation in 2013, where a number of lignin related peaks were detected (Figure 7.21) although all samples were located in wetland areas of the site.

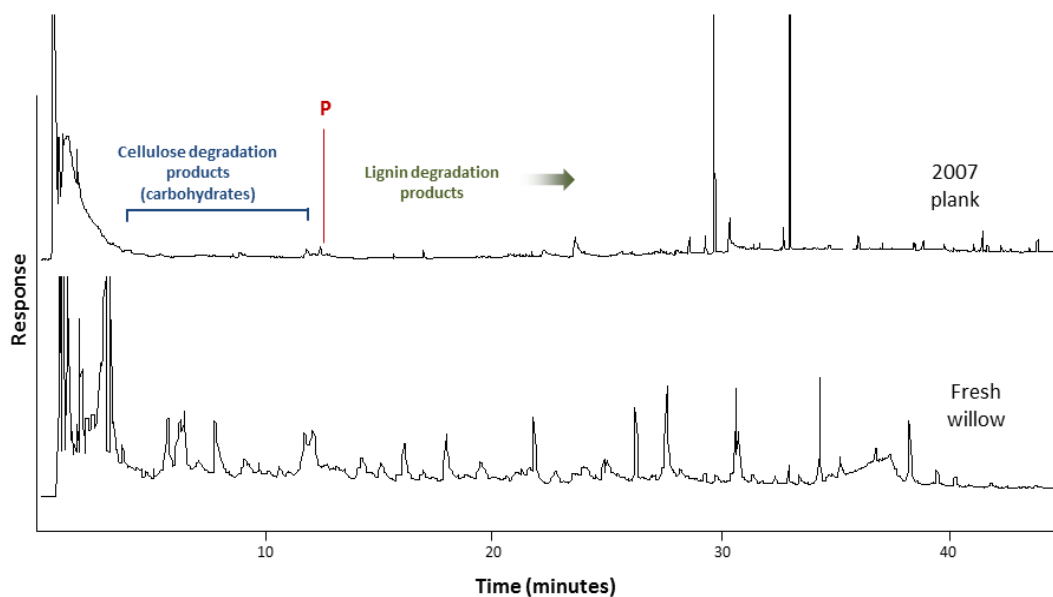


Figure 7.23: py-GC chromatogram for sample excavated from Star Carr in 2007 and stored for four years prior to analysis, compared to a fresh modern willow sample. Very few peaks relating to lignin sub units remain in the Star Carr sample. (Originally in colour).

7.4.2.6 Microscopy

SEM analysis of samples excavated in 2007/2008 was carried out by Ian Panter shortly after excavation, and revealed that in all of the samples the inner, cellulose-rich cell walls were almost completely lost, leaving only a lignin-rich skeleton, which is often characteristic of wood decay (Blanchette *et al.*, 1990). Collapse of this skeleton was also observed, but it was noted that this may have occurred during sample preparation (Panter, 2009). Spherical deposits were seen on the wood using SEM and identified as possible iron oxide crystals, which indicates that exchange with the burial environment has occurred. In addition, some evidence for fungal activity was observed, although this may also have occurred post excavation.

Analysis of several wood samples from the 2013 excavations also reveals thin cell walls, and cell collapse in places. However, regions remain where cell walls appeared more or less intact, suggesting that some cellulose is still present (Figure 7.24).

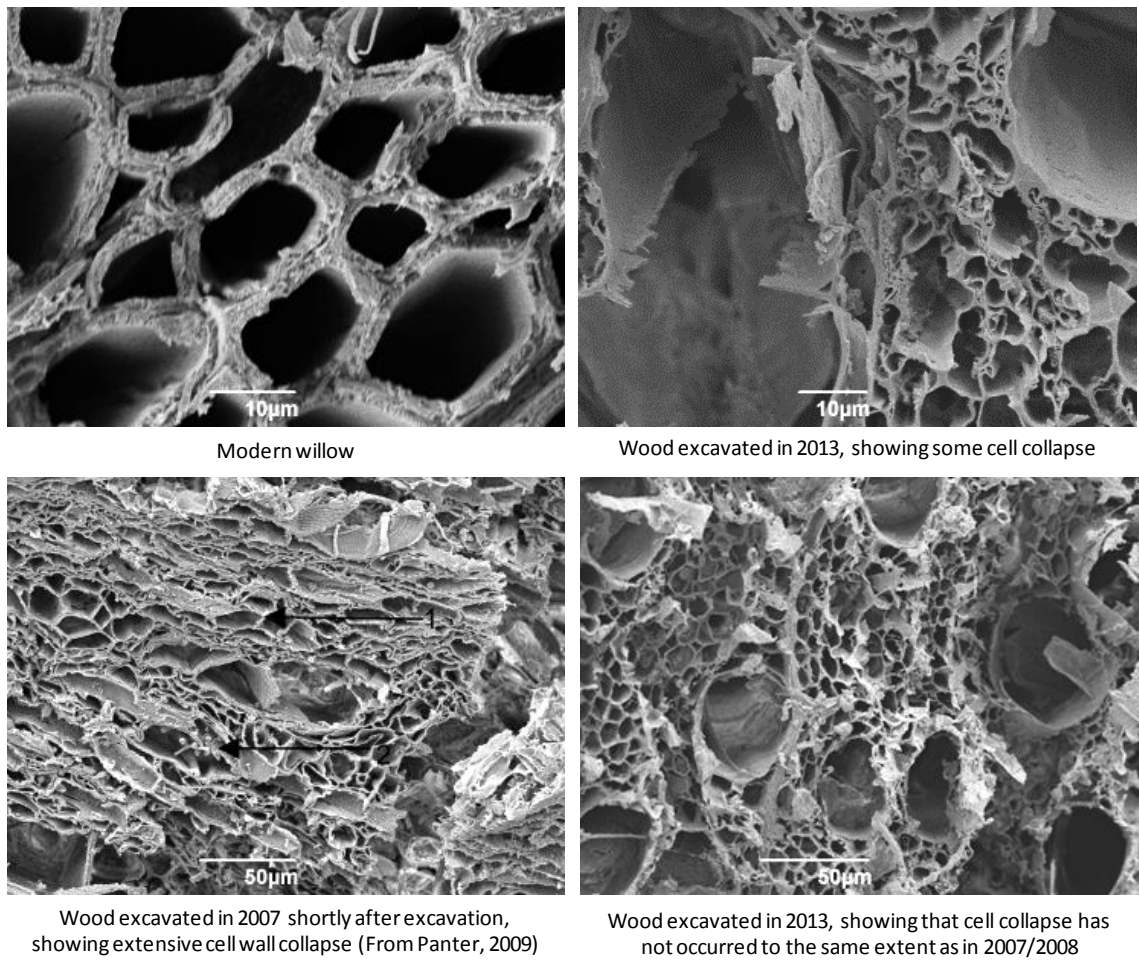


Figure 7.24: SEM images of archaeological wood compared to modern material (top left), showing the difference between the thick, cellulose-rich cell walls in undecayed wood compared to the lignin skeleton seen in wood from Star Carr. Cell collapse does however seem less extensive in the sample excavated in 2013 compared to 2007.

Further SEM analysis was carried out on the '2007 plank', and the presence of large quantities of crystals obscured the cellular structure. These crystals have not been identified, although their plate-like, hexagonal form could be considered characteristic of gypsum (e.g. Shih *et al.*, 2005). Where cell walls were visible (Figure 7.25, right) these were thin and often collapsed.

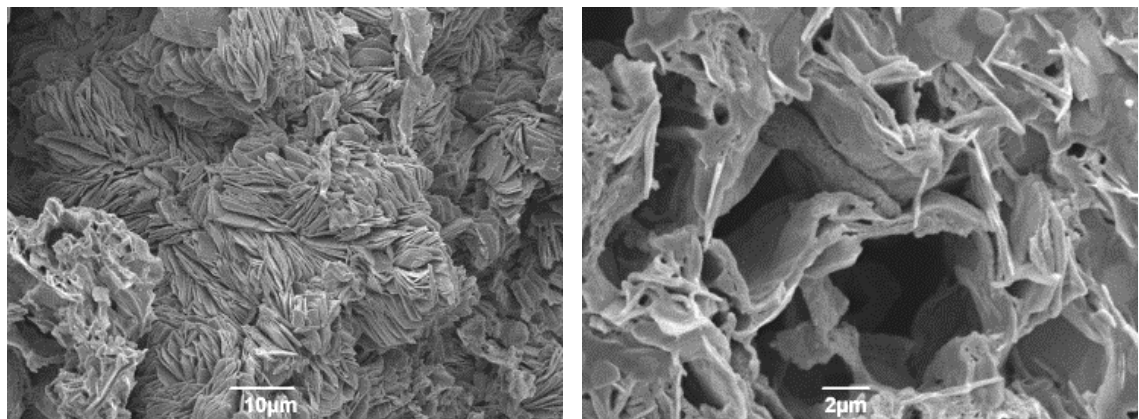


Figure 7.25: SEM images of the plank from 2007 after five years of storage, showing extensive crystal deposits and cell wall collapse

Fungal activity can often be identified under SEM by the presence of long fungal hyphae (e.g. Bjordal *et al.*, 1999) or by obvious cavities in the secondary cell walls (e.g. Kim & Singh, 2000). SEM imaging revealed no presence of biological activity in samples excavated from Star Carr. However, optical microscopy with the use of biological dyes may be more suitable for the detection of biological activity, as it analyses a much larger area of a sample (e.g. Humar *et al.*, 2008). This was not carried out in the current study.

7.4.2.7 Summary of wood analysis

Wood analysed shortly after excavation revealed some deterioration, particularly of the cellulose. However, comparisons with materials from Flag Fen and Must Farm suggest that this is not unusual for a site of this age. Whilst defunctionalisation of lignin is indicated by higher levels of phenol and splitting of the absorption peak at 1240 cm^{-1} in FTIR, the high intensity of later-eluting phenolic compounds in py-GC analysis indicates that lignin is still present in abundance in all analysed samples, meaning that artefacts retain the macroscopic appearance of wood. This is further illustrated by SEM analysis of samples excavated in 2013, where collapse of the cell walls was not extensive. In an archaeological context, this means that information such as cut marks, species and age of the wood can still be determined.

In contrast, analysis of one piece of wood from the 2007 excavations showed that very little organic polymeric material remained, while SEM revealed large areas of crystal formation. In addition, the pH of the water in which 2013 samples had been stored was very low ($\text{pH} < 1$) when analysed some months after excavation, whereas analysis of the sediments upon excavation yielded pH values in the region of 2-3 (Chapter 2). These observations suggest that chemical changes can occur within and around the sample during storage, most likely due to exposure to oxygen. The sample had been stored for approximately four years between excavation and analysis; it is not clear whether this deterioration occurred prior to excavation or during storage.

Whilst lab-based experiments have shown that wood deterioration is less dependent on pH than bone deterioration (Chapter 4), such low pHs as recorded from the surface of the 2007 samples ($\text{pH} < 1$) were not investigated. Cellulose in particular is known to deteriorate via acid catalysed hydrolysis, and it is likely that such low pH values may have facilitated such a rapid loss of polymeric material (e.g. Hoffman & Jones, 1990). Furthermore, after 16 weeks in pH 1 sulfuric acid, a birch sample also appeared to have undergone extensive loss of lignin, suggesting that this too can be chemically driven. Despite this, the relatively good preservation of all archaeological samples analysed from excavations in 2013 suggests that deterioration of wood is not particularly advanced, at least in parts of the site. A possible explanation is that deterioration of the '2007 plank' occurred largely post-excavation. This suggests that drying out of wood would be far more detrimental to its continued survival than high sediment acidity. Introduction of oxygen to the wood leads to increased acidity (as illustrated by the lowering of pH in the water in which all samples were stored); in addition, biological degradation of both the cellulose and lignin may become quickly accelerated.

7.5 Discussion and conclusions

Analysis of both bone and wood from the Star Carr site show that site conditions are contributing to their rapid deterioration. For bone, high sediment acidity appears to be a major factor; much of the bone is either a HA shell, or a HA depleted 'jellybone'. Lab-based experiments have shown that 'jellybone' will further rapidly deteriorate under acidic conditions, without the buffering and stability offered by the HA. Indeed, low Asx values in some of the most degraded bones could be indicative of rapid leaching away of broken down proteins, suggesting that some bones are literally being washed away. It is therefore likely that bones in the present state of preservation would not survive for much longer at the low pH that has been recorded during excavations.

Whilst deterioration of wood at the site has been shown to be largely what we would expect (it is comparable to well-preserved wood from Flag Fen, for example), there are indications that it is highly susceptible to any further alteration; although samples excavated in 2013 were relatively robust, a sample allowed to dry out ('2007 plank') displayed alarming levels of deterioration. Analysis suggests that groundwater may be percolating through the archaeology in areas of the site, and the investigation into site hydrology conducted in 2010 (Brown *et al.*, 2011) suggested that the water-table may have been below the archaeology for long periods. M. Taylor (pers. comm., 2010) reported difficulties in establishing the peat/wood interface during excavations in 2007 and 2008. However, it is possible that this was due to compression of the wood. This is further evidence of drainage of the peat leading to shrinkage. Drying out of the site would put wood at increasing risk of accelerated deterioration due to biological activity (Blanchette, 2000). Indeed, no wood was found in the dryland areas of the site even during the 1950s excavations, further confirming that drying out of the wetland areas would result in the loss of wooden artefacts. Therefore, although low pH may be less detrimental to the survival of wood, drying out of the site could lead to its complete destruction.

Analysis of bone from across Star Carr has highlighted that the modes of deterioration are variable across the site. Bones uncovered from the dryland areas have lost primarily collagen, whereas from the wetland areas, HA has been primarily depleted. This is likely to be due to marked differences in the burial conditions; alterations in acidity, hydrology and oxygen content are all likely to contribute. This variability would also mean that very different management strategies may need to be considered for different parts of the site; for example, we do not know what the effects of altering the pH or re-watering the site would have on the

dryland bones (consisting of mainly HA). In addition, the effects of mitigation strategies would have to consider the different degradation mechanisms of both bone and wood.

The site variability also makes it problematic to assess the time-frame in which diagenesis may have occurred; recently excavated material cannot be directly compared with that uncovered during early excavations without knowing its exact burial location. Despite this, assessment of bone materials from the early excavations showed that a large number of samples were much better preserved than any material uncovered from most recent excavations. This provides evidence that although there may have been localised areas where less well-preserved bone was uncovered during the early excavations, on the whole, site deterioration is likely to have occurred within the last few decades.

Analysis of both bone and wood has provided evidence that deterioration of both materials continues post-excavation, and this indicates that appropriate treatment of excavated organic materials is an important point for consideration. In particular, pH analysis of the water surrounding some of the wood samples from 2013 excavations showed that they had become highly acidic. This is possibly due to oxidation of any reactive sulfate present in the wood following exposure to air. Lab-based experiments have shown that although low pH is not as detrimental to the survival of wood as bone, at pH values of 1, loss of both cellulose and lignin occurred after 16 weeks. Therefore, acidification of wood samples post-excavation could be a problem that requires appropriate treatment and storage.

In contrast, water surrounding bone samples did not show an increase in acidity upon storage; pH remained fairly constant. This is possibly due to the increased porosity of archaeological wood compared to bone, resulting in more sulfides becoming incorporated into the structure, which can then oxidise to sulfuric acid. Alternatively, bone may continue to dissolve to buffer acidity post excavation. Both observations illustrate the care that needs to be taken with organic artefacts following excavation. Ideally, any acidity would be neutralised quickly post-excavation.

CHAPTER 8

CONCLUSIONS AND FUTURE WORK

8.1 Overall conclusions

The application of a suite of complementary analytical techniques has been shown to be most appropriate for the determination of levels of preservation in both bone and wood. By combining bulk analysis techniques (e.g. mass loss and visual analysis) and chemical techniques (e.g. gas and liquid chromatography, FTIR and p-XRD), levels of deterioration can be more confidently determined (Chapter 3). The importance of a multi-analytical approach has been highlighted in the case of experimental wood samples, where analysis by FTIR showed no loss of cellulose whilst py-GC analysis showed that cellulose had in fact degraded, and was possibly left *in situ* (Chapter 5).

Experiments aimed at investigating the effects of high acidity alone have shown that at low pH, bone mineral (HA) rapidly dissolves to buffer acidity, as seen through increased solution pH, high mass loss and peak sharpening in a p-XRD pattern (Chapter 4). The exposed collagen then quickly undergoes degradation, signified by increased leaching into solution. The loss of both components in an archaeological context would mean the loss of critical information; species identification, dating and osteological analysis would all be impossible. Lab-based burial experiments, where the acidity of soil used from Star Carr was less than pH 1, confirmed these findings and showed that when high concentrations of sulfur are present, the HA transforms to gypsum (Chapter 5). The consequences of such a transformation are unknown; however, as HA lends a high degree of stability to the bone collagen, it is likely that its alteration will effect survival of the collagen (e.g. Child *et al.*, 1993; Collins *et al.*, 2002). Burial experiments show that the rate at which HA loss or transformation occurs is determined by both the acidity of the sediments and site hydrology; it is likely that both are having a combined effect.

The effects of acidity on the survival of wood are less obvious. Loss of cellulose and defunctionalisation of lignin has however been observed both in sulfuric acid only for a prolonged period (16 weeks at 80°C) (Chapter 4), and in acidic soils in lab-based burial experiments (Chapter 5). The absence of evidence for biological activity in either context suggests that these changes are purely chemically driven. Despite this, it must be noted that loss of cellulose and lignin defunctionalisation does not result in complete breakdown of the wood. Indeed, in the lab-based burial experiments, the only visual alteration of samples was a darkening of the surface. This suggests that chemical degradation of wood polymers does not result in the loss of archaeological information to the same extent as loss of HA and collagen in bone does. If the macroscopic appearance of wood is retained, species identification, cut mark analysis and dendrochronology can all still be carried out.

Burial experiments have shown that microbial activity is also a major factor in organic deterioration. In particular, the loss of 'jellybone' samples in microbially rich sediments (sand and compost) in the lab-based burials (Chapter 5) indicates that exposed collagen would be rapidly lost through biological deterioration. Biological activity appears to be somewhat suppressed at Star Carr; even where oxygen is present, no evidence for microbial activity was found in either lab-based or *in situ* burial experiments. This has been assumed to be a result of the low pH. However, it needs to be considered that if drying out of the sediments occurs, this may result in increased fungal and microbial activity, leading to the rapid loss of demineralised bone as well as wood.

Analysis of archaeological materials has shown that there are different modes of bone deterioration across the site. In the dryland areas, a HA shell is left behind after collagen depletion, and in the wetland regions the opposite occurs to leave a collagen-rich 'jellybone'. This is likely to be the result of extreme variations in the geochemistry of the sediments across the site (Chapter 2). The mechanisms of formation of the HA shell is unclear, but may be the result of biological activity. The formation of 'jellybones' is highly likely to be the result of dissolution of HA to buffer acidic sediments. Lab-based experiments also showed that archaeological bone is less able to buffer surrounding acidity, and as a result could be more at risk in acidic sediments than estimated by modern replicates.

8.2 Impact for Star Carr

8.2.1 Diagenesis of archaeological material

Geochemical analysis at Star Carr shows that areas of the site are still highly acidic (< pH 2), although pockets of relatively neutral sediments (pH 4-6) remain (Chapter 2; Boreham *et al.*, 2011). In addition, a hydrological survey carried out in 2010, as well as reports by various excavators, suggested that the majority of the archaeological material now lies in fairly dry sediments (Brown *et al.*, 2011).

Whilst the variations in the geochemistry make it difficult to say for certain whether site conditions have changed recently, comparison between material from early excavations and material excavated more recently (2007-2013) suggests that far fewer bones are present in the well-preserved state first reported by Clark (1954). This makes it highly likely that rapid site deterioration has occurred within the last few decades.

Whether this coincided with lowering of the water-table can also not be determined; however, lab-based experiments have shown that acidic conditions cause similar alteration of bones as has been seen in acidic regions of the site, making it highly likely that acidity is the key factor facilitating the decline in bone preservation (Chapter 4). Any bone located in acidic regions of the site would continue to lose HA, as it dissolves to buffer the acidity. The collagen would then be exposed and rapidly lost. Indeed, a large number of samples were uncovered in 2013 that had already undergone severe HA loss. In contrast, many of the samples located in the dryland regions have lost collagen and retained HA (Chapter 7). If the surrounding sediment were to become acidic, it is likely that these would rapidly disappear.

Whilst high acidity is unlikely to result in such rapid loss of wood, the drying out of the site is much greater cause for concern. No wood has ever been found in the dryland areas of the site, highlighting the importance of waterlogging to the survival of wooden artefacts. Waterlogging creates an anaerobic environment where biological deterioration is suppressed. Although anaerobic deterioration can still occur, no evidence for this at the Star Carr site has been found. Indeed, the low pH may be preventing biological activity (e.g. Kim & Singh, 2000), thus protecting wood to some degree.

In contrast to the lack of biological deterioration, chemical deterioration has been shown by experimental studies here to occur at low pH (Chapter 4). Wood analysed at Star Carr is deteriorated to some extent, possibly as a result of this. Whether this would accelerate deterioration in a situation where the wood became aerobic is unknown.

These observations show that material still buried at Star Carr is at risk, particularly if site conditions were to alter further. For example, a particularly dry summer may result in further reduction of the water-table, resulting in increased acidity as more reactive sulfides are oxidised, thus putting both bone and wood at further risk. As both materials have already undergone diagenesis, the effects of this are likely to be highly detrimental and irreversible.

8.2.2 Site management

Both lab and field-based experiments have shown that site hydrology is a major factor determining organic diagenesis, not only because of the introduction of oxygen. If the water-table fluctuates through the samples ('dynamic' hydrology), constant washing away of dissolved species leads to a more rapid breakdown. This suggests that ideally any waterlogged archaeological site would be permanently monitored, meaning that any alterations in pH, redox or water-table height could be quickly recognised.

Potential strategies for slowing down organic deterioration can be considered. Raising the water-table at whole sites has been successfully achieved at a number of archaeological sites, including Sweet Track (Bunning *et al.*, 2001). This would prevent any further oxidation of reactive sulfides to sulfates, and ensure that biological deterioration remains suppressed. An alternative solution could be neutralising the whole site, for example by liming. However, for both potential strategies there is still a great deal of information lacking. Both wood and bone need to be carefully considered, as well as materials in different states of diagenesis. For example, we do not know what would happen to the HA-rich bones located in the dryland areas of the site if the dryland was to be re-wetted.

Rapid changes in both bone and wood from Star Carr have been observed post-excavation (Chapter 7) showing that strategies for the treatment of excavated material may be just as important as site management. Increased acidity in wood samples suggests that sulfide has become incorporated into the porous structure and continue to oxidise to sulfuric acid post-excavation. In order to prevent acidification, samples could either be stored waterlogged (this would also prevent shrinkage) or washed thoroughly prior to any conservation treatment. Although no reduction in pH was observed post-excavation in bone samples, this may be because HA continues to buffer, and therefore these should also be washed thoroughly before storage. This may also prevent the formation of crystals upon drying, which have caused splitting of rib bones.

8.3 Future work

8.3.1 Method development

Although the analytical methods applied throughout the study have been effective for the determination of levels of preservation, scope remains for further development of the methods. In particular, py-GC has been applied non-quantitatively here; if the method employed an appropriate internal standard, quantitation may be achieved (e.g. Bocchini *et al.*, 1998). This would allow direct comparison between samples from different archaeological sites.

Analytical techniques have been selected for their non-destructive or minimally-destructive application. However, the method of p-XRD used here does require a relatively large amount of sample to be powdered (approximately 200 mg). The use of micro-XRD (e.g. Dalconi *et al.*, 2003) should therefore be developed in order for the analysis to be more suitable for the routine analysis of archaeological materials.

Raman microscopy was trialled in Chapter 3; however, appropriate focus of the laser was found to be impossible without impregnating the samples in resin (Chapter 3 Section 3.2.5). This is likely to be due to the wavelength of the laser available. Use of a 785 nm laser, according to Timlin *et al.* (2000) and Raghavan (2011), could potentially provide a completely non-destructive method of determining levels of degradation in both the mineral and collagen fractions of bone.

8.3.2 Biological assessment

Whilst no microbial activity has been confidently identified in any experimental or archaeological materials, it is clear that biological activity may be a key factor in the diagenesis of wood, particularly if the Star Carr site continues to dry out. In addition, it may contribute to the rapid loss of demineralised 'jellybone'. Characterisation of the biological environment of the site has therefore been identified as an important area for future work.

Several methods of microbial characterisation are reported (e.g. Kirk *et al.*, 2004; Ibekwe & Kennedy, 1998) and all have advantages and disadvantages. Traditional techniques such as culturing on agar plates (plate counts) may favour fast growing microbes and not give an accurate view of the microbial diversity of the soil (Kirk *et al.*, 2004).

It is proposed therefore to investigate the possibility of determining both the fatty acid methyl ester (FAME) and phospholipid fatty acid (PLFA) profiles of several soils from across the Star

Carr site, to determine whether high levels of microbial activity can be associated with different geochemical conditions and levels of organic preservation. Rather than specify exact microbes, this type of analysis provides a broad characterisation of types of microbial communities and can indicate the microbial diversity of an environment (Ibekwe & Kennedy, 1998). The advantages of this method are that it is relatively cheap and fast; however, it does not necessarily give an accurate reflection of which microbes are actually active as it also detects dead cells; an alternative method could be DNA characterisation although the high cost of this may make it unsuitable for determining variability across a large area (Ibekwe *et al.*, 2002).

8.3.3 Application to other wetland archaeological sites

Although some comparison with other archaeological sites has been carried out here, the comparison was not extensive. The analytical methods used here have been chosen for their ease of use, cost and ability to be minimally destructive. This makes them ideal for the routine application of identifying changes in preservation at other archaeological sites. Therefore, a more comprehensive comparison with similarly aged sites should be possible, and may allow a more confident assessment of the time-frame in which deterioration at Star Carr has occurred. Although Mesolithic sites with preserved organic materials are rare (Tolan-Smith, 2008) some examples may be found further afield, for example in Ireland, Denmark or the Netherlands (Bailey & Spikins, 2008).

8.3.4 Extended burial experiments

Whilst burial experiments carried out *in situ* (Chapter 6) have been informative, the short time-frame led to levels of degradation being only minimal. Further work should therefore involve prolonged burial experiments. Burial experiments carried out by Nicholson (1996; 1998) for 7 years and Turner-Walker & Peacock (2008) for 4 and 8 years yielded higher levels of deterioration. In addition, experiments where material is removed periodically (e.g. Crowther, 2002) enables a rate of deterioration to be more confidently estimated.

Different species (for bone and wood), cooked and uncooked bone, and different type of bone (long bone/rib) and wood (roundwood/heartwood) have been used here (Chapters 4, 5 & 6), and results have indicated that differences in the levels of deterioration could be seen. In future burial experiments, a wider range of material could be considered in order to more fully understand these differences.

LIST OF ABBREVIATIONS

ATR	Attenuated total reflectance
D (conditions)	Dynamic conditions
EDTA	Ethylenediaminetetraacetic acid
FTIR	Fourier transform infrared spectroscopy
HA	Hydroxyapatite
HPLC	High pressure liquid chromatography
Ka	Thousand years ago
MDE	Method development experiment
NMR	Nuclear magnetic resonance
OPA	o-phthaldialdihyde
Py-GC	Pyrolysis gas chromatography
p-XRD	Powder X-ray diffraction
RP-HPLC	Reverse phase high pressure liquid chromatography
RT	Room temperature
S (conditions)	Stagnant conditions
SEM	Scanning electron microscopy
TEM	Transmission electron microscopy
U_{\max}	Maximum water content

REFERENCES

- Adler, E., 1977. Lignin Chemistry – Past, present and future. *Wood Science and Technology* **11** 169-218
- Aerssens, J., Boonen, S., Lowet, G. & Dequeker, J., 1998. Interspecies differences in bone composition, density and quality: Implications for *in vivo* bone research. *Endocrinology* **139** 663-670
- Almkvist G., 2008. The Chemistry of the Vasa – Irons, acids and degradation. *Doctoral Thesis*, Swedish University of Agricultural Sciences, Uppsala
- Alves, A., Schwanninger, M., Pereira, H. & Rodrigues, J., 2006. Analytical pyrolysis as a direct method to determine the lignin content in wood. Part 1: Comparison of pyrolysis lignin with Klason lignin. *Journal of Analytical and Applied Pyrolysis* **76** 209-213
- Ambrose, S.H. & DeNiro, M.J., 1986. Reconstruction of African human diet using bone collagen carbon and nitrogen isotope ratios. *Nature* **319** 321-324
- Atkins, P., Overton, T., Rourke, J., Weller, M. & Armstrong, F., 2006. Inorganic Chemistry, 4th ed., Oxford University Press, Oxford
- Bada, J.L., 1972. Dating of fossil bones using racemization of isoleucine. *Earth and Planetary Science Letters* **15** 223-231
- Bada, J.L. & Schroeder, R.A., 1975. Amino acid racemisation reactions and their geochemical implications. *Naturwissenschaften* **62** 71-79
- Bada, J.L. & Shou, M.-Y., 1980. Kinetics and Mechanism of Amino Acid Racemization in Aqueous Solution and in Bones, in: Hare, P.E., T.C. H., K.King (Eds.), *Biogeochemistry of Amino Acids*, John Wiley & Sons, United States of America. Pg 235-255
- Bailey, G. & Spikins, P., 2008. Mesolithic Europe. Cambridge University Press, Cambridge.
- Bain, C.G., Bonn, A., Stoneman, R., Chapman, S., Coupar, A., Evans, M., Gearey, B., Howat, M., Joosten, H., Keenleyside, C., Labadz, J., Lindsay, R., Littlewood, N., Lunt, P., Miller, C.J., Moxey, A., Orr, H., Reed, M., Smith, P., Swales, V., Thompson, D.B.A., Thompson, P.S., Van de Noort, R., Wilson, J.D. & Worrall, F., 2011. IUCN UK Commission of Inquiry on Peatlands. *IUCN UK Peatland Programme*, Edinburgh

- Bandick, A.K. & Dick, R.P., 1999. Field management effects on soil enzyme activities. *Soil Biology and Biochemistry* **31** 1471-1479
- Bartlett, R., Bottrell, S.H., Sinclair, K., Thornton, S., Fielding, I.D. & Hatfield, D., 2010. Lithological controls on biological activity and groundwater chemistry in Quaternary sediments. *Hydrological processes* **24** 726-735
- Bartsiokas, A. & Middleton, A.P., 1992. Characterisation and dating of recent and fossil bones by X-ray diffraction. *Journal of Archaeological Science* **19** 63-72
- Beales, N., 2004. Adaptation of microorganisms to cold temperatures, weak acid preservatives, low pH, and osmotic stress: A review. *Comprehensive Reviews in Food Science and Food Safety* **3** 1-20
- Bell, L.S., 1990. Palaeopathology and Diagenesis: An SEM evaluation of structural changes using backscattered electron imaging. *Journal of Archaeological Science* **17** 85-102
- Bell, L.S., Skinner, M.F. & Jones, S.J., 1996. The speed of post mortem change to the human skeleton and its taphonomic significance. *Forensic Science International* **82** 129-140
- Berna, F., Matthews, A. & Weiner, S., 2004. Solubilities of bone mineral from archaeological sites: The recrystallization window. *Journal of Archaeological Science* **31** 867-882
- Bjordal, C.G., Nilsson, T. & Daniel, G., 1999. Microbial decay of waterlogged wood found in Sweden. Applicable to archaeology and conservation. *International Biodeterioration and Biodegradation* **43** 63-73
- Bjordal, C.G., Daniel, G. & Nilsson, T., 2000. Depth of burial, an important factor in controlling bacterial decay of waterlogged archaeological poles. *International Biodeterioration and Biodegradation* **45** 15-26
- Bjordal, C.G. & Nilsson, T., 2007. Reburial of shipwrecks in marine sediments: A long term study on wood degradation. *Journal of Archaeological Science* **35** 862-872
- Blanchette, R.A., Nilsson, T., Daniel, G. & Abad, A., 1990. Biological degradation of wood, in: Rowell, R.M. & Barbour R.J. (Eds), *Archaeological wood properties, chemistry and preservation*. Pg 141-177
- Blanchette, R., 2000. A review of microbial deterioration found in archaeological wood from different environments. *International Biodeterioration and Biodegradation* **46** 189-204
- Bocchini, P., Galletti, G.C., Camarero, S. & Martinez, A.T., 1997. Absolute quantitation of lignin pyrolysis products using an internal standard. *Journal of Chromatography* **773** 227-232

- Bonar, L.C., Roufosse, A.H., Sabine, W.K., Grynepas, M.D. & Glimcher, M.J., 1983. X-ray diffraction studies of the crystallinity of bone-mineral in newly synthesized and density fractionated bone. *Calcified Tissue International* **35** 202-209
- Boreham, S., Conneller, C., Milner, N., Taylor, B., Needham, A., Boreham, J. & Rolfe, C.J., 2011. Geochemical indicators of preservation status and site deterioration at Star Carr. *Journal of Archaeological Science* **38** 2833-2857
- Boskey, A., 2003. Bone mineral crystal size. *Osteoporosis International* **14** S16-S21
- Boyde, A., 2012. Scanning electron microscope studies of bone, in: Bourne, G.H (Ed) *The biochemistry and physiology of bone volume 1: Structure*. Pg 259-310
- Bradley, C., Baker, A., Cumberland, S., Boomer, I. & Morrissey, I.P., 2007. Dynamics of water movement and trends in dissolved carbon in a headwater wetland in a permeable catchment. *Wetlands* **27** 1066-1080
- Bradley, C., Grapes, T., Bassell, L., Brown, A.T.G. & Boomer, I., 2012. Hydrological assessment of Star Carr catchment, Yorkshire. *English Heritage Report*
- Brock, T.D., Brock, K.M., Belly, R.T. & Weiss, R.I., 1972 Sulfolobus: A new genus of sulfur-oxidising bacteria living at low pH and high temperature. *Archiv fur Mikrobiologie* **84** 54-68
- Brown, W.E. & Chow, L.C., 1979. Chemical properties of bone mineral. *Annual Review of Material Science* **66** 213-236
- Brown, K.A., 1985. Sulphur distribution and metabolism in waterlogged peat. *Soil Biology and Biochemistry* **17** 39-45
- Brown, A.G., Ellis, C. & Roseff, R., 2010. Holocene sulphur-rich palaeochannel sediments: diagenetic conditions, magnetic properties and archaeological implications. *Journal of Archaeological Science* **37** 21-29
- Brown, T., Bradley, C., Grapes, T. & Boomer, I., 2011. Hydrological Assessment of Star Carr and the Hertford Catchment, Yorkshire, UK. *Journal of Wetland Archaeology* **11** 36-55
- Brunning, R., Hogan, D., Jones, J., Jones, M., Maltby, E., Robinson, M. & Straker, V., 2000. Saving the Sweet Track: The in situ preservation of a Neolithic wooden trackway, Somerset, UK. *Conservation and Management of Archaeological Sites* **4** 3-20
- Brunning, R., 2006. How does monitoring fit into a wider strategy? A multi-site example from a rural wetland in the UK, in: Kars, H. & van Heeringen (Eds), *Preserving archaeological remains in situ, proceedings of the 3rd conference (Amsterdam)*. Pg 217-226

- Buckland, P.C. 1993. Peatland Archaeology: a conservation resource on the edge of extinction. *Biodiversity and Conservation* **2** 513-527
- Buckley, M., Anderung, C., Penkman, K., Raney, B.J., Gotherstrom, A., Thomas-Oates, J. & Collins, M.J., 2008. Comparing the survival of osteocalcin and mtDNA in archaeological bone from four European sites. *Journal of Archaeological Science* **35** 1756-1764
- Buckley, M., & Collins, M. J., 2011. Collagen survival and its use for species identification in Holocene-lower Pleistocene bone fragments from British archaeological and paleontological sites. *Antiqua* **1** 1-7
- Buscot, F. & Varma, A. 2005. Microorganisms in soils: Roles in genesis and functions. Springer, Berlin.
- Caple, C., 1994. Reburial of waterlogged wood, the problems and potential of this conservation technique. *International Biodeterioration & Biodegradation* 61-72
- Caple, C., 1996. Parameters for monitoring anoxic environments, in: Corfield, M., Hinton, P., Nixon, T. & Pollard, M (Eds) *Preserving archaeological remains in situ: proceedings of the 1st conference*. Pg 113-123
- Caple, C. & Dungworth, D., 1998. Waterlogged anoxic archaeological burial environments. *Ancient Monuments Laboratory Report* **22/98**
- Caple, C., 2004. Towards a benign reburial context: the chemistry of the burial environment. *Conservation and Management of Archaeological Sites* **6** 155-165
- Cappenberg, Th. E., 1974. Interrelations between sulfate-reducing and methane-producing bacteria in bottom deposits of a fresh-water lake. I. Field observations. *Antonie van Leeuwenhoek* **40** 285-295
- Capretti, C., Macchioni, N., Pizzo, B., Galotta, G., Giachi, G. & Giampola, D., 2008. The characterization of waterlogged archaeological wood: The three Roman ships found in Naples (Italy). *Archaeometry* **50** 855-876
- Carrott, J., Hall, A., Johnstone, C. & Large, F., 1997. Evaluation of biological remains from excavations at 47-55 Tanner Row, York. *Reports from the Environmental Archaeology Unit, York* **97/24**
- Caulfield, S., 1978. Star Carr – An Alternative View. *Irish Archaeological Research Forum* **5** 15-22
- Chapman, H.P. & Van de Noort, R., 2001. High-resolution wetland prospection, using GPS and GIS: Landscape studies at Sutton Common (South Yorkshire), and Meare Village East (Somerset). *Journal of Archaeological Science* **28** 365-375

- Child, A.M., Gillard, R.D. & Pollard, A.M., 1993. Microbially-induced promotion of amino acid racemization in bone: isolation of the microorganisms and the detection of their enzymes. *Journal of Archaeological Science* **20** 159-168
- Child, A.M., 1995. Towards an understanding of the microbial decomposition of archaeological bone in the burial environment. *Journal of Archaeological Science* **22** 165-174
- Clark, J.G.D., 1954. Excavations at Star Carr. Cambridge University Press, Cambridge
- Clarke, S., 1987. Propensity for spontaneous succinimide formation from aspartyl and asparaginyll residues in cellular proteins. *International Journal of Protein Research* **30** 808-821
- Coles, B. & Coles, J., 1986. Sweet Track to Glastonbury. Thames and Hudson, London
- Coles, J.M., 1998. Wetland worlds and the past preserved, in: Bernick , K (Ed) *Hidden dimensions, the cultural significance of wetland archaeology*. UBC Press, Vancouver. Pg 3-30
- Collins, M.J., Riley, M.S., Child, A.M. & Turner-Walker, G., 1995. A basic mathematical simulation of the chemical degradation of ancient collagen. *Journal of Archaeological Science* **22** 175-183
- Collins, M.J., Waite, E.R. & van Duin, A.C.T., 1999. Predicting protein decomposition: the case of aspartic-acid racemization kinetics. *Philosophical Transactions of the Royal Society of London Series B – Biological Sciences* **354** 51-64
- Collins, M.J., Nielsen-Marsh, C.M., Hiller, J., Smith, C.I., Roberts, J.P., Prigodich, R.V., Weiss, T.J., Csapo, J., Millard, A.R. & Turner-Walker, G., 2002. The survival of organic matter in bone: A review. *Archaeometry* **44** 383-394
- Collins, M.J., Penkman, K.E.H., Rohland, N., Shapiro, B., Dobberstein, R.C., Ritz-Timme, S. & Hofreiter, M., 2009. Is amino acid racemization a useful tool for screening for ancient DNA in bone? *Proceedings of the Royal Society B – Biological Sciences* **276** 2971-2977
- Colombini, M.P., Orlandi, M., Modugno, F., Tolppa, E-L., Sardelli, M., Zoia, L. & Crestini, C., 2007. Archaeological wood characterization by PY/GC/MS, GC/MS, NMR and GPC techniques. *Microchemical Journal* **85** 164-173
- Conneller, C., 2004. Becoming deer: Corporeal transformations at Star Carr. *Archaeological Dialogues* **11**, 37-56
- Cotter, P. D., & Hill, C., 2003. Surviving the acid test: responses of gram-positive bacteria to low pH. *Microbiology and Molecular Biology Reviews* **67** 429-453

- Covington, A.D., Song, L., Suparno, O., Koon, H.E.C. & Collins, M.J., 2008. Link-lock: An explanation of the chemical stabilisation of collagen. *Journal of the Society of Leather Technologists and Chemists* **92** 1-7
- Cox, M., Earwood, C., Jones, E.B.G., Jones, J., Straker, V., Robinsons, M., Tibbet, M. & West, S., 2001. An assessment of the impact of trees upon archaeology within a relict wetland. *Journal of Archaeological Science* **28** 1069-1084
- Crestini, C., Hadidi, N.M.N. & Palleschi, G., 2009. Characterisation of archaeological wood: A case study on the deterioration of a coffin. *Microchemical Journal* **92** 150-154
- Crisp, M., Demarchi, B., Collins, M., Morgan-Williams, M., Pilgrim, E. & Penkman, K.E.H., 2013. Isolation of the intra-crystalline proteins and kinetic studies in *Struthio camelus* (ostrich) eggshell for amino acid geochronology. *Quaternary Geochronology* **16** 110-128
- Crowther, J., 2002. The experimental earthwork at Wareham, Dorset after 33 years: Retention and leaching of phosphate released in the decomposition of buried bone. *Journal of Archaeological Science* **29** 405-411
- Cullity, B.D., 1978. Elements of X-Ray diffraction: 2nd Edition. Addison-Wesley Publishing, USA
- Currey, J.D., 2002. Bones: Structure and Mechanics. Princeton University Press, Oxfordshire
- Dalconi, M. C., Meneghini, C., Nuzzo, S., Wenk, R., & Mobilio, S., 2003. Structure of bioapatite in human foetal bones: An X-ray diffraction study. *Nuclear Instruments and Methods in Physics Research Section B: Beam Interactions with Materials and Atoms* **200** 406-410
- Dark, P., 1998. Radiocarbon dating of the lake-edge deposits, in: Mellars, P. & Dark, P. *Star Carr in Context*. McDonald Institute for Archaeological Research, Cambridge. Pg 119-124
- Das, K., & Keener, H. M., 1997. Numerical model for the dynamic simulation of a large scale composting system. *Transactions of the ASAE* **40** 1179-1189
- Davis, M., 1996. *In situ* monitoring of wet archaeological environments: a review of available monitoring strategies, in: Corfield, M., Hinton, P., Nixon, T. & Pollard, M (Eds) *Preserving archaeological remains in situ: proceedings of the 1st conference*. Pg 21-25
- Demarchi, B., Collins, M., Bergstrom, E., Dowle, A., Penkman, K., Thomas-Oates, J. & Wilson, J., 2013. New experimental evidence for in-chain amino acid racemization of serine in a model peptide. *Analytical Chemistry* **85** 5835-5842
- Dennison, K.J., 1980. Amino acids in archaeological bone. *Journal of Archaeological Science* **7** 81-86

- Dent, D.L. & Pons, L.J., 1995. A world perspective on acid sulphate soils. *Geoderma* **67** 263-276
- Di Blasi, C., 2008. Modelling chemical and physical processes of wood and biomass pyrolysis. *Progress in Energy and Combustion Science* **34** 47-90
- Dixon, R.A., Dawson, L. & Taylor, D., 2008. The experimental degradation of archaeological human bone by anaerobic bacteria and the implications for recovery of ancient DNA, in: *The 9th International Conference on Ancient DNA and Associated Biomolecules*, Pompeii, Italy
- Dobberstein, R.C., Huppertz, J., von Wurmb-Schwark, N. & Ritz-Timme, S., 2008. Degradation of biomolecules in artificially and naturally aged teeth: Implications for age estimation based of aspartic acid racemization and DNA analysis. *Forensic Science International* **179** 181-191
- Dobberstein, R.C., Collins, M.J., Craig, O.E., Taylor, G., Penkman, K.E.H. & Ritz-Timme, S., 2009. Archaeological collagen: Why worry about collagen diagenesis? *Archaeological Anthropology Science* **1** 31-42
- Dypvik, H., 1984. Geochemical compositions and depositional conditions of Upper Jurassic and Lower Cretaceous Yorkshire clays, England. *Geological Magazine* **121** 489-504
- Egiebor, N.O. & Oni, B., 2007. Acid rock drainage formation and treatment: A review. *Asia-Pacific Journal of Chemical Engineering* **2** 47-62
- Evershed, R.P., Turner-Walker, G., Hedges, R.E.M., Tuross, N. & Leyden, A., 1995. Preliminary results for the analysis of lipids in ancient bone. *Journal of Archaeological Science* **22** 277-290
- Ezra, H.C. & Cook, S.F., 1957. Amino acids in fossil human bone. *Science* **126** 80
- Faix, O., Bremer, J., Schmidt, O. & Stevanovic, T., 1991. Monitoring of chemical changes in white-rot degraded beech wood by pyrolysis-gas chromatography and Fourier-transform infrared spectroscopy. *Journal of Analytical and Applied Pyrolysis* **22** 147-162
- Fantner, G.E., Birkedal, H., Kindt, J.H., Hassenkam, T., Weaver, J.C., Cutroni, J.A., Bosma, B.L., Bawazer, L., Finch, M.M., Cidade, G.A.G., Morse, D.E., Stucky, G.D. & Hansma, P.K., 2004. Influence of the degradation of the organic matrix on the microscopic fracture behaviour of trabecular bone. *Bone* **35** 1013-102
- Faulkner, S.P. & Richardson, C.J., 1989. Physical and chemical characteristics of freshwater wetland soils, in: *Hammer, D (Ed) Constructed wetlands for wastewater treatment*. CRXC Press, Florida
- Feigl, F. & Anger, V., 1972. Spot tests in inorganic chemistry: 6th Edition. Elsevier Science, Amsterdam

- Fell, V., 2005. Fiskerton: Scientific analysis of corrosion layers on archaeological iron artefacts and from experimental iron samples buried for up to 18 months. *English Heritage Centre for Archaeology (Ed.)*
- Fengel, D. & Wegener, W., 1984. Wood: chemistry, ultrastructure, reactions. Walter de Gruyter & Co, Berlin
- Ferraz, A., Baeza, J., Rodriguea, J. & Freer, J., 2000. Estimating the chemical composition of biodegraded pine and eucalyptus wood by DROFT spectroscopy and multivariate analysis. *Bioresource Technology* **74** 201-212
- Field, N. & Pearson, M. P., 2003. Fiskerton: an Iron Age timber causeway with Iron Age and Roman votive offerings, the 1981 excavations. Oxbow Books Ltd
- Florian, M-L. E., 1990. Scope and history of archaeological wood, in: Rowell, R.M and Barbour R.J (Eds.), *Archaeological wood properties, chemistry and preservation*. Pg 3-34
- Gearey, B., Bermingham, N., Chapman, H., Charman, D., Fletcher, W., Fyfe, R., Quartermaine, J. & Van de Noort, R., 2010. Peatlands and the Historic Environment. *IUCN UK Peatland Programme*, Edinburgh
- Gelbrich, J., Mai, C. & Militz, H., 2008. Chemical Changes in wood degraded by Bacteria. *International Biodeterioration & Biodegradation* **61** 24-32
- Gelbrich, J., Kretschmar, E. I., Lamersdorf, N., & Militz, H., 2012. Laboratory experiments as support for development of in situ conservation methods. *Conservation and Management of Archaeological Sites* **14** 7-15
- Gilardi, G., Abis, L. & Cass, A.E.G., 1994. Wide-line solid-state NMR of wood: Proton relaxation time measurements on cell walls biodegraded by white-rot and brown-rot fungi. *Enzyme and Microbial Technology* **16** 676-682
- Giraud-Guille, M.M., 1988. Twisted plywood architecture of collagen fibrils in human compact bone osteons. *Calcified Tissue International* **42** 167-180
- Glimcher, M. J., & Katz, E. P., 1965. The organization of collagen in bone: the role of non-covalent bonds in the relative insolubility of bone collagen. *Journal of ultrastructure research* **12** 705-729
- Gong, J.K., Arnold, J.S. & Cohn, S.H., 1964. Composition of trabecular and cortical bone. *The Anatomical Record* **143** 325-331

- Gordon, C.C. & Buikstra, J.E., 1981. Soil-pH, bone preservation, and sampling bias at mortuary sites, *American Antiquity* **46** 566-571
- Green, J. & Kleeman, C.R., 1991. Role of bone in regulation of systematic acid-base balance. *Editorial review, Kidney International* **39** 9-26
- Green, K.A., *in prep.* The fate of lipids in archaeological burial soils. *PhD thesis*, University of York
- Grupe, G., 1995. Preservation of collagen in bone from dry, sandy soil. *Journal of Archaeological Science* **22** 193-199
- Hamilton, W.A., 1985. Sulphate reducing bacteria and anaerobic corrosion. *Annual Review of Microbiology* **39** 195-217
- Hatcher, P.G. 1984. Dipolar-dephasing ¹³C NMR studies of decomposed wood and coalified xylem tissue: Evidence for chemical structural changes associated with defunctionalisation of lignin structural units during coalification. *Energy & Fuels* **2** 48-58
- Hedges, R. E. M., & Law, I. A., 1989. The radiocarbon dating of bone. *Applied Geochemistry* **4** 249-253
- Hedges, R.E.M., 1990. The chemistry of archaeological wood in: Rowell, R.M and Barbour R.J (Eds.), *Archaeological wood properties, chemistry and preservation*. Pg 111-141
- Hedges, R.E.M. & Millard, A.R., 1995. Bones and groundwater – towards the modelling of diagenetic processes. *Journal of Archaeological Science* **22** 155-164
- Hedges, R.E.M., Millard, A.R. & Pike, A.W.G., 1995. Measurements and relationships of diagenetic alteration of bone from three archaeological sites. *Journal of Archaeological Science* **22** 201-209
- Hedges, R.E.M., 2002. Bone diagenesis: An overview of processes. *Archaeometry* **44** 319-328
- High, K., Penkman, K.E.H., Milner, N. & Panter, I., *in press*. Fading Star: Towards understanding the effects of acidification on organic remains (wood) at Star Carr. Proceedings of the 12th ICOM-CC-WOAM conference, Istanbul 2013
- Highley, T.L. & Kirk, T.K., 1979. Mechanisms of wood decay and the unique features of heartrots. *The American Phytopathological Society* **69** 1151-1157
- Hiller, J.C. & Wess, T.J., 2006. The use of small-angle X-ray scattering to study archaeological and experimentally altered bone. *Journal of Archaeological Science* **33** 560-572

- Hoffman, P., 1981. Chemical wood analysis as a means of characterizing archaeological wood in: Grattan, D., & McCawley, C. (Eds) *Proceedings of the ICOM Waterlogged Wood Working Group Conference*, Ottawa. Pg 73-84
- Hoffman, P., 1986. On the stabilization of waterlogged oakwood with PEG. II. Designing a two-step treatment for multi-quality timbers. *International Institute for Conservation of Historic and Artistic Works* **31** 103-113
- Hoffman, P. & Jones, M.A. 1990. Structure and degradation process for waterlogged archaeological wood in: Rowell, R.M and Barbour R.J (Eds.), *Archaeological wood properties, chemistry and preservation*. Pg 141-177
- Holden, J., West, L.J., Howard, A.J., Maxfield, E., Panter, I. & Oxley, J., 2006. Hydrological control of *in situ* preservation of waterlogged archaeological deposits. *Earth-Science reviews* **78** 59-83
- Holt, D.M. & Jones, E.B.G., 1983. Bacterial degradation of lignified wood cell walls in anaerobic aquatic habitats. *Applied and Environmental Microbiology* **46** 722-727
- Hong, H. & Kester, D.R., 1986. Redox state of iron in the offshore waters of Peru. *Limnology and Oceanography* **30** 512-524
- Hopkins, D.W., 1996. The biology of the burial environment, in: Corfield, M., Hinton, P., Nixon, T and Pollard, M., *Proceedings of the preserving archaeological remains in-situ conference*. Pg 73-85
- Humar, M., Fabric, B., Zupacic, M., Pohleven, F. & Oven, P., 2008. Influence of xylem growth ring width and wood density on durability of oak heartwood. *International Biodeterioration & Biodegradation* **62** 368-371
- Ibekwe, A.M & Kennedy, A.C., 1998. Phospholipid fatty acid profiles and carbon utilization patterns for analysis of microbial community structure under field and green house conditions. *FEMS Microbiology Ecology* **26** 151-163
- Ibekwe, A.M., Kennedy, A.C., Frohne, P.S., Papiernik, S.K., Yang, C-H. & Crowley, D.E., 2002. Microbial diversity along a transect of agronomic zones. *FEMS Microbiology Ecology* **39** 183-191
- Jane, F.W., White, D.J.B. & Wilson, K., 1970. *The structure of wood*, 2nd edition. A&C Black, London
- Jans, M.M.E., Kars, H., Nielsen-Marsh, C.M., Smith, C.I., Nord, A.G., Arthur, P. & Earl, N., 2002. *In-situ* preservation of archaeological bone: a histological study within a multidisciplinary approach. *Archaeometry* **44** 343-352
- Jans, M.M.E., Nielsen-Marsh, C.M., Smith, C.I., Collins, M.J. & Kars, H., 2004. Characterisation of microbial attack on archaeological bone. *Journal of Archaeological Science* **31** 87-95.

- Jans, M.M.E., 2005. Histological characterisation of diagenetic alteration of archaeological bone. *Geoarchaeological and Bioarchaeological Studies Volume 4*. Vrije Universiteit, Amsterdam
- Jensen, O. & Gregory, D.J., 2006. Selected physical parameters to characterize the state of preservation of waterlogged archaeological wood: a practical guide for their determination. *Journal of Archaeological Science* **33** 551-559
- Jones, M. & Eaton, R., 2006. Conservation of Ancient Timbers from the sea in: May, E. & Jones, M. (Eds) *Conservation Science: Heritage Materials*. RSC publishing, Cambridge
- Kamide, K., Okajima, K., Matsui, T. & Kowsaka, K., 1984. Study on the solubility of cellulose in aqueous alkali solution by deuteration IR and ¹³C NMR. *Polymer Journal* **16** 857-866
- Karr, L.P. & Outram, A.K., 2012. Tracking changes in bone fracture morphology over time: environment, taphonomy, and the archaeological record. *Journal of Archaeological Science* **39** 555-559
- Kars, H., 1998. Preserving our *in situ* archaeological heritage: a challenge to the geochemical engineer. *Journal of Geochemical Exploration* **62** 139-147
- Kaufman, D. S., & Manley, W. F., 1998. A new procedure for determining DL amino acid ratios in fossils using reverse phase liquid chromatography. *Quaternary Science Reviews* **17** 987-1000
- Kenward, H. & Hall, A., 2000. Decay of delicate organic remains in shallow urban deposits: are we at watershed? *Antiquity* **74** 519-525
- Kim, Y.S. & Singh, A.P., 2000. Micromorphological characteristics of wood biodegradations in wet environments: A review. *IAWA Journal* **21** 135-155
- Kirk, T. K., & Farrell, R. L., 1987. Enzymatic "combustion": the microbial degradation of lignin. *Annual Reviews in Microbiology* **41** 465-501
- Kirk, J.L., Beaudette, L.A., Hart, M., Moutoglis, P., Klironomos, J.N., Lee, H. & Trevore, J.T., 2004. Review: Methods of studying soil microbial diversity. *Journal of Microbial Methods* **58** 169-188
- Kleen, M. & Gellerstedt, G., 1991. Characterisation of chemical and mechanical pulps by pyrolysis-gas chromatography/mass spectrometry. *Journal of Analytical and Applied Pyrolysis* **19** 139-152
- Kontoyannis, C.G., Orkoula, M.G. & Koutsoukos, P.G., 1997. Quantitative analysis of sulphated calcium carbonates using Raman spectroscopy and X-ray powder diffraction. *Analyst* **122** 33-38

- Koon, H.E.C., Nicholson, R.A. & Collins, M.J., 2003. A practical approach to the identification of low temperature heated bone using TEM. *Journal of Archaeological Science* **30** 1393-1399
- Koon, H.E.C., 2006. Detecting cooked bone in the archaeological record: A study of the thermal stability and deterioration of bone collagen. *PhD Thesis*, University of York, UK
- Koon, H.E.C., O'Connor, T.P. & Collins, M.J., 2010. Sorting the butchered from the boiled. *Journal of Archaeological Science* **37** 62-69
- Landete-Castillejos, T., Estevez, J.A., Martinez, A., Ceacero, F., Garcia, A. & Gallego, L., 2007. Does chemical composition of antler bone reflect the physiological effort made to grow it? *Bone* **40** 1095-1102
- Lane, P. J. & Schadla-Hall, R. T., 2004. The Many Ages of Star Carr: Do 'Cites' Make the 'Site'? In: A. Barnard (Ed.) *Hunter-gatherers in History, Archaeology and Anthropology*, Oxford: Berg. Pg 145-161
- Lee-Thorp, J.A. & Van der Merwe, N.J., 1991. Aspects of the chemistry of modern and fossil biological apatites. *Journal of Archaeological Science* **18** 343-345
- Li, C., & Zhao, Z. K., 2007. Efficient acid-catalyzed hydrolysis of cellulose in ionic liquid. *Advanced Synthesis & Catalysis* **349** 1847-1850
- Lillie, M. & Smith, R. 2007. The *in situ* preservation of archaeological remains: using lysimeters to assess the impacts of saturation and seasonality. *Journal of Archaeological Science* **34** 1494-1504
- Luder, W.F., 1942. Acids and bases: their relationship to oxidizing and reducing agents. *Journal of Chemical Education* **19** 24-26
- Margolis, H.C. & Moreno, E.C., 1992. Kinetics of hydroxyapatite dissolution in acetic, lactic and phosphoric acid solutions. *Calcified Tissue International* **50** 137-143
- Martinez, A.T., Speranza, M., Ruiz-Duenas, F.J., Ferreria, P., Camarero, S., Guillen, F., Martinez, M.J., Gutierrez, A. & del Rio, J.C., 2005. Biodegradation of lignocellulosics: microbial, chemical and enzymatic aspects of the fungal attack of lignin. *International Microbiology* **8** 195-204
- Matthiesen, H., 2004. In situ measurement of soil pH. *Journal of Archaeological Science* **31** 1373-1381
- Matthiesen, H., Dunlop, A.R., Jensen, J.A., de Beer, H. & Christensson, A., 2006. Monitoring of preservation conditions and evaluation of decay rates of urban deposits – results from the first five years of monitoring at Bryggen in Bergen, in: Karrs, H. & van Heeringen (Eds),

- Preserving archaeological remains in situ, proceedings of the 3rd conference (Amsterdam)*. Pg 163-174
- McFarlane, D. A., & Ford, D. C., 1998. The age of the Kirkdale Cave palaeofauna. *Science* **25** 3-6
- Mellars, P. & Dark, P., 1998. *Star Carr in Context*. McDonald Institute for Archaeological Research, Cambridge
- Milner, N., Conneller, C., Elliott, B., Koon, H., Panter, I., Penkman, K., Taylor, B. & Taylor, M., 2011a. From riches to rags: organic deterioration at Star Carr. *Journal of Archaeological Science* **38** 2818-2832
- Milner, N., Lane, P., Taylor, B., Conneller, C. & Schadla-Hall, T., 2011b. Star Carr in a Postglacial lakescape: 60 years of reseach. *Journal of Wetland Archaeology* **11** 1-19
- Milner, N & Taylor, B., 2012. Excavations at Flixton Island: Interim report. *Unpublished report*
- Milner, N., Taylor, B., Conneller, C. & Schadla-Hall, T., 2013a. *Star Carr: Life in Britain after the Ice Age*. *Archaeology for all: Council for British Archaeology*. York
- Milner, N., Taylor, B., Bamforth, M., Conneller, C., Elliot, B., High, K., Knight, B. & Taylor, M., 2013b. Postglacial : Assessment report for Star Carr, excavations 2013. *Unpublished report*
- Mosely, H., 1996. Archaeology and development, in: Corfield, M., Hinton, P., Nixon, T. & Pollard, M (Eds) *Preserving archaeological remains in situ: proceedings of the 1st conference*. Pg 47-50
- Needham, A., 2007. *Star Carr soils analysis*. University of York: *unpublished report*
- Nicholson, R.A., 1993. A morphological investigation of burnt animal bone and an evaluation of its utility in archaeology. *Journal of Archaeological Science* **20** 411-428
- Nicholson, R.A., 1996. Bone degradation, burial medium and species representation: Debunking the myths, an experiment-based approach. *Journal of Archaeological Science* **23** 513-533
- Nicholson, R.A., 1998. Bone degradation in a compost heap. *Journal of Archaeological Science* **25** 393-403
- Nielsen-Marsh, C.M. & Hedges, R.E.M., 2000. Patterns of diagenesis in Bone I: the effects of site environments. *Journal of Archaeological Science* **27** 1139-1150
- Nielsen-Marsh, C.M., Hedges, R.E.M., Mann, T. & Collins, M.J., 2000. A preliminary investigation of the application of differential scanning calorimetry to the study of collagen degradation in archaeological bone. *Thermochimica Acta* **365** 129-139

- Nudelman, F., Pieterse, K., George, A., Bomans, P. H., Friedrich, H., Brylka, L. J., Hilbers, P.A.J., de With, G. & Sommerdijk, N. A., 2010. The role of collagen in bone apatite formation in the presence of hydroxyapatite nucleation inhibitors. *Nature materials* **9** 1004-1009
- O'Connor, T.P., 1987. On the structure, chemistry and decay of bone, antler and ivory in: Starling, K & Watkinson, D. (Eds), *Archaeological bone, antler and ivory*. Pg 6-8
- O'Connor, T.P., 1989. The animal bones: bones from Anglo-Scandinavian Levels and 16-22 Coppergate. York Archaeological Trust for Excavation and research Ltd, United Kingdom
- Orgel, J.P.R.O., Miller, A., Irving T.C., Fischetti, R.F., Hammersley, A.P. & Wess, T.J., 2001. The *in situ* supermolecular structure of type 1 collagen. *Structure* **9** 1061-1069
- Oxley, I., 1996. The *in situ* preservation of underwater sites, in: Corfield, M., Hinton, P., Nixon, T. & Pollard, M (Eds) *Preserving archaeological remains in situ: proceedings of the 1st conference*. Pg 159-173
- Pandey, K.K. 1998. A study of chemical structure of soft and hardwood and wood polymers by FTIR Spectroscopy. *Journal of Applied Polymer Science* **71** 1969-1975
- Pandey, K.K. & Pitman, A.J. 2003. FTIR studies of the changes in wood chemistry following decay by brown-rot and white-rot fungi. *International Biodeterioration & Biodegradation* **52** 151-160
- Panter, I. & Spriggs, J., 1996. Condition assessment and conservation strategies for waterlogged wood assemblages, in: Hoffman, P., Grant, T., Spriggs, J., Daley, T. (Eds), *Wet Organic Archaeological Materials*, York. Pg 185-201
- Panter, I., 2009. Report on the decay analysis of wood and antler samples from Star Carr, North Yorkshire. *York Archaeological Trust report*
- Panter, I., 2013. Must Farm Palaeochannel: Storage, recording and conservation of 8 waterlogged logboats. *English Heritage report*
- Paschalis, E.P., Verdelis, K., Doty, S.B., Boskey, A.L., Mendelsohn, R. & Yamaughii, M., 2001. Spectroscopic characterization of collagen cross-links in bone. *Journal of Bone and Mineral research* **16** 1821-1828
- Patrick, W.H. & Mahaptra, I.C., 1968. Transformation and availability to rice of nitrogen and phosphorus in waterlogged soils. *Advances in Agronomy* **20** 323-359
- Penel. G., Leroy, G., Rey, C. & Bres, E., 1998. MicroRaman spectral study of the PO₄ and CO₃ vibrational modes in synthetic and biological apatites. *Calcified Tissue International* **63** 475-481

- Penkman, K.E.H., Kaufman, D.S., Maddy, D. & Collins, M.J., 2008. Closed –system behaviour of the intra-crystalline fraction of amino acids in mollusc shells. *Quaternary Geochronology* **3** 2-25
- Person, A., Bocherens, H., Saliege, J.F., Paris, F., Zeitoun, V. & Gerard, M., 1995. Early diagenetic evolution of bone-phosphate – an X-ray-diffractometry analysis. *Journal of Archaeological Science* **22** 211-221
- Piga, G., Santos-Cubedo, A., Moya Sola, S., Brunetti, A., Malgosa, A. & Enzo, S., 2009 An X-ray diffraction (XRD) and X-ray fluorescence (XRF) investigation in human and animal fossil bones from Holocene to Middle Triassic. *Journal of Archaeological Science* **36** 1857-1868
- Piga, G., Santos-Cubedo, A., Brunetti, A., Piccinini, M., Malgosa, A., Napolitano, W. & Enzo, S., 2011. A multi-technique approach by XRD, XRF, FT-IR to characterize the diagenesis of dinosaur bones from Spain. *Palaeogeography, Palaeoclimatology, Palaeoecology* **310** 92-107
- Piispanen, R. & Saranpaa, P., 2001. Variation of non-structural carbohydrates in silver birch (*Betula pendula* Roth) wood. *Trees* **15** 444-451
- Pleshko, N., Boskey, A. & Mendelsohn, R., 1991. Novel infrared spectroscopic methods for the determination of crystallinity of hydroxyapatite minerals. *Biophysics Journal* **60** 786-793
- Pollard, A.M., 1996. The chemical nature of the burial environment, in: Corfield, M., Hinton, P., Nixon, T. & Pollard, M (Eds) *Preserving archaeological remains in situ: proceedings of the 1st conference*. Pg 60-65
- Pollard, A.M., 2006. Prediction of rates of decay of archaeological organic material using soil carbon cycling modelling, in: Karris, H. & van Heeringen (Eds), *Preserving archaeological remains in situ, proceedings of the 3rd conference (Amsterdam)*. Pg 55-64
- Postgate, J.R., 1965. Recent advances in the study of the sulfate-reducing bacteria. *Bacteriological Reviews* **29** 425-441
- Powell, K.L., Pedley, S., Daniel, G & Corfield, M., 2001. Ultra structural observations of microbial succession and decay of wood buried at a Bronze Age archaeological site. *International Biodeterioration & Biodegradation* **47** 165-173
- Price, F.T. & Casagrande, D.J., 1991. Sulfur distribution and isotopic composition in peats from the Okefenokee Swamp, Georgia and the Everglades, Florida. *International Journal of Coal Geology* **17** 1-20
- Pryor, F., 1991. Flag Fen: Prehistoric Fenland Centre. English Heritage, Avon

- Ragahavan, M., 2011, Investigation of mineral and collagen organisation in bone using Raman spectroscopy. *Doctoral Thesis*, University of Michigan
- Reddy, K.R. & Patrick Jr, W.H., 1975. Effect of alternate aerobic and anaerobic conditions on redox potential, organic matter decomposition and nitrogen loss in a flooded soil. *Soil Biology and Biochemistry* **7** 87-94
- Reiche, I., Favre-Quattropani, L., Calligaro, T., Salomon, J., Bocherens, H., Charlet, L. & Menu, M., 1999. Trace element composition of archaeological bones and post-mortem alteration in the burial environment. *Nuclear Instruments and Methods in Physics Research B* **150** 656-662
- Reiche, I., Favre-Quattropani, L., Vignaud, C., Bocherens, H., Charlet, L. & Menu, M., 2003. A multi-analytical study of bone diagenesis: the Neolithic site of Bercy (Paris, France). *Measurements and Science technology* **14** 1608-1619
- Reiche, I., lebon, M., Chadefaux, C., Muller, K., Le Ho, A-S., Gensch, M. & Schade, U., 2010. Microscale imaging of the preservation state of 5,000-year-old archaeological bones by synchrotron infrared microspectroscopy. *Analytical and Bioanalytical Chemistry* **397** 2491-2499
- Rho, J.Y., Kuhn-Spearing, L. & Zioupos, P., 1998. Mechanical properties and the hierarchical structure of bone. *Medical Engineering & Physics* **20** 92-102
- Rhodes, B., 2014. The diagenesis of demineralised bone under acidic conditions. *MChem Research Project, University of York*
- Rich, A. & Crick, F.H.C., 1961. The molecular structure of collagen. *Journal of Molecular Biology* **3** 483-506
- Rieck, F., 1997. Recent excavations at Nydam. *The Danish National Museums Nydam Project 1989–1997*. Amersfoort, C.J.C. Reuvensteizing
- Robb, G.A. & Robinson, J.D.F., 1995. Acid drainage from mines. *The Geographical Journal* **161** 47-54
- Roberts, S.J., Smith, C.I., Millard, A.R. & Collins, M.J., 2002. The taphonomy of cooked bone: characterising boiling and its physio-chemical effects. *Archaeometry* **44** 485-494
- Rosswall, T., 1975. Introduction, in: Weilgolaski, F.E (Ed) *Fennoscandian Tundra Ecosystems. Part 1, Plants and Micro-organisms*. Ecological Studies **16** Springer-Verlag, Berlin
- Rowley-Conwy, P., 1998. Faunal remains and antler artefacts, in: Mellars, P. & Dark, P. *Star Carr in Context*. McDonald Institute for Archaeological Research, Cambridge. Pg 99-107

- Russell, J. B., & Dombrowski, D. B., 1980. Effect of pH on the efficiency of growth by pure cultures of rumen bacteria in continuous culture. *Applied and Environmental Microbiology* **39** 604-610
- San Antonio, J.D., Schweitzer, M.H., Jensen, S.T., Kalluri, R., Buckley, M. & Orgel, J.P.R.O., 2011. Dinosaur peptides suggest mechanisms of protein survival. *PLoS One* **6**
- Sanchez, C., 2009. Lignocellulosic residues: Biodegradation and bioconversion by fungi. *Biotechnology Advances* **27** 185-194
- Sandström, M., Jalilehvand, F., Damian, E., Fors, Y., Gelius, U., Jones, M. & Salome, M., 2005. Sulfur accumulation in the timbers of King Henry VIII's warship Mary Rose: A pathway in the sulfur cycle of conservation concern. *Proceedings of the National Academy of Sciences of the United States of America* **102** 14165-14170
- Sato, N., Gutain, A.T., Kang, K., Daimon, H. & Fujie, K., 2004. Reaction kinetics of amino acid decomposition in high-temperature and high-pressure water. *Industrial and Engineering Chemistry Research* **43** 3217-3222
- Scalbert, A., Monties, B. & Janin, G., 1989. Tannins in wood: Comparison of different estimation methods. *Journal of Agricultural Food Chemistry* **37** 1324-1329
- Schwarzel, K., Renger, M., Sauerbrey, R. & Wessolek, G., 2002. Soil characteristics of peat soils. *Journal of Plant Nutrition and Soil Science* **165** 479-486
- Schwertmann, U. & Cornell, R. M., 2000. Iron oxides in the laboratory: 2nd Edition. Wiley-VCH, Weinheim
- Seaby, D., 1991. Gravimetric density determination of wood using the DDD 200 wood decay detecting drill. *Unpublished report* Department of Agriculture for Northern Island
- Shaw, P.E., Tatu, J.H. & Berry, R.E., 1967. Acid-catalysed degradation of D-fructose. *Carbohydrate Research* **5** 266-273
- Shih, W., Rahardianto, A., Lee, R. & Cohen, Y. 2005. Morphometric characterization of calcium sulphate dehydrate (gypsum) scale on reverse osmosis membranes. *Journal of Membrane Science* **252** 253-263
- Shoulders, M.D. & Raines, R.T., 2009. Collagen structure and stability. *Annual Review of Biochemistry* **78** 929-958
- Smith, G.G. & Evans, R.C., 1980. The Effect of Structure and Conditions on the Rate of Racemization of Free and Bound Amino Acids, in: Hare, P.E., T.C, H., King, K. (Eds.), *Biochemistry of Amino Acids*, John Wiley & Sons, United States of America. Pg 257-282

- Smith, D.N., Roseff, R. & Butler, S., 2001. The sediments, pollen, plant macro-fossils and insects from a Bronze Age channel fill at Yoxall Bridge, Staffordshire. *Experimental Archaeology* **6** 1-12
- Sposito, G., 2008. *The Chemistry of soils*. Oxford University Press, New York
- Spriggs, J.A., 1981. The conservation of timber structures at York – A progress report, in: Grattan, D., & McCawley, C. (Eds) *Proceedings of the ICOM Waterlogged Wood Working Group Conference*, Ottawa. Pg 143-152
- Steinbergs, A., Iismaa, O., Freney, J.R. & Barrow, N.J., 1961. Determination of total sulphur in soil and plant material. *Analytical Chimica Acta* **27** 158-164
- Stout, S.D. & Teitelbaum, S.L., 1976. Histological analysis of undecalcified thin sections of archaeological bone. *American Journal of Physical Anthropology* **44** 263-269
- Surovell, T.A & Stiner, M.C., 2001. Standardising Infra-red measures of bone mineral crystallinity: an experimental approach. *Journal of Archaeological Science* **28** 633-642
- Taylor, M., 1992. Flag Fen: the wood. *Antiquity* **66** 476-498
- Timlin, J.A., Carden, A. & Morris, M.D., 2000. Raman spectroscopic imaging markers for fatigue-related microdamage in bovine bone. *Analytical Chemistry* **72** 2229-2236
- Tiquia, S. M., Wan, H. C., & Tam, N. F., 2002. Microbial population dynamics and enzyme activities during composting. *Compost Science & Utilization* **10** 150-161
- Tolan-Smith, C., 2008. Mesolithic Britain, in: Bailey, G. & Spikins, P (Eds), *Mesolithic Europe*. Cambridge University Press, Cambridge. Pg 132-157
- Tuomela, M., Vikam, M., Hatakka, A. & Itavaara, M., 2000. Biodegradation of lignin in a compost environment: A review. *Bioresource Technology* **72** 169-183
- Turner-Walker, D. & Syversen, U., 2002. Quantifying histological changes in archaeological bones using BSE-SEM image analysis. *Archaeometry* **44** 461-468
- Turner-Walker, G., 2008. The chemical and microbial degradation of bones and teeth in: Pinhasi, R. & Mays, S. (Eds), *Advances in Human Palaeopathology*. Pg 3-30
- Turner-Walker, G., & Jans, M., 2008. Reconstructing taphonomic histories using histological analysis. *Palaeogeography, Palaeoclimatology, Palaeoecology*, **266** 227-235
- Turner-Walker, G., Peacock, E.E., 2008. Preliminary results of bone diagenesis in Scandinavian bogs. *Palaeogeography Palaeoclimatology Palaeoecology* **266** 151-159

- Van Bergen, P.F., Poole, I., Ogilvie, T., Caple, C. & Evershed, R., 2000. Evidence for demethylation of syringyl moieties in archaeological wood using pyrolysis-gas chromatography/mass spectrometry. *Rapid Communications in Mass Spectrometry* **14** 71-79
- Van de Noort, R., 1998. The Humber wetlands survey: An integrated approach to wetland research and management in: Bernick, K (Ed) *Hidden dimensions, the cultural significance of wetland archaeology*. UBC Press, Vancouver. Pg 3-30
- Van de Noort, R., & O'Sullivan, A., 2006. Rethinking wetland archaeology. Duckworth, London
- Very, J-M. & Baud, C-A., 1984. X-ray diffraction of calcified tissues in: Dickson, G.R (Ed), *Methods of calcified tissue preparation*. Pg 369-390
- Very, J.M., Gibert, R., Guilhot, B., Debout, M. & Alexandre, C., 1997. Effect of aging on the amide group of bone matrix, measured by FTIR spectrophotometry, in adult subjects deceased as a result of violent death. *Calcified Tissue International* **60** 271-275
- Vinciguerra, V., Napoli, A., Bistoni, A., Petrucci, G. & Sgherzi, D., 2007. Wood decay characterization of a naturally infected London plane-tree in urban environment using Py-GC/MS. *Journal of Analytical Applied Pyrolysis* **78** 228-231
- Warren, L. A., 2011. Acid rock drainage, in: Reitner, J (Ed) *Encyclopedia of Geobiology*, Springer Pg5-8
- Weiner, S. & Traub, W., 1992. Bone structure: from ångstroms to microns. *Faseb Journal* **6** 879-885
- Welch, J. & Thomas, S., 1996. Groundwater modelling of waterlogged archaeological deposits, in: Corfield, M., Hinton, P., Nixon, T. & Pollard, M (Eds) *Preserving archaeological remains in situ: proceedings of the 1st conference*. Pg 16-20
- Wess, T.J., Drakopoulos, M., Snigirev, S., Wouters, J., Paris, O., Fratzl, P., Collins, M., Hiller, J. & Nielsen, K., 2001. The use of small-angle X-ray diffraction studies for the analysis of structural features in archaeological samples. *Archaeometry* **43** 117-129
- Wheeler, A., 1978. Why were there no fish remains at Star Carr? *Journal of Archaeological Science* **5** 85-89
- Williams, J., Fell, V., Graham, K., Simpson, P., Collins, M., Koon, H. & Griffin, R., 2006. Re-watering of the Iron Age Causeway at Fiskerton, England, in Karris, H. & van Heeringen (Eds), *Preserving archaeological remains in situ, proceedings of the 3rd conference (Amsterdam)*. Pg 181-198
- Wilson, M.A., Godfrey, I.M., Hanna, J.V., Quezada, R.A. & Finnie, K.S., 1993. The degradation of wood in old Indian Ocean shipwrecks. *Organic Geochemistry* **20** 599-610

- Wilson, L., & Pollard, A. M., 2002. Here today, gone tomorrow? Integrated experimentation and geochemical modelling in studies of archaeological diagenetic change. *Accounts of Chemical Research* **35** 644-651
- Wilson, A. M., Huettel, M., & Klein, S., 2008. Grain size and depositional environment as predictors of permeability in coastal marine sands. *Estuarine, Coastal and Shelf Science* **80** 193-199
- Xiang, Q., Lee, Y.E., Pettersson, P.O. & Torget, R.W., 2003. Heterogeneous aspects of acid hydrolysis of α -cellulose. *Applied Biochemistry and Biotechnology* **105-108** 505-514
- Yablokov, V.Y., Smeltsona, I.L., Zelyaev, A. & Mitrofanova., 2009. Studies of the rate of thermal decomposition of glycine, Alanine and serine. *Russian Journal of Organic Chemistry* **79** 1344-1346
- Zapata, J., Perez-Sirvent, C., Martiez-Sanchez, M.J. & Tovar, P., 2006. Diagenesis, not biogenesis: Two late Roman skeletal examples. *Science of the Total Environment* **369** 357-368
- Zevenhuizen, L.P.T.M., Dolfig, J., Eshuis, E.J. & Scholten-Loerselman, I.J., 1979. Inhibitory effects of copper on bacteria related to the free ion concentration. *Microbial Ecology* **5** 139-146